Università degli Studi di Firenze

DOTTORATO DI RICERCA IN
"*Scienze della Terra*"

CICLO XXV

COORDINATORE Prof. Rook Lorenzo

Distribution of mercury and other trace elements in the Mt. Amiata region (Southern Tuscany, Italy)

Settore Scientifico Disciplinare GEO/09

Dottorando
Dott. Rimondi Valentina

Tutore
Prof. Costagliola Pilario

Anni 2010/2012

ABSTRACT

This PhD project focuses on the Hg mining district of Mt. Amiata (Southern Tuscany- Italy), and to the environmental consequences deriving from the mining activity occurring in this region. In the Mt. Amiata, mercury (Hg) was produced for about one century, ending almost 30 years ago (1980s). Different aspects of Hg environmental impact of mining activity in the Mt. Amiata Hg are taken into consideration in this research project, carried on with the partnerships of different national and international research centres, as USGS and Regione Toscana. The work especially addresses to the Paglia River Basin (PBR), which is the main natural collector of Hg drained by the east sector of the Mt. Amiata. The main goals of the work are then: i) to establish an updated picture of Hg and methyl-Hg (MMHg) diffusion and distribution in the PBR; ii) to estimate the mass load of Hg transported by this river; iii) to characterize the speciation of Hg − and hence its bioavailability − in different environmental matrices; iv) to define the regional background for Hg.

The results of this study report an elevated and pervasive distribution of Hg in all the environmental compartments of Paglia River (water, sediment, soil, roasted discarded materials). Especially, MMHg is widely distributed in this ecosystem, resulting in its great bioaccumulation in local fish, which present MMHg concentrations highly exceeding the recommended value of the U.S. Environmental Protection Agency (US EPA).

Coupling the XAS and SEC techniques, this study shows as Hg is essentially present in the extremely insoluble form of cinnabar, and related alteration product, in sediments of Paglia River that precede mining activity, while a more soluble mineral assemblage, constituted by Hg^0 and $HgCl_2$, characterizes the post-mining and recent sediments. These compounds were likely leached from the original calcine deposits, and they suggest an enhanced mobility and hence bioavailability of Hg in the PBR as a consequence of mining activity and of the roasting process. As these last compounds may easily solubilize releasing free Hg(II), they represent a main risk for the environment, possibly favouring methylation reactions. The occurrence of these compounds may then possibly relate with the elevated bioavailability of MMHg in the PBR.

Results of this study indicate that significant amount of Hg is transported annually by the Paglia River, in the order of tens of kg. This transport occurs mainly in the form of particulate Hg, which can deposit along the river course. The hydrodynamic of Paglia River prevents however a definitive storage of Hg, which is further mobilized up to Tiber River, possibly impacting this ecosystem. Notwithstanding mining activity promotes Hg diffusion in the environment, pristine sediments analyzed in this work report Hg concentrations much higher than the crustal level, indicating the presence of a wide geogenic anomaly centred in the area of Mt. Amiata. Preliminary results indicate it might range 2-6 μg/g, being much higher than the Hg values common encountered in the crust. The establishment of a reliable background is of fundamental importance for this area in order to fix reliable thresholds for the remediation projects going to be carried out at these mines.

RIASSUNTO

Lo lavoro svolto nell'ambito di questo dottorato è rivolto allo studio del distretto minerario del Monte Amiata (Toscana meridionale, Italia) e alle ricadute ambientali connesse al passato minero-metallurgico di questa regione, dove il mercurio (Hg) è stato prodotto fino all'inizio anni '80. Il progetto di ricerca, svolto in collaborazione con diversi enti di ricerca, nazionali e internazionali tra cui USGS e Regione Toscana, indaga differenti aspetti connessi all'inquinamento ambientale da Hg (+ altri metalli in tracce) legati alla principale miniera del distretto, Abbadia San Salvatore. Lo studio in particolare si concentra sul bacino del F. Paglia, che rappresenta la principale via di drenaggio naturale del Hg proveniente dal settore orientale del M. Amiata. Gli obiettivi di questo lavoro sono: i) definire e aggiornare i dati pregressi circa la distribuzione e diffusione del Hg e metil-Hg (MMHg) in vari comparti abiotici e biotici del bacino del F. Paglia, ii) stimare le quantità di Hg trasportate in soluzione da questo fiume, iii) definire la speciazione del Hg − e dunque la sua biodisponibilità – in differenti matrici ambientali; iv) stabilire il background regionale di Hg.

I risultati di questo progetto indicano una distribuzione pervasiva di Hg in tutti i comparti ambientali analizzati (sedimenti fluviali e acque del F. Paglia, suoli e scarti minerari). La presenza di MMHg è elevata in questo ecosistema, come dimostrato dal forte bioaccumulo di questo contaminante nei pesci del Paglia con concentrazioni molto superiori al limite stabilito dall'Agenzia di Protezione Ambientale degli USA (US EPA).

Tramite l'utilizzo di tecniche XAS e SEC, questo studio indica che i sedimenti fluviali del F. Paglia che precedono l'attività mineraria sono composti solo da cinabro, minerale altamente insolubile, e sue fasi di alterazione. Composti maggiormente solubili di Hg, come Hg^0 e $HgCl_2$, caratterizzano invece i sedimenti successivi all'attività mineraria del F. Paglia, derivanti del ruscellamento superficiale e lisciviazione di questi minerali dalle calcine della miniera di Abbadia. A seguito dell'attività mineraria e dei processi di arrostimento del minerale, la mobilità e quindi la biodisponibilità di Hg è quindi incrementata. Tali composti rappresentano un forte rischio per l'intero ecosistema del F. Paglia, poiché la loro solubilizzazione comporta il rilascio di Hg(II), che può andare incontro a processi di metilazione. Non è quindi da escludere che la speciazione del Hg negli attuali sedimenti fluviali possa risultare determinate per spiegare l'elevata produzione di MMHg nel bacino del Paglia e il conseguente bioaccumulo nei pesci di questo fiume.

I bilanci di massa svolti per il F. Paglia indicano che quantità dell'ordine di decine di kg/anno di Hg sono trasportate annualmente fuori dal distretto amiatino, prevalentemente in forma di particolato, rappresentando una possibile, ma tuttora da chiarire, sorgente di inquinamento per il F. Tevere di cui il Paglia è affluente. Nonostante, l'attività minerarie pregressa sia determinante per l'attuale diffusione del Hg nell'ambiente, le ricerche svolte nell'ambito di questo progetto di dottorato evidenziano che i sedimenti considerati *pristine* contengono quantità di Hg molto superiori (2-6 μg/g) al clarke crustale per questo elemento, definendo quindi una marcata anomalia naturale (geogenica) nell'area del Monte Amiata. Tenere conto di tali valori è fondamentale per gli interventi di bonifica che sono attualmente in atto o in corso di progettazione nell'area del Monte Amiata.

Contents

ABBREVIATIONS

AAS:	Atomic absorption spectrometry
As:	Arsenic
ASSM:	Abbadia San Salvatore mine
CVAAS:	Cold Vapor Atomic Absorption Spectrometry
CVAFS:	Cold Vapor Atomic Fluorescence Spectrometry
DMMHg:	Dimethyl-mercury
FDA:	Food and Drug Administration
Hg:	Mercury
Hg^0:	Elemental mercury
Hg_D:	Dissolved Hg
Hg_{SPM}:	Hg bound to SPM
Hg_T:	Total Hg
K_D:	Partition coefficient
Mg:	Megagrams
MMHg:	Methyl-mercury
PEC:	Probable Effect Concentration
PCA:	Principal Component Analysis
PRB:	Paglia River Basin
Sb:	Antimony
SEC:	Sequential chemical extractions
SPM:	Suspended particulate matter
SSL:	Soil screening levels
UNEP:	United Nations Environment Programme
US EPA:	Environmental Protection Agency
XAS:	X-Ray Absorption Spectroscopy
WHO:	World Health Organization

CHAPTER 1

– INTRODUCTION –

1.1 Mercury: general aspects

Mercury (Hg) and its main mineral, cinnabar (HgS) started to be known by humans in ancient times and their applications still continue today. In the elemental form, Hg is a silver-white colored metal (Hg^0), the only one to be liquid in standard conditions (UNEP/WMO, 1998). The symbol *Hg* (***H****ydrar****g****yrum*, "watery silver" in Greek), derives from this peculiar and unique characteristic. The unusual properties of Hg explain its large use starting from the antiquity in various sectors of human life, ranging from medicine, agriculture to scientific and industrial applications. Although present also in nature, metallic Hg started to be produced 2000 years ago by Romans in Almadén (Spain) by heating cinnabar and condensing the vapour. The first use of cinnabar dates back to Neolithic Age (ca. > 4000 BCE), when the mineral was used as pigment and was found as preservative of human bones in Italy and Spain (Parsons and Percival, 2005). The massive use of Hg started in the 1500, when it was employed to recover low-grade silver ores in South and Central America by amalgamation technique. For this purpose, Hg started to be traded, and for more than 300 years Hg was sent by Spain, Slovenia and Peru to South America (Parsons and Percival, 2005). This technique was later used in the gold rushes of the 18th and 19th centuries in North America. Nriagu (1994) estimated that ~196,000 tons Hg were lost from 1570 to 1900 in the Americas, causing the first widespread and high diffusion of Hg all over the world (Fig. 1.1.) (Schuster et al., 2002; Hylander and Meili, 2003).

Thanks to its low resistivity and good electrical conductivity, Hg is now a component of different electrical and electronic products, as electrical wiring and switches, fluorescent lamps, batteries, thermostats, and measuring and control devices (e.g. barometers and pressure gauges) (Eisler, 1987). In the industrial field, Hg is used principally for the production of chlorinated compounds as vinyl chloride monomer (VCM), and in chlor-alkali industry where Hg is the cathode in the electrolytic production of NaOH and Cl from NaCl; minor applications are reported in nuclear reactors and as an addictive for paper production (Gray, 2003). In agriculture, Hg has been used as fungicide for seeds and bulbs (Gray, 2003),

particularly in the extremely toxic forms of methyl- and ethyl-Hg. However, following the several cases of poisoning associated to these treatments, the use in this sector has been banned.

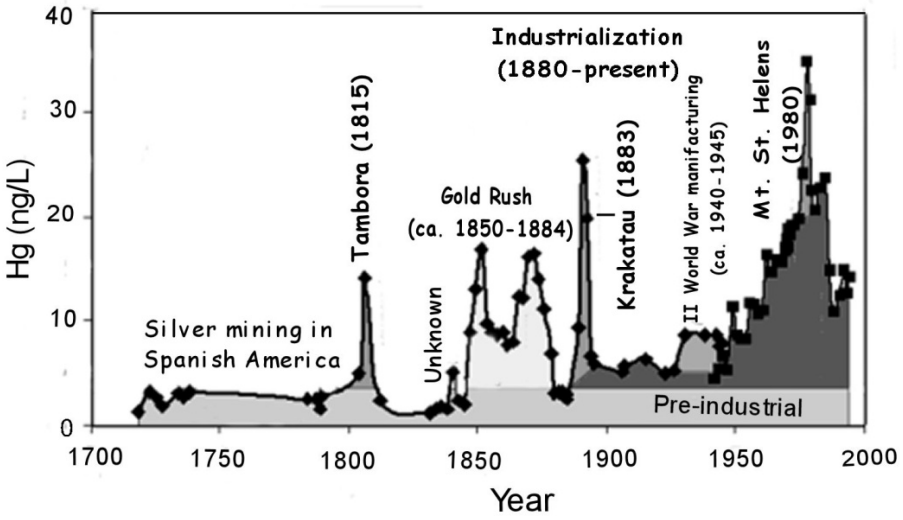

Fig. 1.1. *Mercury concentration profile in log ice core mapping Hg distribution in the last 270 years (modified from Schuster et al., 2002).*

Since the first industrial period (1870-1915), the increased use of Hg in different human activities has multiplied the emission sources to the environment, as documented by the Hg accumulation profile in 270-year ice core record (Fig. 1.1) (Schuster et al., 2002). The peak of Hg demand (10,000 t yr^{-1}) was registered during the World War II and the 1970s (Hylander and Meili, 2003). In the last decades, the industrial use of Hg has however declined due to the increased awareness about its toxicity. Thanks to technological development, Hg is then substituted in many goods by less toxic elements or different technologies (Hylander and Meili, 2003), resulting in a global demand reduced to 3000-3800 tons in the year 2005 (UNEP, 2006). Present-day major uses for Hg are for artisanal and small-scale Au mining, for VCM and chlor-alkali production (Pacyna et al., 2010; Pirrone et al., 2010).

The toxicity of Hg was already recognized in ancient times, mainly as the result of its effects on miners. Roman slaves were indeed sent to work in the Spanish mines, where the life expectancy was of three years (Parsons and Percival, 2005). In the second century BCE, Romans prohibited Hg mining in Italy, aware of the risk associated to this exploitation. However, between the 16th century and the middle of 20th, Hg was thought to have curative proprieties and was employed as an ointment, in vapor baths, assumed by mouth, and especially used as a remedy against syphilis (Parsons and Percival, 2005). Nowadays, Hg is known to be a pervasive pollutant, accumulating in organisms, and being highly toxic (US

EPA, 1997). Globally, about 1 million tons Hg were extracted from various ore bodies in the world (Hylander and Meili, 2003), concurring to the alteration of the global Hg cycle. Mercury concentrations in the atmosphere are now 3-5 fold higher than in pre-industrial times, while Hg deposition to lands has increased up to 20-fold since the 1840s (Schuster et al., 2002; Krabbenhoft et al., 2005), consequently enhancing the exposure of Hg to humans. The tragedies of Japan and Iraq between the 1950s and 1970s as a result of methyl-Hg mass poisoning, focused the world attention to the risk associated to the use of Hg in human activities. Mercury production then started to be regulated at least in industrialized countries (Pirrone et al., 2010), and the European Commission adopted a legislation to ban Hg exports between the EU countries and to store excess Hg (EU, 2008).

1.2 Mercury global cycle

The natural Hg geochemical cycle can be schematically synthesized in three steps, regulated by the redox reactions between Hg(0) and Hg(II), and involving: atmospheric transport, deposition to lands and oceans, and re-volatilization (Fig. 1.2). The overall lifetime of Hg in this complex atmosphere-ocean-land system ranges between 3000 and 10,000 yr (Mason and Sheu, 2002; Selin, 2009). Mercury is emitted into the atmosphere from both natural and anthropogenic sources (Pirrone et al., 2003; Nacht et al., 2004; Selin, 2009). The first ones include the contributions of both primary natural sources, as those related to emissions from volcanoes, degassing of areas naturally enriched in Hg (global mercury belts) and geothermal vents (Selin, 2009), and secondary natural sources, deriving from re-emission of Hg previously deposited on waters, lands and vegetation (Gårfeldt et al., 2002; Selin, 2009), the so-called re-cycled Hg (Schroeder and Munthe, 1998). Primary natural sources common account for 500 megagrams (Mg) yr^{-1} Hg (Fig. 1.2) (Mason et al., 2012), although this number is highly uncertain (Selin et al., 2008). Volcanic activity represents the 78% of natural emitters (Bagnato et al., 2009; Zambardi et al., 2009), highly influencing the global Hg budget. Rytuba (2005) reported for instance that following the two historical eruptions of Tambora (1815) and Krakatau (1885), Hg deposition to land increased of three times and returned to background few years after the eruptions; peaks of Hg concentrations in ice cores were moreover observed following these episodes (Fig. 1.1) (Schuster et al., 2002). Contributions of Hg from areas naturally enriched in Hg, the so-called mercuriferous belts (§1.4), can in addition be elevated (Nacht et al., 2004; Kocman and Horvat, 2011; Llanos et al., 2011). Total emission from Almadén, the worlds principal Hg geochemical anomaly, represents for example the 0.1% of the modern global anthropogenic emission rate (Ferrara et

al., 1998a). Oceans are one of the main pool for Hg, containing approximately 350,000 Mg of this element (Selin et al., 2008; Selin, 2009; Mason et al., 2012). The chemical equilibrium established between Hg contents in waters and atmosphere controls the main processes affecting Hg, i.e. the volatilization from surface oceans and the deposition from atmosphere (Mason et al., 1994). As the large majority of aquatic systems contains dissolved Hg at concentrations that are supersaturated relative to equilibrium conditions, evasion of Hg^0 occurs by oceans and inland waters (Morel et al., 1998; Schroeder and Munthe, 1998). Oceanic evasion is then the principal way of Hg re-cycling (Mason et al., 1994; Pirrone et al., 2003; Mason, 2009; Pirrone et al., 2010), estimated to 2000-2800 Mg yr^{-1} (Fig. 1.2) (Mason and Sheu, 2002). Terrestrial emissions, including volatilization from soils and vegetation, range from 300-2800 Mg yr^{-1} of Hg global emissions, with an additional contribution of 300-600 Mg yr^{-1} from biomass burning (Holmes et al., 2010; Mason et al., 2012) (Fig. 1.2).

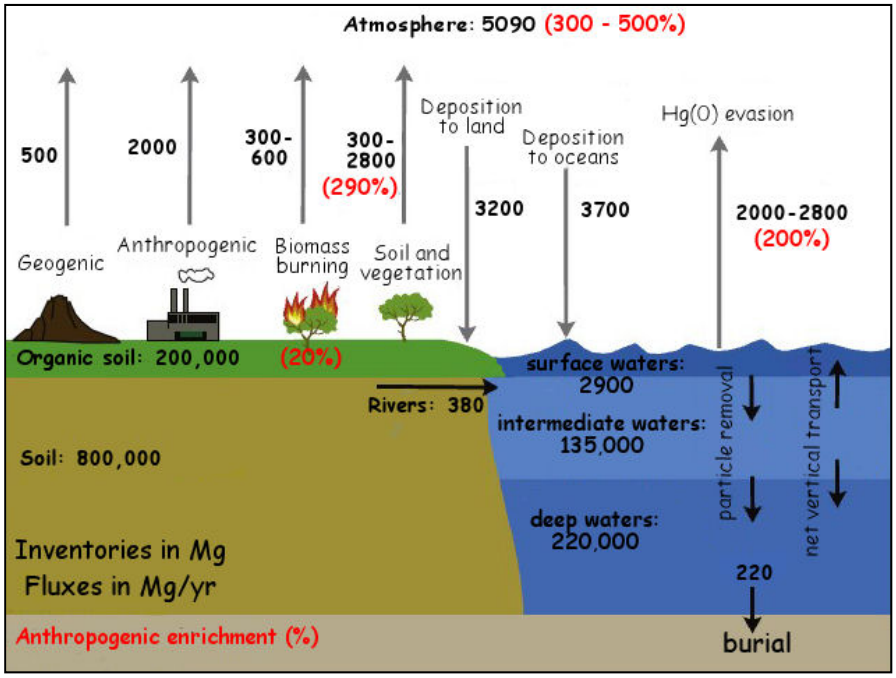

Fig. 1.2. *The global cycle for Hg. Fluxes and inventories are expressed in megagrams (Mg) yr^{-1} and Mg, respectively; anthropogenic enrichment of natural fluxes are reported in red and expressed in % (modified from Mason et al., 2012).*

Although termed as natural, the fluxes described above are highly affected by human activity (Selin et al., 2009), which altered the biogeochemical Hg cycle releasing to the atmosphere the Hg stored in long-term geological sinks. As a consequence natural fluxes of Hg between the atmosphere and the oceans/land are highly enhanced with respect to the pre-industrialization time (Fig. 1.2) (Selin, 2009; Mason et al., 2012), and emissions from

"natural" processes are nearly the 70% of the global emission budget (Pirrone et al., 2010). Anthropogenic Hg fluxes (1926-2600 Mg yr^{-1}; Cinnirella and Pirrone, 2006; Pacyna et al., 2006; Holmes et al., 2010; Pirrone et al., 2010; Mason et al., 2012) are mainly related to fossil fuel combustion, incineration of waste, cremation, small artisanal gold mining and volatilization from landfill (UNEP, 2002). Mercury production from mining is another source of Hg to the atmosphere, although its extent is difficult to be quantified. In 2000, nearly 1800 Mg of Hg were produced in the world, resulting in a Hg emission of 50 Mg (Maxson, 2006).

Mercury is emitted to the atmosphere as Hg^0, although minor emissions of Hg(II) and Hg bound to particulate matter may come from anthropogenic sources (Selin, 2009) (Fig. 1.2). In soils, Hg^0 may be formed by reduction of Hg(II)-species, which predominantly occurs by photochemical reduction of Hg(II) (Gustin et al., 2002), although it could be triggered by the presence of Fe^{2+} and fulvic/humic acids acting as reductants (Gabriel and Williamson, 2004). Mercury evasion from soils is controlled by soil moisture, incident light and temperature (Krabbenhoft et al., 2005). Similarly, photoreduction is also the principal mechanism that regulates Hg^0 evasion from waters (Morel et al., 1998; Fitzgerald and Lamborg, 2005). In the atmosphere, greater than 95% of Hg exists in the elemental state (Fitzgerald and Gill, 1979), although particle-bound Hg(II) and some gaseous Hg(II) ("reactive gaseous Hg" or RGM) are reported (Banic et al., 2005). RGM, consisting of halides, $Hg(OH)_2$ and other unidentified Hg(II) compounds (Schroeder and Munthe, 1998), is highly water-soluble (10^5 times more than Hg^0; Lindberg and Stratton, 1998), and this water solubility highly influences RGM removal from the atmosphere and its deposition on the biosphere. Hg^0 in the atmosphere is slowly oxidized to Hg(II) (Morel et al., 1998), mainly at the water-air interface and by action of O_3, HClO, HSO_3^-, OH^-, and Br^- (Donohue et al., 2006). Gaseous elemental Hg exhibits higher volatility, lower reactivity, and hence lower deposition rates than oxidized Hg(II) (Banic et al., 2005). Thanks to its long residence time in the atmosphere (ca. 1 yr) (Fizgerald and Lamborg, 2004), Hg^0 can be regarded as a global pollutant, as it distributes everywhere over the planet. The return of Hg to the Earth's surface occurs mainly by wet and dry atmospheric deposition of Hg(II), being general higher to the oceans than to lands (Morel et al., 1998). Models elaborated in the last decade generally agree that global deposition to the oceans is between 2800 and 5800 Mg yr^{-1} (Mason and Sheu, 2002; Selin, 2009; Mason et al., 2012); in 2008, a recent study reported a value of 3700 Mg (Fig. 1.2) (Holmes et al., 2010). Atmospheric deposition is the principal source of Hg for the open-seas (Mason et al., 2012), although the importance of riverine discharges is questionable. Estimations of riverine Hg discharge to the oceans considering 927 rivers worldwide (Sunderland and Mason, 2007)

indicate that large amounts of Hg are transported to the estuarine environments (> 2800 Mg yr^{-1}), but only a small portion of that is then transferred to the open oceans (~ 380 Mg yr^{-1}) (Fig. 1.2). On the contrary, other studies show that Hg transport by rivers is essential to explain the seasonal variations registered on Hg fluxes in the Arctic Ocean (Fisher et al., 2012).

Newly deposited Hg has been shown to preferentially re-volatilize in a short time, a phenomenon known as prompt recycling (Selin, 2008). It is estimated that 5% to 60% of deposited Hg is promptly recycled to the atmosphere, the higher values being for waters and snows (Hintelmann et al., 2002). In the terrestrial system, >90% Hg resides on soils (Selin, 2009). Mason and Sheu (2002) calculated that the Hg total burden in the first 15 cm of soil is in the order of 10^6 Mg, increased by approximately 15% by human activity (Selin et al., 2008). The ultimate sink for Hg occurs in the oceans, where Hg is buried to the deep oceanic sediments. This process however occurs at very slow rates, removing from the re-cycle about 200 Mg Hg each year (Fig. 1.2).

1.3 Mercury geochemistry

In natural aquatic environments, Hg occurs in three valence state (0, I, II) and may be present in various chemical and physical forms. The reactions establishing between the different species determine the mobility and toxicity of Hg, and its potential for methylation. The main Hg dissolved species are elemental Hg(0)], complexes of Hg(II) and organic forms, chiefly methyl-Hg (CH_3Hg^+ or MMHg), dimethyl-Hg [$(CH_3)_2Hg$] or DMMHg), and some ethyl-Hg (Akagi et al., 1975). The chemical and physical properties of these forms regulate the geochemical cycle of Hg (Fig. 1.3). Hg(0) generally represents 10% - 30% of the dissolved Hg both in oceans and freshwater systems (Kim and Fitzgerald, 1996), and it is produced by biotic reduction of Hg(II) by aquatic organisms (Mason et al., 1995), abiotic reduction by humic substances (Allard and Arsenie, 1991), and degradation of organic forms (Mason and Sullivan, 1998). Most of surface waters are supersaturated in Hg(0), especially in summer (Ullrich et al., 2011), resulting in Hg lost from the aquatic compartments for its volatilization to the atmosphere (Fig. 1.3). The monovalent oxidation state is of minor importance, as Hg(I) exists only as the dimer (Hg_2^{2+}) in acidic environments, disproportionating to Hg(II) and Hg(0) in presence of OH^-, F^- and CN^- (Davis et al., 1997). Hg(II) is then the stable species at neutral pH (Davis et al., 1997; Ullrich et al., 2001), and it occurs as a complex ion (Morel et al., 1998). Among inorganic ligands, Hg is preferentially complexed to hydroxide [$Hg(OH)^+$, $Hg(OH)_2$, $Hg(OH)^{3-}$] or to chloride ($HgCl^+$, HgClOH, $HgCl_2$, $HgCl_3^-$, $HgCl_4^{2-}$), depending on

the chloride concentrations and the pH (Fig. 1.4) (Morel et al., 1998). The species $HgCl_2$ and $Hg(OH)_2$ are the most abundant for the range of pH and Eh common encountered in natural systems (Fig. 1.4) (Gabriel and Williamson, 2004).

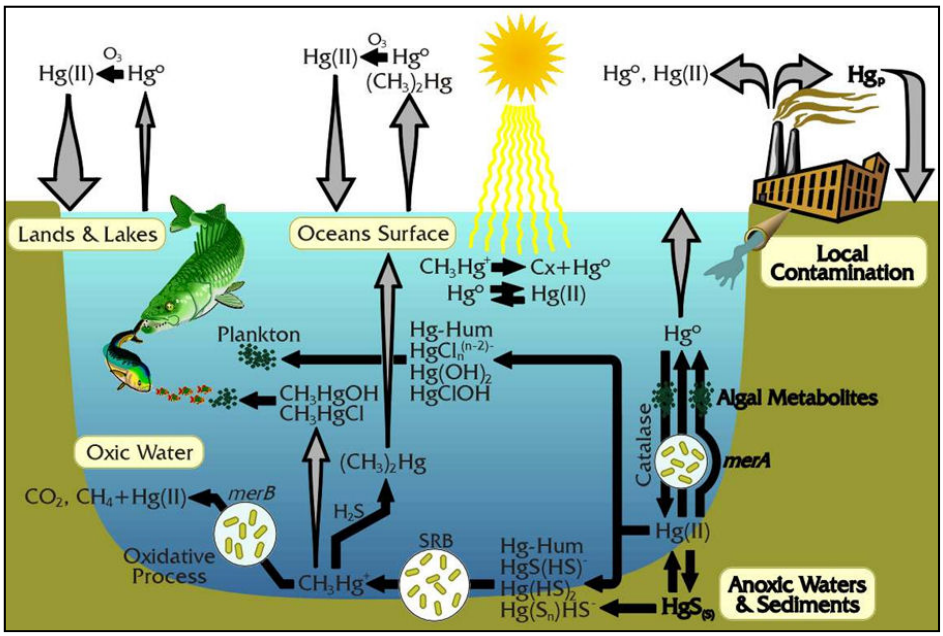

Fig. 1.3. *The biogeochemical cycle of Hg. Black arrows represent the transformation or uptake of Hg, gray arrows the flux of Hg between various compartments, while the width of gray arrows is approximately proportional to the importance of each flux in nature (modified from Schaefer et al., 2002).*

Organomercurials are present in surface waters due to natural processes, such as biotic methylation (§1.3.1), or to human activities. In freshwater systems, MMHg is the most ubiquitous organomercury compound, whereas DMMHg is normally not detected (Ullrich et al., 2001). Thanks to the kinetic hindering of its decomposition reactions, MMHg has a remarkable stability in natural waters (Ullrich et al., 2001), being degraded only by biotic pathways and in a lesser extent by photochemically reactions (§1.3.1). In estuarine and marine systems, the proportion of MMHg is typically less than 5% of total Hg (Coquery et al., 1997), whereas up to 30% of MMHg can be found in fluvial and lake systems (Ullrich et al., 2011), increasing much in anoxic water. The methylmercuric hydroxide, CH_3HgOH, is the common species for MMHg in freshwater systems, while in seawater it is present mainly as CH_3HgCl (Ullrich et al, 2001). In contrast to freshwater systems, DMMHg dominates in deep oceanic waters (Mason and Fitzgerald, 1990, 1991), and little or no DMMHg appears to be present in surface waters (Mason and Fitzgerald, 1990, 1991). Unlike MMHg, DMMHg is readily lost by evaporation and rapidly decomposes in the environment.

Mercury and particularly MMHg establish strong reactions with organic matter found in soils and in waters, as humic and fulvic acids (Ravichandran, 2004). In natural systems, Hg speciation is then largely dominated by organic rather than inorganic complexes. In freshwaters, 90% of Hg is assumed to be complexed by organic matter (Hersterberg et al., 2001; Ullrich et al., 2001), whose reduced sulfur species (e.g. sulfide and thiols) are good binders for Hg (Ravichandran, 2004); most of MMHg (>70%) is however probably associated to dissolved organic carbon in lake water (Ullrich et al., 2001). Moreover, much of the common inorganic Hg forms in waters, as Cl^- and OH^- are further complexed with organic ligands (Gabriel and Williamson, 2004), showing that >99% of Hg in solution is as $HgOH^+$–fulvic acid complex (Reddy and Aiken, 2001).

Although organic complexation likely dominates in oxic environments, under anoxic conditions the chemistry of Hg is mainly controlled by sulfide, and Hg(II) and CH_3Hg^+ tend to form complexes with sulfur (notably sulfide). In waters, as sulfide concentrations increase, Hg speciation is dominated by HgS^0, followed by $HgHS_2^-$, HgS_2^- and finally $Hg(HS)_2^0$ (Benoit et al., 1999). Sulfide ligands control Hg speciation even at very low total sulfide concentrations of 1 nM (Dyrssen and Wedborg, 1991). Methyl-Hg also forms high stable complexes with sulfur, mainly in the form of CH_3HgS (Ullrich et al., 2001), although the chloride complex dominates even at low concentrations (0.1 n*M*) of H_2S and thiols (Dyrssen and Wedborg, 1991). In sediments and soils, Hg(II)-sulfides, existing in the form of cinnabar (α-HgS) and metacinnabar (β-HgS), are the main insoluble Hg compounds of natural systems (Ullrich et al., 2001). Thanks to this low solubility (K_{ps} in the order of 10^{-53}; Morel et al., 1998), the availability of free Hg in the environment is severely limited (Gray, 2003; Navarro, 2008), and cinnabar formation in sulfidic waters, soils and sediments represents an important detoxification process (Stein et al., 1996). Mercuric oxide (HgO), which is sparingly soluble ($K_{ps} = 10^{-4}$), is however also encountered in contaminated environments (Sakamoto et al., 1995).

One of the most important aspect of Hg is its strong tendency to sorb on surfaces, which determines the high affinity of Hg, and in lesser extent of MMHg, to suspended particles in waters (Krabbenhoft et al., 2005). Then suspended matter plays a fundamental role in transporting Hg and MMHg in aquatic systems, being particularly important in coastal particulate-rich areas (Coquery et al., 1997). Particulate Hg consists of Hg bound to inorganic particles and particulate organic matter (Morel et al., 1998; Ullrich et al., 2001). In terrestrial soils, humic and fulvic acids are considered the most important complexing agents (Biester and Scholtz, 1997), and in lesser amounts clay minerals, amorphous oxides, oxyhydroxydes

of Fe, Al, Mn, amorphous FeS (Gabriel and Williamson, 2004). Among inorganic sorbents, FeOOH and MnOOH are the principal phases controlling Hg mobility, followed by clay minerals (Schuster, 1991) in the sequence of illite > montmorillonite > kaolinite. Organic Hg species show however greater affinity for montmorillonite, less allopane, and finally kaolinite (Gabriel and Williamson, 2004).

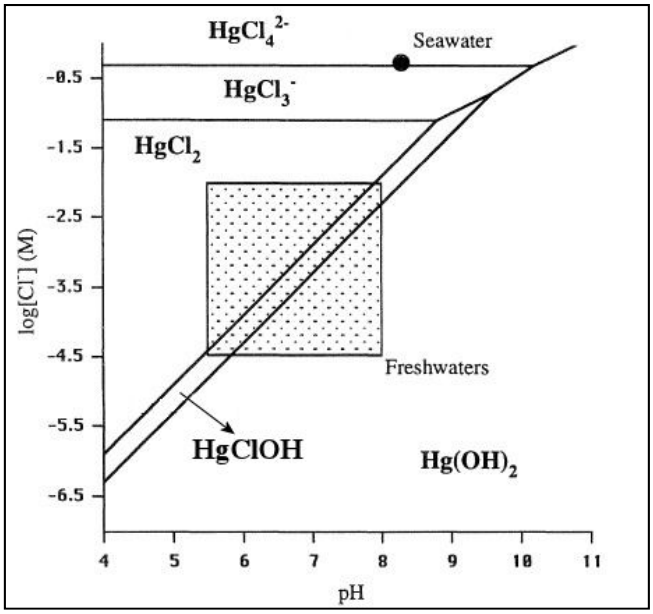

Fig. 1.4. *Speciation of Hg as a function of pH and chloride concentrations. Ionic strength corrections are neglected. Seawater has a pH of 8.3 and a chloride concentration of 0.55 M. The pH-Cl− fields for freshwater and seawater are even reported (modified from Morel et al., 1998).*

1.3.1 Mercury methylation and demethylation

The process of methyl-Hg formation (methylation) in sediment and water represents a key step of Hg cycle, because it increases the bioavailability and toxicity of Hg and enhances the exposure of humans to MMHg. Mercury *methylation* involves the transfer of a alkyl-anion group (CH_3^-) from an organic compound to inorganic Hg, while the opposite process, degrading MMHg to inorganic Hg, terms *demethylation*. Once released into the environment, all forms of inorganic Hg can be potentially converted into this compound (Gray, 2003) (Fig. 1.3). Particularly, MMHg is believed to be formed by ionic Hg and divalent compounds, although it possibly forms from metallic Hg (Ullrich et al., 2001).

Methylation occurs both abiotically and biotically or as a mixture of both processes (Ullrich et al, 2001). Abiotic methylation may occur in presence of suitable methyl-donor, as humic substances (Nagase et al., 1984); furthermore laboratory data have shown that Hg is photochemically methylated by the presence of acetate (Akagi et al., 1975). Notwithstanding

the importance of abiotic versus biotic methylation is still a matter of debate, it is widely accepted that methylation is mainly microbially mediated. Berman and Bartha (1986) report that in anoxic sediments MMHg from abiotic methylation is one order of magnitude less than that derived by biotic one. Methyl-Hg is synthesized by a wide variety of bacteria and fungi, ranging from anaerobes to aerobes (Hamdy and Noyes, 1975; Compeau and Bartha, 1985), but the most common methylating agents are the sulfate-reducing bacteria (SRB) (Gilmour et al., 1992; Weber, 1993; Schaefer et al., 2002; Benoit et al., 2003; Shao et al., 2012), and in a lesser extent iron-reducing bacteria (Kerin et al., 2006; Graham et al., 2012). Peaks of MMHg production in estuarine systems have been correlated with the increased activity of SRB (Compeau and Bartha, 1985; Meritt and Amirbahman, 2009).

Methylation occurs mainly in anaerobic conditions, therefore the main sites for methylation are wetlands, saturated soils and aquatic sediments (Benoit et al., 2003; Krabbenhoft et al., 2005). In lake sediments, the most productive zone for MMHg is below the oxic/anoxic interface, which can be only few millimeters thick (Krabbenhoft et al., 2005). Methyl-Hg production is influenced by the availability of Hg for methylation, the speciation of Hg, and the factors regulating the activity of the methylating bacteria (Fitzgerald and Lamborg, 2005). For instance, addition of low concentrations of sulfate stimulates MMHg production, as sulfates are essential for the SRB methabolism (Fitzgerald and Lamborg, 2005). However, the amount of sulfate should be not so high to cause accumulation of sulfide and limiting the availability of Hg for methylation (Gilmour and Henry, 1992). An important parameter for methylation is the bioavailability of Hg for bacteria, which depends by Hg speciation rather than the absolute content of Hg in the media. As microbial uptake of Hg occurs by diffusion of Hg species through the cellular membranes, the uptake of Hg neutral species is believed to be generally favoured (Morel et al., 1998; Ullrich et al., 2001). $HgCl_2$ and HgS^0 are then the most suitable species for methylation in oxygenated and anoxic environments, respectively (Benoit et al., 1999).

Similar to methylation, demethylation is mainly microbially mediated (Ullrich et al., 2001), and could occur by either oxidative and reductive pathways, and as a result of both detoxification mechanisms or metabolic processes (Meritt and Amirbahman, 2009). In reductive demethylation, the end product of the process is CH_4 and either Hg(II) or Hg(0), and demethylation is a detoxification mechanism operated by Hg-resistant bacteria by means of the mercury resistance (*mer-)* operon gene (Oremland et al., 1991; Marvin-DiPasquale et al., 2000; Schaefer et al., 2002). This process occurs both in aerobic and anaerobic sediments, generally in highly contaminated environments, and both in *gram*-positive and *gram*-negative

bacteria (Meritt and Amirbahman, 2009). In the complete reduction mechanism by *mer*-operons, *Mer* B firstly breaks the bondage of Hg(II)−CH_3, forming CH_4 and Hg(II), and then *Mer* A reduces Hg(II) to Hg(0) (Marvin-DiPasquale, et al., 2000; Meritt and Amirbahman, 2009). In anoxic environments, the reduction of Hg(II) to Hg(0) may be the result of respiratory processes of bacteria, without involving a *mer*-operon pathway (Krabbenhoft et al., 2005; Meritt and Amirbahman, 2009). Species of the genus *Geobacter* are able to reduce Hg(II) in presence of acetate and Fe(III), which act as electron donors and acceptors, respectively (Wiatrowski et al., 2006). In oxidative demethylation, CO_2 and Hg(II) are the dominant products of the process, which occurs in anaerobic and aerobic freshwater sediments (Ullrich et al., 2001; Meritt and Amirbahman, 2009) and is at least partially mediated by SRB, methanogenic bacteria and aerobes (Oremland et al., 1991). Photodemethylation, that is the only prominent way of abiotic MMHg degradation (Ullrich et al., 2001), is largely triggered by the UV light penetrating in the sediment column.

Once formed in the aquatic web, MMHg is effectively taken up by aquatic biota, and as a result of its slowly elimination by the organisms, it increases as the organism get older; even small amounts of MMHg in the environment can then result in great accumulation in fish, i.e. to *bioaccumulation* (Burgess, 2005). In aquatic web, MMHg binds to organic matter and, thanks to its ability to cross biological membranes, accumulates in phytoplankton and bacteria, which are in turn eaten by zooplankton and benthic invertebrates (Burgess, 2005). Phytoplankton and invertebrates are then consumed by small fish which are in turn eaten by large fish. At each step of the food wed, concentrations of MMHg is higher in the predator than in the prey, resulting in *biomagnification* (Ullrich et al., 2001) (Fig. 1.3). As a consequence, the concentrations of MMHg in fish can be 10^6-10^7 times those of waters where they live (Burgess, 2005). Furthermore, the percentages of MMHg on total Hg generally increase going up in the aquatic web, and in large predatory fish, muscle tissue contains more than 90% MMHg (Bloom et al., 1992; Downs et al., 1998), while in sediments MMHg rarely exceeds few % with respect of total Hg (Ullrich et al., 2001).

The most common pathway of Hg to humans is through diet, particularly by consumption of fish products (Gray, 2003). In humans, more than 94%-95% MMHg is adsorbed in the gastro-intestinal tract (US EPA, 2001), and thanks to its lipophilic affinity, it concentrates in the nervous system (US EPA, 1997). Methyl-Hg main health effect is neurotoxicity (WHO, 1990; Gupta et al., 2005), resulting in paresthesia, deafness, dysarthria, ataxia, coma and even death (Gupta et al., 2005). The vulnerability to methyl-Hg is especially high in developing fetus as MMHg can be transported across placenta and can accumulate in fetal brains (WHO, 1990).

Recent studies on this matter have demonstrated that an inverse correlation exists between the intelligence of children and the MMHg concentration in their cord blood (Trasande et al., 2005).

The toxicology consequence of MMHg exposure to humans were firstly recognized in the 1950s and 1970s in Japan and Iraq. In Minamata (Japan) local populations were exposed to extremely high levels of MMHg by consumption of contaminated fish, discharged to the sea by a local manufacturing site (Gupta et al., 2005). This was the first known case of mass poisoning by MMHg, which directly caused the death of more than one hundred people and affected tens of thousands by cerebral damages (Hylander and Goodsite, 2006). Following this tragedy the symptomatology associated with Hg poisoning is named as "Minamata disease". Similar to Japan, in Iraq, the population was exposed to MMHg through ingestion of contaminated food (grain seeds) treated with MMHg. 6530 cases of MMHg poisoning among people were reported, and of these cases 459 persons died (Gupta et al., 2005). Following these tragedies, the employ of MMHg compounds in agriculture was banned, and consumption advisories for Hg in fish were set in order to protect humans from indirectly exposure to MMHg. The present-day established limits are of 0.3 μg/g (w/w) for the U.S. Environmental Protection Agency (US EPA, 2001), while the World Health Organization (WHO, 1989) and the U.S. Food and Drug Amnistration (FDA, 1984) have suggested limits of 0.5 and 1 μg Hg /g, respectively.

1.4 Global mercury belts and their environmental impact

The natural enriched Hg areas concentrate along the three planetary metallogenic belts of Circum-Pacific, Mediterranean, and Central Asia (Fig. 1.5) (Baeyens et al., 2003), known as the *global mercury belts* (Fitzgerald and Lamborg, 2005). A peculiar characteristic of these Hg deposits is their localization in past or presently developing parts of the lithosphere, as in: i) intracontinental rifts (aulacogens) in ancient cratons of the Early and Middle Paleozoic, ii) intraplate riftogenesis in orogenic belts, and iii) active continental margins of Mesozoic and Cenozoic. These areas correspond to deep lithospheric faults originating in the mantle (Borisenko et al., 2005), suggesting that the development of the Hg ore-forming systems may be triggered by mantle magmatism phenomena, such as mantle plumes (Baeyens et al., 2003); a mantle origin for the ore deposits of China, Russia, Ukraine and Kyrgyzstan has been recently demonstrated by the He isotopic composition of the mineralizing fluids at these ores (Borisenko et al., 2005).

Historically, three-fourths of the Hg global production has come from the following five mining regions, and related Hg belts: Almadén (Spain), Idrjia (Slovenia), Mt. Amiata (Italy), California Coast Range (USA) and Huancavelica (Peru) (Gray, 2003; Rytuba, 2003). The site of Almadén in particular constitutes the largest Hg geochemical anomaly in the world, estimated to contain before mining 250,000 tons Hg, equal to one-third of Hg global resources (Hernandez et al., 1999; Higueras et al., 2006). The Mediterranean basin concentrates by itself approximately the 65% of Hg world resources (Ferrara et al., 1991). Despite their common location, Hg deposits in the Mediterranean are not co-genetic, and each of them should be considered as a small isolated Hg belt, formed in different times and geological settings (Rytuba, 2003).

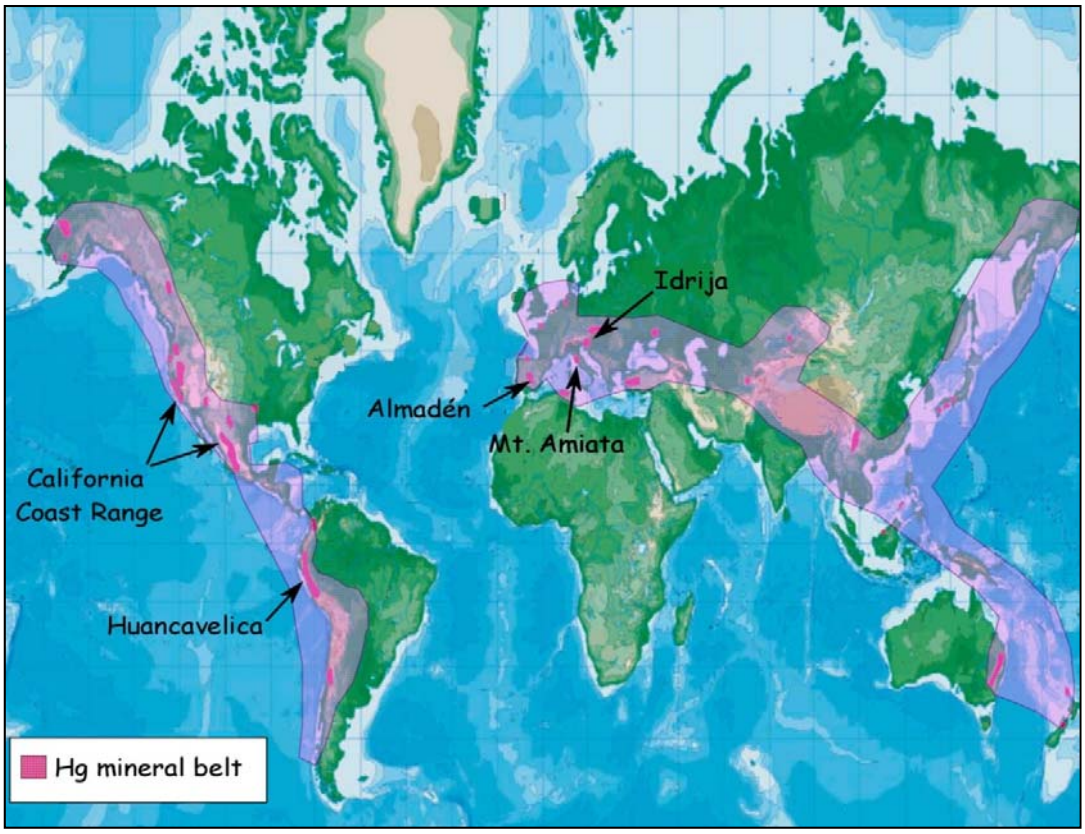

Fig. 1.5. *The distribution of Hg mineral belts on a global scale. The five most important mining regions for Hg production are highlighted (modified from Rutyba, 2003).*

Mercury deposits can be divided in three typologies, depending on their age and association with geologic formations: Almadén-type, silica carbonate-type, and hot-spring-type (Rytuba, 2003, 2005). The Almadén-type deposits are localized in Silurian quartzite, associated with mafic submarine vent complexes, as submarine calderas, dikes and sills and oval craters (Rytuba, 2003), and are the largest Hg deposits, containing from 10 to 100 million metric tons

of ore mineral. The grade of these deposits is extremely rich, ranging between 2.0 and 20 weight % Hg (Rytuba, 2005). As easily guessed by the name, these deposits are typical of Almadén and have been rarely documented outside Spain. The silica carbonate−type Hg deposit is spatially associated to serpentinite, and has been altered to mineral assemblage of silica and carbonate minerals (Rytuba, 2002, 2005). These deposits are generally small or medium in size, with an ore mineral reservoir of 0.1−10 million metric tons, and the ore containing 0.2−0.8 weight % Hg (Rytuba, 2002). Main representations of these deposits are located in the California Coast Range mercury belt with the famous New Idria and New Almadén mines. Hot-spring Hg deposits are closely associated to volcanic centers, and eventually meteoric-dominated geothermal systems (Rytuba, 2003). Many of these deposits are geologically young, and the common occurrence of Hg-rich thermal fluids leads to still active deposition of ore minerals. The Mt. Amiata Hg district can be considered as one of the main examples of this typology (Rytuba, 2005).

Cinnabar is the main ore mineral in all the deposits, with only few exceptions (Rytuba, 2002, 2003). Elemental Hg can be found in association with cinnabar in Almadén- and silica carbonate-type of deposits, while Hg chlorides, sulphates and oxide minerals locate in the upper parts of hot-spring deposits, mainly as a product of supergene alteration of cinnabar (Rytuba, 2005). Mercury transport in hydrothermal solutions forming Hg deposits occurs mainly by sulfide complexes, in particular by $Hg(HS)_2$ and $HgS(HS)^-$ (Barnes and Seward, 1997), which lead to extensive deposition of cinnabar and metacinnabar. Hydrated forms of Hg^0 are however believed to be potential transporting species when native Hg is found as primary mineral (Barnes and Seward, 1997). In addition to the mobility of Hg as an aqueous ion, Hg can be transported as dry vapor or as a component in steam. Mobilization of Hg as a dry vapour is reported among the volcanic centers, as in the case of Mt. Amiata, Italy (Schröcke, 1972), where Hg-rich vapour precipitates cinnabar thanks to the presence of bacterial H_2S (Morteani et al., 2011).

In Hg mine sites all over the world, the recovery of Hg from cinnabar is accomplished by heating the ore at 650-700 °C (roasting process). Hg^0 is then obtained from the dissociation of cinnabar by the following reaction:

$$\mathbf{HgS_{(s)} + O_{2(g)} = Hg^0_{(g)} + SO_{2\,(g)}}$$

Mercury vapour is then recovered as liquid Hg by cooling the vapour. Beside Hg, a mix of liquid Hg and not fully combusted materials (condenser soot) is recovered by the condensers

and further processed to extract pure liquid Hg by addition of lime. At the end of the process, exhausted ore rocks are termed as waste calcines.

The release of Hg from mine impacted areas represents a serious risk for biota and humans, which may be exposed to high levels of Hg for long time after the operations have ceased (Gray et al., 2000; Hines et al., 2000). Abandoned mines are of concern especially for the high concentrations of Hg in discarded materials at these sites (Bailey et al., 2002; Gray et al., 2003, 2006; Navarro, 2008). The concentration of Hg in calcines generally ranges from 10 to 800 μg/g (Rytuba, 2003), although up to several weight percents Hg have been reported (Gray et al., 2004). Moreover, the speciation of Hg in waste calcines is generally made by secondary-formed soluble Hg compounds, which represent an importance source of easily leachable Hg (Biester et al., 2000; Kim et al., 2004; Stetson et al., 2009; Gray et al., 2010). Acid mine drainage (AMD) and physical remobilization of waste piles, tailings, and contaminated riverbanks provide indeed large amounts of Hg to local ecosystems (Navarro, 2008). Volatilization of Hg^0 during ore roasting also accounts for remarkable dispersion of elemental Hg (Rytuba, 2005). It has been estimated for example that 37,033 tons of Hg were emitted into the environment during the operation period of the Idrija mine (Gosar and Teršic, 2012). Due to its pervasive character, Hg is widely documented in both abiotic and biotic compartments surrounding Hg mines, resulting in decades of persistent contamination after the end of mining (Gray et al., 2000; Gosar and Teršic, 2012). In streams directly affected by mining runoff, Hg can reach hundreds or thousands μg/g in sediments and waters (Gosar et al., 1997; Gray et al., 2000, 2004, 2006; Qiu et al., 2006; 2012), and then is readily taken up by biota living in those ecosystems (Hines et al., 2000). Dramatically high Hg levels have been reported in macroinvertebrates and bacteria (Hines et al., 2000), aquatic snails (Gray et al., 2012), and fish (Horvat et al., 2003; Qiu et al., 2009), up to mammalians that feed with contaminated food, and which in turn are eaten by humans (Gnamuš et al., 2000). The transport of Hg mainly occurs by rivers, both in dissolved and particulate forms, resulting in Hg contamination up to coastal areas and marine ecosystems hundreds of kms away from the primary source. Covelli et al. (2008) estimate for instance that 900 tons/Hg accumulated in the Gulf of Trieste, as a result of the 500-years long runoff by Isonzo River (Idrija mine, Slovenia).

Human exposure to Hg may result from direct and indirect pathways (Rytuba, 2005). Direct pathways are mainly represented by inhalation of Hg vapours, which can be elevated as a result of volatilization from contaminated calcines and soils (Qiu et al., 2006; Higueras et al., 2006; Martínez-Coronado et al., 2011), and by accidental ingestion of Hg-rich dusts (Rytuba,

2003). Indirect pathways relate however to the ingestion of Hg by consumption of contaminated food, such as edible plants, rice and fish (Qiu et al., 2012), and are more dangerous as they generally involve methyl-Hg exposure. Due to the strong consumption of local contaminated fish, high Hg concentrations have been for instance reported in people living near the Palawan mine (Philippines), where 21 residents have been treated for Minamata disease (Gray et al., 2003).

1.5 The Mt. Amiata Hg district

In Southern Tuscany (Italy), a wide Hg metallogenic province clusters around the volcano-geothermal area of Mt. Amiata (Fig. 1.6), as a result of the post-collisional events of Northern Apennines orogenesis. Mercury deposits are found in strict association to Sb(Au) mineralization, testifying their origin from the same metallogenic process (Morteani et al., 2011). However, Hg deposits are physically separated from Sb(Au) ones (Fig. 1.6) (Klemm and Neumann, 1984;), which is common to most Hg mineralization worldwide (Morteani et al., 2011).

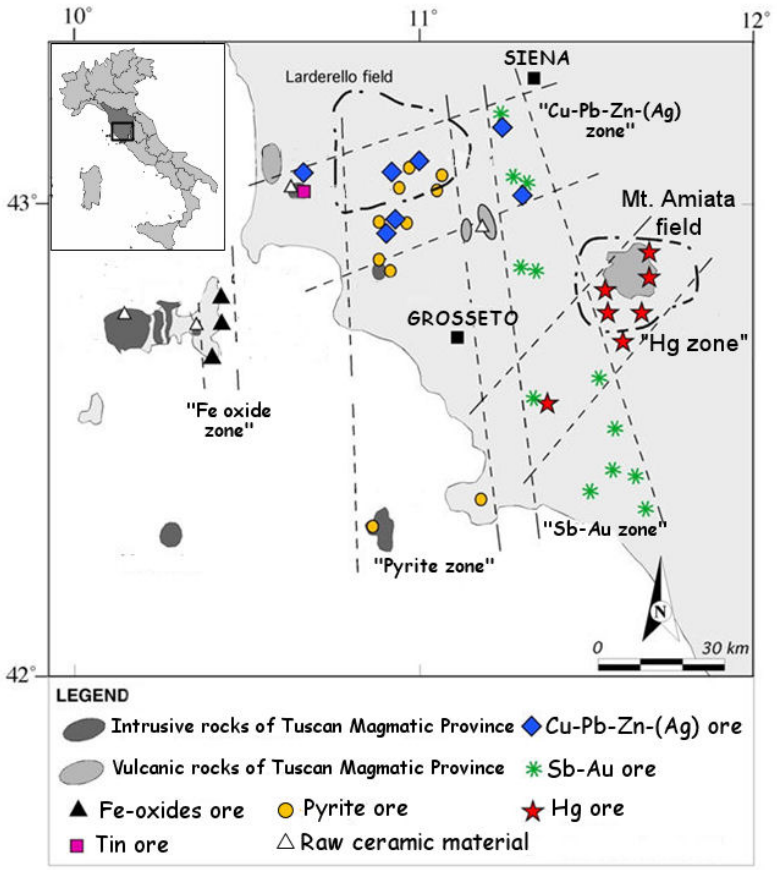

Fig. 1.6. *The metallogenic province of Southern Tuscany (Italy) (modified from Tanelli and Lattanzi, 1986).*

The Hg-Sb(Au) mineralization is a world-class example of epithermal deposits, which metallogenesis articulated as a two-step process (Brogi et al., 2011). In Southern Tuscany, following Baroni et al. (1994) and Brogi et al. (2011), during a first phase Hg and Sb(Au) were mobilized to the shallower levels of the crust, as a result of their leaching from the Paleozoic phyllite of the Metamorphic Complex of Tuscany (Elter and Pandeli, 1991) occurred during the Late Oligocene−Early Miocene greenshist metamorphism. These authors then suggest that during the Pliocene−Pleistocene, these elements were re-mobilized by the convective hydrothermal circulation associated to the Mt. Amiata geothermal anomaly, forming the modern ores (Tanelli, 1983; Brogi et al., 2011; Morteani et al., 2011). Such geothermal anomaly, which is actively exploited for energy production (Bertini et al., 2005), is related to the emplacement of a magmatic body at 6-7 km depth beneath the Mt. Amiata (Gianelli et al., 1988) during the Early Pliocene (Pasquarè et al., 1983; Marinelli et al., 1993). Recent studies suggest that Hg and minor Sb(Au) mobilization and deposition should be considered as still going on process in the Mt. Amiata region (Morteani et al., 2011), and the mineralization appears to be controlled by deep deformation structures which gave rise to the Mt. Amiata volcanic eruptions in the Pleistocene (Brogi and Fabbrini, 2009; Brogi et al., 2010). Fractionation of Hg and Sb(Au) to the gas and liquid phase respectively, explains the physical separation of these elements in the Tuscan deposits (Moreteani et al., 2011) and worldwide (Klemm and Neumann, 1984).

Mining exploitation for Hg started with the Etruscans (8^{th}-1^{th} centuries BC), it was interrupted during the Romans (Strappa et al., 1977), and started again in 1849, when the first Hg was produced at the Siele mine. In the past millennium, production of Hg from Mt. Amiata develops at a larger scale, rapidly becoming one of the most important in the world. In 1948, 42 mines and 4 smelting plants were operating in the area (Bellander et al., 1998; Ferrara et al., 1998b). In the 1970s−1980s, due to the low cost of Hg and its substitution in many technological and industrial applications, the Mt. Amiata mines gradually closed. The mining center of Abbadia San Salvatore (1897-1982) was one of the largest in Europe and one of the most productive. In 1982, the mine definitely ceased its activity with a total production of more than 50,000 tons Hg (Bacci, 1998). The Mt. Amiata ore had a Hg content of 0.6-2% and was extracted in closed pits up to 400 meters deep (Bellander et al., 1998). The primary assemblage in the Mt. Amiata mines is essentially cinnabar, and the rare observations of free Hg have been interpreted as a consequence of local phenomena of sublimation (Savoia, 1919). Non-economic minerals found in association with cinnabar are marcasite, pyrite, stibnite, and rare arsenical sulfides (realgar and orpiment) (Falini, 1960; Zucchetti 1964), whereas typical

gangue mineral is calcite, and very rare celestite, gypsum, native sulphur and hydrocarbons (Klemm and Neumann, 1984; Morteani et al., 2011). Mercury mobilization and deposition is believed to have occurred mainly by uprising aqueous solutions, where Hg was complexated with H_2S, which is abundant in this area. H_2S-rich exhalations ("putizze"; Loppi et al., 1998) and high H_2S levels in CO_2-rich manifestations are indeed well documented around the Mt. Amiata volcano (Frondini et al., 2008, 2009; Tassi et al., 2009). H_2S is believed to originate by bacterial reduction and/or thermochemical reduction of gypsum in the Burano Evaporites and or anhydrite levels in the Tuscan Metamorphic Complex (Elter and Pandeli, 1991) (Morteani et al., 2011; Tassi et al., 2012). Besides aqueous transport, Hg was additionally deposited from dry vapour in Tuscan deposits (Barnes and Seward, 1997), as suggested by the still elevated Hg concentrations in present-day geothermal vapours (Falini, 1960).

Mercury mineralization occurs principally in Tuscan formations and Ligurian-Subligurian Units (Abbadia San Salvatore), and secondarily in Pliocenic sandstones, and in the Quaternay volcanites of Mt. Amiata (Abbadia San Salvatore) (Tanelli, 1983). Mercury mineralization presents as veinlets of cinnabar and impregnations replacing the carbonatic matrix and cement of calcarenites, limestones and sandstones of the Ligurian (Subligurian) Unit (Dini, 2003), of carbonatic sandstones of Pietraforte and of Pliocene sands (Zucchetti, 1964; Klemm and Neumann, 1984). Additionally, botryoidal cinnabar aggregates named "fragole" ("strawberries") are sometimes located in open fractures in sandstones (Dini, 2003). A common characteristic of all the ore bodies is their "impounding structure" (Zucchetti, 1964), as they generally develop beneath an impermeable formation, as shales, that caused the deposition of the mineral from the ascending solutions. For instance, in Fig. 1.7 the section of the mineralized body in Abbadia San Salvatore is reported, where the ore body develops in marls and marly limestones ("Sopranummulitico") and massive biocalcarenites ("Nummulitico" or "Bancone") (Subligurian Units), and the roof of the deposits are represented by "Argille Verdi" (Argille = Shales) of the Cretaceous Flysh (Ligurid Units), which acted as a seal for the ascending mineralizing fluids (Arisi Rota, 1971; Klemm and Neumann, 1984).

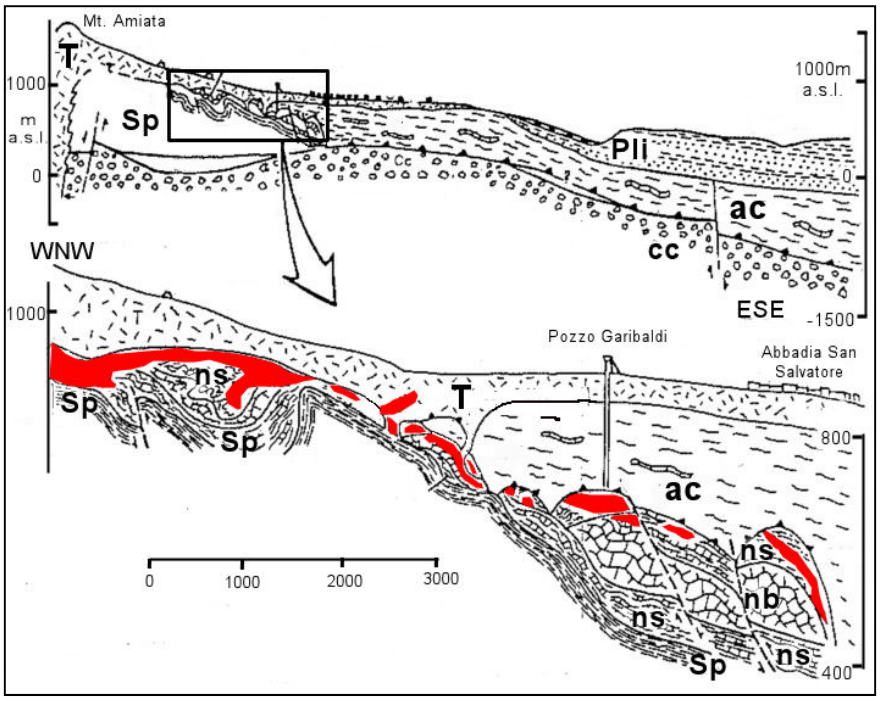

Fig. 1.7. *Schematic representation of the Hg deposit of Abbadia San Salvatore collocated E of Mt. Amiata. The ore bodies are located in the following formations: "Sopranummulitico" marls and marly limestone, "Nummulitico Bancone" massive calcarenite, and in altered volcanic rocks. Abbreviations: Cc, Calcare Cavernoso (Norian); Sp, Scisti Policromi (Cretaceous); ns, "Sottonummultico" (Paleocene) and "Sopranummulitico" (Eocene); nb, "Bancone Nummulitico" (Eocene); ac, Cretaceous Flysh (Ligurian Units); Pli, Pliocene sandstones; T, Quaternary volcanic rocks; Hg ore bodies are in red (modified from Klemm and Neumann, 1984).*

After 30 years from the end of mining, remediation strategies have been carried on only in few mining sites at Mt. Amiata, despite exhausted roasted cinnabar are still disposed near to the smelting plants, without providing for their proper disposal. Residues of calcines and metallic Hg are widely observable in soils, particularly in the proximity of the roasting plants and condensers, where Hg droplets are visible at naked eyes.

The first information about Hg distribution in the Mt. Amiata region is dated back to 1966, when a wide Hg contamination of stream sediments and waters was reported, as a result of the still going on mining activity (Dall'Aglio, 1966; Dall'Aglio et al., 1966). After the closure of the last mine in 1982, the first comprehensive dataset on Hg diffusion in different compartments of Mt. Amiata was compiled, and showed high levels of Hg in air, soil, sediments, water and biotic compartment of the Mt. Amiata ecosystem (Ferrara et al., 1991). Furthermore, Hg was found to have been taken up in great amount by plants (Bacci et al., 1994), fungi (Bargagli and Baldi, 1984), and aquatic organisms of local rivers (Bacci et al., 1978), increasing its bioavailability in this area. Moreover, the elevated Hg levels in the

coastal area of the Thyrennian Sea and in associated benthic organisms (Baldi and D'Amato, 1986; Barghigiani and Ristori, 1995; Barghigiani et al., 1996) were at least partly attributed to the intensive and long-lasting mining in the Mt. Amiata.

Most of the studies made up to now in this region were focused on Hg contamination in the atmosphere, that was determined both by monitoring the Hg contents in lichens and green plants (Bargagli et al., 1986; 1987) both by direct measurement of Hg in atmosphere (Breder and Flucht, 1984; Edner et al., 1993; Ferrara et al., 1998b). The last study on this matter, conducted by the use of the LIDAR remote sensing technique, reported that a still high flux of Hg^0 was emitted from the mining area of Abbadia San Salvatore (66 g h^{-1}; Ferrara et al., 1998b) after 15 years from the closure of mine, and anomalously high concentrations of 10-20 ng m^{-3} Hg were established for this area (Ferrara et al., 1998b). Many of the more recent studies were moreover devoted to investigate the importance of Hg emissions from geothermal plants located in the Mt. Amiata, which represent an additional source of Hg to the atmospheric environment (Bargagli et al., 1997; Loppi, 1998; Bacci et al., 2000). Discriminating geothermal from mining contamination represents an important aspect of environmental research, as the contributions of these sources may sometimes overlap.

Despite the importance of this mining district, studies on Hg distribution in geologic matrices are scant and relatively old. In particular, many of these works dated back to the last years of the mining activity, and need therefore to be updated, in order to delineate the present-day contamination levels, and to guide any remediation strategy in this area. Moreover, previous studies never measured Hg species such as methyl-Hg, which is however fundamental to evaluate the ecosystem effects of mining activity, and to establish its possible bioavailability for biota and humans.

1.6 Aims of the work

In this work, the distribution and the effects of Hg and related heavy metals in the Mt. Amiata region are investigated. As introduced in the previous section, the Mt. Amiata has been one the worldwide principal mining site for Hg, hence representing a suitable area in order to study Hg geochemistry and its effects to the environment. Specifically, different aspects of Hg dispersion by the natural drainage system of the Paglia River are taken into consideration. This river is the SE drainage basin of the Mt. Amiata district, collecting waters from different mines located at the head of its tributaries (Fig. 1.8), then causing the dispersion of Hg far away from the local mine sites. Moreover, as the Paglia River is a tributary of the Tiber River

(Fig. 1.8), the principal river course of Central Italy discharging to the Mediterranean Sea, the interest of this work is not limited to the local scale but may extend to the regional one.

In this thesis, the attention is particularly focused on the Abbadia San Salvatore Hg mine, which is located almost at the head of the Paglia River, known in the first tract as Pagliola Creek (Fig. 1.8). As a consequence of the intensive mining activity, high amounts of calcines are presently improperly disposed around the mining and urban areas of Abbadia. Running surface waters act then as important carriers of Hg, which is easily and widely transported to the Paglia River downstream ecosystem. As the remediation strategy for this mine site is planned to begin in a short time, this thesis may furnish useful comparison data for the future post-remediation monitoring, and could help to define updated remediation strategies for this mine.

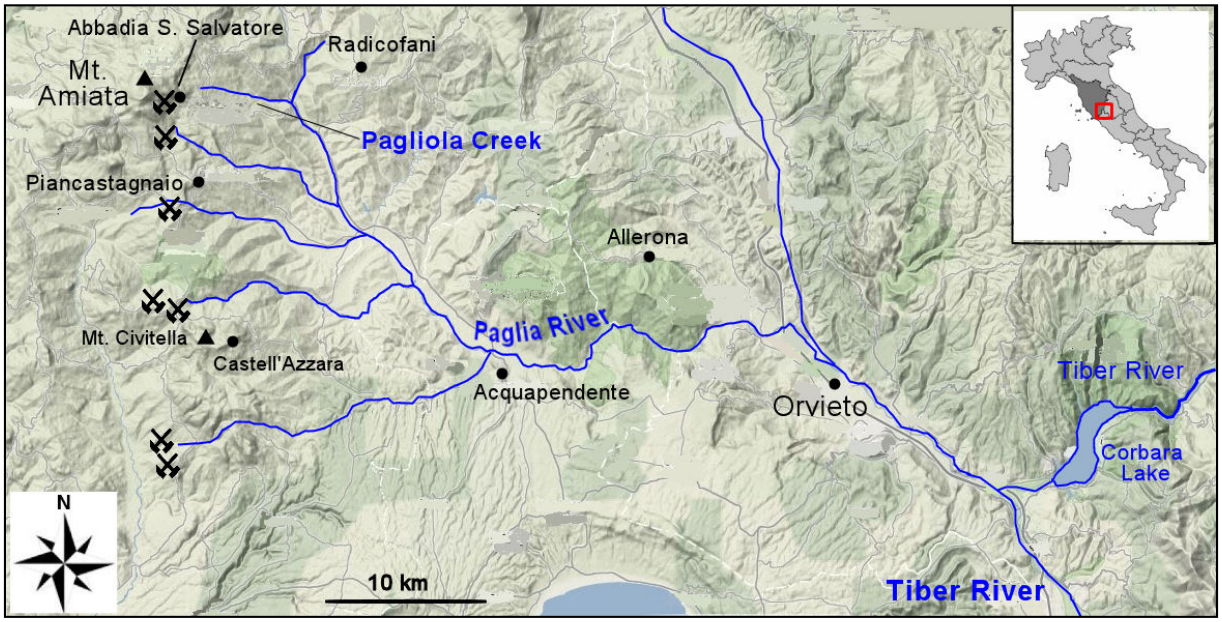

Fig. 1.8. *The Paglia River Basin in the Mt. Amiata district. The main Hg mines belonging to this basin are shown.*

The specific aspects and purposes of this thesis can be resumed in four parts:

- **Part I (Chapter 2)**, representing an extensive survey on Hg and MMHg distribution in different environmental matrices belonging to the Paglia River course carried out in collaboration with the U.S. Geological Survey (USGS); the main objectives of this section are then to characterize the principal source of Hg contamination, i.e. calcines and soils of the mining area, and to evaluate the extent of Hg runoff in the environment on the targets of contamination, water and sediments of the Paglia River. Levels of

MMHg are moreover measured in fish of the Paglia River to highlight Hg bioaccumulation in local biota;

- **Part II (Chapter 3)**, where the annual mass load of Hg transported by the Paglia River waters is quantified in collaboration with the Regione Toscana. The principal aims of this work are then to localize punctual and diffuse source of contamination in the basin and to evaluate the impact of Hg discharged to the Tiber River and possibly to the Mediterrenean Sea;
- **Part III (Chapter 4)**, where the speciation of Hg in different geological materials is determined by means of different techniques, ranging from Chemical Sequential Extractions to X-Ray Absorption Spectroscopy; as the solubility of Hg compounds is extremely variable, ranging from practically insoluble compounds (Hg sulphides) to water-soluble species (Hg sulphates and chlorides), this part of the work is fundamental to understand the potential bioavailability of Hg in the Paglia River ecosystem;
- **Part IV (Chapter 5)**, in order to determine the Hg regional background in the area of Mt. Amiata, which is a crucial step to discriminate between natural and anthropogenic contaminated geological matrices in this perturbed environment.

References

AKAGI H., FUJITA Y., TAKABATAKE E. (1975). Photochemical methylation of inorganic mercury in the presence of mercuric sulfide. *Chem. Lett.*, **2**: 171−176.

ALLARD B. AND ARSENIE I. (1991). Abiotic reduction of mercury by humic substances in aquatic systems — an important process for the mercury cycle. *Water Air Soil Pollut.,* **56**: 457−464.

ARISI ROTA F., BRONDI A., DESSAU G., FRANZINI M., MONTE AMIATA S.P.A. (1971), STABILIMENTO MINERARIO DEL SIELE, STEA B., VIGHI L. (1971). I Giacimenti minerari. In: La Toscana meridionale. *Rend. Soc. Ital. Mineral. Petrol.*, **27**, Spec. Is.: 357–544.

BACCI E., GAGGI C., DUCCINI M., BARGAGLI R., RENZONI A. (1994). Mapping mercury vapours in an abandoned cinnabar mining area by azalea (*Azalea indica*) leaf trapping. *Chemosphere*, **29**: 641−656.

BACCI E., GAGGI C., LANZILLOTTI E., FERROZZI S. (1998). Studio per l'individuazione dei residui di mercurio in forme mobili e della presenza di altri elementi in tracce di interesse ai fini della predisposizione di un progetto di bonifica dell'area di pertinenza della ex miniera di mercurio di Abbadia San Salvatore (SI). ENI SpA − Divisione AGIP, Mining Italiana SpA. Roma, 17 pp.

BACCI E., GAGGI C., LANZILLOTTI E., FERROZZI S., VALLI L. (2000). Geothermal power plants at Mt. Amiata (Tuscany ± Italy): mercury and hydrogen sulphide deposition revealed by vegetation. *Chemosphere*, **40**: 907−911.

BACCI E., LEONZIO C., RENZONI A. (1978). Mercury Decontamination in a River of Mount Amiata. *Bull. Environ. Contam. Toxicol.*, **20**: 577−581.

BAEYENS W., DEHANDSCHUTTER B., LEERMAKERS M., BOBROV V.A., HUS R., BAEYENS-VOLANT D. (2003). Natural mercury levels in geological enriched and Geological active areas: case study of Katun River and Lake Teletskoye, Altai (Siberia). *Water Air Soil Pollut.,* **142**: 375–393.

BAGNATO E., ALLARD P., PARELLO F., AIUPPA A., CALABRESE S. , HAMMOUYA G. (2009). Mercury gas emissions from La Soufrière Volcano, Guadeloupe Island (Lesser Antilles). *Chem. Geol.*, **266**: 267−273.

BALDI F. AND D'AMATO M.L. (1986). Mercury pollution in marine sediment cores near cinnabar deposits and chlor-alkali plant. *Sci. Total Environ.*, **57**: 111−120.

BANIC C., BLANCHARD P., DASTOOR A., HUNG H., STEFFEN A., TORDON R., POISSANT L., WIENS B. (2005). Geogenic and mining sources of mercury in the environment. In: Parsons M.B. and Percival J.B. (Eds.), Mercury: sources, cycles and effects. Mineralogical Association of Canada, Short Course Series, Vol. 34. Halifax, Nova Scotia, pp. 157−177.

BAILEY E.A., GRAY J.E., THEODORAKOS P.M. (2002). Mercury in vegetation and soils at abandoned mercury mines in Southwestern Alaska, USA. *Geochem. Explor. Environ. Anal.*, **2**: 275−285.

BARGAGLI R. AND BALDI F. (1984). Mercury and methyl mercury in higher fungi and their relation with the substrata in a cinnabar mining area. *Chemosphere*, **13**: 1059−1071.

BARGAGLI R., BARGHIGIANI C., MASERTI B.E. (1986). Mercury in vegetation of the Mt. Amiata area (Italy). *Chemosphere*, **15**: 1035−1042.

BARGAGLI R., CATENI D., NELLI L., OLMASTRONI S., ZAGARESE B. (1997). Environmental Impact of Trace Element Emissions from Geothermal Power Plants. Arch. *Environ. Contam. Toxicol.*, **33**: 172–181.

BARGAGLI R., IOSCO F.P., BARGHIGIANI C. (1987). Assessment of mercury dispersal in an abandoned mining area by soil and lichen analysis. *Water Air Soil Pollut., **36***: 219−225.

BARGHIGIANI C. AND RISTORI T. (1995). Preliminary results on the role of rivers in total Hg concentrations in marine sediments and benthic organisms of a coastal area of Italy. *Water Air Soil Pollut.*, **80**: 1017−2020.

BARGHIGIANI C., RISTORI T., LOPEZ ARENAS J. (1996). Mercury in marine sediment from a contaminated area of the northern Tyrrhenian Sea: < 20 pm grain-size fraction and total sample analysis. *Sci. Total Environ., **192***: 163−173**.**

BARNES H.L. AND SEWARD T.M. (1997). Geothermal Systems and Mercury Deposits. In: Barnes H.L. (Ed.), Geochemistry of Hydrothermal Ore Deposits, Chap. 14. John Wiley & Sons Inc., New York, 3th Edition, pp. 699-736.

BARONI F., PROTANO G., RICCOBONO F. (1994). Mercury content in the rocks of Tuscany. A geochemical contribution to geology of Hg-ores. *Atti Accad. Fisiocritici Siena serie XV*, **XIII**: 59−66.

BELLANDER T., MERLER E., CECCARELLI F., BOFFETTA P. (1998). Historical Exposure to Inorganic Mercury at the smelter works of Abbadia San Salvatore, Italy. 81−90. *Ann. Occup. Hyd.*, **42**: 81−90.

BENOIT J.M., GILMOUR C.C., MASON R.P., HEYES A. (1999). Sulfide controls on mercury speciation and bioavailability to methylating bacteria in sediment pore waters. *Environ. Sci. Technol.,* **33**: 951−957.

BENOIT J.M., GILMOUR C.C., HEYES A., MASON R.P., MILLER C.L. (2003). Geochemical and Biological Controls over Methylmercury Production and Degradation in Aquatic Ecosystems. In: Chai Y. and Braids O.C. (Eds.), Biogeochemistry of Environmentally Important Trace Elements. *ACS Symposium Series* 835. American Chemical Society, Washington DC, pp. 262–297.

BERMAN M. AND BARTHA R.(1986). Levels of chemical versus biological methylation of mercury in sediments *Bull. Environ. Contam. Toxicol*., **36**: 401−404.

BERTINI G., CAPPETTI G., FIORDALISI A. (2005). Characteristics of geothermal fields in Italy. *Giorn. Geol. App.*, **1**: 247–254

BIESTER H. AND SCHOLZ C. (1997). Determination of mercury binding forms in contaminated soils: mercury pyrolysis versus sequential extractions. *Environ. Sci. Technol.*, **31**: 233–239.

BIESTER H., GOSAR M., COVELLI S. (2000). Mercury Speciation in Sediments Affected by Dumped Mining Residues in the Drainage Area of the Idrija Mercury Mine, Slovenia. *Environ. Sci. Technol.*, **34**: 3330−3336.

BLOOM N.S. (1992). On the chemical form of mercury in edible fish and marine invertebrate tissue. *Can. J. Fish. Aquat. Sci.,* **49**: 1010−1017.

BORISENKO A.S., OBOLENSKIY A.A., NAUMOV E.A. (2005). Global tectonic settings and deep mantle control on Hg and Au-Hg deposits. In: Mao J. and Bierlein F.P. (Eds.), Mineral Deposit Research: Meeting the Global Challenge, Chap. 1. Springer-Verlag Berlin Heidelberg, pp. 3−6.

BREDER R. AND FLUCHT R. (1984). Mercury levels in the atmosphere of various regions and locations in Italy. *Sci. Total Environ.*, **40**: 231−244.

BROGI A. AND FABBRINI L. (2009). Extensional and strike-slip tectonics across the Monte Amiata–Monte Cetona transect (Northern Apennines, Italy) and seismotectonic implications. *Tectonophysics*, **476**: 195–209.

BROGI A., FABBRINI L., LIOTTA D. (2011). Sb–Hg ore deposit distribution controlled by brittle structures: The case of the Selvena mining district (Monte Amiata, Tuscany, Italy). *Ore Geol. Rev.*, **41**: 35–48.

BROGI A., LIOTTA D., MECCHERI M., FABBRINI L.(2010). Transtensional shear zones controlling volcanic eruptions: the Middle Pleistocene Monte Amiata volcano (inner Northern Apennines, Italy). *Terra Nova*, **22**: 137–146.

BURGESS N.M. (2005). Mercury in biota and its effects. In: Parsons M.B. and Percival J.B. (Eds.), Mercury: sources, cycles and effects. Mineralogical Association of Canada, Short Course Series, Vol. 34. Halifax, Nova Scotia, pp. 235−258.

CINNIRELLA S. AND PIRRONE N. (2006). Spatial and temporal distributions of mercury emissions from forest fires in Mediterranean region and Russian federation. *Atmos. Environ.*, **40**: 7346–7361.

COMPEAU G.C. AND BARTHA R. (1985). Sulfate-Reducing Bacteria: Principal Methylators of Mercury in Anoxic Estuarine Sediment. *Appl. Environ. Microbiol.*, **50**: 498-502.

COQUERY M., COSSA D., SANJUAN J. (1997). Speciation and sorption of mercury in two macrotidal estuaries. *Mar. Chem.,* **58**: 213−227.

COVELLI S., FAGANELI J., DE VITTOR C., PREDONZANI S., ACQUAVITA A., HORVAT M. (2008). Benthic fluxes of mercury species in a lagoon environment (Grado Lagoon, Northern Adriatic Sea, Italy. *Appl. Geochem.*, **23**: 529–546.

DALL'AGLIO M. (1966). Distribuzione del mercurio nelle acque superficiali. *Atti Soc. Tosc. Sc. Nat. A*, **36**: 577−595.

DALL'AGLIO M., DA ROIT R., ORLANDI C., TONANI F. (1966). Prospezione geochimica del mercurio. Distribuzione del mercurio nelle alluvioni della Toscana. *L'Industria Mineraria*, Serie II, XVII, **9**: 391−398.

DAVIS A., BLOOM N.S., QUE HEE S.S. (1997). The Environmental Geochemistry and Bioaccessibility of Mercury in Soils and Sediments: A Review. *Risk Anal., **17**: 557-569.*

DINI A. (2003). Ore deposits, industrial minerals and geothermal resources. In: Poli G., Perugini D., Rocchi S., Dini A. (Eds.). Miocene to Recent Plutonism and Volcanism in the Tuscan Magmatic Province. *Per. Mineral.*, Spec. Is., **72**: 41−52.

DONOHOUE D.L., BAUER D., COSSAIRT B., HYNES A.J. (2006). Temperature and pressure dependent rate coefficients for the reaction of Hg with Br and the reaction of Br with Br: a pulsed laser photolysis-pulsed laser induced fluorescence study. *J. Phys. Chem. A,* **110**: 6623–6632.

DOWNS S.G., MACLEOD C.L., LESTER J.N. (1998). Mercury in precipitation and its relation to bioaccumulation in fish: a literature review. *Water Air Soil Pollut.,* **108**: 149-187.

DRYSSEN D. AND WEDBORG M. (1991). The sulfur–mercury (II)system in natural waters. *Water Air Soil Pollut.,* **56**: 507–519.

EDNER H. RAGNARSON P., SVANBERG S., WALLINDER E., FERRARA R., MASERTI B.E., BARGAGLI R. (1993). Atmospheric mercury mapping in a cinnabar mining area. *Sci. Total Environ.*, **133**: 1−15.

EISLER R. (1987). Mercury hazards to fish, wildlife, and invertebrates: A synoptic review. U.S. Fish and Wildlife Service, Biological Report 85 (1.10), 90 pp.

ELTER F.M. AND PANDELI E. (1991). Structural features of the metamorphic Paleozoic–Triassic sequences in deep geothermal drillings of the Mt Amiata area (SE Tuscany Italy). *Boll. Soc. Geol. It.*, **110**: 511–522.

EU − EUROPEAN UNION (2008). Regulation (EC) No 1102/2008 of the European Parliament and of the Council of 22 October 2008. Official Journal of the European Union, L 304/75.

EU − EUROPEAN UNION (2005). Community strategy concerning mercury. Brussels: Commission of the European Communities.

FALINI F. (1960). Notizie preliminari di una campagna di indagini e ricerche per minerali di mercurio nella regione del M. Amiata (province di Siena e Grosseto). *Per. Mineral.*, **XXIX**: 19−45.

FDA (1984). Mercury In Fish Cause for Concern? U.S. Food and Drug Administration.

FERRARA R., MASERTI B.E., BREDER R. (1991). Mercury in abiotic and biotic compartments of an area affected by a geochemical anomaly (Mt. Amiata, Italy). *Water Air Soil Pollut.,* **56**: 219-233.

FERRARA R., MASERTI B.E., ANDERSSON M., EDNER H., RAGNARSON P., SVANBERG S., HERNANDEZ A. (1998A). Atmospheric mercury concentrations and fluxes in the Almadén district (Spain). *Atm. Environ.*, **32**: 3897−3904.

FERRARA R., MAZZOLAI B., EDNER H., SVANBERG S., WALLINDER E. (1998B). Atmospheric mercury sources in the Mt. Amiata area, Italy. *Sci. Total Environ.*, **213**: 13−23.

FISHER J. A., JACOB D. J., SOERENSEN A. L., AMOS H. M., STEFFEN A., SUNDERLAND E. M. (2012). Riverine source of Arctic Ocean mercury inferred from atmospheric observations. *Nature Geoscience*, **5**: 499−504.

FITZGERALD W.F. AND GILL G.A (1979). Sub-Nanogram Determination of Mercury by Two-Stage Gold Amalgamation and Gas Phase Detection Applied to Atmospheric Analysis. *Anal. Chem.*, **15**: 1714−1720.

FITZGERALD W. AND LAMBORG C. (2005). Geochemistry of mercury in the environment. In: Holland, H., Turekian, K. (Eds.), Environmental Geochemistry, Treatise on Geochemistry, Vol. 9. Elsevier, pp. 107–148.

FRONDINI F., CALIRO S., CARDELLINI C., CHIODINI G., MORGANTINI N. (2009). Carbon dioxide degassing and thermal energy release in the Monte Amiata volcanic-geothermal area (Italy). *Appl. Geochem.*, **24**: 860−875.

FRONDINI F., CALIRO S., CARDELLINI C., CHIODINI G., MORGANTINI N., PARELLO F. (2008).Carbon dioxide degassing from Tuscany and Northern Latium (Italy). *Global Planet. Change*, **61**: 89−102.

GABRIEL M.C. AND WILLIAMSON D.G. (2004). Principal biogeochemical factors affecting the speciation and transport of mercury through the terrestrial environment. *Environ. Geochem. Health,* **26**: 421–434.

GÅRDFELDT K., SOMMAR J., FERRARA R., CECCARINI C., LANZILLOTTA E., MUNTHE J., WÄNGBERG I., LINDQVIST O., PIRRONE N., SPROVIERI F., PESENTI E., STRÖMBERG D. (2003). Evasion of mercury from coastal and open waters of the Atlantic Ocean and the Mediterranean Sea. *Atmos. Environ.*, **37**, suppl. 1: S73– S84.

GIANELLI G., PUXEDDU M., BATINI F., BERTINI G., DINI I., PANDELI E., NICOLICH R. (1988). Geological model of a young volcano-plutonic system: the geothermal region of Monte Amiata (Tuscany, Italy). *Geothermics*, **17**: 719–734.

GILMOUR C.C., HENRY E.A., MITCHELL R. (1992). Sulfate stimulation of mercury methylation in freshwater sediments. *Environ. Sci. Technol.,* **26**: 2281−2287.

GNAMUŠ A., BYRNE A., HORVAT M. (2000). Mercury in the Soil-Plant-Deer-Predator Food Chain of a Temperate Forest in Slovenia. *Environ. Sci. Technol.*, **34**: 3337−3345.

GOSAR M., PIRC S., BIDOVEC S. (1997). Mercury in the Idrijca River sediments as a reflection of mining and smelting activities of the Idrija mercury mine. *J. Geochem. Explor.*, **58**: 125-131.

GOSAR M. AND TERŠIČ (2012). Environmental geochemistry studies in the area of Idrija mercury mine, Slovenia. *Environ. Geochem. Health*, **34**: 27−41.

GRAHAM A.M., AIKEN G.R., GILMOUR C.C. (2012). Dissolved Organic Matter Enhances Microbial Mercury Methylation Under Sulfidic Conditions. *Environ. Sci. Technol.*, **46**: 2715−2723.

GRAY J.E. (2003). Introduction. In: Gray J.E. (Ed.), Geologic Studies of Mercury by the U.S. Geological Survey. *U.S. Geological Survey Circular 1248*, U.S. Geological Survey, Reston Virginia, 7 pp.

GRAY J.E., GREAVES I.A., BUSTOS D.M., KRABBENHOFT D.P. (2003). Mercury and methylmercury contents in mine-waste calcine, water, and sediment collected from the Palawan Quicksilver Mine, Philippines. *Environ. Geol.*, **43**: 298−307.

GRAY J.E., HINES M.E., HIGUERAS P.L., ADATTO I., LASORSA B.K. (2004). Mercury speciation and microbial transformations in mine wastes, stream sediments, and surface waters at the Almaden Mining District, Spain. *Environ. Sci. Technol.*, **38**: 4285−4292.

GRAY J.E., HINES M.E., BIESTER H. (2006). Mercury methylation influenced by areas of past mercury mining in the Terlingua district, Southwest Texas, USA. *Appl. Geochem.*, **21**: 1940–1954.

GRAY J.E., HINES M.E., KRABBENHOFT D.P., THOMS B. (2012). Methylation of Hg downstream from the Bonanza Hg mine, Oregon. *Appl. Geochem.*, **27**: 106−114.

GRAY J.E., PLUMLEE G.S., MORMAN S.A., HIGUERAS P.L., CROCK J.G., LOWER H.A., WITTEN M.L. (2010). In Vitro Studies Evaluating Leaching of Mercury from Mine Waste Calcine Using Simulated Human Body Fluids. *Environ. Sci. Technol.*, **44**: 4782–4788.

GRAY J.E., THEODORAKOS P.M., BAILEY E.A., TURNER R.R. (2000). Distribution, speciation, and transport of mercury in stream−sediment, stream−water, and fish collected near abandoned mercury mines in southwestern Alaska, USA. *Sci. Total Environ.,* **260**: 21−33.

GUPTA S., BARLOW M., DONALDSON S. (2005). Mercury exposure and human health effects: a Canadian perspective. In: Parsons M.B. and Percival J.B. (Eds.), Mercury: sources, cycles and effects. Mineralogical Association of Canada, Short Course Series, Vol. 34. Halifax, Nova Scotia, pp. 259−286.

GUSTIN M.S., BIESTER H., KIM C.S. (2002). Investigation of the light enhanced emission of mercury from naturally enriched substrates. *Atmos. Environ.*, **36**: 3241– 3254.

HAMDY M.K. AND NOYES O.R. (1975). Formation of Methyl Mercury by Bacteria. *Appl. Microbiol.*, **30**: 424−432.

HERNÁNDEZ A., JÉBRAK M., HIGUERAS P., OYARZUN R., MORATA D., MUNHÁ J. (1999). The Almadén mercury mining district, Spain. *Miner. Deposita*, **34**: 539−548.

HESTERBERG D., CHOU J. W., HUTCHISON K. J., AND SAYERS D. J. (2001). Bonding of Hg(II) to reduced organic sulfur in humic acid as affected by S/Hg ratio. *Environ. Sci. Technol.,* **35**: 2741−2745.

HIGUERAS P., OYARZUN R., LILLO J., SÁNCHEZ-HERNÁNDEZ J.C., MOLINA J.A., ESBRÍ J.M., LORENZO S. (2006). The Almadén district (Spain): Anatomy of one of the world's largest Hg-contaminated sites. *Sci. Total Environ.*, **236**: 112−124.

HINES M.E., HORVAT M., FAGANELI J., BONZONGO J-C.J., BARKAY T., MAJOR E.B., SCOTT K.J., BAILEY E.A., WARWICK J.J., LYONS W.B. (2000). Mercury Biogeochemistry in the Idrija River, Slovenia, from above the Mine into the Gulf of Trieste. *Environ. Res. A*, **83**: 129−139.

HINTELMANN H., HARRIS R., HEYES A., HURLEY J.P., KELLY C.A., KRABBENHOFT D.P., LINDBERG S., RUDD J.W., SCOTT K.J., ST LOUIS V.L. (2002). Reactivity and mobility of

new and old mercury deposition in a boreal forest ecosystem during the first year of the METAALICUS study. *Environ. Sci. Technol.* **36**: 5034−5040.

HOLMES C.D., JACOB D.J., CORBITT E.S., MAO J., YANG X., TALBOT R., SLEMR F. (2010). Global atmospheric model for mercury including oxidation by bromine atoms. *Atmos. Chem. Phys.*, **10**: 12037–12057.

HORVAT M., NOLDE N., FAJON V., JEREB V., LOGAR M., LOJEN S., JACIMOVIC R., FALNOGA I., LIYA Q., FAGANELI J., DROBNE D.(2003). Total mercury, methylmercury and selenium in mercury polluted areas in the province Guizhou, China. *Sci. Total Environ.*, **304**: 231−256.

HYLANDER L.D. AND MEILI M. (2003). 500 years of mercury production: global annual inventory by region until 2000 and associated emissions. *Sci. Total Environ.*, **304**: 13−27.

HYLANDER L.D. AND GOODSITE M.E. (2006). Environmental costs of mercury pollution. *Sci. Total Environ.*, **368**: 352−370.

KERIN E.J., GILMOUR C.C., RODEN E., SUZUKI M.T., COATES J.D., MASON R.P. (2006). Mercury Methylation by Dissimilatory Iron-Reducing Bacteria. *Appl. Environ. Microbiol.*, **72**: 7919−7921.

KIM J.P. AND FITZGERALD W.F. (1986). Sea-air partitioning of mercury in the equatorial Pacific Ocean. *Science,* **231**: 1131−1133.

KIM C.S., RYTUBA J.J., BROWN JR. G.E. (2004). Geological and anthropogenic factors influencing mercury speciation in mine wastes: an EXAFS spectroscopy study. *Appl. Geochem.*, **19**: 379–393.

KLEMM D.D. AND NEUMANN N. (1984). Ore-controlling factors in the Hg–Sb province of southern Tuscany, Italy. In: Wauschkuhn A. et al. (Eds.). Syngenesis and Epigenesis in the Formation of Mineral Deposits. Springer-Verlag, Heidelberg, pp. 482−503.

KOCMAN D. AND HORVAT M. (2011). Atmospheric distribution and deposition of mercury in the Idrija Hg mine region, Slovenia. *J. Environ. Manage.*, **92**: 2038−2046.

KRABBENHOFT D.P., BRANFIREUN B.A. HEYES A. (2005). Geogenic and mining sources of mercury in the environment. In: Parsons M.B. and Percival J.B. (Eds.), Mercury: sources, cycles and effects. Mineralogical Association of Canada, Short Course Series, Vol. 34. Halifax, Nova Scotia, pp. 139−156.

LINDBERG S.E., AND STRATTON W.J. (1998). Atmospheric Mercury Speciation: Concentrations and Behavior of Reactive Gaseous Mercury in Ambient Air. *Environ. Sci. Technol.*, **32**: 49−57.

LLANOS W., KOCMAN D., HIGUERAS P., HORVAT M. (2011). Mercury emission and dispersion models from soils contaminated by cinnabar mining and metallurgy. *J. Environ. Monitor.*, **13**: 3460−3468.

LOPPI S. (1998). Distribuzione ambientale di mercurio, arsenico, boro e antimonio nell'area geotermica del M. Amiata. *Atti Mus. Stor. Nat. Maremma*, **17**: 79−89.

MARINELLI G., BARBERI F., CIONI R. (1993). Sollevamenti neogenici e intrusioni acide della Toscana e del Lazio settentrionale. *Mem. Soc. Geol. It.*, **49**: 279–288.

MARTÍNEZ-CORONADO A., OYARZUN R., ESBRÍ J.M., LLANOS W., HIGUERAS P. (2011). Sampling high to extremely high Hg concentrations at the Cerco de Almadenejos,

Almadén mining district (Spain): The old metallurgical precinct (1794 to 1861 AD) and surrounding areas. *J. Geochem. Explor.*, **109**: 70−77.

MARVIN-DIPASQUALE M., AGEE J., MCGOWAN C., OREMLAND R.S., THOMAS M., KRABBENHOFT D., GILMOUR C. (2000). Methyl-mercury degradation pathways: a comparison among three mercury impacted ecosystems. *Environ. Sci. Tech.*, **34**: 4908–4916.

MASON R.P. (2009). Mercury emissions from natural processes and their importance in the global mercury cycle. In: Pirrone N. and Mason R.P. (Eds.), Mercury Fate and Transport in the Global Atmosphere: Emissions, Measurements, and Models, Chap. 7. Springer, New York (USA), pp.173−191.

MASON R.P., CHOI A.L., FITZGERALD W.F, HAMMERSCHMIDT C.R., LAMBORG C.H., SOERENSEN A.L., SUNDERLAND E.M. (2012). Mercury biogeochemical cycling in the ocean and policy implications. *Environ. Res.*, **119**: 101−117.

MASON R.P. AND FITZGERALD W. F. (1990). Alkylmercury species in the equatorial Pacific. *Nature,* **347**: 457−459.

MASON R.P. AND FITZGERALD W.F. (1991). Mercury speciation in open ocean waters. *Water Air Soil Pollut.,* **56**: 779−789.

MASON R.P., FITZGERALD W.F., MOREL F.M.M. (1994). The biogeochemical cycling of elemental mercury: Anthropogenic influences. *Geochim. Cosmochim. Acta,* **58**: 3191−3198.

MASON R.P., MOREL F.M.M., HEMOND H.F. (1995). The role of microorganisms in elemental mercury formation in natural waters. *Water Air Soil Pollut.,* **80:** 775−787.

MASON R.P. AND SHEU G-R. (2002). Role of the ocean in the global mercury cycle. *Glob. Biogeochem. Cy.,***16**: 1093−1107.

MASON R. P. AND SULLIVAN K. A. (1998). Mercury and methylmercury transport through an urban watershed. *Water Res.,* **32**: 321−330.

MAXSON P. (2006). Mercury flows and safe storage of surplus mercury. Technical Report, Concorde East/West Sprl for the European Commission – Environment Directorate, 82 pp.

MERITT K.A. AND AMIRBAHMAN (2009). Mercury methylation dynamics in estuarine and coastal marine environments — A critical review. *Earth-Sci. Rev.*, **96**: 54–66.

MOREL F.M.M., KRAEPIEL A.M.L., AMYOT M. (1998). The chemical cycle and bioaccumulation of mercury. *Annu. Rev. Ecol. Svst.*, **29**: 543−66.

MORTEANI G., RUGGIERI G., MÖLLER P., PREINFALK C. (2011). Geothermal mineralized scales in the pipe system of the geothermal Piancastagnaio power plant (Mt. Amiata geothermal area): a key to understand the stibnite, cinnabarite and gold mineralization of Tuscany (central Italy). *Miner. Deposita*, **46**: 197–210.

NACHT D.M., GUSTIN M.S., ENGLE M.A., ZEHNER R.E., GIGLINI A.D. (2004). Atmospheric Mercury Emissions and Speciation at the Sulphur Bank Mercury Mine Superfund Site, Northern California. *Environ. Sci. Technol.*, **38**: 1977−1983.

NAGASE H., OSE Y., SATO T., ISHAKAWA T. (1984). Mercury methylation by compounds in humic material. *Sci. Total Environ.,* **32**: 147−156.

NAVARRO A. (2008). Review of characteristics of mercury speciation and mobility from areas of mercury mining in semi-arid environments. *Rev. Environ. Sci. Biotechnol.*, **7**: 287–306.

NRIAGU J.O. (1994). Mercury pollution from the past mining of gold and silver in the Americas. *Sci. Total Environ.*, **149**: 167–181.

OREMLAND R.S., CULBERTSON C.W., WINFREY M.R. (1991). Methylmercury decomposition in sediments and bacterial cultures: involvement of methanogens and sulfate reducers in oxidative demethylation. *Appl. Environ. Microbiol.*, **57**:130–137.

PACYNA E.G., PACYNA J.M., STEENHUISEN F., WILSON S. (2006). Global anthropogenic mercury emission inventory from 2000. *Atmos. Environ.*, **40**: 4048–4063.

PACYNA E.G., PACYNA J.M., SUNDSETH K., MUNTHE J., KINDBOM K., WILSON S., STEENHUISEN F., MAXSON P. (2010). Global emission of mercury to the atmosphere from anthropogenic sources in 2005 and projections to 2020. *Atmos. Environ.*, **44**: 2487–2499.

PARSONS M.B. AND PERCIVAL J.B. (2005). Geogenic and mining sources of mercury in the environment. In: Parsons M.B. and Percival J.B. (Eds.), Mercury: sources, cycles and effects. Mineralogical Association of Canada, Short Course Series, Vol. 34. Halifax, Nova Scotia, pp. 1−20.

PASQUARÈ G., CHIESA S., VEZZOLI L. ZANCHI A.(1983). Evoluzione paleogeografica e strutturale di parte della Toscana meridionale a partire dal Miocene superiore. *Mem. Soc. Geol. Ital.*, **25**: 145–157.

PIRRONE N., CINNIRELLA S., FENG X., FINKELMAN R.B., FRIEDLI H.R., LEANER J., MASON R., MUKHERJEE A.B., STRACHER G.B., STREETS D.G., TELMER K. (2010). Global mercury emissions to the atmosphere from anthropogenic and natural sources. *Atmos. Chem. Phys.*, **10**: 5951–5964.

PIRRONE N., FERRARA R., HEDGECOCK I.M., KALLOS G., MAMANE Y., MUNTHE J., PACYNA J.M., PYTHAROULIS I., SPROVIERI F., VOUDOURI A., WANGBERG I. (2003). Dynamic processes of mercury over the Mediterranean region: results from the Mediterranean Atmospheric Mercury Cycle System (MAMCS) project. *Atmos. Environ.*, **37**, Suppl. 1: 21–39.

QIU G., FENG X., MENG B., SOMMAR J., GU C. (2012). Environmental geochemistry of an active Hg mine in Xunyang, Shaanxi Province, China. *Appl. Geochem.*, **27**: 2280−2288.

QIU G., FENG X., WANG S., SHANG L. (2006). Environmental contamination of mercury from Hg-mining areas in Wuchuan, northeastern Guizhou, China. *Environ. Pollut.*, **142**: 549−558.

QIU G., FENG X., WANG S., FU X., SHANG L. (2009). Mercury distribution and speciation in water and fish from abandoned Hg mines in Wanshan, Guizhou province, China. *Sci. Total Environ.*, **407**: 5162−5168.

RAVICHANDRAN M. (2004). Interactions between mercury and dissolved organic matter − a review. *Chemosphere*, **55**: 319–331.

REDDY M.M. AND AIKEN G.R. (2001). Fluvic acid sulfide ion competition for mercury ion binding in the Florida Everglades. *Water Air Soil Pollut.*, **132**: 89–104.

RYTUBA J.J. (2002). Mercury geoenvironmental models. In: Seal RR, Foley N (Eds.), Geoenvironmental analysis of ore deposits, US Geological Survey Open File Report 02-195, pp. 161–175.

RYTUBA J.J. (2003). Mercury from mineral deposits and potential environmental impact. *Environ. Geol.*, **43**: 326–338.

RYTUBA J.J. (2005). Geogenic and mining sources of mercury in the environment. In: Parsons M.B. and Percival J.B. (Eds.), Mercury: sources, cycles and effects. Mineralogical Association of Canada, Short Course Series, Vol. 34. Halifax, Nova Scotia, pp. 21−41.

SAKAMOTO H., TOMIYASU T., YONEHARA N. (1995). The contents and chemical forms of mercury in sediments from Kagoshima Bay, in comparison with Minamata Bay and Yatsushiro Sea, Southwestern Japan. *Geochem. J.,* **29**: 97−105.

SAVOIA U. (1919). Qua e là per le contrade minerarie d'Italia - Le miniere cinabrifere italiane. *La Miniera Italiana* III, **7−8**: 233−248.

SCHAEFER J.K., LETOWSKI J., BARKAY T. (2002). mer -Mediated Resistance and Volatilization of Hg(II) Under Anaerobic Conditions. *Geomicrobiol. J.*, **19**: 87−102.

SCHROEDER W.H. AND MUNTHE J. (1998). Atmospheric mercury – an overview. *Atm. Environ.*, **32**: 809−822.

SCHUSTER E. (1991). The behavior of mercury in the soil with special emphasis on complexation and adsorption processes-a review of the literature. *Water Air Soil Pollut.*, **56**: 667–680.

SCHUSTER P.F., KRABBENHOFT D.P., NAFTZ D.L., DEWAYNE CECIL L., OLSON M.L., DEWILD J.F., SUSONG D.D., GREEN J.R., ABBOTT M.L. (2002). Atmospheric Mercury Deposition during the Last 270 Years: A Glacial Ice Core Record of Natural and Anthropogenic Sources. *Environ. Sci. Technol.*, **36**: 2303−2310.

SELIN N.E. (2009). Global Biogeochemical Cycling of Mercury: A Review. *Annu. Rev. Env. Resour.*, **34**: 43−63.

SELIN N.E., JACOB D.J., YANTOSCA R.M., STRODE S., JAEGLÉ L., SUNDERLAND E.M. (2008). Global 3-D land-ocean atmosphere model for mercury: present-day versus preindustrial cycles and anthropogenic enrichment factors for deposition. *Glob. Biogeochem. Cycles,* **22**: GB2011, 13 pp.

SHAO D., KANG Y., WU S., WONG M.H. (2012). Effects of sulfate reducing bacteria and sulfate concentrations on mercury methylation in freshwater sediments. *Sci. Total Environ.*, **424**: 331–336.

STEIN E.D., COHEN Y., WINER A.M. (1996). Environmental distribution and transformations of mercury compounds. *Crit. Rev. Environ. Sci. Technol.*, **26**: 1−43.

STETSON S.J., GRAY J.E., WANTY R.B., MACALADY D.L. (2009). Isotopic variability of mercury in ore, mine-waste calcine, and leachates of mine-waste calcine from areas mined for mercury. *Environ. Sci. Technol.*, **43**: 7331–7336.

STRAPPA O. (1977). Storia delle miniere di mercurio del Monte Amiata. *L'Industria Mineraria*, **XXVIII**, I-II-III parts, 252−259; 336−348; 433−439.

SUNDERLAND E.M. AND MASON R.P. (2007). Human impacts on open ocean mercury concentrations. *Global Biogeochem. Cycles*, **21**: GB4022, 15 pp.

TANELLI G. (1983). Mineralizzazioni metallifere e minerogenesi della Toscana. *Mem. Soc. Geol. It.*, **8**: 91–109.

TASSI F., FIEBIG J., VASELLI O., NOCENTINI M. (2012). Origins of methane discharging from volcanic-hydrothermal, geothermal and cold emissions in Italy. *Chem. Geol.*, **310-311**: 36−48.

TANELLI G. AND LATTANZI P. (1986). Metallogeny and mineral exploration in Tuscany: state of the art. *Mem. Soc. Geol. It.*, **31**: 1986, 299−304.

TASSI F., VASELLI O., CUCCOLI F., BUCCIANTI A., NISI B., LOGNOLI E., MONTEGROSSI G. (2009). A Geochemical Multi-Methodological Approach in Hazard Assessment of CO_2-Rich Gas Emissions at Mt. Amiata Volcano (Tuscany, Central Italy). *Water Air Soil Pollut*., Focus **9**: 117–127.

TRASANDE L., LANDRIGAN P.J., SCHECHTER C. (2005). Public Health and Economic Consequences of Methyl Mercury Toxicity to the Developing Brain. *Environ. Health Persp.*, **113**: 590−596.

ULLRICH S.M., TANTON T.W., ABDRASHITOVA S.A. (2001). Mercury in the Aquatic Environment: A Review of Factors Affecting Methylation. Crit. Rev. *Environ. Sci. Technol.*, **31**: 241–293.

UNEP (2002). Global mercury assessment. Technical Report, United Nations Environment Programme, Chemicals. Geneva, Switzerland.

UNEP (2006). Summary of Supply, Trade and Demand Information on Mercury. Analysis requested by UNEP Governing Council decision 23/9 IV. Technical Report, United Nations Environment Programme, Chemical Branch, DTIE. Geneva, Switzerland.

UNEP/WMO (1998). Atmospheric Input of Mercury to the Mediterranean Sea. MAP Technical Reports Series No. 122, United Nations Environment Programme. Athens, Greece.

US EPA (1997). Mercury study report to Congress. U.S. Environmental Protection Agency, I-VIII, EPA-452/R-97-003.

US EPA (2001). Water quality criterion for the protection of human health: Methylmercury. U.S. Environmental Protection Agency, EPA-823-R-01-001. Washington, USA.

WEBER J.H. (1993). Review of possible paths for abiotic methylation of mercury(II) in the aquatic environment. *Chemosphere*, **26**: 2063−2077.

WIATROWSKI H.A., WARD P.M., BARKAY T. (2006). Novel reduction of mercury(II) by mercury-sensitive dissimilatory metal reducing bacteria. *Environ. Sci. Technol.*, **40**: 6690–6696.

WHO (1990). Methylmercury, Environmental Health Criteria 101. World Health Organization, Geneva, Switzerland.

WHO (1989). Mercury − Environmental Aspects, Environmental Health Criteria 86. World Health Organization, Geneva Switzerland.

ZAMBARDI, T., SONKE, J.E., TOUTAIN, J.P., SORTINO, F., SHINOHARA, H. (2009). Mercury emissions and stable isotopic compositions at Vulcano Island (Italy). *Earth Planet. Sci. Lett.*, **277**: 236–243.

ZUCCHETTI S. (1964). Giacimenti minerari – I giacimenti mercuriferi secondary della Toscana e l'età della loro metallogenesi. *Lincei – Rend. Sc. Fis. Mat. Nat.*, **XXXVI**: 658−668.

CHAPTER 2

PART I - CONCENTRATION, DISTRIBUTION, AND TRANSLOCATION OF MERCURY AND METHYLMERCURY IN MINE-WASTE, SEDIMENT, SOIL, WATER, AND FISH COLLECTED NEAR THE ABBADIA SAN SALVATORE MERCURY MINE, MT. AMIATA DISTRICT, ITALY

Valentina Rimondi[1], John E. Gray[2], Pilario Costagliola[1], Orlando Vaselli[1], and Pierfranco Lattanzi[3]

[1]Dipartimento Scienze di della Terra, Università di Firenze, Via G. La Pira 4, Firenze, 50121 Italy
[2]U.S. Geological Survey, MS 973, Federal Center, Denver, CO 80225 USA
[3]Dipartimento di Scienze della Terra, Università di Cagliari, Via Trentino 51, Cagliari, 09127 Italy

Published to Science of the Total Environment, **414**: 318−327.

Keywords: mercury, methylmercury, mining, sediment water, fish

Abstract

The distribution and translocation of mercury (Hg) are studied in the Paglia River ecosystem, located downstream from the inactive Abbadia San Salvatore mine (ASSM). The ASSM is part of the Mt. Amiata Hg district, Southern Tuscany, Italy, which was one of the world's largest Hg districts. Concentrations of Hg and methyl-Hg have been determined in mine-waste calcine (retorted ore), sediment, water, soil, and freshwater fish collected from the ASSM and the downstream Paglia River. Concentrations of Hg in calcine samples range from 25 to 1500 μg/g, all of which exceed the industrial soil contamination level for Hg of 5 μg/g used in Italy. Stream and lake sediment samples collected downstream from the ASSM range in Hg concentration from 0.26 to 15 μg/g, of which more than 50% exceeds the probable effect concentration for Hg of 1.06 μg/g, the concentration above which harmful effects are likely to be observed in sediment-dwelling organisms. Stream and lake sediment methyl-Hg concentrations show a significant correlation with TOC, indicating considerable methylation and potential bioavailability of Hg. Stream water contains Hg as high as 1400 ng/L, but only one water sample exceeds the 1000 ng/L drinking water Hg standard used in Italy. Concentrations of Hg are elevated in freshwater fish muscle samples and range from 0.16 to 1.2 μg/g (wet weight), average 0.84 μg/g, and 96% of these exceeds the 0.3 μg/g (methyl-Hg,

wet weight) US EPA fish muscle standard recommended to protect human health. Analysis of fish muscle for methyl-Hg confirms that >90% of the Hg in these fish is methyl-Hg. Such highly elevated Hg concentrations in fish indicate active methylation, significant bioavailability, and uptake of Hg by fish in the Paglia River ecosystem. Methyl-Hg is highly toxic and the high Hg concentrations in these fish represent a potential pathway of Hg to the human food chain.

2.1 Introduction

Active and inactive Hg mines represent a significant source of Hg to the environment as a result of the disposal of Hg-rich mine-waste calcine (retorted ore) at these sites. Extraction of Hg during mining is generally carried out in retort or rotary furnace, where ore is heated to 600-700 °C, leading to the thermal decomposition of cinnabar (HgS) to elemental mercury (Hg^0). Condensation of Hg vapor to liquid elemental Hg is the final step in ore processing and elemental Hg is the product sold on the international market. Retorting of cinnabar ore is an incomplete process, and thus, mine-waste calcines generally contain elevated Hg concentrations due to the presence of unconverted cinnabar as well as the formation of metacinnabar, Hg^0, and other insoluble and soluble Hg salts during retorting (Kim et al., 2000, 2003; Gray et al., 2010). Runoff from mine-waste calcines produces adverse effects to ecosystems located downstream from Hg mines (Gosar et al., 1997; Gray et al., 2002, 2003; Higueras et al., 2006). Stream sediment and water downstream from Hg mines are also characterized by anomalously high Hg concentrations even decades after the end of Hg mining (Gosar et al., 1997; Gray et al., 2000; Hines et al., 2000; Qiu et al., 2005).

The most significant environmental concern associated with downstream transportation of Hg is potential conversion of inorganic Hg to methyl-Hg (CH_3Hg^+), the most toxic form of Hg (Eisler, 1987). Methyl-Hg is a neurotoxin (WHO, 1976; Clarkson, 1990) and high intake of Hg by humans may result in health effects such as deafness, blindness, and even death (NAS, 1978; Eisler, 1987; US EPA, 1997). In natural environments, methylation of inorganic Hg is mainly the result of microbial activity, primarily by the action of sulfate reducing bacteria (Compeau and Bartha, 1985), which is particularly enhanced in organic-rich sediment (Hines et al., 2000; Ullrich et al., 2001). Despite the generally low organic contents in mine-waste calcine, areas mined for Hg have been shown to have active formation of methyl-Hg resulting in high concentrations of methyl-Hg in calcine in some instances (e.g., up to 11,100 ng/g, Almadén, Spain; (Gray et al., 2004)), thus, representing a potentially significant source of

methyl-Hg to ecosystems surrounding Hg mines. Methyl-Hg formation is potentially hazardous because it is water soluble, bioavailable, and bioaccumulates in living organisms (NAS, 1978; US EPA, 1997), and generally increases in the food chain with increasing trophic levels (biomagnification) (NAS, 1978). Consumption of fish containing high concentrations of Hg is the dominant exposure pathway of methyl-Hg to humans because generally more than 90% of Hg in fish is methyl-Hg (Fitzgerald and Clarkson, 1991; Bloom, 1992; Mason et al., 2000). In order to limit exposure of methyl-Hg to humans, the US EPA established a consumption advisory for methyl-Hg in fish muscle of 0.3 μg/g (wet weight) (US EPA, 2009b).

The Monte Amiata Hg district, Southern Tuscany, Italy, is part of the large circum-Mediterranean Hg belt, which hosts 65% of the world's cinnabar deposits (Bargagli et al., 1986). Monte Amiata was one of the five mining regions (Almadén, Spain; Idrija, Slovenia; California Coast Ranges, USA; Monte Amiata, Italy; Huancavelica, Peru) that dominated the historical global production of elemental Hg (Ferrara et al., 1999). Several presently inactive mines constitute the Monte Amiata district (Fig. 2.1).

Presently, detailed study of Hg diffusion through abiotic and biotic compartments at Monte Amiata district is lacking. Speciation of Hg is unknown in the sediment and water column in the Monte Amiata area, and in addition, determinations of Hg in fish have not been made since the 1970s (Bacci and Renzoni, 1973). Significant production of Hg from the Monte Amiata Hg district and the presence of large deposits of mine-waste calcine containing high concentrations of Hg potentially contaminate surrounding streams and rivers located downstream from Hg mines. Furthermore, potential conversion of inorganic Hg to methyl-Hg leads to increased bioavailability of Hg and potential exposure of Hg to the food chain in this area. This study is focused on the largest mine in the Monte Amiata district, the ASSM. The objective of this study is to evaluate (1) environmental effects of past Hg mining to the ecosystem downstream from the ASSM, (2) the source of Hg to the surrounding environment, (3) the distribution and transport of Hg and methyl-Hg in sediment and water runoff from the ASSM, and (4) potential exposure of Hg to humans in the area through the measurement Hg and methyl-Hg concentrations in freshwater fish. Samples of calcine, soil, stream sediment, stream and lake water, and fish have been analyzed for both Hg and methyl-Hg in this study.

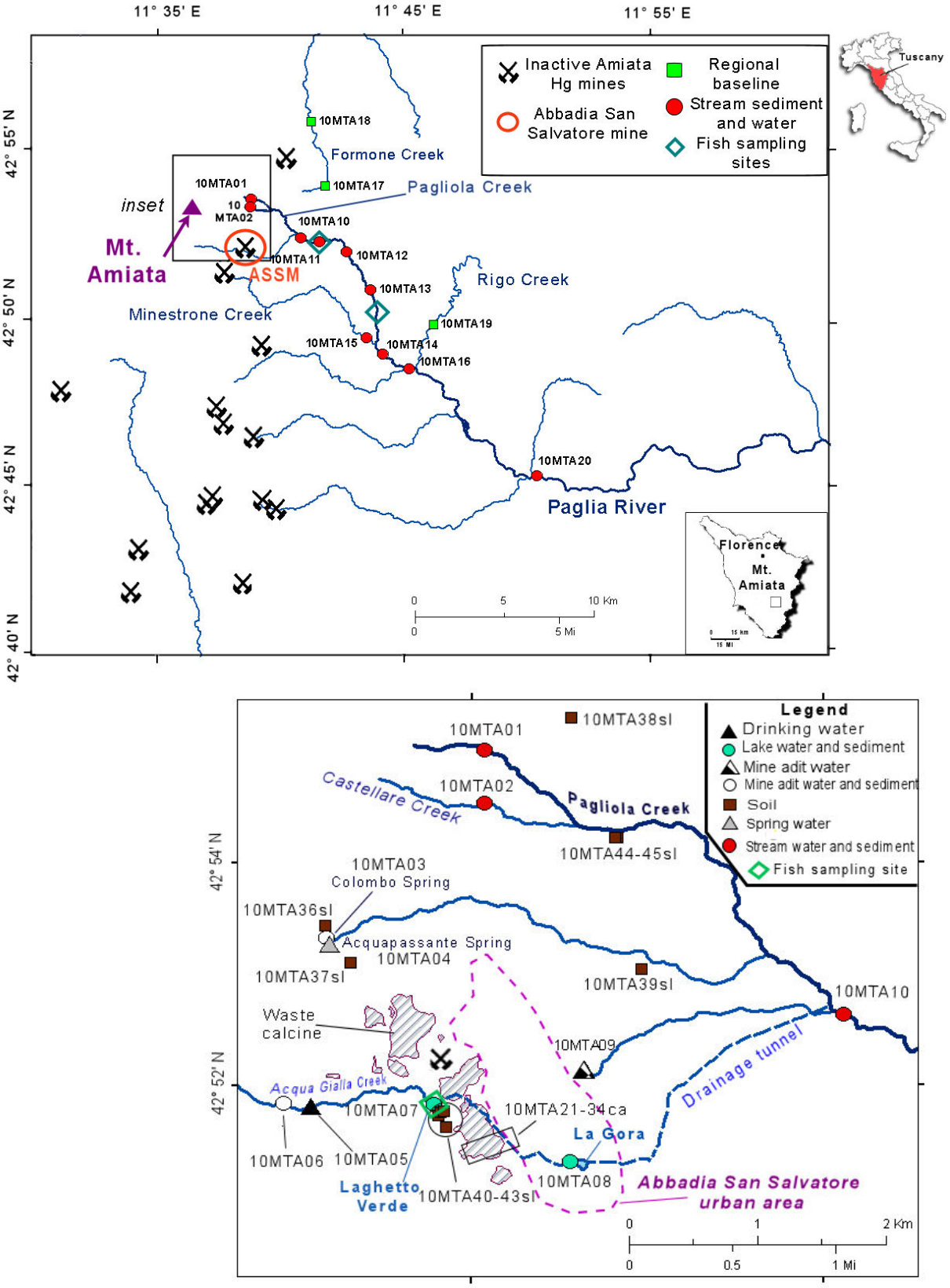

Fig. 2.1a,b. *Location of sediment, water, mine-waste calcine, and soil samples collected in this study.*

2.2 Study Area

The area of study is the ASSM of the Monte Amiata Hg district, Italy (Fig. 2.1). Similar to most Hg deposits worldwide, cinnabar is the dominant ore mineral at the ASSM, but minor pyrite, and rare stibnite, marcasite, and arsenic-bearing sulphides have also been reported (Falini, 1960; Morteani et al., 2011). Typical gangue is microcrystalline calcite and quartz, and rare celestite, gypsum, native sulphur, and hydrocarbons (Klemm and Neumann, 1984). The Monte Amiata district deposits were originally worked by the Etruscans (about 800 BC), but these mines were later closed by the Romans (Barghigiani and Ristori, 1994; Ferrara et al., 1991). Deposits in the area were rediscovered in 1868 (Barghigiani and Ristori, 1994) and mines were thereafter reopened. About 102,000 t of Hg (3 million flasks of Hg of 34.5 kg each) were produced from the 1860s to 1980 (Ferrara et al., 1998), ranking it as the 4th largest Hg producing district worldwide. Samples for this study were collected in and around the town of Abbadia San Salvatore (42^{o} 53' N, 11^{o} 40' E) (Fig. 2.1), where the retort for the majority of the mines of the Monte Amiata district is located. Precipitation averages about 85 cm per year at Abbadia San Salvatore and temperatures during field work varied from about 19-27 ^{o}C. During sample collection from September 2-8, 2010, weather was generally dry, and sunny to partly cloudy. Streams sampled in the area are generally perennial.

2.3 Methods

2.3.1 Sample collection and preparation

Samples of mine-waste calcine (n = 15) were collected from waste piles of the ASSM, which are located adjacent to the town of Abbadia San Salvatore (Fig. 2.1, Table 2.1). Calcine was collected as grab samples about 50 cm below the surface to avoid the highly-oxidized near-surface environment. Calcine samples were collected at this depth in the mine waste piles to access moist, potentially anoxic areas with generally more active anaerobic methylating bacteria, and therefore, the highest possibility of Hg methylation. Soil samples were collected from near the ASSM retort emission stack (n = 4) and from other sites (n = 6) located more distal from the retort area east and north of ASSM (Fig. 2.1, Table 2.1). Soil was collected from a 2-5 cm depth from the A-horizon following the removal of the forest floor O-horizon leaves and tree litter. Sediment (n = 17) and various water samples (n = 20) were collected from sites in and around the ASSM and from regional baseline sites (Fig. 2.1, Table 2.2). Stream and lake sediment was collected from surface-layer, bed-load alluvium, and composited from several localities at each site. There were 15 stream sediment samples

collected in this study, but only 2 lake sediment samples. The lake sediment samples were collected from two small lakes, which are located along Acqua Gialla Creek (Fig. 2.1b). These lakes are open systems where sediment and water flows in and through these lakes and eventually exits at the downstream point of discharge. All calcine, soil, and stream and lake sediment samples for Hg and methyl-Hg analysis were stored in amber glass vessels with Teflon-lined lids and were frozen until analysis. Solid samples for additional geochemical analysis were air dried, sieved to minus-80-mesh (0.18 mm), and pulverized.

Unfiltered water samples were collected from the same sites as stream and lake sediment samples, with the exception of one stream drainage (10MTA17) where there was no water, and four additional sites where only water was collected from mine adits and a drainage tunnel (10MTA03, 04, 05, and 09; Table 2.2). These unfiltered water samples were collected primarily to evaluate the variation of Hg and methyl-Hg concentrations in water downstream from the ASSM and throughout the region. Water samples for Hg and methyl-Hg analysis were collected in Teflon bottles pre-cleaned by boiling in concentrated HNO_3 for 48 hours. Within eight hours of collection, the water samples were acidified with ultra-pure HCl using a final acid concentration of 0.5% v/v.

Freshwater fish were collected from the Paglia River and Pagliola Creek (Fig. 2.1) and from a small lake located next to the mine area (Laghetto Verde) using dip nets or rod and reel angling techniques. Fish were chilled in a cooler during the day and frozen within four hours of collection. Species of fish collected included barbel (*Barbus plebejus*), chub (*Leiciscus cephalus*), roach (*Chondrostoma genei*), and carp (*Cyprinus carpio*). A total of 86 fish were caught and analyzed for Hg in this study. Seventy of the fish were later thawed and dissected with a stainless steel knife to obtain muscle samples (fillet) for analysis. From Pagliola Creek (site 10MTA11, Fig. 2.1) there were 59 fish collected, 52 roach and 7 barbel, from which muscle was removed and analyzed for Hg; an additional 5 barbel and 2 roach were collected from this site that were analyzed as whole fish. From the site on the Paglia River (near site 10MTA13, Fig. 2.1) 9 fish were collected, 6 chub, 2 barbel, and 1 roach, which were dissected and muscle was collected for analysis; an additional 9 fish were collected from this site, 7 roach and 2 barbel, and analyzed as whole fish. There was one carp collected from Laghetto Verde, from which muscle was removed and analyzed. Fish collected were small, ranging from 8-19 cm in fork length and weighing between 7-90 g, with the exception of the carp collected from Laghetto Verde that was 25 cm in length, weighing 320 g. All fish samples were freeze dried, pulverized, and then analyzed dry. Fish were weighed prior to freezing and then again after freeze drying to obtain wet weight conversions.

Sample	Location	Hg (µg/g)	Methyl-Hg (ng/g)	TOC (%)
Calcine				
10 MTA 21ca	Abbadia San Salvatore mine	130	11	2.9
10 MTA 22ca	Abbadia San Salvatore mine	120	26	3.7
10 MTA 23ca	Abbadia San Salvatore mine	48	4.5	1.1
10 MTA 24ca	Abbadia San Salvatore mine	76	6.8	2.3
10 MTA 25ca	Abbadia San Salvatore mine	25	0.34	0.23
10 MTA 26ca	Abbadia San Salvatore mine	74	1.7	0.55
10 MTA 27ca	Abbadia San Salvatore mine	110	1.1	n.d.
10 MTA 28ca	Abbadia San Salvatore mine	32	0.39	0.11
10 MTA 29ca	Abbadia San Salvatore mine	1200	11	0.16
10 MTA 30ca	Abbadia San Salvatore mine	1500	8.8	0.44
10 MTA 31ca	Abbadia San Salvatore mine	110	0.60	0.030
10 MTA 32ca	Abbadia San Salvatore mine	130	2.3	0.35
10 MTA 33ca	Abbadia San Salvatore mine	380	11	0.20
10 MTA 34ca	Abbadia San Salvatore mine	250	3.6	0.27
10 MTA 35ca	Abbadia San Salvatore mine	140	0.86	0.10
Soil				
Mining area				
10 MTA 40sl	Abbadia San Salvatore mine	400	29	7.5
10 MTA 41sl	Abbadia San Salvatore mine	280	44	8.1
10 MTA 42sl	Abbadia San Salvatore mine	150	45	14
10 MTA 43sl	Abbadia San Salvatore mine	170	7.9	7.0
Baseline areas				
10 MTA 36sl	north Abbadia San Salvatore	2.4	18	6.5
10 MTA 37sl	north Abbadia San Salvatore	14	29	9.1
10 MTA 38sl	north Abbadia San Salvatore	0.64	0.95	2.2
10 MTA 39sl	east Abbadia San Salvatore	1.0	1.5	2.5
10 MTA 44sl	east Abbadia San Salvatore	2.7	1.4	4.8
10 MTA 45sl	east Abbadia San Salvatore	1.9	1.2	4.8

Table 2.1. *Geochemical data for calcine and soil collected in the Monte Amiata area.*

2.3.2 Chemical analysis

Mine Waste Calcine, Stream Sediment, and Soil

The concentration of Hg was determined in the calcine, soil, and sediment samples using an aqua-regia digestion following EPA method 1631 (Bloom and Fitzgerald, 1988). The Hg ions in the digestate were reduced by acidic $SnCl_2$ to Hg^0 and purged from the sample with argon. The released Hg was measured by cold vapor atomic absorption (using a Leeman Hydra AF instrument, Leeman Labs Inc., Hudson, New Hampshire). Methyl-Hg analysis followed EPA

method 1630 using cold-vapor atomic fluorescence spectrometry (CVAFS) (Bloom, 1989). During methyl-Hg analysis, sediment and mine-waste samples were extracted into methylene chloride during digestion to avoid possible methylation artifact effects (Bloom et al., 1997). An ethylating agent was then added to the extract to form a volatile methyl-ethylmercury derivative, and then purged onto graphitized carbon traps as a means of preconcentration and interference removal. The samples were then isothermally chromatographed, pyrolitically broken down to Hg^0 and detected using CVAFS (using a Tekran Model 2500, Tekran Instruments, Toronto, Canada). All Hg and methyl-Hg determinations were performed by Battelle Marine Science Laboratory, Sequim, Washington. Quality control for Hg and methyl-Hg analysis was established using blank spikes, matrix spikes, standard reference materials (SRM's), and/or sample replicates. Blank and matrix spikes were run as 1 per every 10 samples, replicates and SRM's were run as 1 per every 20 samples, and 3 method blanks were run every 20 samples. Recoveries for Hg on blank spikes were 99-100% and were 75-125% on matrix spikes. There were no blank spikes for methyl-Hg. Recoveries for methyl-Hg matrix spikes varied from 74-101%. The relative percent difference in sample replicates was ≤17% for Hg and was ≤20% for methyl-Hg. Replicates used were separate laboratory aliquots of individual samples (field samples). For the SRM, IAEA-405 analyzed in this study, recoveries ranged from 94-98% and 74-95% of the certified values for Hg and methyl-Hg, respectively. Method blanks contained Hg and methyl-Hg below the lower limit of determination, which was 0.01μg/g for Hg and 0.04 ng/g for methyl-Hg.

The mine-waste calcine, soil, and sediment samples were also analyzed for total organic carbon (TOC) because the process of Hg-methylation depends on organic matter. Determination of TOC was by subtracting carbonate C from total C concentrations. Total C was determined using an automated C-analyzer with an infrared detector that measures CO_2 gas liberated as the sample is combusted at 1370^o C. Carbonate C was determined by liberating CO_2 following treatment with 2 N $HClO_4$; this CO_2 was collected in a solution of monoethanolamine that is then coulometrically titrated using platinum and silver/potassium-iodide electrodes. The relative percent difference in stream sediment, soil, and calcine sample replicates was ≤15% for TOC and the lower limit of determination was 0.05%. Determinations for total C and carbonate C in all mine-waste calcine and stream sediment samples were performed at SGS Laboratory, Toronto, under a contract with the U.S. Geological Survey.

		Stream/Lake Sediment			Stream/lake Water	
Sample	**Location**	**Hg (µg/g)**	**Methyl-Hg (ng/g)**	**TOC (%)**	**Hg (ng/L)**	**Methyl-Hg (ng/L)**
			Upstream from mine			
10 MTA 01	Pagliola Creek	0.27	1.2	0.62	3.2	0.29
10 MTA 02	Castellare Creek	0.10	0.041	0.44	4.3	0.33
			Mine adits			
10 MTA 03	Colombo Spring	1.3	1.5	2.1	130	1.7
10 MTA 06	Acqua Gialla Creek	1.8	0.94	0.79	390	0.39
10 MTA 09	Galleria Italia	n.a	n.a	n.a	170	0.15
					Spring water	
10 MTA 04	Acquapassante Spring	n.a	n.a	n.a	2.6	<0.02
					Drinking water	
10 MTA 05	Galleria XXII	n.a	n.a	n.a	2.8	<0.02
			Downstream from mine			
10 MTA 10	Pagliola Creek	10	6.4	2.1	450	1.3
10 MTA 11	Pagliola Creek	13	5.8	0.50	1400	3.0
10 MTA 12	Paglia River	14	5.2	1.0	450	1.2
10 MTA 13	Paglia River	0.79	0.20	0.23	140	1.0
10 MTA 14	Paglia River	0.35	0.36	0.27	21	0.26
10 MTA 15	Minestrone Creek	0.26	0.22	0.24	3.7	0.15
10 MTA 16	Paglia River	0.42	0.25	0.29	11	0.14
10 MTA 20	Paglia River	10	0.69	0.25	3.8	0.10
			Lakes			
10 MTA 07	Laghetto Verde	15	8.7	2.4	55	0.67
10 MTA08	La Gora	11	4.7	1.0	290	0.77
			Regional Baselines			
10 MTA 17	Formone Creek	0.023	0.068	0.42	n.a	n.a
10 MTA 18	Formone River	0.057	3.0	0.55	1.9	0.19
10 MTA 19	Rigo Creek	0.034	0.089	0.24	1.5	0.045

Table 2.2. *Geochemical data for sediment and water collected in the Monte Amiata area.*

Water

Concentrations of Hg were determined in the water samples using cold-vapor atomic fluorescence spectrometry (CVAFS) following EPA method 1631e (US EPA, 2002). The water samples were digested for Hg by subjecting them to BrCl oxidation for a minimum of 24 hrs. Mercuric ions in the oxidized sample were reduced to Hg^0 with $SnCl_2$, and then purged onto gold-coated sand traps as a means of preconcentration and interference removal. Mercury vapor was thermally desorbed to a second analytical gold trap and then sent to a fluorescence cell and analyzed by CVAFS (Bloom, 1989). For methyl-Hg analysis, the water samples were processed following a distillation and ethylating method (Horvat et al., 1993). An ethylating agent was added to each sample to form a volatile methyl-ethylmercury derivative, and then purged onto graphite carbon traps as a means of preconcentration and interference removal. The sample was then isothermally chromatographed, pyrolitically broken down to Hg^0, and detected using a CVAFS detector (Bloom, 1989). Sample results were corrected for distillation efficiency. All Hg and methyl-Hg determinations in water were made using a Tekran Model 2500. Recoveries for Hg on blank spikes were 99-103% and for methyl-Hg were 94-105%. Recoveries for Hg on matrix spikes were 98-102% and for methyl-Hg were 75-102%. The relative percent difference in water sample replicates varied from 3-11% for Hg and 2-26% for methyl-Hg. The SRM, NIST 1641d was analyzed with the samples and Hg recovery was 97-101% of the certified value. Although no SRM for methyl-Hg is available for water, the SRM tissue sample DORM-3 was analyzed along with the water samples to evaluate method accuracy and methyl-Hg recovery was 93-100% of the certified value. Method blanks were below the lower limit of determination of 0.1 ng/L for Hg and 0.02 ng/L for methyl-Hg in water samples.

2.4 Results and discussion

Comparative standards for Hg (Table 2.3) are used throughout the text for comparison to solid, water, and fish samples collected in this study. The probable effect concentration (PEC) for Hg of 1.06 μg/g in sediment is the concentration above which harmful effects are likely to be observed in sediment dwelling organisms (MacDonald et al., 2000). A similar Hg concentration of 1.0 μg/g has been established as the limit in Italy for public and residential use of soil (commonly referred to as the "green limit"). For industrial use of soil, Italy has established a Hg limit of 5.0 μg/g (IME, 2006), while no national standards have been set for methyl-Hg. The recommended US EPA Soil Screening Levels (SSL) for inorganic Hg are 310

µg/g in industrial soil and 23 µg/g for residential soil (US EPA, 2008). Limits recommended by the US EPA for methyl-Hg in industrial and residential soil are 100 and 7.8 µg/g, respectively. Comparative standards are also shown for water and fish (Table 2.3).

Location	Unfiltered water		Sediment, calcine, or soil		Fish (muscle)	References
	Hg (ng/L)	**Methyl-Hg (ng/L)**	**Hg (µg/g)**	**Methyl-Hg (ng/g)**	**Hg (µg/g, wet weight)**	
Monte Amiata, Italy						*1*
Downstream from mines	3.8-1400	0.14-3.0	0.26-14	0.20-8.7	0.16-1.2	
Mine-waste calcine	--	--	25-1500	0.34-26	--	
Soil	--	--	0.64-400	0.95-45	--	
Lakes	55-290	0.66-0.77	11-15	4.7-8.7	0.49	
Almadén Hg district, Spain						*2, 3, 4, 5*
Downstream from mines	7.6-13,000	0.41-30	3.0-2,300	0.32-82	0.72-1.9	
Mine-waste calcine	--	--	160-34,000	< 0.2-3,100	--	
Soil	--	--	6-8,889	--	--	
Mine-pit lake	2200-2800	0.040-0.065	935	3	--	
Idrija Hg mine, Slovenia						*6, 7, 8*
Downstream from mines	6.0-322	0.01-0.6	0.77-1347	0.01-11	1.1-1.8	
Mine-waste calcine	--	--	10-727	6.5-14	--	
Hg mines, California USA						*9, 10, 11*
Downstream from mines	1,400-19,000	0.96-4.5	0.4-220	1.1-150	0.1-2.1	
Mine-waste calcine	2-450,000	<0.003-47	10-1500	--	--	
Hg mines, southwest Alaska, USA						*12, 13*
Downstream from mines	1.0-2500	0.01-1.2	0.90-5500	0.05-31	0.03-0.62	
Mine-waste calcine and soil	--	--	3.5-46,000	0.2-41	--	
Hg mines, Nevada, USA						*14*
Downstream from mines	6.0-2000	0.039-0.92	0.17-170	0.12-0.95	--	
Mine-waste calcine	--	--	14-14,000	<0.05-96	--	
Palawan Hg mine, Philippines						*15*
Downstream from mines	170-330	<0.02-0.33	3.7-15	0.28-3.9	0.03-1.1*	
Mine-waste calcine	18,000-31,000	<0.02-1.4	28-660	0.13-3.2	--	
Mine-pit lake	120-940	1.7-3.1	6.9-400	2.0-21	--	
Wanshan Hg mine, China						*16, 17*
Downstream from mines	15-9300	0.31-22	90-930	3.0-20	0.061-0.68	
Mine-waste calcines	--	--	5.7-400	0.17-1.1	--	
Soil	--	--	5.1-790	0.13-15	--	

Table 2.3−continued on next page

Table 2.3−continued

	Comparative baselines distal from mines					
Lake Baikal, Russia	0.14-2.02	0.002-0.161	0.005-0.072	--	--	18
Lake San Antonio, Calif., USA	0.6-1.8	--	--	--	--	19
Baselines streams, SW Alaska, USA	0.1-1.4	0.04-0.2	0.02-0.78	0.1-0.3	--	12
Uncontaminated streams, Canada	--	--	0.01-0.7	--	--	20
Streams and lakes, Antarctica	0.27-1.9	0.02-0.33	--	--	--	21
	Comparative standards					
Probable effect concentration, sediment	--	--	1.06	--	--	22
US EPA, residential soil screening level	--	--	23	7.8	--	23
US EPA, industrial soil screening level	--	--	310	100	--	23
Italian industrial soil limit	--	--	5.0	--	--	24
Italian residential soil limit	--	--	1.0	--	--	24
Italian drinking water standard	1,000	--	--	--	--	24
International drinking water standard	6,000	--	--	--	--	25
US EPA drinking water standard	2,000	--	--	--	--	26
US EPA, acute aquatic life water standard	2,400	--	--	--	--	26
US EPA, chronic aquatic life water standard	770	--	--	--	--	26
US EPA, methyl-Hg standard fish muscle	--	--	--	--	0.3	26

* marine fish

Table 2.3. *Comparative Hg and methyl-Hg data for Hg mines, baselines, and standards worldwide. References are: 1 This study, 2 (Gray et al., 2004), 3 (Berzas Nevado et al., 2003), 4 (Higueras et al., 2003), 5 (Higueras et al., 2006), 6 (Hines et al., 2000), 7 (Gosar et al., 1997), 8 (Horvat et al., 2004), 9 (Rytuba, 2000), 10 (Rytuba, 2003), 11 (Davis et al., 2008), 12 (Gray et al., 2000), 13 (Bailey et al., 2002), 14 (Gray et al., 2002), 15 (Gray et al., 2003), 16 (Qiu et al., 2005), 17 (Qiu et al., 2009), 18 (Leermakers et al., 1996), 19 (Gill and Bruland, 1990), 20 (Painter et al., 1994), 21 (Lyons et al., 1999), 22 (MacDonald et al., 2000), 23 (US EPA, 2008), 24 (IME, 2006), 25 (WHO, 2005), and 26 (US EPA, 2009b).*

2.4.1 Calcine

Concentrations of Hg in mine waste calcine samples collected in the Monte Amiata district range from 25 to 1500 μg/g, whereas methyl-Hg vary from 0.34 to 26 ng/g (Table 2.1). All concentrations of Hg found in ASSM calcine exceed the PEC for Hg (MacDonald et al., 2000), but the PEC is established for sediment and is not directly applicable to mine waste calcine, thus, the industrial SSL is a more appropriate point of comparison for calcine. Only three ASSM calcine samples exceed the US EPA industrial Hg SSL of 310 μg/g (US EPA, 2008) (Table 2.1; Fig. 2.2), whereas all ASSM calcine samples exceed the much lower industrial SSL for Hg of 5 μg/g used in Italy (IME, 2006) (Fig. 2.2). More important than the concentration of Hg is the concentration of methyl-Hg, which is highly toxic to all organisms (Eisler, 1987; US EPA, 1997). All concentrations of methyl-Hg in the ASSM calcine samples

are lower than the US EPA methyl-Hg industrial SSL of 100 μg/g (US EPA, 2008) (Table 2.3).

Concentrations of Hg in the ASSM calcine samples are elevated compared to sediment collected from local baseline sites in this study and worldwide Hg baselines (Table 2.3; Fig. 2.2). Elevated Hg concentrations in mine-waste calcine worldwide are generally a result of the incomplete process of Hg ore retorting, thus, minor unconverted cinnabar is present in calcine.

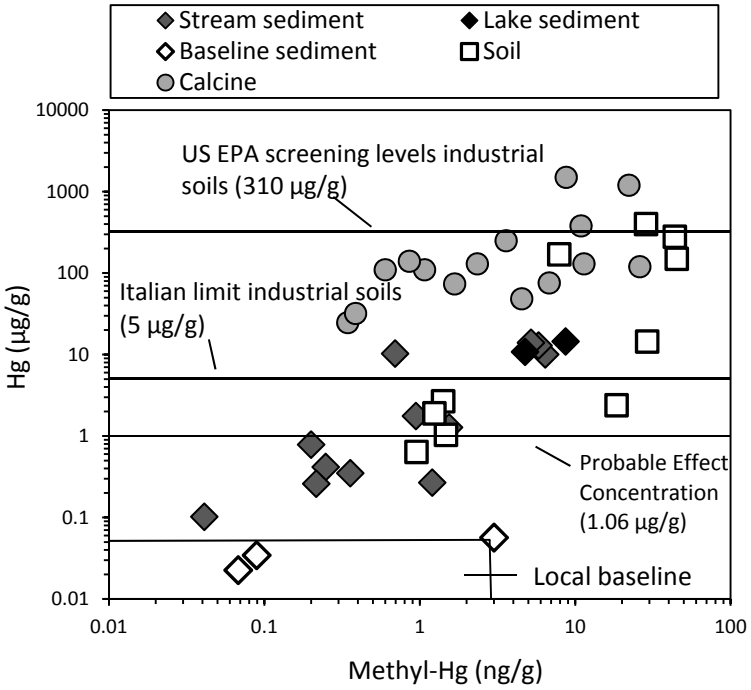

Fig. 2.2. *Concentrations of methyl-Hg versus Hg in calcine, sediment, and soil samples collected in the Monte Amiata area. The limit in Italy for industrial soil, the US EPA screening level for industrial soil, and the Probable Effect Concentration (PEC) are shown for reference. Local baseline data are also shown for reference (Table 2.1).*

In addition, Hg^0 and other insoluble and soluble Hg compounds, formed during ore retorting, are also found in calcine (Kim et al., 2000, 2003; Esbrí et al., 2010; Gray et al., 2010). Concentrations of Hg and methyl-Hg in calcine from the ASSM are similar to those reported in calcine collected from other Hg mines worldwide (Table 2.3). Much higher concentrations of Hg have been reported for the Hg districts of Almadén, Spain, and Alaska and Nevada in the USA (Table 2.3). Furthermore, the ASSM calcine samples contain lower methyl-Hg concentrations than calcine at Almadén, and Hg mines in California and Nevada, USA (Table 2.3). Methylation of Hg is generally enhanced in anaerobic, organic-rich environments (Compeau and Bartha, 1985; Ullrich et al., 2001). In the Monte Amiata area, calcines are low

in TOC and such low organic matter contents likely limit the ability of bacteria to methylate Hg.

2.4.2 Stream and lake sediment

Sediment samples were collected from the Paglia River and its tributaries and from lakes located along the Paglia River (Fig. 2.1) to evaluate Hg contamination and Hg methylation as result of past Hg mining and ore retorting. Local baselines were established by sampling sites distal from Hg mines in the region, although collection of uncontaminated baseline samples was difficult in this area as there are many Hg mines and potentially undiscovered Hg deposits (e.g., the region has high "geogenic" Hg). Stream sediment samples collected downstream from the ASSM range in Hg concentration from 0.26 to 14 μg/g (Table 2.2). The two lake sediment samples contain among the highest concentrations of Hg for sediment in this study (11 and 15 μg/g; Table 2.2), but similar Hg concentrations (10 to 14 μg/g, 10MTA10-12; Table 2.2) are found for Paglia River sediment samples collected from sites 3 to 5.5 km downstream from the ASSM (Fig. 2.3). The two lake sediment samples contain highly elevated Hg compared to the sediment sample collected upstream (10MTA06, 1.8 μg/g, Table 2.2), but the lakes are located downstream, and receive runoff, from calcine piles containing high Hg concentrations, whereas site 10MTA06 is upstream from these calcines (Fig. 2.1b). In addition, sediment collected at a site 20 km downstream from the ASSM contains a Hg concentration of 10 μg/g, but this site clearly receives sediment runoff from additional Hg mines of the Monte Amiata district located at the headwaters of other tributaries of the Paglia River (Fig. 2.1). Sediment collected upstream from the ASSM and from regional baseline sites contains significantly lower Hg concentrations (0.023-0.27 μg/g), but is generally higher than the range of concentrations of Hg of 0.0123 to 0.056 μg/g reported for upper continental crust (Rudnick and Gao, 2003). Not all samples collected upstream from the ASSM are uncontaminated with respect to Hg, for example, mineralized rocks are observed in bed load sediment at site 10MTA01 and this sample contains a Hg concentration of 0.27 μg/g, which is higher than the baseline sites (Table 2.2; Fig. 2.3). This site likely receives runoff from undiscovered Hg-bearing mineralized rock, which is to be expected in an area with abundant mines and Hg-rich mineral deposits. Higher baseline concentrations of Hg are common in areas of past Hg mining worldwide as there are many Hg deposits, rocks, and minerals in these areas that contain elevated Hg (Berzas Nevado et al., 2003; Gray et al., 2004).

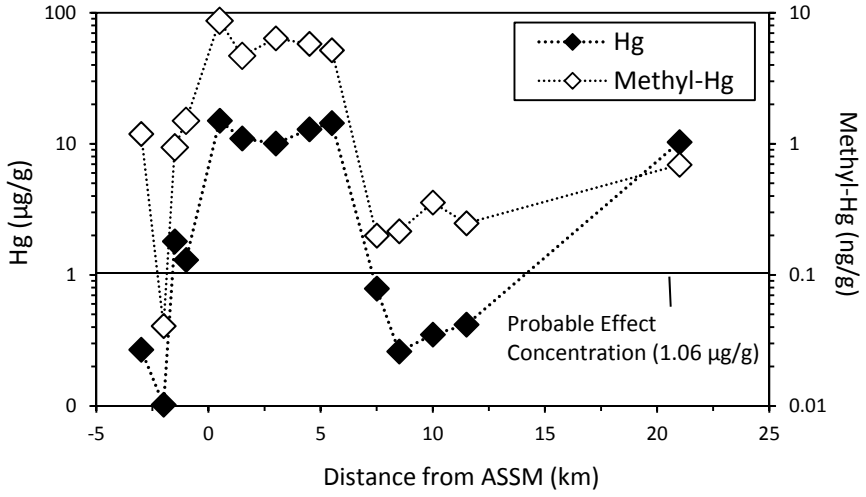

Fig. 2.3. *Concentration of methyl-Hg and Hg in sediment versus distance from the ASSM. The Probable Effect concentration (PEC) is shown for reference (MacDonald et al., 2000). Positive distances shown are downstream from the ASSM, negative distances are upstream from the ASSM.*

High concentrations of Hg found in stream sediment samples collected downstream from the ASSM are mainly the result of runoff from deposits of ASSM calcines, which were discarded on site and continue to erode into local streams. Although minor calcine is observed in streams proximal to the ASSM, Hg concentrations in stream sediment samples are generally lower than those found in ASSM calcine (Tables 2.1 and 2.2; Fig. 2.2). Concentrations of Hg in sediment samples collected from the Paglia River remain high and relatively constant for about 6 km (Fig. 2.3), followed by a sharp decrease, and an increase at site 10MTA20 about 20 km downstream from the ASSM (as previously noted, site 10MTA20 receives runoff from other Hg mines of the Monte Amiata district). The sharp decrease in the sediment Hg concentration at about 6 km downstream (0.79 µg/g, 10MTA13) is a result of increased dilution as several tributaries flow into the Paglia River from the east and north upstream from this site and the river at this site is larger with higher discharge than the sites upstream.

Concentrations of Hg in stream sediment samples collected in this study are similar to, but generally lower than, those reported in streams and rivers near other Hg districts worldwide (Table 2.3). More than 50% of stream and lake sediment samples collected downstream from the ASSM (Fig. 2.2) exceeds the PEC for Hg of 1.06 µg/g (MacDonald et al., 2000).

Stream and lake sediment samples collected downstream from the ASSM contain methyl-Hg concentrations that range from 0.20 to 8.7 ng/g (Table 2.2). Concentrations of methyl-Hg in sediment show a similar trend to that in Hg (Fig. 2.3). Concentrations of methyl-Hg in sediment show a significant correlation with TOC (r^2 =0.52, p= 0.001; Fig. 2.4), a finding

which has been observed in other studies (Olson and Cooper, 1976; Gray and Hines, 2009). Data for stream sediment samples also indicate a strong correlation between concentrations of Hg and methyl-Hg (r^2 = 0.73, p << 0.01, Fig. 2.5). These correlations indicate significant methylation of Hg and potential bioavailability of Hg in sediment of the Paglia River downstream from the ASSM, especially at sites with higher TOC.

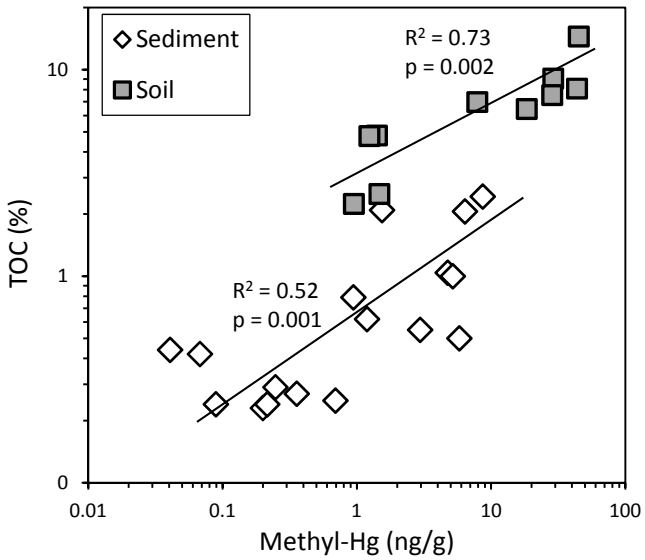

Fig. 2 4. *Concentration of methyl-Hg versus TOC for sediment and soil samples.*

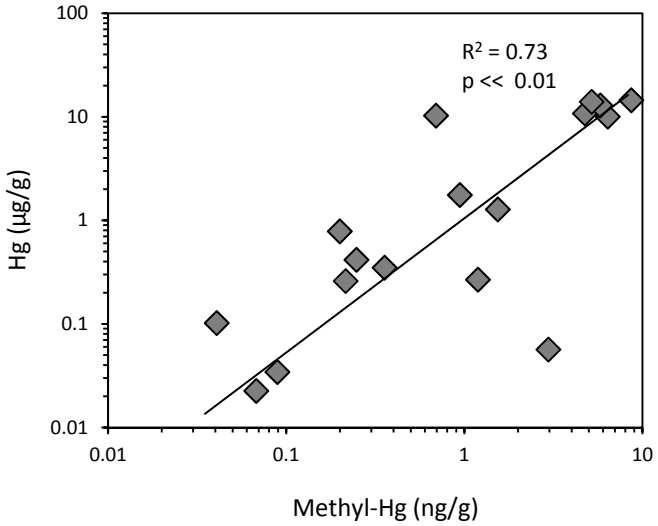

Fig. 2.5. *Concentration of methyl-Hg versus Hg in sediment samples.*

2.4.3 Soil

Soil was sampled inside the abandoned ASSM next to retort stacks in order to evaluate the extent of Hg contamination and methylation of Hg in the area. Additional soil samples were

collected from sites located more distal from the mine north and south of the town (Fig. 2.1), where there has not been any retorting activity. Concentrations of Hg in soil range from 0.64 to 400 μg/g (Table 2.1) and are highly elevated in samples collected proximal to the retort stack (150 to 400 μg/g). High concentrations of Hg in soil around other Hg mines worldwide are common (Table 2.3). For example, Hg concentrations were found to be as high as 8,889 μg/g in soil near the Almadén retort, Spain and were as high as 790 μg/g in soil in the Wanshan district, China (Table 2.3). Soil collected near the abandoned ASSM retort are enriched in Hg by several orders of magnitude when compared to the 0.01 to 0.50 μg/g range of Hg concentration reported for uncontaminated soil worldwide (Senesi et al., 1999). In addition, concentrations of Hg in soil collected north and east of the ASSM decrease consistently with increasing distance from the retort, decreasing from 14 to 0.64 μg/g at distances of 1 to 3 km. Such high Hg concentrations in soil are the result of local Hg deposition from emission of Hg via retort stacks during cinnabar ore retorting. Previous research has estimated that more than 10,000 t of Hg^0 escaped during the century-long activity at the ASSM (Ferrara et al., 1998).

Soil samples collected distal from the ASSM contain Hg concentrations less than the US EPA residential and industrial SSL's (US EPA, 2008) (Table 2.3). Conversely, concentrations of Hg in all soil samples collected proximal to the ASSM retort stack exceed the 23 μg/g US EPA residential SSL, but only one soil sample (10MTA40) exceeds the 310 μg/g US EPA industrial SSL for Hg (Tables 2.1 and 2.3). In addition, concentrations of Hg in all soil samples collected near the ASSM retort exceed the 5 μg/g Italian SSL for Hg for industrial use (Tables 2.1 and 2.3). Soil samples collected distal from the ASSM contain Hg concentrations that exceed the Italian residential SSL of 1 μg/g, with the exception of 10MTA38 that contains a Hg concentration of 0.64 μg/g (Table 2.1).

Methyl-Hg concentrations in soil in this study range from 0.95 to 45 ng/g (Table 2.1) and are higher than those reported in soil in Wanshan, China, and Southwestern Alaska, USA (Table 2.3). Methyl-Hg in soil collected near the ASSM is generally higher than that found in the stream sediment and calcine samples in this study, which is likely due to the generally higher TOC in these samples (Table 2.1). There is a significant correlation between methyl-Hg and TOC ($r^2 = 0.73$, $p = 0.002$; Fig. 2.4) in the collected soil samples that is consistent with the strong affinity of methyl-Hg for organic matter (Ullrich et al., 2001). Despite these high methyl-Hg concentrations, all soil samples in this study are considerably below the US EPA

methyl-Hg SSL of 100 (Table 2.3) for industrial soil, but 60% of the soil samples exceeds the and 7.8 μg/g residential SSL (US EPA, 2008).

2.4.4 Water

Water was collected from streams, lakes, springs, local baselines, mine adits, and from a town drinking water supply in and around the ASSM area (Fig. 2.1, Table 2.2). Water collected from streams draining the ASSM is elevated in Hg and methyl-Hg and ranges from 3.7 to 1400 ng/L and 0.10 to 3.0 ng/L, respectively (Table 2.2). Water with highly elevated Hg and methyl-Hg concentrations is collected at site 10MTA10 (Fig. 2.1) − this site was 300 m downstream from the point at which a drainage tunnel discharges water from underground workings of the ASSM (Fig. 2.1). However, the sample (10MTA11) with the highest Hg (1400 ng/L) and methyl-Hg concentration (3.0 ng/L) was located about 1.5 km downstream from the ASSM discharge tunnel, and in addition, this site was located near the point where sewage water from the town of Abbadia San Salvatore is discharged into the Paglia River.

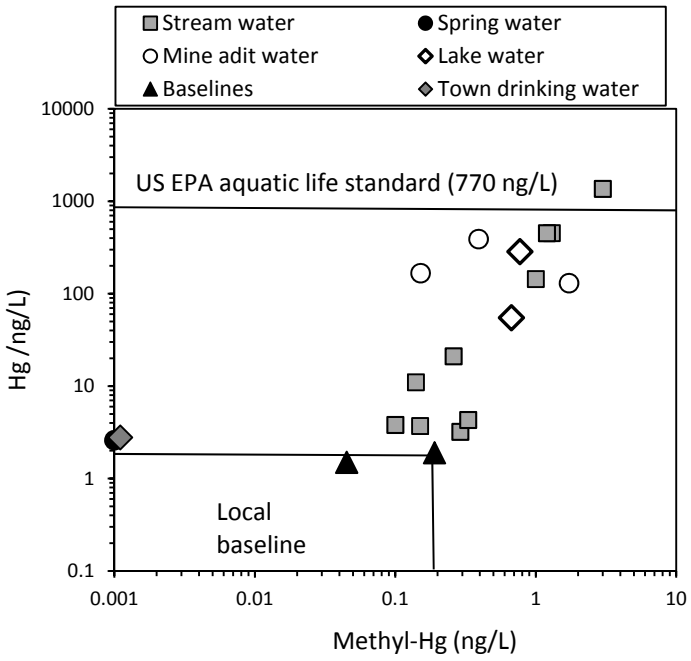

Fig. 2.6. *Concentration of Hg versus methyl-Hg in water samples collected in this study.*

Such sewage potentially influences Hg in water at this site. Stream water at site 10MTA11 was also unusually turbid, with abundant suspended particulates visible in the stream, and was likely affected by Hg attached to particulates derived from sewage discharge or by runoff from calcines in and around in the town of Abbadia San Salvatore, or both. Additional water samples collected from sites downstream from 10MTA11 on the Paglia River generally

contain decreased concentrations of Hg and methyl-Hg with increasing distance (data not shown).

Water collected from two lakes and three mine adits is also elevated in Hg and methyl-Hg and varies from 55 to 390 ng/L and 0.15 to 1.7 ng/L, respectively (Table 2.2; Fig. 2.6). Spring water (Hg = 2.6 ng/L, methyl-Hg ≤ 0.02 ng/L) and water used as a source of drinking water (Hg = 2.8 ng/L, methyl-Hg ≤ 0.02 ng/L) for the town of Abbadia San Salvatore were also collected and these samples contain Hg and methyl-Hg similar to the local baseline water samples (Table 2.2; Fig. 2.6). Concentrations of Hg in all water samples collected in this study are below established drinking water standards for Hg including (1) the 2000 ng/L drinking water standard used in the USA (US EPA, 2009b) and (2) the 6000 ng/L international drinking water standard (WHO, 2005) (Table 2.3). Only one sample (10MTA11) exceeds the Hg concentration of 770 ng/L (Fig. 2.6), the standard recommended to protect against chronic effects to aquatic wildlife in the USA (US EPA, 2009b) and this sample also exceeds the 1000 ng/L Hg concentration used as the drinking water standard of Italy (IME, 2006) − all other water samples contain Hg below these two standards (Table 2.3). There is no recommended standard for methyl-Hg in water. Concentrations of Hg and methyl-Hg in water collected from adits, lakes, and streams in and around the ASSM are elevated when compared to local baselines (Fig. 2.6) and these water data indicate significant runoff of Hg from the ASSM and transference of methyl-Hg from the sediment column to water in the area.

2.4.5 Fish

Concentrations of Hg are elevated in fish muscle collected in this study and range from 0.16 to1.2 μg/g (wet weight), and average 0.84 μg/g (Fig. 2.7). Of the fish muscle samples, 96% (66 of 70 samples) exceeds the 0.3 μg/g (methyl-Hg, wet weight) US EPA fish muscle standard recommended to protect human health (US EPA, 2009b). A subset of 17 fish muscle samples was analyzed for methyl-Hg and these data confirm that ≥90% of the Hg in these fish is methyl-Hg (Fig. 2.8), which is consistent with the conclusion of other studies indicating that 90 to 100% of Hg in freshwater fish is methyl-Hg (Fitzgerald and Clarkson, 1991). Thus, Hg concentrations in fish muscle analyzed in this study are directly comparable to the 0.3 μg/g methyl-Hg US EPA standard.

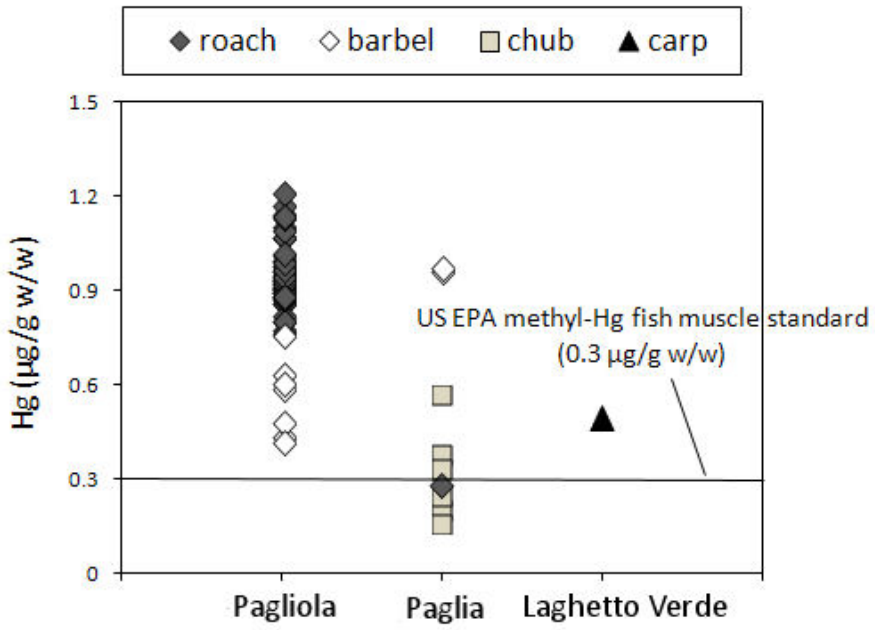

Fig. 2 7. *Concentration of Hg in fish muscle collected in the study area.*

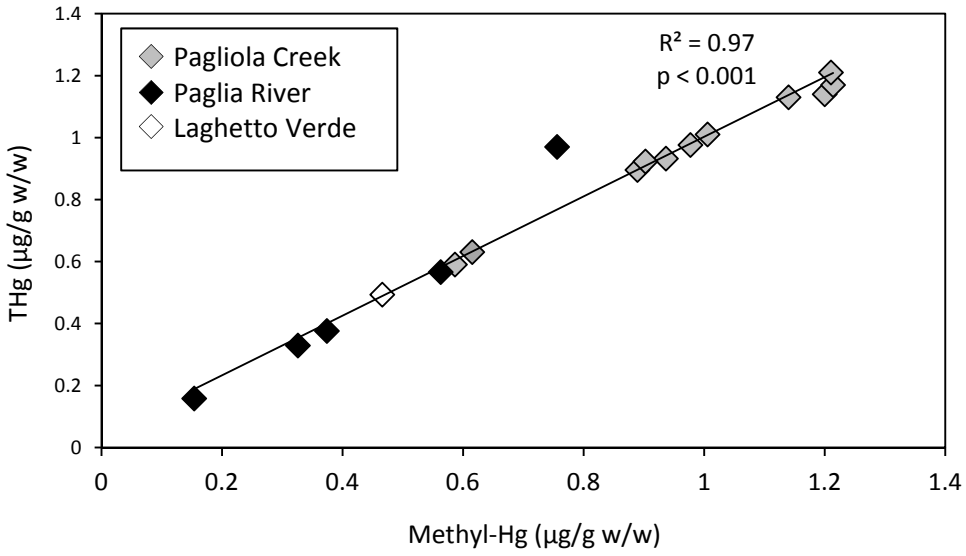

Fig. 2 8. *Concentration of Hg versus methyl-Hg in fish muscle samples collected in this study.*

Concentrations of Hg found in the fish muscle samples collected in this study are among the highest found downstream from areas mined for Hg (Table 2.3). The fish muscle Hg results found in the ASSM area are surprising considering that the fish collected are small and that they are bottom feeding, herbivorous fish. Generally, bottom feeding fish are low in the fish order and generally have lower Hg concentrations compared to higher order, carnivorous fish

(US EPA, 1997). No correlation was found for Hg in fish versus fish wet weight or Hg in fish versus fish length (data not shown).

Elevated Hg concentrations in freshwater fish collected from areas downstream from Hg mines is not unusual (Table 2.3), e.g., fish collected downstream from Hg mines in California, USA, are reported to contain Hg concentrations as high as 2.1 μg/g (muscle, wet weight) (Davis et al., 2008). In addition, elevated concentrations of Hg in fish were reported from the ASSM area as early as 1973, when Hg in fish muscle was reported to be as high as 8.0 μg/g in fish collected from the Paglia River (Bacci and Renzoni, 1973). The Bacci and Renzoni (1973) study was carried out during the time of active Hg mining and Hg retorting at the ASSM and these fish muscle data suggest that there was much higher Hg bioavailability at that time. Presently, in the ASSM area, exposure of Hg to humans consuming fish caught from Pagliola Creek and Paglia River is potentially high, although fish collected from this area are small and unlikely to be typically used for food sources. In the United States, water bodies with average fish muscle Hg concentrations exceeding 0.3 μg/g are posted with an advisory recommending against human consumption of fish caught this water body (US EPA, 1997). There is presently no human health advisory posted recommending against consumption of fish contaminated with Hg for either Pagliola Creek or the Paglia River.

2.5 Conclusions

Downstream transport of Hg from the ASSM is the dominant source of Hg to the Paglia River ecosystem. Concentrations of Hg and methyl-Hg are elevated in sediment and water in the Paglia River downstream from the ASSM, which is a result of runoff from mine-waste calcine and active methylation of Hg in this ecosystem. More than 50% of the stream sediment samples collected downstream from the ASSM in this study exceeds the PEC for Hg of 1.06 μg/g. Correlation of methyl-Hg concentrations with TOC in sediment indicates active methyl-Hg formation at sites with abundant organic matter. Concentrations of Hg in soil range from 0.64 to 400 μg/g and are highly elevated in samples collected proximal to the retort stack (150 to 400 μg/g). All soil samples collected near the ASSM retort exceed the 5.0 μg/g Italian SSL for Hg for industrial soil use, whereas most soil collected distal from the ASSM contains Hg below this industrial limit. Water collected from streams draining the ASSM is elevated in Hg and methyl-Hg and vary from 3.7 to 1400 ng/L and 0.10 to 3.0 ng/L, respectively, whereas the local baseline stream water sites varies in Hg and methyl-Hg from 1.5 to 1.9 ng/L and 0.045 to 0.19 ng/L, respectively. Of the freshwater fish collected, 96% of the fish muscle

samples exceeds the 0.3 µg/g (methyl-Hg, wet weight) US EPA fish muscle standard. Data show a progressive increase in the ratio of methyl-Hg/Hg in calcine (0.001-0.022%), stream sediment and soil (0.01-5.3%), water (0.04-10 %), and fish muscle (90-100%) (Fig. 2.9). Concentrations of Hg and methyl-Hg in fish indicate significant bioavailability and transference of Hg to fish in the Paglia River ecosystem downstream from the ASSM.

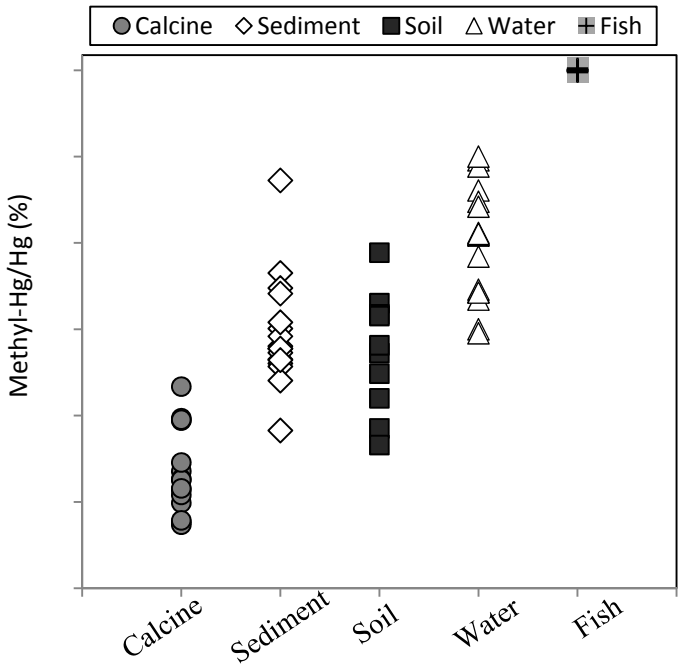

Fig. 2.9. *Ratio of methyl-Hg/Hg for calcine, sediment, soil, water, and fish of the Monte Amiata Hg district.*

Acknowledgements

This study was funded by the U.S. Geological Survey (USGS), the University of Florence, the Italian Ministry of Instruction, University, and Research (grant number MIUR PRIN 2008), and the township of Abbadia San Salvatore, Italy. Brenda Lasorsa (Battelle Marine Sciences Laboratory, Sequim, WA, USA) provided Hg and methyl-Hg analyses of samples. We thank Ian Ridley and Bronwen Wang, reviewers for the USGS, and three anonymous reviewers for Science of the Total Environment for constructive comments that helped to improve this paper. Use of trade names is for descriptive purposes and does not imply an endorsement by the U.S. Geological Survey.

References

BACCI E. AND RENZONI A. (1973). Indagine preliminare sul contenuto in mercurio totale in alcuni pesci dei fiumi del Monte Amiata. *Rass. Med. Sper.*, **20**: 60−67.

BAILEY E.A., GRAY J.E., THEODORAKOS P.M. (2002). Mercury in vegetation and soils at abandoned mercury mines in Southwestern Alaska, USA. *Geochem. Explor. Environ. Anal.*, **2**: 275−285.

BARGAGLI R., BARGHIGIANI C., MASERTI B.E. (1986). Mercury in vegetation of the Mount Amiata area (Italy). *Chemosphere*, **15**: 1035−1042.

BARGHIGIANI C. AND RISTORI T. (1994). The distribution of mercury in a Mediterranean area. In: Watras CJ, Huckabee JW, editors. Mercury Pollution: Integration and synthesis. Lewis Publishers, Boca Raton, pp. 41−49.

BERZAS NEVADO J.J., GARCIA BERMEJO L.F., RODRIGUEZ MARTIN-DOIMEADIOS R.C. (2003). Distribution of mercury in the aquatic environment at Almadén, Spain. *Environ. Pollut.*, **122**: 261−271.

BLOOM N.S. (1989). Determination of picogram levels of methylmercury by aqueous phase ethylation, followed by cryogenic gas chromatography with cold vapor atomic fluorescence detection. *Can. J. Fish. Aquat. Sci.*, **46**: 1131−1140.

BLOOM N.S. (1992). On the chemical form of mercury in edible fish and marine invertebrate tissue. *Can. J. Fish. Aquat. Sci.*, **49**: 1010−1017.

BLOOM N.S., COLMAN J.A., BARBER L. (1997). Artifact formation of methyl mercury during aqueous distillation and alternative techniques for the extraction of methyl mercury from environmental samples. *Fresenius J. Anal. Chem.*, **358**: 371−377.

BLOOM N.S. AND FITZGERALD W.F. (1988). Determination of volatile mercury species at the picogram level by low-temperature gas chromatography with cold-vapour atomic fluorescence detection. *Anal. Chim. Acta*, **208**: 151−161.

CLARKSON T.W. (1990). Human health risks from methylmercury in fish. *Environ. Toxicol. Chem.*, **9**: 957−961.

COMPEAU G.C. AND BARTHA R. (1985). Sulfate-reducing bacteria: Principal methylators of mercury in anoxic estuarine sediment. *Appl. Environ. Microbiol.*, **50**: 498-502.

DAVIS J.A., GREENFIELD B.K., ICHIKAWA G., STEPHENSON M. (2008). Mercury in sport fish from the Sacramento–San Joaquin Delta region, California, USA. *Sci. Total. Environ.*, **391**: 66−75.

EISLER R. (1987). Mercury hazards to fish, wildlife, and invertebrates: A synoptic review. U.S. Fish and Wildlife Service, Biological Report 85(1.10), 90 pp.

ESBRÍ J.M., BERNAUS A., ÁVILA M., KOCMAN D., GARCÍA-NOGUERO E.M., GUERRERO B., GAONA X., ÁLVAREZ R., PEREZ-GONZALEZ G., VALIENTE M., HIGUERAS P., HORVAT M., LOREDO J. (2010). XANES speciation of mercury in three mining districts–Almadén, Asturias (Spain), Idria (Slovenia). *J. Synchrotron Rad.*, **17**: 179−186.

FALINI F. (1960). Notizie preliminari di una campagna di indagini e ricerche per minerali di mercurio nella regione del M. Amiata (province di Siena e Grosseto). *Per. Mineral.*, **XXIX**: 19−45.

FERRARA R., MASERTI B.E., BREDER R. (1991). Mercury in abiotic and biotic compartments of an area affected by a geochemical anomaly (Mt. Amiata, Italy). *Water Air Soil Pollut.*, **56**: 219−233.

FERRARA R., MASERTI B.E., MAZZOLAI B., DI FRANCESCO F., ANDERSSON M., EDNER H., SVAMBERG S., WALLINDER E. (1999). Atmospheric mercury in abandoned mine structures and restored mine buildings. In: Ebinghaus R., Turner R.R., Lacerda D.,

Vasiliev O., Salomons W. (Eds.), Mercury Contaminated Sites Characterization, Risk Assessment and Remediation. Springer Verlag, Heidelberg, pp. 249−257.

FERRARA R., MAZZOLAI U.B., EDNER H., SVANBERG S., WALLINDER E. (1998). Atmospheric mercury sources in the Mt. Amiata area, Italy. *Sci. Total Environ.*, **213**: 12−23.

FITZGERALD W.F. CLARKSON T.W. (1991). Mercury and monomethylmercury: Present and future concerns. *Environ. Health Perspect.*, **96**: 159−166.

GILL G.A. AND BRULAND K.W. (1990). Mercury speciation in surface freshwater systems in California and other areas. *Environ. Sci. Technol.*, **24**: 1392−1400.

GOSAR M., PIRC S., BIDOVEC M. (1997). Mercury in the Idrijca River sediments as a reflection of mining and smelting activities of the Idrija mercury mine. *J. Geochem. Explor.*, **58**: 125-131.

GRAY J.E., CROCK J.G., FEY D.L. (2002). Environmental geochemistry of abandoned mercury mines in west-central Nevada, USA. *Appl. Geochem.*, **17**: 1069−1079.

GRAY J.E., GREAVES I.A., BUSTOS D.M., KRABBENHOFT D.P. (2003). Mercury and methylmercury contents in mine-waste calcine, water, and sediment collected from the Palawan Quicksilver Mine, Philippines. *Environ. Geol.*, **43**: 298−307.

GRAY J.E. AND HINES M.E. (2009). Biogeochemical mercury methylation influenced by reservoir eutrophication, Salmon Falls Creek Reservoir, Idaho, USA. *Chem. Geol.*, **258**: 157−167.

GRAY J.E., HINES M.E., HIGUERAS P.L., ADATTO I., LASORSA B.K. (2004). Mercury speciation and microbial transformations in mine wastes, stream sediments, and surface waters at the Almadén mining district, Spain. *Environ. Sci. Technol.*, **38**: 4285−4292.

GRAY J.E., PLUMLEE G.S., MORMAN S.A., HIGUERAS P.L., CROCK J.G., LOWER H.A., WITTEN M.L. (2010). In Vitro Studies Evaluating Leaching of Mercury from Mine Waste Calcine Using Simulated Human Body Fluids. *Environ. Sci. Technol.*, **44**: 4782–4788.

GRAY J.E., THEODORAKOS P.M., BAILEY E.A., TURNER R.R. (2000). Distribution, speciation, and transport of mercury in stream−sediment, stream−water, and fish collected near abandoned mercury mines in southwestern Alaska, USA. *Sci. Total Environ.,* **260**: 21−33.

HIGUERAS P., OYARZUN R., BIESTER H., LILLO J., LORENZO S. (2003). A first insight into mercury distribution and speciation in soils from the Almadén mining district, Spain. *J. Geochem. Explor.*, **80**: 95−104.

HIGUERAS P., OYARZUN R., LILLO J., SÁNCHEZ-HERNÁNDEZ J.C., MOLINA J.A., ESBRÍ J.M., LORENZO S. (2006). The Almadén district (Spain): Anatomy of one of the world's largest Hg-contaminated sites. *Sci. Total Environ.*, **236**: 112−124.

HINES M.E., HORVAT M., FAGANELI J., BONZONGO J-C.J., BARKAY T., MAJOR E.B., SCOTT K.J., BAILEY E.A., WARWICK J.J., LYONS W.B. (2000). Mercury Biogeochemistry in the Idrija River, Slovenia, from above the Mine into the Gulf of Trieste. *Environ. Res. A*, **83**: 129−139.

HORVAT M., LIANG L., BLOOM N.S. (1993). Comparison of distillation with other current isolation methods for the determination of methyl mercury compounds in low level environmental samples: part II. Water. *Anal. Chim. Acta*, **282**: 153−168.

HORVAT M., TOMAN M., STERGARŠEK J., KOTNIK J., FAJON V., GIBIČAR D. (2004). Mercury and selenium in fish species in the Idrijca river polluted due to past mercury mining. *RMZ - Materials and Geoenvironment*, **51**: 1073−1077.

IME (2006). Decreto legislativo 3 aprile 2006, n. 152: Norme in materia ambientale. Gazzetta Ufficiale della Repubblica Italiana n. 88 del 14-4-2006, suppl. ord. n. 96, Titolo V, All.5. Tab. 1. Istituto Poligrafico dello Stato, Roma.

KIM C.S., BLOOM N.S., RYTUBA J.J., BROWN G.E., JR. (2003). Mercury Speciation by X-ray Absorption Fine Structure Spectroscopy and Sequential Chemical Extractions: A Comparison of Speciation Methods. *Environ. Sci. Technol.*, **37**: 5102−5108.

KIM C.S., BROWN G.E., JR., RYTUBA J.J. (2000). Characterization and speciation of mercury-bearing mine wastes using X-ray absorption spectroscopy. *Sci. Total Environ.*, **261**: 157−168.

KLEMM D.D. AND NEUMANN N. (1984). Ore-controlling factors in the Hg–Sb province of southern Tuscany, Italy. In: Wauschkuhn A. et al. (Eds.). Syngenesis and Epigenesis in the Formation of Mineral Deposits. Springer-Verlag, Heidelberg, pp. 482−503.

LEERMAKERS M., MEULEMAN C., BAEYENS W. (1996). Mercury distribution and fluxes in Lake Baikal. In: Baeyens W, Ebinghaus R, Vasiliev O, editors. Global and Regional Mercury Cycles: Sources, Fluxes and Mass Balances. Kluwer Academic Publishers, Dordrecht, Netherlands, pp. 303−315.

LYONS W.B., WELCH K.A., BONZONGO J.C. (1999). Mercury in aquatic systems in Antarctica. *Geophys. Res. Lett.*, **26**: 2235−2238.

MACDONALD D.D., INGERSOLL C.G., BERGER T.A. (2000). Development and evaluation of consensus-based sediment quality guidelines for freshwater ecosystems. *Arch. Environ. Contam. Toxicol.*, **39**: 20−31.

MASON R.P., LAPORTE J.M., ANDRES S. (2000). Factors controlling the bioaccumulation of mercury, methylmercury, arsenic, selenium, and cadmium by freshwater invertebrates and fish. *Arch. Environ. Contam. Toxicol.*, **38**: 283−297.

MORTEANI G., RUGGIERI G., MÖLLER P., PREINFALK C. (2011). Geothermal mineralized scales in the pipe system of the geothermal Piancastagnaio power plant (Mt. Amiata geothermal area): a key to understand the stibnite, cinnabarite and gold mineralization of Tuscany (central Italy). *Miner. Deposita*, **46**: 197–210.

NAS (1978). An Assessment of Mercury in the Environment. Washington, D.C.: National Academy of Sciences, National Research Council, 185 pp.

OLSON B.H. AND COOPER R.C. (1976). Comparison of aerobic and anaerobic methylation of mercuric chloride by San Francisco Bay sediments. *Water Res.*, **10**: 113−116.

PAINTER S., CAMERON E.M., ALLAN R., ROUSE J. (1994). Reconnaissance geochemistry and its environmental relevance. *J. Geochem. Explor.*, **51**: 213−246.

QIU G., FENG X., WANG S., SHANG L. (2005). Mercury and methylmercury in riparian soil, sediments, mine-waste calcines, and moss from abandoned Hg mines in east Guizhou province, southwestern China. *Appl. Geochem.*, **20**: 627−638.

QIU G., FENG X., WANG S., FU X., SHANG L. (2009). Mercury distribution and speciation in water and fish from abandoned Hg mines in Wanshan, Guizhou province, China. *Sci. Total Environ.*, **407**: 5162−5168.

RUDNICK S. AND GAO S. (2003). Composition of the continental crust. In: Holland H.D., Turekian K.K. (Eds.), The Crust, Treatise on Geochemistry, Vol. 3. Elsevier, Oxford, pp. 1–64.

RYTUBA J.J. (2000). Mercury mine drainage and processes that control its environmental impact. *Sci. Total Environ.*, **260**: 57−71.

RYTUBA J.J. (2003). Mercury from mineral deposits and potential environmental impact. *Environ. Geol.*, **43**: 326–338.

SENESI G.S., BALDASSARE G., SENESI N., RADINA B. (1999). Trace element inputs into soils by anthropogenic activities and implications for human health. *Chemosphere*, **39**: 343-377.

ULLRICH S.M., TANTON T.W., ABDRASHITOVA S.A. (2001). Mercury in the Aquatic Environment: A Review of Factors Affecting Methylation. Crit. Rev. *Environ. Sci. Technol.*, **31**: 241–293.

US EPA (1997). Mercury study report to Congress. U.S. Environmental Protection Agency, I-VIII, EPA-452/R-97-003.

US EPA (2002). Method 1631, Revision E: Mercury in water by oxidation, purge and trap, and cold vapor atomic fluorescence spectrometry. U.S. Environmental Protection Agency, EPA 821-R-02-019.

US EPA (2008). Human health medium specific screening levels. U.S. Environmental Protection Agency.

US EPA (2009a). Mercury in Solids and Solutions by Thermal Decomposition, Amalgamation, and Atomic Absorption Spectrophotometry in Test Methods for Evaluating Solid Waste. U.S. Environmental Protection Agency, Office of Solid Waste and Emergency Response. Washington, D.C.

US EPA (2009b). National Recommended Water Quality Criteria. U.S. Environmental Protection Agency.

WHO (1976). Environmental health criteria. Vol.1. Mercury. World Health Organization, Geneva, Switzerland.

WHO (2005). Mercury in Drinking-water. WHO/SDE/WSH/05.08/10. World Health Organization, Geneva, Switzerland.

CHAPTER 3

PART II - MASS LOADS OF DISSOLVED AND PARTICULATE HG (AND AS AND SB) IN THE MT. AMIATA MINING DISTRICT, SOUTHERN TUSCANY (ITALY)

Abstract

Total dissolved and particulate mercury mass balances are estimated in different hydrological seasons (March and September 2011 and March 2012) in the Paglia River Basin (PRB) (Central Italy). Paglia River drains one of the largest Hg-rich region worldwide: the Mt. Amiata ore district. Quantification of Hg mass loads in this Hg mine district can allow to: (1) identify the contamination sources, (2) evaluate the effect of Hg on the environment, and (3) determine those processes able to affect Hg transport. Our data indicate that up to 34 g d^{-1} of Hg is transported during the rainy season as a result of direct drainage of the former Abbadia San Salvatore Mine (ASSM), which mainly contributes to the Hg concentrations measured in the Paglia River. Specifically, up to 99% of Hg is transported as particulate Hg. The observed Hg fluxes in the PRB are up to 100 times higher than those that would derive only by natural denudation processes of rocks and soils. Spatial distribution of Hg loads indicate that particulate Hg is deposited along the river course, forming a natural sink from where it is later re-suspended, possibly with partitioning to the dissolved phase. In low flow conditions, Hg deriving from this sink results in fluxes in the PRB that are directly comparable to those provided by rainfall. However, extraordinary hydrologic conditions (prolonged absence of rainfall) can severely reduce the amount of Hg transported in the basin, as evidenced in March 2012, when Hg loads are 20-fold lower than in March and September 2011. The mechanism of Hg transport in the basin appears however similar in all sampling seasons, suggesting that the water flow controls only the quantities of Hg mobilized rather than the way it is transported. Preliminary estimation of yearly Hg flux shows that up to 11 kg of Hg can directly be related to downstream transport by ASSM during baseline conditions.

Keywords: mercury, mass loading, particulate matter, Mt. Amiata

3.1 Introduction

Mercury (Hg) is a heavy metal of environmental concern due to its elevated toxicity to humans and living organisms (WHO, 1976). Differently from other metals, Hg has no known biological functions (Eisler, 1987). In natural environments, the key reaction is the conversion of Hg to methyl−Hg, which bioaccumulates and biomagnifies in the aquatic organisms, as fish (US EPA, 1997). Seafood consumption thus is the major route of methyl-Hg to humans (e.g. Holmes, 2009). The Mediterranean basin is characterized by a wide Hg geochemical anomaly, mainly represented by the large cinnabar deposits of Almadén (Spain), Idrija (Slovenia), Izmir and Kenya (Turkey), Medjerda (Tunisia), and Mt. Amiata (Italy) (Cossa and Coquery, 2005). Approximately 65% of the world's Hg resources are located in the Mediterranean region (Ferrara et al., 1997), which occupies only 1% of the total Earth's surface area (Renzoni et al., 1998). This mercuriferous belt is claimed to be partly responsible of the high concentrations of MMHg in seafood (Ferrara et al., 1991), that are twice those of the same species living in the Atlantic Ocean (Horvat et al., 2003; Cossa and Coquery, 2005), thus representing a risk for people living in this area and consuming large amount of local seafood (Renzoni et al., 1998). Other authors suggest that the elevated water temperatures of the Mediterranean Sea (about 10 °C warmer than those of Atlantic Ocean for the same depth) are responsible for the particularly elevated methyl-Hg rates in this ecosystem (Bacci, 1989; Cossa et al., 1997; Horvat et al., 2003), and consequently accumulation in local fish. Studies of Hg geochemistry in the Mediterranean Sea started in the early 1970s with the Mediterranean Action Plan of the UNEP's Regional Seas Programme, in order to delineate the cycle, the distribution, and particularly to identify the principal Hg sources to the basin. Besides atmospheric inputs and direct discharges of wastewater effluents, rivers resulted to be important contributors of Hg to the sea, carrying Hg mainly as a result of runoff from contaminated wastes (UNEP/WHO, 1996). First attempts to estimate Hg delivered by rivers reported up to 130 t yr^{-1} (UNEP/ECE/UNIDO/FAO/UNESCO/WHO/IAEA, 1984), which are now considered largely overestimated (Bacci, 1989). Following more recent studies (Cossa and Coquery, 2005; Rajar et al., 2007), between 8 and 14 t yr^{-1} are presently discharging by European rivers to the Mediterranean Sea. While rivers with considerable annual Suspended Particulate Matter (SPM) discharges were considered in these calculation, as Po (Italy), Isonzo (Slovenia-Italy), Rhone (France), Ebro (Spain) and Nilo (Egypt), rivers draining the most important Hg mining districts were generally overlooked, with the exception of the Isonzo River. Only indirect estimates about Hg loads of Tiber River have been provided

(Cossa and Coquery, 2005), notwithstanding it receives waters from the Paglia River, which drains the Mt. Amiata Hg district (Southern Tuscany, Italy), that is considered the 4th worldwide largest Hg producing district. However, high Hg in particulate matter carried on for decades after the end of mining (Gray et al., 2000; Faganeli et al., 2003; Covelli et al., 2007) suggests that detailed estimates of Mediterranean Hg budget cannot disregard Hg delivered by streams draining Hg districts. For example, Hg loads are estimated as high as 1,500 kg yr^{-1} for the Isonzo River (Idrija Hg mine, Slovenia; Širka et al., 1999), 4−30 kg yr^{-1} for the Guadalupe River (New Idrija Hg mine, USA; Thomas et al., 2002), and up to 470 kg yr^{-1} for the Sacramento River (California Coast Ranges mines, USA; Choe et al., 2003; David et al., 2009). However, the derivation of mass loads on a yearly time scale faces with the impossibility of performing continuous monitoring of hydrological parameters, as SPM, whose fate is strictly related to that of Hg although its temporal variability is enormous, and difficult to be predicted (Horowitz et al., 2001). Therefore, approximations are made in most of the studies, e.g. SPM annual fluxes are estimated from discrete measured values (Širca et al., 1999; Ganguli et al., 2000; Choe et al., 2003), derived from log-log regressions relating SPM to discharge or Hg water contents to SPM (Wall et al., 2005; David et al., 2009), or derived by indirectly analysis of topography, rainfall and land use (Thomas et al., 2002).

At a local scale, quantification of metal loadings to streams in a mining district is particularly important, because it offers the opportunity to identify contaminant sources, and to assist in decisions about remediation of contaminated areas. The main requirement for a reliable load estimation is the accurate measurement of the flow discharge as it mainly influences the final calculation. In mountain streams, where mines are generally located, flow discharge measurements by flow meters are particularly complicated by the presence of cobbles of river bottom, pools and riffles (Kimball, 1997). Moreover, flow meters do not account for the hyporheic flux, resulting in an underestimation of the flow discharge (Bencala et al., 1990). In these conditions, tracer-dilution techniques provide an accurate estimate of flow discharge, and they are applied since many years to detail metal loadings from mine drainage (Kimball et al., 2001; 2009; 2010). Recently, this method was applied in Southern Tuscany to the Merse River (Kimball et al., 2007), as the whole region is affected by centuries of mining activities (Tanelli, 1983). To the best of our knowledge, this is the only published case where this technique was used in the field of the Italian environmental geosciences.

In this study, tracer-dilution methods are applied to the Paglia River, as common to other Hg districts worldwide, mining of Hg has extensively affected the Mt. Amiata area and this watershed; high concentrations of Hg in sediments and waters of Paglia River and active

formation of methyl−Hg were recently documented by Rimondi et al. (2012). Therefore, the aims of this study are to (1) quantify the mass load of Hg in the Paglia River, and (2) evaluate the downstream transport of Hg and potential contamination of river sediment.

3.2 Study site

The Paglia River Basin (PRB) covers an area of about 1,330 km^2 between three Italian regions, Tuscany, Umbria and Latium, and is the major tributary of the Tiber River, the third river for length of Italy, which flows directly to the Mediterranean Sea (Fig. 3.1a). The upper sector of PRB is part of the NW−SE trending Radicofani basin tectonic depression, derived by the Pliocene and Pleistocene development of Northern Apennines orogenesis (e.g. Pascucci et al., 2006), and filled up with marine sediments of the Early Pliocene (River Paglia Unit; e.g. Castaldi and Chiocchini, 2012). Olistostromes of the Late Cretaceous-Eocene allochtonous formations of Santa Fiora Flysh (Ligurian Units) are recognized in the upper sector of the basin (Castaldi and Chiocchini, 2012), together with the Quaternay volcanic rocks related to the magmatic activity of Mt. Amiata volcano, the shoshonite and ultra-potassium latite lavas of the Radicofani neck (e.g. D' Orazio et al., 1994), and the potassic lavas of the Roman Magmatic Province (e.g. Peccerillo, 2002). The latter occur in the southern sector of the watershed. The Ligurian Units (Oligocene−Late Cretaceous), composed by ophiolites and associated pelagic sequence and calcareous turbidites, border the RB and generally overly the Tuscan Nappe, consisting of a metamorphic basement (Carboniferous-Lower Triassic), a Mesozoic carbonate-evaporite sequence and Oligocene-Middle Miocene sandstones (Macigno formation).

The head of the Paglia River is located at Mt. Amiata (1,048 m s.l.), where it starts as Pagliola Creek. After ~5 km it forms the Paglia River as it is fed by the Cacarello Creek (Fig. 3.1b). The Paglia River represents the most important water collector of the eastern side of volcanic−geothermal area of Mt. Amiata. Mercury ore bodies in Mt. Amiata consist essentially of cinnabar, while common non-economic minerals are As-sulphides (realgar and orpiment), and stibnite (Arisi Rota et al., 1971; Morteani et al., 2011). For about 1/3 of its length, Paglia River is fed by creeks draining the Hg mines: Pagliola (Abbadia San Salvatore mine), Minestrone (Cerro del Tasca mine), Senna (Senna mine) Siele (Siele mine), and Stridolone (Cornacchino and Poggiali mines) (Fig. 3.1a). The Paglia River system has a torrential character (mean slope of 8%), particularly in the tract of Pagliola Creek, while downstream the river shows a larger waterbed with a mean slope of 1%. This area is characterized by a Mediterranean (temperate) climate (hot and dry summer; cold and rainy

winter). Data from the thermo−pluviometric station of Abbadia San Salvatore (825 m a.s.l.) indicate that the mean annual temperature (1953−2000 period) is 10.5 °C with a mean annual precipitation of 1,480 mm (1925−2000 period) in 105 rainy days (Ciccacci et al., 2009). About 2/3 of annual total precipitation is concentrated in the semester autumn−winter (Ciccacci et al., 1988). The concomitance of multiple rainy days after the dry summer periods, scarce vegetation cover and erodible underlying lithologies induces severe denudation processes in this area and leads to the formation of peculiar landform morphologies, called *biancane* and *calanchi* (Ciccacci et al., 2009).

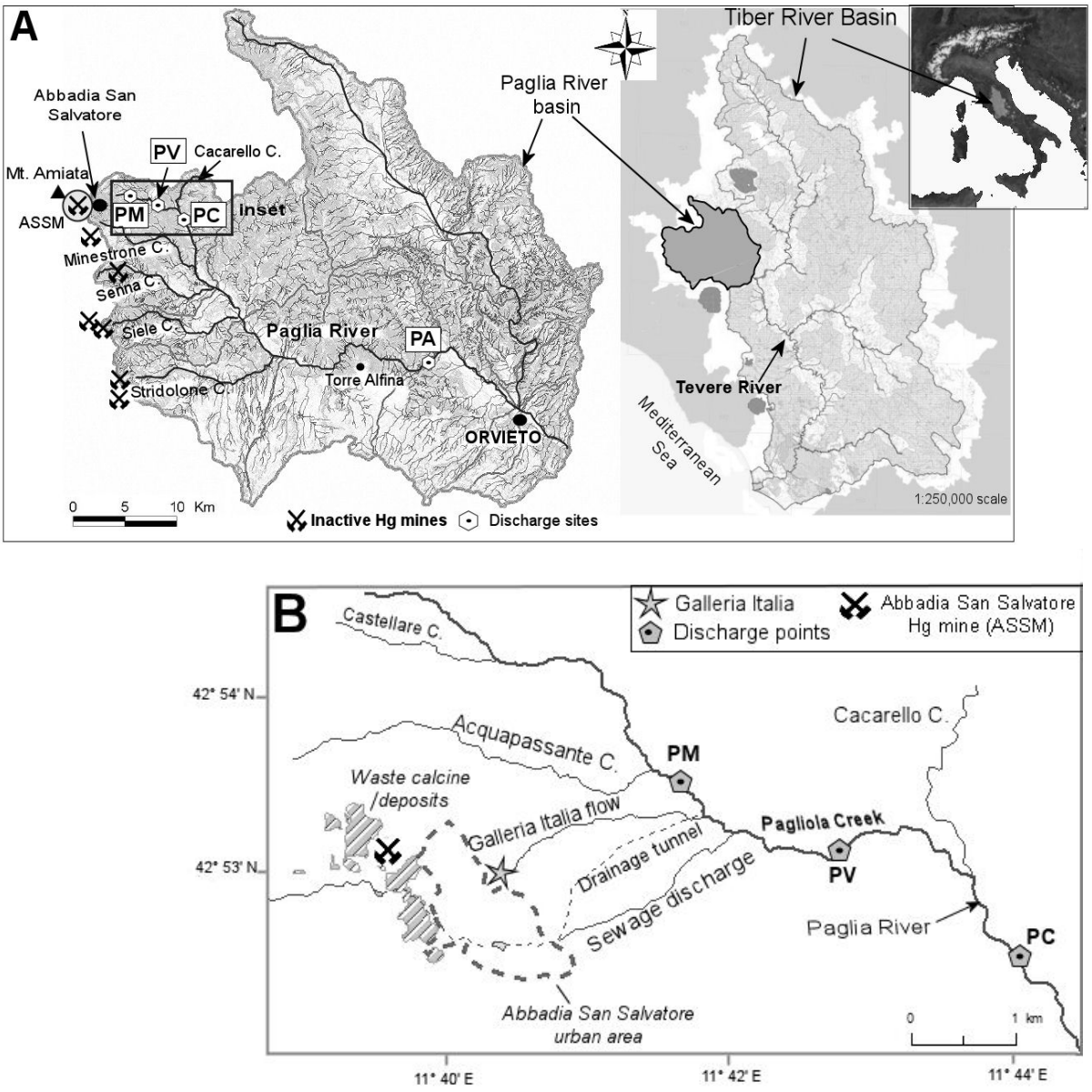

Fig. 3.1 a,b. *Schematic map of the Tiber River and Paglia River basins (A), the Mt. Amiata Hg district, Abbadia San Salvatore mine (ASSM), and sites of river discharge measurements, PM, PV, PC, PA (see text for explanation of labels) located 5, 6 and 35 km downstream from ASSM, respectively. Panel B shows a detail of the rectangular inset in (A).*

This study focuses on the upper part of PRB, which is directly impacted by the past mine activity of ASSM, and represents the most outstanding Hg mine of the whole basin. In the first kms of its course, Pagliola Creek is fed by waters of the Galleria Italia. This water discharge represents the drainage system of the ASSM as it collects all waters from the underground working tunnels. A second drainage system, located at the base of Abbadia San Salvatore, named Galleria Ribasso, is presently dry. A tunnel draining the mining area and associated waste calcine piles, and the sewage system of the town are additionally discharging their waters to the Pagliola Creeks (Fig. 3.1b). Due to the torrential regime of the upper part of the Paglia River (Moretti et al., 1988), hydrological periods are difficult to be defined. In particular, in association with powerful rainy events floods, flash floods and associated sliding like mud- and debris-flows are described (Di Tria et al., 1999). Such events, coupled with the severe denudation processes that characterize this area, lead to elevated transport of suspended material to the Paglia River. Up to the conjunction with Cacarello Creek, water discharges are relatively constant throughout the year because waters from the Galleria Italia and the sewage system are the main water suppliers to the Paglia River. Downstream, discharges are affected by rainfall, the lowest and highest water levels being recorded at the end of summer time (September-October) and in winter and spring (November-March), respectively.

3.3 Materials and methods

3.3.1 Sampling sites and procedures

Surface water samples were collected to study the spatial and temporal changes in concentrations, partitioning and load of Hg and other trace metals, such as As and Sb. All samples were referred to the distance from the ASSM, which likely represents the main local punctual source of Hg to the river course of Paglia. Water samples were collected in four sites along the Paglia River (Fig. 3.1a, b): (1) one site upstream ASSM that can be referred to a "background" site for the Amiata region (Pagliola Monte, PM); (2) two sites located just downstream ASSM, in order to quantify the mass loads of runoff from the ASSM (Pagliola Valle, PV, Paglia Casetta, PC), and (3) one site at the end of the Hg district (Paglia Allerona, PA), which was collected to account for all Hg runoff from the southeastern part of the Mt. Amiata district (Fig. 3.1a, b). As no stations for continuous monitoring of flow discharge were available in this area, sampling campaigns were carried out in order to sample the most different water flow conditions, i.e. March 2011, after abundant rainfall occurred during winter and spring times, and at the beginning of September 2011, after almost three months of

drought. The 2011 samplings represent therefore the baseline conditions for Paglia River. The 2012 spring was characterized by a striking hydrological deficit for the Tuscany watersheds, due to the scarce precipitations occurred in the autumn- spring seasons. As a consequence, the last campaign was performed in March 2012 and aimed to define how mass loads varied as result of the prolonged absence of rainy events. Therefore, the data obtained for the latter campaign are representative of extraordinary flow conditions for the Paglia River.

Ancillary parameters were collected at each sampling station. Temperature, pH and electrical conductivity were measured in the field. For each sampling site three aliquots of water were filtered in the field with 0.45 μm membrane filters, as follows: (1) 50 mL to determine the main cations and NH_4^+, acidified with 0.5 % concentrated Suprapur HCl; (2) 50 mL to determine dissolved As, acidified in the field with 0.5 % concentrated Ultrapure HCl; (3) 50 mL to determine all the dissolved trace elements but As (Li, B, Al, Cr, Mn, Fe, Co, Ni, Cu, Zn, Mo, Ag, Cd, Ba, Te, Tl, Pb, Bi, U), acidified in the field with 1% concentrated Ultrapure HNO_3. Four additional aliquots of unfiltered waters were then sampled: (1) 125 mL to determine the main anions, F^- and Br^-; (2) 50 mL to determine total As, acidified in the field with 0.5 % concentrated Ultrapure HCl and 1% concentrated Ultrapure HNO_3; (3) 50 mL to determine all the total trace elements but As (Li, B, Al, Cr, Mn, Fe, Co, Ni, Cu, Zn, Mo, Ag, Cd, Ba, Te, Tl, Pb, Bi, U), acidified in the field with 1% concentrated Ultrapure HNO_3; (4) 2L to determine SPM. Waters for trace elements were collected in acid pre-cleaned high-density PE bottles, while samples for SPM were transported from the sampling sites on ice, and preserved at 4 °C until analysis. As explained before, in this study we refer to dissolved constituent concentration as the accepted fraction passing the 0.45 μm-filter (Stordal et al., 1996). It should be pointed out that this cutoff may result in an overestimation of the truly dissolved concentrations (Stordal et al., 1996), due to the presence of colloids passing this filter pore size (Cidu and Frau, 2009).

All mercury sampling and analysis were performed following the appropriate "clean hands−dirty hands" procedures (US EPA, 1996). Waters for total Hg (Hg_T) and dissolved Hg (Hg_D) were collected in US EPA certified pre−cleaned bottles double packed in zip−lock bags. Water filtration was made in the field by means of 0.45 μm sterilized cellulose membrane filters. Samples for Hg analysis were then stored at 4 °C, and later acidified within 8 h of collection with Baker Instra-Analyzed HCl, using a final acid concentration of 0.5% v/v. Particulate Hg fraction (Hg_P) was obtained by the difference between total Hg

(particulate + dissolved) and total dissolved Hg. The concentration of Hg on SPM particles [Hg_{SPM}], in units of µg/g, was then determined as $[Hg_{SPM}] = \frac{[Hg_P]}{[SPM]}$.

3.3.2 Analytical methods

Major cations (Ca^{2+}, Mg^{2+}, Na^{+}, K^{+}), NH_4^{+}, anions (SO_4^{2-}, Cl^{-}, NO_3^{-}), Br^{-} , and F^{-} were determined by ion chromatography (Methom 861 and 761, respectively), and HCO_3^{-} by automatic titration with 0.01 M HCl (Metrohm basic Titrino 794). Analytical errors calculated as the difference between the sum of cations plus that of anions (Appelo and Postma, 1993), expressed in meq/L (TZ^{+}, TZ^{-}), were below the accepted limit of 5%. Concentration of Hg in water samples was determined using cold−vapor atomic fluorescence spectrometry (CVAFS) following EPA method 1631e (US EPA, 2002). Both the unfiltered and filtered water samples were digested for total mercury by subjecting them to bromine monochloride oxidation for a minimum 24 hours. Mercuric ions in the oxidized sample were reduced to Hg^0 with $SnCl_2$, and then purged onto gold−coated sand traps as a means of preconcentration and interference removal. Mercury vapor was thermally desorbed to a second "analytical" gold trap, and from that into a fluorescence cell (Bloom, 1989). Recoveries for Hg on blank spikes were 96–113% and 98−109% on matrix spike. The relative percent difference in water sample replicates was less than 5%. The SRM NIST 1641d was analyzed with the samples, and Hg recovery was 97–105% of the certified value. Method blanks were below the lower limit of determination of 0.1 ng/L for Hg.

SPM, expressed in mg/L, were calculated by two independent laboratories, Battelle Marine Science (Washington, USA) and Dipartimento di Scienze della Terra of Firenze (Italy) in order to check for consistency. Battelle lab followed the Standard Methods for the Analysis of Water and Wastewater Method 2540D (Eaton et al., 1999). A known volume of water was siphoned onto a pre−weighed 0.45 µm glass fiber filter. Then the filters were dried at 105°C for 24 hours and weighed to determine the mass of the suspended solids. Slight modifications to the method were made by the Dipartimento di Scienze della Terra, which employed 0.45 µm acetate cellulose filters, that were dried at 60°C up to reach a constant weight. Results between these two labs were well consistent, as differences between analytical values were <10%. Acetate filters were then directly analyzed for trace elements by a complete dissolution with *aqua regia* (HCl/HNO_3 3:1 v/v) for 3h. Concentrations of trace elements metals on SPM were then calculated by subtracting the average metal concentrations of blank filters.

Concentrations of trace elements in waters and particulate water (Li, B, Al, Cr, Mn, Fe, Co, Ni, Cu, Zn, Mo, Ag, Cd, Ba, Te, Tl, Pb, Bi, U) were determined by ICP−MS and hydride generation ICP–MS (As). Concentrations of Fe were determined by both ICP-MS and ICP-OES to avoid instrumental interferences at low concentrations. The detection limits varying according to the instrument performances, and the values obtained for each analytical sequence are reported in tables and calculated as 10 times the standard deviation of the blank solutions. Both precision and accuracy were evaluated using the standard reference solutions NIST1643e and E-S-2 (SP Science). Estimated analytical errors were less than 10%. Field blank solutions were prepared for each campaign, and analyzed to check contamination during sampling.

3.3.3 Discharge measurements and mass flux calculations

In this study different methods were applied to sites PM, PV, PC and PA in order to accurately determine flow discharges. In order to prevent underestimation of the real water flows by flow meters, both flow meters and tracer dilution method were applied at sites PM, PV and PC, located in the mountain part of the Paglia River. At PA the discharge was measured by the Istituto Idrografico Regionale of Umbria using a magnetic flow meter, as the great width of the river prevented the use of the tracer dilution technique at this site. Due to the extremely low flow at site PM during the dry season, the flow was in this case estimated by measuring the time employed for water to fill up a bucket of 5 L.

Dilution measurements were made through injection of a specific tracer (NaCl) as a slug injection (Hudson and Fraser, 2005). In this approach the tracer is added in the stream as a near−instantaneous slug or gulp. Ordinary NaCl salt was chosen as a tracer because of i) its low cost; ii) the easiness of detection at small concentrations by common conductivity meters (Wood and Dykes, 2002), and iii) the low concentrations of Na and Cl that characterized these waters. In each of the five measurements, between 3 and 7 kg of salt were dissolved in approximately 30 L of stream water in order to have a net increase of conductivity with respect to baseline. After the solution was careful homogenized to allow complete salt dissolution, it was injected in the stream. The electrical conductivity was measured about 100−150 m downstream from the salt injection point, a distance that allowed a lateral and longitudinal thorough mixing of tracer solution (Hudson and Fraser, 2002), at 10s time interval starting from the time the salt was added to the stream. Conductivity curves were reconstructed in the field with two electrical conductivity meters for each sample site in order to account for any inhomogeneous distribution of the salt wave (Kilpatrick et al., 1989;

Kilpatrick, 1993). During the experiment, water samples were collected to reconstruct specific calibration constants for each site and conductivity meter, through the analysis of chloride by ion chromatography in laboratory. The following equation, based on the mass balance principle, was then applied to compute the stream discharge (Q) (Kilpatrick and Cobb, 1985; Kite, 1993):

$$Q = \frac{M}{\int_0^T K \times (EC_T - EC_0)\, dt} \quad (1)$$

where M is the mass of salt added to the stream expressed as Cl^- mass, EC_T is the conductivity at time t during the passage of salt wave, EC_0 is the baseline conductivity, and K is the calibration factor to convert EC to Cl^- concentrations. This denominator particularly defines the area of the salt wave curve reported as an example in Fig. 3.2. The discharge values reported in this study were expressed as the average of results obtained by the two salt curves.

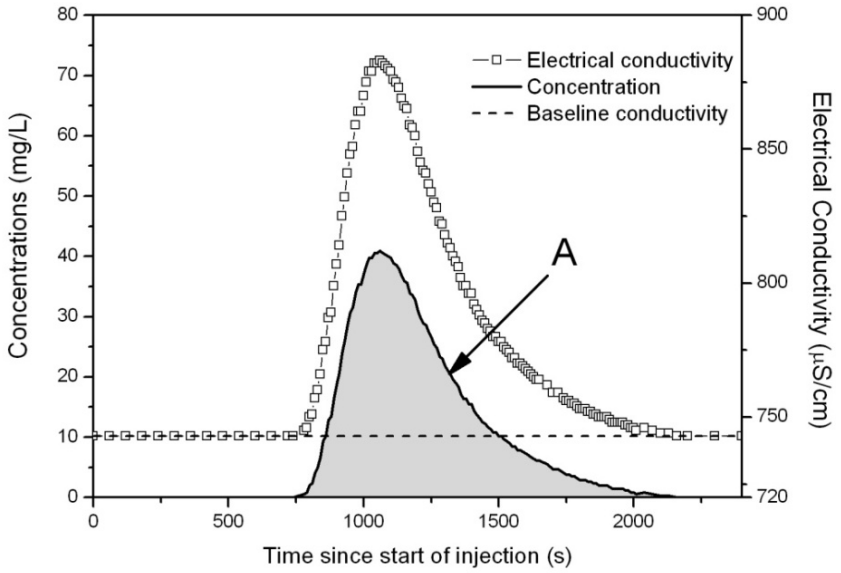

Fig. 3.2. *Electrical conductivity and related extrapolated Cl^- curves obtained for site PC during March 2012. The shadow area is the quantity that must be calculated in equation 1.*

Daily loadings of Hg and other trace elements were calculated assuming that the measured values for discharges, trace elements concentrations in water and in particulate matter were constant for 24h. Dissolved and particulate loads were then calculated by the following equations:

$$FM_D = ([Me_D] \times Q) \quad (2)$$

$$FM_P = ([Me_{SPM}] \times Q_{SPM}) \quad (3)$$

where [Me_D] corresponds to the concentrations of metal in the dissolved form, Q to the water discharge for 24h, [Me_{SPM}] to the concentration of selected element on suspended matter, and Q_{SPM} to the daily discharge of SPM. The sum of (2) and (3) represented the total load of that particular element in the stream.

3.4 Results and discussion

3.4.1 Major chemistry and hydrology

Sampling dates, distance from the ASSM, temperature, pH, conductivity, Total Dissolved Solids (TDS), main cations and anions, NH^{4+}, Br^- and F^- are reported in Table 3.1. Values of pH vary between 7.9 and 8.8, indicating an alkaline environment, which is typical of worldwide freshwater systems draining carbonate formations (Drever, 1997). Cations are mostly represented by Ca^{2+} (~ 67% of TZ^+), followed by Mg^{2+} (~ 18%), Na^+ (~ 13%), and K^+ (~ 3%), whereas anions mainly consist of HCO_3^- (~ 51% of TZ^-), SO_4^{2-} (~ 42%), and Cl^- (~ 7%). Accordingly, the Langelier-Ludwig diagram (Langelier and Ludwig, 1942) indicates that most of the waters are (Ca^{2+} + Mg^{2+})– HCO_3^- in composition (Fig. 3.3), suggesting their circulation in the Mesozoic carbonatic formations of the Tuscan sequence (Frondini et al., 2009). The waters of PC and PV sites collected during the dry seasons (September 2011 and March 2012) are however shifted to the quadrant of sulphate-rich waters, pointing toward the Ca-SO_4 end-member, represented by the Galleria Italia waters (Fig. 3.3). This observation highly indicates mixing of river waters with those coming from the drainage system of the Abbadia mine, whose composition is likely affected by the circulation in the carbonate-evaporite formations of the Tuscan sequence. Main changes in water geochemistry are in particular observed during the low water discharge seasons when the Galleria Italia input is not diluted by the Paglia River Ca-HCO_3 waters. The highest concentrations of nitrogen species, as NO_3^- and NH_4^+, are similarly observed during the dry season of Paglia River, and particularly for sites PV and PC. Due to the location of these sites, ~ 5 km downstream the point where sewage water from the town of Abbadia is discharged into the Pagliola Creek River, such observations suggests important geochemical modification of waste waters to the upper part of PRB.

Sample	Distance [A] (km)	T (°C)	Conductivity (μS/cm)	pH	HCO_3^-	SO_4^{2-}	Cl^-	NO_3^-	Br^-	F^-	Ca^{2+}	Mg^{2+}	K^+	Na^+	NH_4^+	TDS
March 2011																
PM	−1	11.0	487	7.9	259	50	10	0.50	0.04	0.11	70	12	1.9	15	0.10	418
PV	+ 4.5	10.5	535	8.0	223	115	10	2.33	0.01	0.24	86	14	4.2	15	0.59	469
PC	+ 5.5	10.7	501	8.2	244	94	11	1.85	0.03	0.22	82	14	3.9	18	0.48	470
PA	+ 35	11.0	648	8.0	305	75	11	5.11	0.04	0.32	92	18	6.5	24	0.19	539
September 2011																
PM	−1	19.3	807	8.0	275	161	34	0.02	< d.l.	0.14	102	20	3.9	39	0.43	635
PV	+ 4.5	18.4	843	8.1	116	309	15	19	< d.l.	0.68	136	16	9.6	15	1.68	637
PC	+ 5.5	17.0	846	8.3	113	314	14	11	< d.l.	0.72	135	16	8.8	16	0.32	628
PA	+ 35	25.2	609	8.3	218	110	22	4.20	< d.l.	0.82	67	16	12	27	0.33	477
March 2012																
PM	−1	9.9	611	8.8	281	109	23	1.01	0.02	0.18	88	16	2.5	26	< d.l.	546
PV	+ 4.5	13.4	750	8.7	220	229	18	4.84	0.02	0.53	118	16	19	9.3	2.21	636
PC	+ 5.5	10.7	749	8.7	207	230	18	5.70	0.03	0.51	118	16	7.2	20	0.61	623
PA	+ 35	11.8	601	8.2	250	110	26	4.90	0.03	0.71	72	17	11	29	< d.l.	520

[A] Refers to the distance from ASSM; all elements concentrations are in mg/L.

Table 3.1. *Conductivity, pH, T and major chemistry of Paglia River waters during the three different field campaigns.*

Water discharges calculated from the tracer dilution are commonly higher than those obtained by flow meters (Kimball, 1997). In this study, differences between these techniques ranged from 12 to 39% with a mean of 25 ± 11%, which is in agreement with that reported by Kimball (1997). As the results obtained by tracer dilution were considered more reliable in the conditions of this study, we referred to these values for data discussion and mass load calculations.

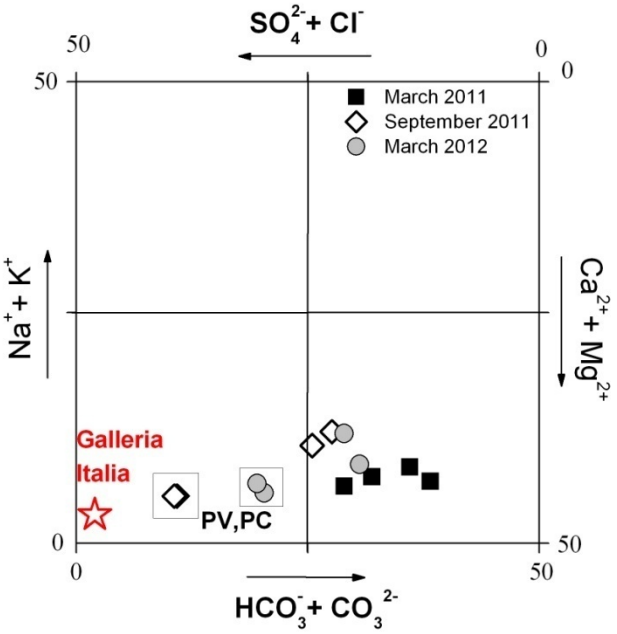

Fig. 3.3. *Langelier-Ludwig diagram for the Paglia River waters. Square-contoured samples refers to PV and PC sites for September 2011 and March 2012 sampling periods.*

Flow discharges range between < 5 L/min and 9,570 L/s, while SPM is between 1.3 and 85.7 mg/L (Table 3.2). As expected, the highest discharges are measured in March 2011, which corresponds to the flood regime for Paglia River, while the flow values are one order of magnitude lower during September 2011 (Table 3.2). Flow discharges range between <5L/min and 410 L/s and between 20 and 820 L/s for September 2011 and March 2012, respectively, highlighting the dramatic hydrological deficit of the Paglia River during the spring 2012. Highest SPM concentrations are generally reported during March 2011 (8.6-85.7; Table 3.2); with the exception of PA, the transport of SPM is 10 times lower during March 2012 than in 2011, suggesting that the singularity of the hydrological conditions in this season has severely reduced the transport of SPM in the PRB. A clear relation between Q and SPM is not evident (Fig. 3.4a); SPM values indeed increase independently from the discharge rate, as outlined by the highest values reported for sites PV and PC, coupled with their relatively low water flows (Table 3.2). The spatial trends for both Q and SPM are however

similar during the three sampling periods (Fig. 3.4b): (1) Q increases with the distance from the mine; (2) SPM shows a peak at site PV during the low flow periods, and at PC during high flow; 3) SPM decreases at PA (Fig. 3.4b). The peculiar evolution of SPM, coupled with the peak of 78.7 mg/L SPM recorded at PV during the dry period (higher than the 44.8 SPM value reported for the same station in wet season; Table 3.2), suggest that SPM is introduced to PRB by: 1) a seasonally-dependent source, i.e. surface runoff, which generally determines higher SPM during the rainy season, and 2) a seasonally-independent source, which supplies the river with SPM even during low water flow periods, resulting in extremely elevated SPM at sites PV during September 2011. It is to note that the sewage system of Abbadia has been considered to potentially highly affect SPM in waters, causing anomalously high turbidity to the Pagliola Creek downstream water locations (Rimondi et al., 2012), i.e. at PV and PC. The decrease in SPM registered after PV may indicate deposition of SPM after this site during dry seasons. On the contrary, PA dilutes the amount of SPM introduced in the basin, as suggested by the lowest measured SPM obtained at this site for all the sampling seasons (Fig. 3.4a; square-contoured symbols).

	Q (L/s)	**SPM** (mg/L)	**Hg_T** (ng/L)	**Hg_D** (ng/L)	**Hg_P** (ng/L)	**Hg_{SPM}** (µg/g)	**log K_D**
March 2011							
PM	420	10.4	17.3	2.4	15.0	1.4	5.8
PV	1380	44.8	286	13.6	272	6.1	5.7
PC	1820	85.7	113	7.6	105	1.2	5.2
PA	9570	8.6	14.4	4.7	9.6	1.1	5.4
September 2011							
PM	< 5 L/min	9.4	2.4	1.6	0.80	0.09	4.7
PV	170	78.7	1512	10.7	1501	19.1	6.3
PC	170	58.7	228	7.0	221	3.8	5.7
PA	410	1.5	13.9	2.8	11.1	7.6	6.4
March 2012							
PM	20	1.3	2.9	1.8	1.1	0.9	5.7
PV	190	27.4	77.7	10.4	67.3	2.5	5.4
PC	220	14.2	47.3	7.9	39.4	2.8	5.6
PA	820	9.9	15.2	3.2	12.0	1.2	5.6

Table 3.2. *SPM, Hg_T, Hg_D, Hg_P, Hg_{SPM} concentrations and partition coefficients (log K_D) for sites PM, PV, PC and PA along the Paglia River.*

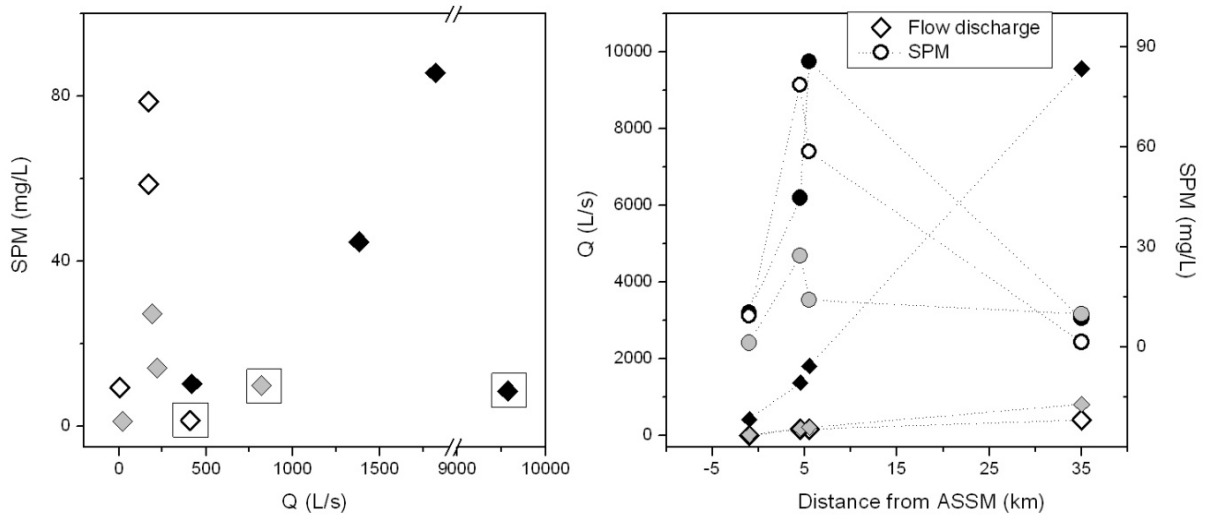

Fig. 3.4 a,b. *(a) Relationships between discharge and SPM; (b) spatial evolution of discharge and SPM in relation to the distance from ASSM. For both figures, black, white and gray symbols refer to March 2011, September 2011 and March 2012, respectively. Square-contoured symbols refer to site PA.*

3.4.2 Trace elements in water and in particulate matter

Concentrations of Hg_T, Hg_D are reported in Table 3.2. They are in agreement with the results reported for the same area by Rimondi et al. (2012). Concentrations of Hg_T are below the 2,000 ng/L US EPA established limits for Hg in drinking waters, and generally < 770 ng/L, i.e. below the limit to protect aquatic wildlife in the USA against chronic effects (US EPA, 2009). Only one water sample at PV in September 2011 had a value of 1,512 ng/L Hg (Table 3.2), exceeding both the environmental quality standard limits for superficial waters defined by the Italian legislation (1,000 ng/L; GURI, 2006a) and US EPA (770 ng/L; US EPA, 2009). Notwithstanding Hg in waters generally well correlates to SPM (Balogh et al., 1997; Coquery et al., 1997; Choe et al., 2003), in this study only a weak correlation between these variables, although statistically significantly is observed ($R^2 = 0.34$; $p < 0.05$; Fig. 3.5a). However, a strong influence by the two extremes of the variables, i.e. 1512 Hg_T and 85.7 SPM, is evident (Fig. 3.5a). If these values are removed from the dataset, the improved Hg_T vs SPM correlation ($R^2 = 0.85$; $P << 0.01$), suggests that the distribution of Hg in water can be at least partially explained by SPM.

Concentrations of Hg_{SPM} range from 0.09 to 19.1 μg/g (Table 3.2). Such concentrations are particularly elevated if compared to those usually reported for continental crust (UCC) (~ 0.012 − 0.06 μg/g) (Taylor and McLennan, 1995; Wedepohl, 1995; Rudnik and Gao, 2003), which are commonly applied to SPM (Schäfer et al., 2006). These values are even higher than those shown by some catchments impacted by human activities (Balogh et al., 1997;

Paraquetti et al., 2004; Schäfer et al., 2006), and mining (Thomas et al., 2002; Choe et al., 2003), and generally higher than 0.15 µg/g, the limit established by US EPA to avoid negative effects on aquatic wildlife (Schäfer et al., 2006). In this study Hg_{SPM} is not correlated to seasonal variation of discharge, and the highest Hg in SPM is reported during the dry seasons (Table 3.2). Such finding is quite common in medium watersheds (Coynel et al., 2007), as high water flows promote strong erosion of less contaminated sediments, dilution by soil erosion, and/or higher percentages of relatively coarse material (Coynel et al., 2007). However, for all seasons, all Hg species in both water and particulate report a clear trend with respect to their distance from ASSM (Fig. 3.6a). The highest Hg concentrations are always measured at PV (PC), indicating that the ASSM is likely the main point source of particulate Hg for PRB. The lowest particulate Hg is generally reported at sites PM (0.09-1.4 µg/g), which is located upstream from the influence of ASSM, and notably at PA (1.1-7.6 µg/g), located at the furthest distance from ASSM. Despite the highest discharges have been measured at this site, the lowest Hg_{SPM} is here observed (Fig. 3.6b), suggesting that PA is able to dilute the amount of Hg entering the basin, or that Hg is deposited between PC and PA. In addition, Hg_{SPM} is not clearly correlated to SPM (Fig. 3.5b); in particular, these variables have a better correlation in March 2012, when the runoff of the basin was completely reset by the prolonged absence of rainfall, while the correlation is lacking for the other seasons, when high (March 2011) or minor (September 2011) runoffs occurred in the basin (Fig. 3.5b). These observations confirm, as already outlined for SPM, that the introduction of particulate Hg in the Paglia River can be mainly related to a point source(s), which is independent from the river discharge (see later paragraphs for further details). The increase of the water flows, which triggers additional mobilization of particulate by surface runoff (i.e. increase of SPM), acts as a dilution factor for the Hg contents in particulate by addition of non-contaminated or less contaminated particulate matter.

Concentrations of other trace elements in water and SPM are listed in Tables 3.3, 3.4 and 3.5. The main dissolved contaminants in water have contents below the most common national and international limits (Table 3.3), particularly for As, Cd, Cr, Ni and Cu, which are the selected elements to be analyzed for quality standards of water by the Italian legislation (GURI, 2006a) (Table 3.3). However, particularly elevated concentrations of Al and Fe in unfiltered waters are reported for all the analyzed stations, and particularly for PV (up to 9,900 and 8,900 µg/L for Fe and Al, respectively) (Table 3.4). Elevated Fe is mainly due to the Galleria Italia waters, which occasionally have caused the change in color of the Pagliola Creek that turned to be red−brown due to the high amount of Fe- colloidals during overflow

episodes. Similarly, the high amount of Al in river waters can be related to leaching of Al silicates under acidic conditions (Drever, 1997).

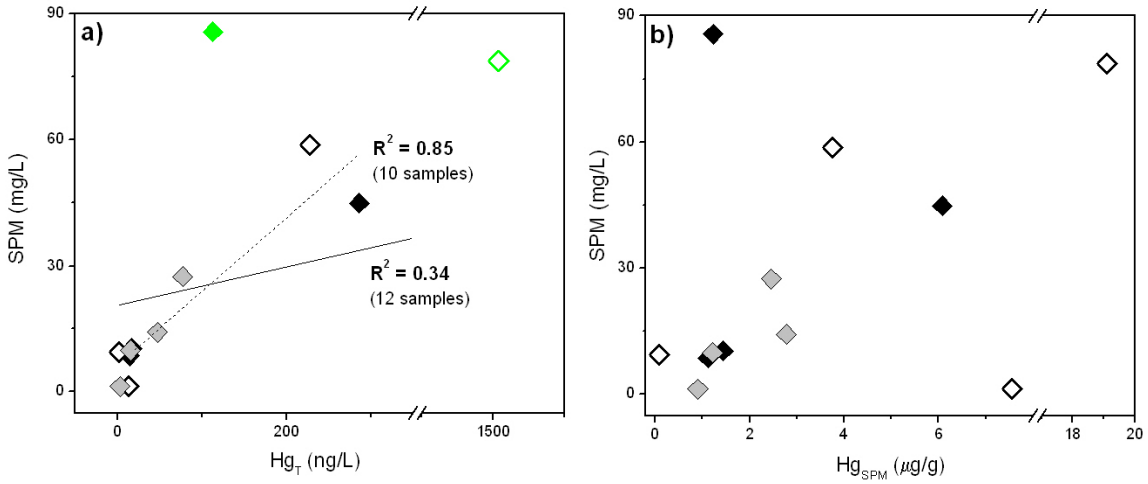

Fig. 3.5 a,b. *(a) Binary diagrams of SPM versus Hg_T, and (b) SPM versus Hg_{SPM}. Black, white and gray symbols refer to March 2011, September 2011 and March 2012, respectively. Green symbols referred to data that were excluded from the calculation of linear regression for R^2 = 0.85 (see text for explanation).*

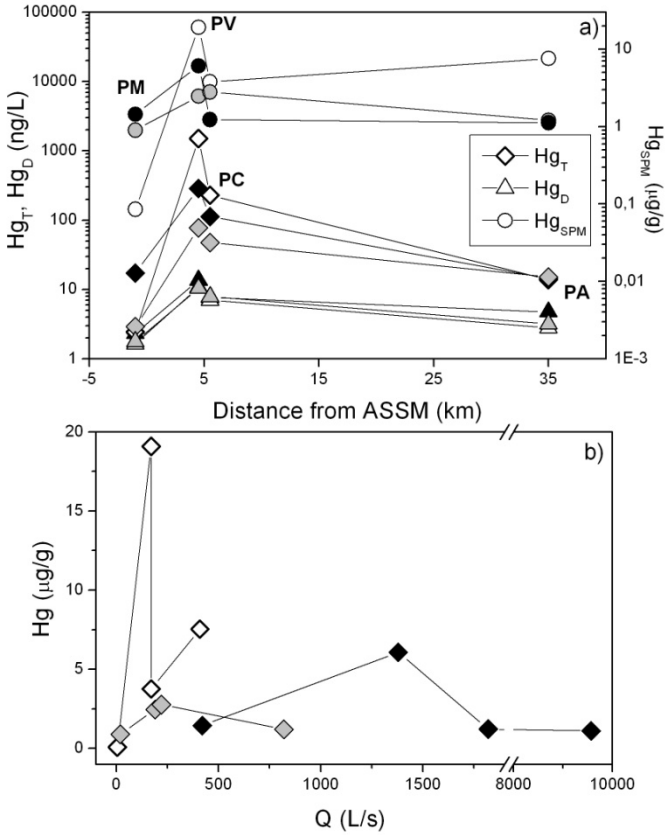

Fig. 3.6 a,b. *a) Spatial distribution of Hg_T, Hg_D and Hg_{SPM} in relation to the distance to the Hg mine of Abbadia San Salvatore (ASSM); b) distribution of Hg_{SPM} with respect to flow discharges. Black, white and gray symbols refer to March 2011, September 2011 and March 2012, respectively. Refer to the text for labels PM, PV, PC, and PA.*

	Li	B	Al	Cr	Mn	Fe	Co	Ni	Cu	Zn	Rb	Sr	Mo	Cd	Ba	Tl	Pb	U	Sb	As
March 2011																				
PM	6.7	42	42	<1	3.1	<30	0.27	0.9	1.6	<6	2.3	540	0.3	<0.05	16	<0.05	<0.2	0.4	0.24	<0.5
PV	13	59	53	<1	42	<30	0.9	4.3	1.7	<6	13	550	0.4	<0.05	16	<0.05	<0.2	0.5	0.34	4.3
PC	13	66	33	<1	23	<30	0.6	2.9	2.2	<6	9.1	520	0.4	<0.05	18	<0.05	<0.2	0.6	0.28	0.9
PA	10	97	10	<1	3.1	<30	0.17	0.8	2.2	<6	7.3	650	0.7	<0.05	31	<0.05	<0.2	2.2	0.23	<0.5
September 2011																				
PM	11	120	23	<1	46	<15	0.19	0.9	1.8	<6	4.7	870	0.8	<0.24	27	<0.1	<0.7	0.8	0.3	<0.2
PV	41	74	56	<1	**121**	23	2.2	14	<1.2	<6	57	480	0.7	<0.24	15	<0.1	<0.7	0.49	<0.03	2.1
PC	40	78	52	<1	56	26	1.2	11	1.4	6.8	49	470	0.6	<0.24	14	<0.1	<0.7	0.42	0.1	1.6
PA	16	160	3	<1	14	<15	0.21	0.8	2	<6	25	680	1.4	<0.24	35	<0.1	<0.7	3.2	0.3	1.2
March 2012																				
PM	8.1	55	n.d.	<0.6	2.5	<30	0.18	1.5	<1.3	<3	3.6	650	0.5	<0.03	21	0.01	<0.2	0.7	0.3	<0.1
PV	28	80	49	<0.6	**100**	<30	1.1	6.3	<1.3	<3	42	500	0.6	<0.03	15	0.03	<0.2	0.7	0.2	1.8
PC	28	80	39	<0.6	79	<30	0.86	5.4	<1.3	<3	34	520	0.6	<0.03	14	0.01	<0.2	0.6	0.2	1.4
PA	14.8	130	7	<0.6	13	<30	0.22	1.1	<1.3	<3	21	610	0.9	0.2	32	0.02	<0.2	3.0	0.3	1.7
(A)	n.e.	n.e.	500–2,000	100	50	300	n.e.	100	1,300	5,000	n.e.	n.e.	n.e.	5	n.e.	0.5	15	30	6	50
(B)	n.e.	n.e.	n.e.	50	50	200	50	20	1,000	3,000	n.e.	n.e.	n.e.	5	n.e.	n.e.	10	n.e.	5	10

All elements concentrations are in µg/L

(A) Maximum contamination level (Clean Water Act, EPA, 2009);
(B) Italian maximum permissible limits in surface waters (GURI, 2006a).

Table 3.3. *Concentrations of trace elements in filtered waters of Paglia River. Limits for the most common heavy metals are reported for the Italian, and USA limits. n.e. stands for not established. Values above (A), (B) are reported in bold. Te, Bi, Ag were always < d.l.*

	Li	B	Al	Cr	Mn	Fe	Co	Ni	Cu	Zn	Rb	Sr	Mo	Cd	Ba	Tl	Pb	U	Sb	As
March 2011																				
PM	6.7	42	690	< 1	10	300	0.47	1.5	2.0	<6	2.4	540	0.3	<0.05	17	<0.05	0.2	0.5	0.2	<0.5
PV	13	61	5,100	3.4	106	4,800	3.4	11	7.6	28	23	590	0.4	0.06	35	0.1	2.5	0.9	0.5	6.9
PC	13	70	5,200	7.0	90	4,700	2.3	7.8	5.4	21	15	540	0.4	<0.05	30	<0.05	1.5	0.8	0.3	1.1
PA	10	95	340	1.0	15	460	0.36	1.3	2.6	<6	7.9	670	0.7	<0.05	32	<0.05	0.3	2.3	0.2	0.5
September 2011																				
PM	11	120	38	<1	52	30	0.2	1.1	1.8	<6	4.9	810	0.8	<0.24	30	<0.1	<0.7	0.9	0.3	<0.2
PV	41	99	8,900	1.7	244	9,900	4.7	16	2.7	61	57	440	0.7	<0.24	24	<0.1	1.0	0.8	0.5	7.6
PLC	40	97	7,800	1.0	133	7,900	3.1	12	1.8	55	50	440	0.6	<0.24	21	<0.1	<0.7	0.7	0.2	6.1
PA	17	170	370	<1	36	380	0.4	0.9	2.2	<6	25	610	1.3	<0.24	39	<0.1	<0.7	3.1	0.3	1.4
March 2012																				
PM	8.1	56	39	<0.6	1.3	<30	0.17	1.5	<1.3	<3	3.6	660	0.5	2.4	20	0.01	<0.2	0.7	0.3	<0.1
PV	28	81	3,000	<0.6	130	3,500	1.8	5.6	1.4	23	44	520	0.6	<0.03	17	0.03	0.26	0.8	0.2	3.6
PLC	28	81	1,550	<0.6	95	1,800	1.2	5.2	<1.3	13	35	530	0.6	<0.03	18	0.02	0.2	0.7	0.2	2.1
PA	15	130	220	<0.6	23	<30	0.34	0.7	1.4	<3	21	620	0.9	<0.03	33	0.03	0.27	3.0	0.3	1.8

All elements concentrations are in µg/L

Table 3.4. *Concentrations of trace elements in unfiltered waters of Paglia River water. Te, Bi and Ag were always < d.l.*

	Li	B	Al	Cr	Mn	Fe	Co	Ni	Cu	Zn	Ga	Rb	Sr	Mo	Ag	Cd	Ba	Pb	U	Sb	As
March 2011																					
PM	34	50	62,310	<d.l.	732	32,803	**21**	50	60	**1,038**	6	24	123	2	1	3	78	20	3	<d.l.	7
PV	24	14	112,660	18	1,260	70,950	**33**	65	48	**435**	13	22	159	1	<d.l.	2	94	15	2	<d.l.	**25**
PC	33	21	60,290	30	930	51,100	**21**	45	43	**333**	14	27	154	1	<d.l.	1	65	15	1	<d.l.	11
PA	35	14	38,280	29	945	34,090	16	43	53	**257**	10	46	228	1	<d.l.	1	125	24	1	1	7
September 2011																					
PM	n.d.	n.d.	n.d.	n.d.	n.d.	n.d.	n.d.	n.d.	n.d.	n.d.	n.d.	n.d.	n.d.	n.d.	n.d.	n.d.	n.d.	n.d.	n.d.	n.d.	n.d.
PV	12	<d.l.	112,380	45	1,818	86,780	**41**	58	41	**744**	6	20	157	1.2	0.25	<d.l.	120	26	3	7	**62**
PC	6	<d.l.	131,990	45	1,696	98,210	**35**	37	36	**982**	5	10	156	<d.l.	0.36	<d.l.	112	11	3	3	**71**
PA	27	<d.l.	25,000	80	1,745	31,130	17	42	66	**241**	7	44	231	2.4	0.28	<d.l.	137	24	1	7	14
March 2012																					
PM	n.d.	n.d.	n.d.	n.d.	n.d.	n.d.	n.d.	n.d.	n.d.	n.d.	n.d.	n.d.	n.d.	<d.l.	n.d.	n.d.	n.d.	n.d.	n.d.	n.d.	n.d.
PV	8	<d.l.	113,030	16	3,696	135,610	**36**	n.d.	28	**976**	7	20	258	<d.l.	0.26	2	200	11	4	< d.l.	**81**
PLC	24	13	122,490	37	6,991	149,250	**48**	35	n.d.	**1,197**	14	40	358	<d.l.	0.09	1	353	20	4	< d.l.	**77**
PA	66	<40	31,430	26	2,651	42,210	**22**	n.d.	70	**205**	14	66	342	<d.l.	n.d.	2	327	51	2	< d.l.	**26**
(A)	n.e.	n.e.	n.e.	150	n.e.	n.e.	20	120	120	150	n.e.	n.e.	n.e.	n.e.	n.e.	2	n.e.	100	n.e.	10	20

All elements concentrations are in μg/g.

(A) Italian maximum permissible limits in soil designated to public green, private and residential uses (GURI, 2006b).

Table 3.5. *Concentrations of major trace elements and heavy metals in SPM of Paglia River. < d.l. stands for under detection limit; n.d. for not determined. Values above (A) are reported in bold. Bi and Tl were always < d.l.*

3.4.3 Partition coefficient

The behavior of Hg in aquatic system is primarily dependent on its distribution between dissolved and particulate forms (Hissler and Probst, 2006). Although they are not related to thermodynamic factors, partition coefficients (K_d), calculated as $K_d(\frac{L}{kg}) = \frac{\left[Hg_{SPM}\,(\frac{\mu g}{g})\right]}{\left[Hg_D\,(\frac{mg}{L})\right]}$), are widely used to describe processes affecting Hg (Balogh et al., 1997; Hissler and Probst 2006; Kocman et al., 2010).

Log-transformed distribution coefficients [log(K_D)] for the Paglia River range from 4.7 to 6.4 (Table 3.2), in the upper range of typical values commonly reported for Hg from other rivers (Leermakers et al., 1995; Paraquetti et al., 2004; Hissler and Probst, 2006), particularly for those impacted by mining activity (Ganguli et al., 2000; Thomas et al., 2002; Kocman et al., 2010). Such elevated log(K_D) values evidence that most Hg is associated with the particulate phase.

In this study, log(K_D) values are found to be quite similar in the different hydrological periods, suggesting that water discharges have minor influence in determining the partitioning of Hg between particulate and dissolved species (Hurley et al., 1995). However, contrarily to what is often observed (Hissler and Probst, 2006), log(K_D) values do not depend on common variables such as SPM, pH and inorganic ligands (Cl^-) (data not shown). Moreover, the decrease of log(K_D) with SPM, the so-called "particle concentration effect" commonly observed for Hg and other particle-bound constituents (Choe et al., 2003; Flanders et al., 2010; Kocman et al., 2010) and attributed to increase amount of filter-passing elements (i.e. colloidal fraction) with increasing SPM, was not observed in this work. This finding suggests that Hg colloidal complexation and transport in the Paglia River can have minor importance.

The longitudinal profiles of log(K_D) between PM and PA are quite different during the two main hydrological periods (Fig. 3.7): March and September 2011. During high flow period, log(K_D) values progressively decrease from upstream to downstream locations (PM−PC; Fig. 3.7), whereas low flow conditions (September 2011) show a steep increase in log (K_D) at PV site (Fig. 3.7). In both seasons, however, log(K_D) strongly drops down between PV and PC. In particular, at PC we observed a strong reduction of the hydrological gradient of Paglia River, corresponding to the transition from the mountain part of the river course (Pagliola Creek) to the flood plain (Paglia River). The abrupt decrease of log(K_D) after PV can then possibly relate to depositional processes (Hissler and Probst, 2006; Flanders et al., 2010), occurring in that part of the river where the water flow flows down.

During low flow conditions, the increase in log (K_D) at PV indicates the introduction of particle bound Hg to the river, suggesting the mine as a source of further Hg to the Pagliola Creek, accordingly a similar increase in Hg_{SPM} is recorded at this site (Fig. 3.6a). As explained later on, the particulate Hg deposited at PV could be re-suspended during low water periods, causing the increase in log (K_D). Variations in log(K_D) at PA are presumably not strictly related to ASSM, due to the relatively large distance between these sites (~ 35 km). At PA the log (K_D) increase during the dry season is therefore associated with additional particulate Hg entering the basin from the Hg mines located in the southern sector of Mt. Amiata (Fig. 3.1a). The addition of particulate Hg at PV and PA is apparently masked during the high flow regime, when the highest SPM in the basin dilutes the contribution of Hg-contaminated SPM, resulting in log(K_D) decrease between PM and PC, and comparable log(K_D) values at PC and PA (Fig. 3.7).

In March 2012, with the exception of PM, log(K_D) values are quite similar in all the locations (Fig. 3.7), and no decrease of log(K_D) between PV and PC is observed. Therefore, data suggest that the exceptional hydrological conditions of March 2012, resulting in a lower content of SPM (Table 3.2), have prevented the sedimentation of particulate Hg along the Paglia River course, which was then further transported downstream along the PRB. Similarly, in those conditions the contribution of Hg particulate from Hg mines south of Abbadia was remarkably absent, or minor.

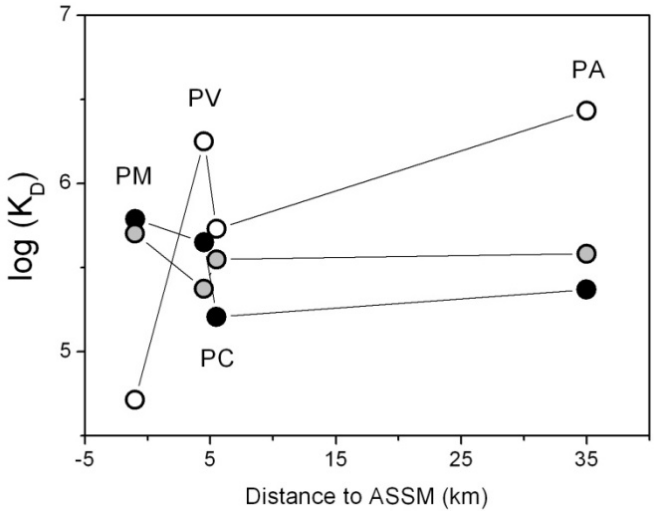

Fig. 3.7. *Spatial and seasonal evolution of Hg distribution coefficient (log K_D) between particulate (µg/g) and dissolved (ng/L) phases. Black, white and gray symbols refer to March 2011, September 2011 and March 2012, respectively. Refer to the text for labels PM, PV, PC, and PA.*

3.4.4 Normalization and enrichment factor

To determine Hg contamination in the particulate matter, i.e. concentrations exceeding natural backgrounds, it is necessary to determine the natural component of the observed concentration. Since grain size and provenance are the two most important parameters that control the concentrations of trace metals in sediments (Loring, 1990), normalizing their content to a proper conservative element can help, in principle, to discriminate the natural versus anthropogenic input of Hg in the particulate matter of PRB. The main requirement for a suitable normalizing element is its natural origin, then its presence in sediments should not be a consequence of external contamination, i.e. industrial activities or mining (Kocman et al., 2010), but it should result only from natural weathering of continental crust. Generally speaking, the most suitable elements to be used as normalizing factors are Al and Fe (Martin and Meybeck, 1979; Szefer, 1990; Loring and Rantala, 1992; Lin et al., 2012), because of their i) high natural concentrations in stream sediments and SPM, ii) minimal input by anthropogenic sources, and iii) presence in primary and secondary aluminosilicates (Daskalakis and O'Connor, 1995). Nevertheless, Zr, Sc and Li can also be used as reference elements. Loring (1990) showed that Li correlates with trace metals in fine−grained sediments equally or even more strongly than Al. In addition, Martin and Meybeck (1979) pointed out that, besides Al and Fe, any element for which the river dissolved transport is negligible, i.e. <10%, can be used for normalization, suggesting that Ga may also be used for this purpose. Owing to the fact that Fe is added to Paglia River by mine waters, its use in this study was avoided. Similarly, Al was excluded due to its probable "non lithogenic" contribution to SPM. As a consequence, SPM concentrations were normalized to Li and Ga. Both elements produced similar results, and here only those data related to Li normalization are presented and discussed.

In Fig. 3.8 trace elements concentrations normalized to Li are plotted against the same ratio in the Upper Continental Crust (UCC), whose values were derived by Taylor and McLennan (1995) and Rudnick and Gao (2003). Trace elements and heavy metals but Hg, As and Sb, generally plot on the 1:1 line, suggesting that no particular contamination of these elements affects the SPM of Paglia River. However, strong deviations from the continental ratio are observed for Hg, As, Sb and Zn (Ag). Besides the expected enrichment in Hg, As/Li_{SPM} and Sb/Li_{SPM} enrichments are observed, likely due to the presence of As and Sb minerals (e.g. realgar, orpiment and stibnite) often found in association with cinnabar mineralization (Arisi Rota et al., 1971; Morteani et al., 2011). Similarly, the widespread diffusion of

Cu−Pb−Zn(Ag) polymetallic sulphide deposits in Southern Tuscany (Tanelli, 1983) may result in high natural background of these base metals, and Ag with respect to the continental crust. Enrichments in Fe, Al and Mn are moreover observed, suggesting that significant amounts of these metals are mobilized by mine runoff.

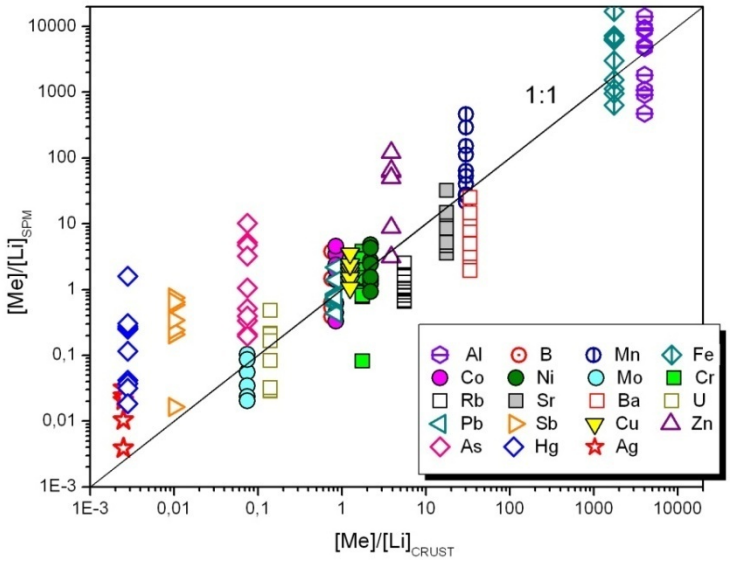

Fig. 3.8. *Trace element [Me]/Li ratios for the Paglia River versus the same ratios in the average Earth's crust (Taylor and McLennan, 1995) plotted independently from sampling periods. The solid black line represents the 1:1 ratio; trace metal located above (below) the 1:1 line are enriched (depleted) with respect to the Earth crust.*

Quantitatively, in this study we evaluated the enrichments for Hg, Sb and As by means of the Enrichment Factor (EF) and Index of Geoaccumulation (Igeo) (Müller, 1981), calculated as follows:

$$\boldsymbol{EF_{Li}^{M} = \frac{([Me]/[Li])_{sample}}{([Me]/[Li])_{background}}}$$

$$\boldsymbol{I_{geo} = \log_2 \frac{[Me]_{sample}}{1.5[Me]_{background}}}$$

where $[Me]/[Li]_{sample}$ and $[Me]/[Li]_{background}$ are the ratios of trace metal to reference element in the sample and in background sediment, $[Me]_{sample}$ is the concentration of trace metal in the sample divided by its concentration in background material. I_{geo} values are commonly applied to assess the contamination level in natural matrices as the presence of the constant 1.5 in the denominator of the mathematical expression allows to predict natural fluctuations of the metal in the environment and small anthropogenic influences (Loska et al., 2004). Earth's crust values are generally employed as background concentrations (Lin et al., 2012), basing on the

concept that if continental rocks are weathered and there is no anthropogenic contribution to the system, the composition of trace metal in sediment (or particulate matter) is supposed to be the same as in the crust. However, concentrations of metals in rocks and soils from which particulate matter is derived may significantly be higher than those in the crust due to the natural geochemical anomalies (e.g. ore deposits). For this reason, more meaningful EFs and Igeo values are obtained when they are referred to local background levels (Feng et al., 2004; Reimann and De Claritat, 2005; Yiğiterhan and Murray, 2008; Song et al., 2011). Background values for Hg, As and Sb in Southern Tuscany are estimated to 0.3, 7, and 0.4 µg/g respectively (Benvegnù et al., 1993; Protano et al., 1998), and were calculated taking into account the mineralizations of this region. As these values significantly differ from those reported for the continental crust (0.056 µg/g Hg, 1.5 µg/g As and 0.2 µg/g Sb; Taylor and McLennan, 1995), we referred to these local concentrations to calculate EFs and I_{geo}.

EF_{Li} for Hg, As and Sb are between 1−106, 1−29, 1−29 respectively while I_{geo} have values of 1−5; <0−4 <0−3, respectively (Table 3.6), highlighting a large variability of contamination conditions. According to the contamination categories of Sutherland (2000), SPM is between minimal and highly enriched in As (Sb) and between significant and very high for Hg (Table 3.6). Moreover, following Müller, (1981), in September 2011, SPM sampled at PV results to be between heavy and extremely contaminated by Hg, and heavily contaminated by As and Sb (Table 3.6). This enrichment sequence is generally respected: $EF_{Li}^{Hg} > EF_{Li}^{Sb} > EF_{Li}^{As}$, showing that Hg is by far the most enriched metal in SPM, followed by Sb and then by As. The spatial variability of EFs with increasing distance from ASSM is similar among the different seasons, with the highest values reported at site PV, and a generally decrease thereafter (Fig. 3.9). The EFs values are higher during low flow condition (September 2011). It is to note that EF_{Li}^{Hg} of March 2012 resembles those observed during March 2011 (Fig. 3.9), ranging 1-21 and 2-17, respectively (Table 3.6).

Similar EFs' spatial trends suggest that, despite the degree of metal enrichment in SPM is different among seasons, the mechanism of Hg(As, Sb) transport in the Paglia River is similar in different hydrological seasons, and is not affected by water flows. Notwithstanding the dramatic hydrological deficit of March 2012 with the consequent strong decrease of SPM, SPM enrichment in Hg equaled that of March 2011, and this metal was similarly transported downstream ASSM. According to the similar evolution of Hg_{SPM} along the river course, EFs suggest that most contaminated particulate is supplied to the basin at site PV, which is spatially and directly influenced by ASSM, while lower EFs are observed for those sites

located further downstream, possibly resulting from: 1) deposition of polluted particulate (decrease of SPM and log(K_D) after PV), and/or 2) dilution effect of downstream sites (addition of relatively unpolluted SPM during March and September 2011). The most elevated EFs referred to the dry seasons show, as outlined in the previous section, that a point source of metals (and SPM) exists in the basin, which constantly mobilizes metals independently from the hydrological seasons. Particularly, the addition of contaminated SPM may derive either from the Galleria Italia mine adit either by resuspension of previously deposited particulate Hg. This contribution is however masked during high water flows by the increase amount of SPM entering the basin.

	EF_{Li}^{Hg}	EF_{Li}^{Sb}	EF_{Li}^{As}	I_{geo}^{Hg}	I_{geo}^{Sb}	I_{geo}^{As}
March 2011						
PM	3	n.d.	1	2	n.d.	<0
PV	17	n.d.	3	4	n.d.	1
PC	2	n.d.	1	1	n.d.	0.1
PA	2	1	1	1	<0	<0
September 2011						
PM	n.d.	n.d.	n.d.	<0	n.d.	n.d.
PV	106	29	15	5	3	4
PC	17	10	13	3	3	2
PA	18	12	2	4	0.4	3
March 2012						
PM	n.d.	n.d.	n.d.	1	n.d.	n.d.
PV	21	n.d.	29	2	n.d.	3
PC	8	n.d.	9	3	n.d.	3
PA	1	n.d.	1	1	n.d.	1

Table 3.6. *Calculated enrichment factors (EF) and Index of Geoaccumulation (Igeo) for selected elements (Hg, As and Sb)in the SPM of Paglia River.*

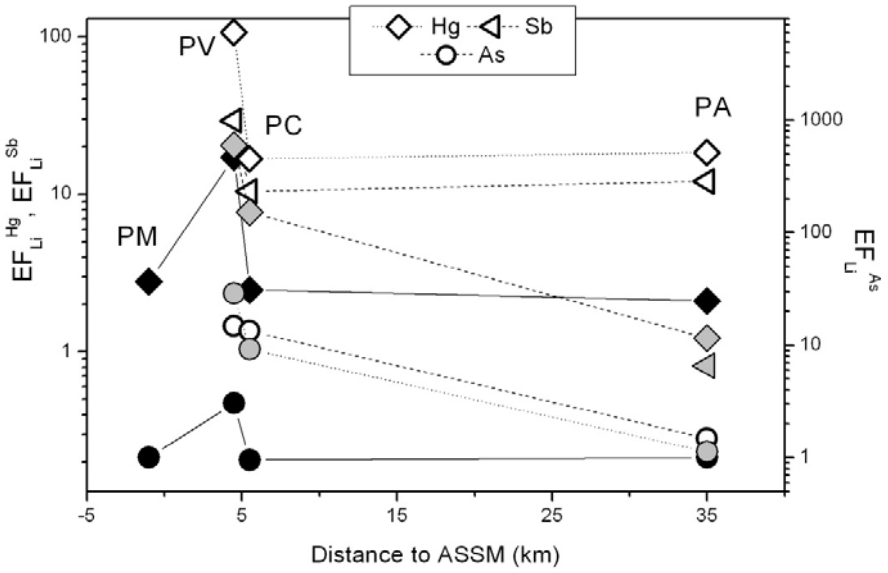

Fig. 3.9. *Spatial evolution of EFs for Hg, As and Sb from the Abbadia San Salvatore Hg mine. Black and white symbols refer to the high (March 2011), and low (September 2011) water flows, respectively. Gray symbols are for March 2012.*

3.4.5 Mercury, arsenic and antimony mass loads

Total, particulate and dissolved fluxes were calculated for Hg, As and Sb (Table 3.7). Arsenic and Sb were considered because of both their elevated contents in SPM and their environmental significance. The highest total Hg mass flux is recorded in March 2011, when up to 34 g d^{-1} Hg are transported at PV. Similar, though lower loads, are found at PC (18 g d^{-1}) and PA (12 g d^{-1}), while at PM Hg flux is two orders of magnitude lower than those calculated at the other sites (0.6 g d^{-1}; Table 3.7). During the 2011 measurements, downstream from PV, transported loads of total and particulate Hg decrease with increasing distance from the mine (Fig. 3.10). Specifically, a considerable decrease in Hg load is reported after PV, while it shows a more gradual decrease between PC and PA (Fig. 3.10). In spite of minor variations, in March 2012 loads are similar among sampling sites, i.e. ~ 1 g d^{-1} (Fig. 3.10). Mercury fluxes are highly variable between rainy (March 2011) and dry (September 2011) seasons with the exception of PV, whose Hg load in September 2011 is comparable (24 g d^{-1}) to that of March 2011 (34 g d^{-1}) (Table 3.7). On the contrary, one order of magnitude lower loads are observed in March 2012 (Table 3.7). Dissolved Hg loads account between 1 and 33% of the total Hg flux, suggesting that total loads can almost entirely ascribed to the variations of particulate Hg. As previously reported for other mining districts worldwide (Faganeli et al., 2003; Hissler and Probst, 2006; Schäfer et al., 2006), the transport of Hg in the Paglia River is then dominantly occurring as suspended particles.

	$F-Hg_T$	$F-Hg_D$	$F-Hg_P$	$F-As_T$	$F-As_D$	$F-As_P$	$F-Sb_T$	$F-Sb_D$	$F-Sb_P$
March 2011									
PM	0.6	0.09	0.5	3	n.d.	3	9*	9	n.d.
PV	34	2	33	193	60	134	41*	41	n.d.
PC	18	1	17	149*	n.d.	149	44*	44	n.d.
PA	12	4	8	50*	n.d.	50	190*	190	n.d.
September 2011									
PM	n.d.	n.d.	n.d.	n.d.	n.d.	n.d.	n.d.	n.d.	n.d.
PV	24	0.17	24	113	34	79	9	0	9
PC	3.4	0.10	3.3	85	24	62	4	1	3
PA	0.5	0.10	0.4	43	43	1	11	11	0.36
March 2012									
PM	0.005	0.003	0.002	n.d.	n.d.	n.d.	1*	1	n.d.
PV	1.3	0.17	1.1	119	30	89	5*	5	n.d.
PC	0.9	0.15	0.7	84	27	58	4*	4	n.d.
PA	1.1	0.22	0.9	139	120	18	21*	21	n.d.

* Total fluxes are intended as the sum of dissolved flux *F-(Hg, As, Sb)$_D$* plus particulate *F-(Hg, As, Sb)$_P$*; when one of these two terms is not determined (n.d.), the total flux equals either dissolved or particulate flux.

Table 3.7. *Loads of selected elements, Hg, As and Sb reported as total ($F-Me_T$), dissolved ($F-Me_D$) and particulate ($F-Me_P$) loads.*

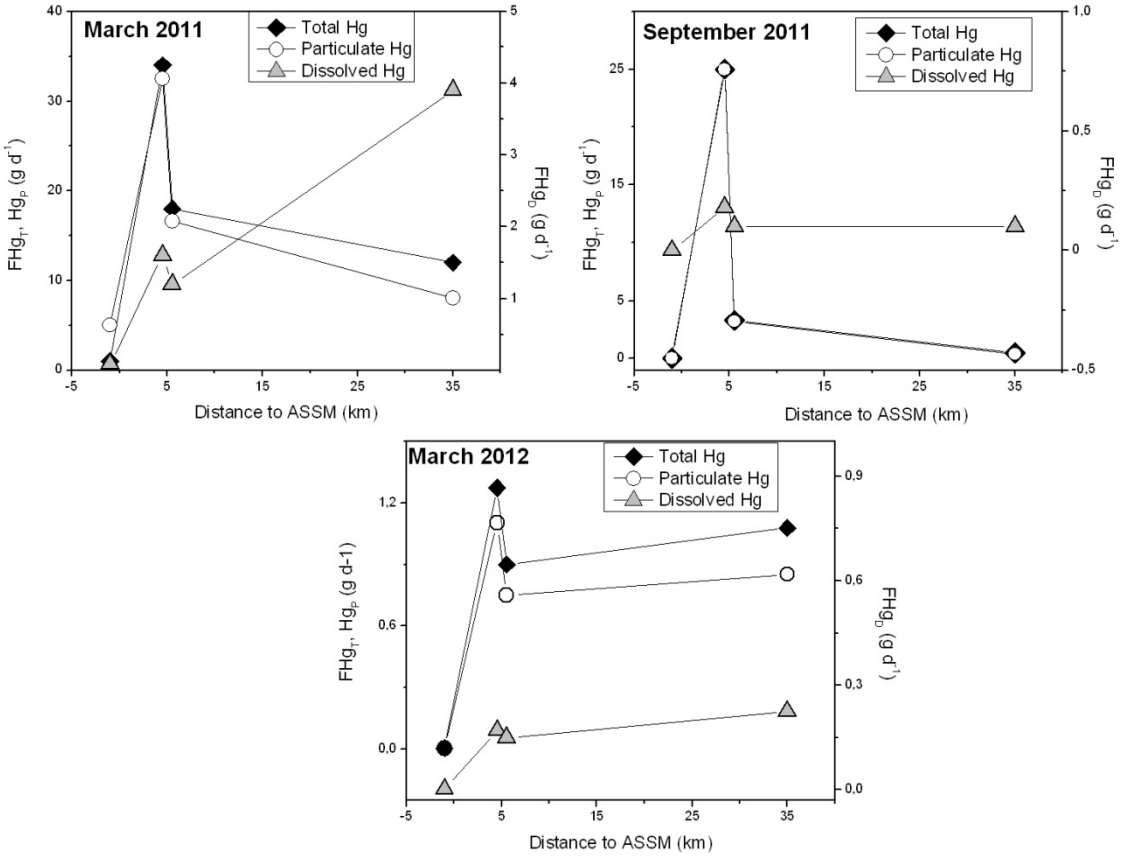

Fig. 3.10. *Spatial relation of Hg fluxes determined for each station in different hydrological periods.*

The Abbadia San Salvatore Hg mine represents a point source of pollution for Hg, supplying ~ 100% of the total Hg budget to the PRB, as suggested by the highest mass loads reported for sites located 5 km downstream from ASSM. The decrease of particulate loads between sites PV and PC recorded in 2011 is likely due to the deposition of particulate Hg along this section of the river, which is largely influenced by the reduced water flow, resulting from the decreased hydrological gradient between these two sites, and significantly reducing the particulate loads of Hg downstream from PV. The generally positive correlation between Hg loads and seasonal discharge, i.e. loads are higher during the wet season (March 2011), suggests the importance of runoff associated with heavy winter rains as an important factor promoting the mobilization of metals in the PRB. However, the similar Hg loads reported at PV during both wet and dry seasons in 2011 support the hypothesis that a water flow-independent source of Hg exists in the basin, which supplies a constant amount of Hg independently from the discharge. Such a source may be represented by the Hg deposited along the river reaches, a sort of transient sink, from which Hg is re-suspended in low flow regimes. Studies on the dynamics of Paglia River bed have evidenced that human interventions have severely altered its morphology, resulting in bed narrowing (Cencetti et al., 2004) and channel incision (Ciccacci et al., 1988; Cencetti et al., 2004). This would indeed prevent a definitive stacking of Hg as river bed bottom deposit, promoting on the contrary Hg mobilization and transport downstream the Paglia River. Thanks to this effective mobilization, important quantities of Hg might theoretically be directly discharged into the Tiber River, provoking a contamination of its ecosystem.

The Hg loads measured in March 2012, contrarily to those of 2011, should be regarded as representative of an extraordinary event for the Paglia River. The prolonged absence of rainfall in the basin results indeed in Hg loads are 30-fold lower than those observed during the previous year. The constancy of Hg loads among the studied sites, ~ 1 g d^{-1}, suggests that these hydrological conditions were able to prevent a marked deposition of Hg along the river course, which was then further transported downstream. This season could therefore depict the condition of a *steady-state flow*, which occurs when Hg introduced in the river exactly balances the quantity that can be transported in such hydrological conditions by the flow. However, as outlined by the EFs, the mechanism of Hg transport in the basin is unaffected by the particular conditions of this season, suggesting therefore that the hydrologic conditions of the Paglia River control the absolute quantities of Hg mobilized in the basin rather than the mechanism of its diffusion.

Similarly to Hg, maximum loads for As and Sb are reported in March 2011, when up to 190 g d^{-1} As and 193 g d^{-1} Sb are mobilized at PV and PA, respectively (Table 3.7). Although particulate load for Sb is available only for the September field campaign, data show a similar behavior for both elements, whose loads drop down after PV (from 9 to 3 g d^{-1}; Fig. 3.11). However, differently from As and Hg, maximum loads for Sb are always reported for site PA (Fig. 3.11), showing spatially diffused sources of this contaminant to the watershed, possibly due to the contribution of other mines located south of ASSM. Common to Hg, As transport is generally occurring as particulate phase, ranging between 51 to 100%, although some exceptions are observed, since dissolved loads up to 43 and 126 g d^{-1} are transported at PA in September 2011 and March 2012, respectively, accounting for about 98 and 95% of total As load. Due to its preferential association to the dissolved phase (Martin and Meybeck, 1979), major loads for Sb are recognized to be partitioned in this fraction (~ 100%). However, commonly to all three metals, dissolved loads increase at site PA (Fig. 3.10 and 3.11, Table 3. 6), suggesting that re-suspension of particulate Hg(As, Sb) accumulated in the local sink may in turn transiently affect the partitioning of Hg between particulate and dissolved forms (Wayne et al., 1996), determining an increase of Hg in dissolved species in some sector of the Paglia River. This effect is particularly evident for As and Sb, whose loads are mainly determined by dissolved fractions at PA. As the dissolved Hg species are the more promptly available to methylation reactions (Ullrich et al., 2001), possible conversion of Hg to methyl-Hg would be expected in the PRB. Nevertheless, increase of methyl-Hg bioavailability with increasing distance from the ASSM was not reported in sites located near to Allerona (Rimondi et al., 2012), suggesting that methyl-Hg formation is probably not enhanced by the increase of dissolved Hg species.

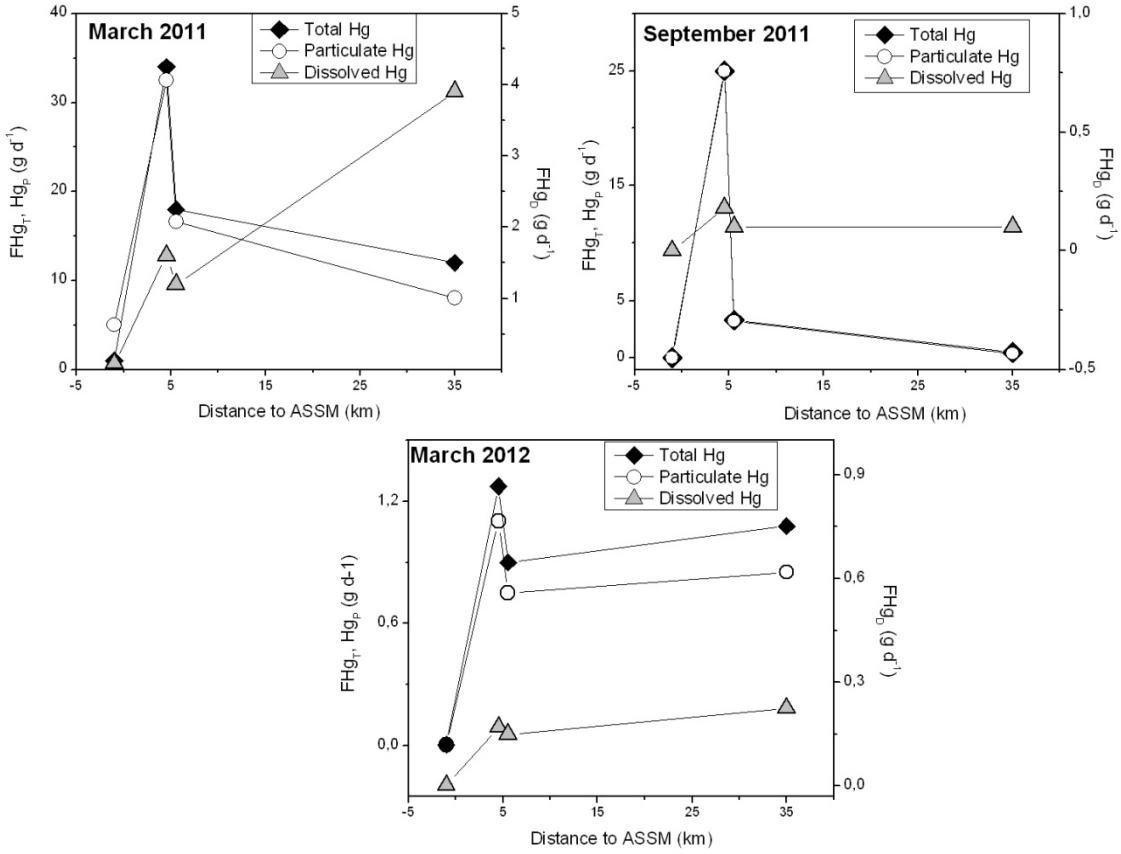

Fig. 3.11. *Spatial relation of As and Sb fluxes determined for each station in different hydrological periods Open symbols refers to Sb, full colored symbols to As.*

3.4.6 Anthropogenic contribution to Hg fluxes

In order to determine how much of the observed Hg, As and Sb transport (i.e. load) was originated from natural processes, i.e. how continental erosion processes contributed to the river flux, we calculated the theoretical flux for each sampling site. Theoretical flux (F_T), related only to natural denudation of Earth's crust, was calculated as follows (Szefer, 1990):

$$F_T = [Me]_{AM} \times F_{SPM} \times [Li_{SPM}]/[Li_{UCC}]$$

where $[Me]_{AM}$ is the Southern Tuscany natural background for Hg, As and Sb (cf. § 3.4.4), F_{SPM} is the daily SPM flux, and $[Li_{SPM}]/[Li_{UCC}]$ is the ratio of Li content in particulate matter to that of the superficial Earth's crust. Metal sources to the Paglia River were then identified by defining the ratio, $FR = F_{OBS}/F_T$, between observed flux and theoretical flux. When FR is comprised between 0.5 and 1.5, natural erosion of continental crust is mainly responsible for the observed flux, while for FR >1.5 anthropogenic sources contribute to the mass transport (Szefer, 1990). FR values are significant only when the analyzed element is transported

principally as particulate phase. On the contrary, if the element partitions mainly as the dissolved form, the obtained FR are artificially elevated. In order to minimize such high FR values, especially for Sb, the ratios in this study were then calculated referring only to the observed particulate fluxes. The percentage ratio between the F_T and F_{OBS} (F_T/F_{OBS} (%)) was calculated in order to quantify how much of the observed flux was due to natural denudation phenomena.

Background fluxes for Hg, As and Sb, FR values and F_T/F_{OBS} (%) are reported in Table 3.8. Maximum background fluxes are observed during the rainy season, when up to 7, 156 and 9 g d^{-1} are mobilized for Hg, As and Sb, respectively. These data are considered as baseline fluxes, i.e. related only to the natural erosion of continental rocks, i.e. without any anthropogenic source. The regional elevated concentrations of these metals in soils and sediments of the Mt. Amiata area (Protano et al., 1998), as a result of widespread diffusion of these elements in Tuscany mineral deposits, are mainly responsible for elevated background fluxes in Paglia River. Moreover, this phenomenon is accentuated by the highly erosional rate characterizing the PRB (5-6 cm y^{-1}) (Della Seta et al., 2007), which promotes mobilization of naturally metal-enriched sediments in the basin, particularly by the action of heavy winter rains.

Values of FR are between 1 and 108, ~1−72 and 10−29 for Hg, As and Sb, respectively and contrary to background fluxes, are higher during dry seasons (September 2011−March 2012), increasing from one to two orders of magnitude with respect to rainy season (Table 3.8). Higher FR are referred to PV for Hg and As, while at PA for Sb (Table 3.8). Percentage contributions of background flux to the observed (particulate) one (F_T/F_{OBS} %) range between 1 to 82 % for Hg, from to 1 to >100 % for As and from 3 to 10 % for Sb, and are higher during the wet season (Table 3.8). Data suggest that a significant proportion of Hg is mobilized as result of anthropogenic activity, i.e. Hg mining activity at ASSM, as FR values are significantly higher than 1, particularly at PV. However, in summertime the absence of rainy events steeply decreases the amount of Hg deriving by denudation phenomena, increasing the percentage of Hg flux related to anthropogenic activity, i.e. discharge from the Galleria Italia becomes the predominant fraction of the observed Hg flux. Similar conclusions can be drawn for As, whose mass transport during March 2011 was almost completely associated to natural denudation phenomena (FR ~ 1). As data for Sb particulate fluxes were available only for September 2011, it was not possible to observe any FR seasonal variations as noted for Hg and As. However a small increase of FR between PC and PA (10 and 13, respectively) and associated decrease of F_T/F_{OBS} (from 10 to 8), confirm that ASSM does not

represent the only punctual source of Sb to the basin, the contributions to Sb fluxes mainly deriving from those mines located in the southern Mt. Amiata district.

	Hg			As			Sb		
	F_T (g d^{-1})	FR	F_T/F_{OBS} (%)	F_T (g d^{-1})	FR	F_T/F_{OBS} (%)	F_T (g d^{-1})	FR	F_T/F_{OBS} (%)
March 2011									
PM	0.2	3	35	4	0.6	>100	0.3	n.d.	n.d.
PV	2	17	6	44	3	33	3	n.d.	n.d.
PC	7	2	40	156	1	100	9	n.d.	n.d.
PA	4	2	47	88	0.6	>100	5	n.d.	n.d.
September 2011									
PM	n.d.	n.d.	n.d.	n.d.	n.d.	n.d.	n.d.	n.d.	n.d.
PV	0.2	108	1	5	15	7	0.3	29	3
PC	0.2	17	6	5	13	7	0.3	10	10
PA	0.02	18	5	0.5	2	68	0.03	13	8
March 2012									
PM	n.d.	n.d.	n.d.	n.d.	n.d.	n.d.	n.d.	n.d.	n.d.
PV	0.05	21	5	1	72	1	0.1	n.d.	n.d.
PC	0.1	8	13	2	25	4	0.1	n.d.	n.d.
PA	0.7	1	82	16	1	90	0.9	n.d.	n.d.

Table 3.8. *Theoretical fluxes (F_T), flux ratio (FR) and percent ratio between theoretical and observed fluxes (F_T/F_{OBS}) of Hg, As and Sb at selected sites PM, PV, PC and PA.*

3.4.7 Mercury loads: comparison with other mining districts and annual estimate

The maximum calculated daily loads in the Paglia River (site PV) are generally in the range or higher than those reported for Hg mining impacted basins with similar drainage area, such as those draining the most important Hg mines of the Californian Coast Ranges (Table 3.9). Higher loads were however reported for the Isonzo River (Idrija mine), which has a drainage basin (1,533 km^2) much larger than that considered for Paglia River in this study (cf. § 3.2). For similar reasons, much higher Hg loads were measured at the outlet of the Sacramento River, that together with the Cache Creek drain 154,000 km^2, being the 96th river in the world on the base of its water discharge (David et al., 2009).

Although the data presented above suggest the importance of Hg transport in the Paglia River, they do not provide a representative estimate of Hg transport by the river on an annual time scale. However, as Hg is essentially transported bound to the particulate fraction, reasonable estimate of Hg fluxes are generally obtained from the mean annual concentration of Hg_{SPM} and established SPM fluxes in the basin, neglecting the contribute of Hg_D (Balogh et al.,

1997; Thomas et al., 2002; Schäfer et al., 2006; Leicht et al., 2007). Nevertheless, computations of SPM fluxes are time-consuming, as much of SPM in river basin is transported in few days of the year (Horowitz et al., 2001; Moatar et al., 2006), then requiring an accurate choice of sampling frequency. Thus, reliable annual estimates of Hg loads are difficult, particularly in those basins where SPM fluxes are extremely variable, i.e. where different erosive factors occur together: elevated runoff during storm events, high acclivity, erodible formations, as it is the case for the Paglia River (Della Seta et al., 2007). Accordingly, the importance of episodic transport of Hg following storm events is stressed in different mining districts (Table 3.9). In these conditions, enormous quantities of SPM are indeed mobilized as a result of higher runoff, increased capacity for the stream to erode contaminated bank, and transport sediments (White and Kirchner, 2000), resulting in up to 80-fold increase of Hg transport (White and Kirchner, 2000). Particularly, 8 days of flood event in the Isonzo River (Idrija mine) were enough to mobilize up to three times the amount of Hg transported in a whole year (Širca et al., 1999). Although in this study was not possible to continuously monitor SPM, estimate of yearly Hg load was performed at PV considering the mean of the daily loads measured in March and September 2011 (~ 30 g d^{-1}), as representative of the whole year. This simplification is consistent with the finding that Hg loads at PV are pretty much unaffected by flow discharge. In this condition annual Hg load accounts to ~ 11 kg yr^{-1}, being comparable to Hg loads observed elsewhere, and particularly being 10 times higher than those determined at the New Idrija Hg mine (Table 3.9), one of the most important Hg mine in North America. It should however be emphasized that this estimated annual flux has to be considered as a conservative estimate, being derived during flow baseline conditions for the Paglia River. In these calculations is indeed neglected the potentially high input of Hg during rainfall events, which may possible increase the estimate up to one order of magnitude (Ganguli et al., 2000). Particularly, *flash flood* events are well documented in the Paglia River. They are able to rapidly mobilize high volumes of suspended material during heavy winter rainfall (Di Tria et al., 1999), likely resulting in an additional increase of Hg budget for the basin.

Hg mine districts and locations	Hg loads		
	daily loads (g d^{-1})*		annual loads (kg yr^{-1})
	baseline	*episodic flux*	
Abbadia San Salvatore mine (Mt. Amiata, Italy)[a]	30	--	11
Idrija mine (Slovenia)[b]	4,000	4,700 kg (8 d)	1,500
New Almadén mine (CCR[1], California)[c]	30	22 (2 d)	4-30
New Idrija (CCR[1], California)[d]	7	--	1.5
Gambonini mine (CCR[1], California)[e]	1.7	30 kg (2 d)	--
Cache Creek mines (CCR1, California)[f]	--	134-2,400 (3 d)	4.5-12.5
CCR[1] mines (California)[g,h]	< d.l.-57 kg d^{-1}	--	61-470

[a]this study; [b]Sirka et al. (1999); [c]Thomas et al. (2002); [d]Ganguli et al. (2000); [e]White and Kirchner (2000); [f]Domalgaski et al. (2004); [g]Choe et al. (2003); [h]David et al. (2009); [1]California Coast Ranges

Table 3.9. *Reported total Hg loads calculated for creeks and rivers draining worldwide Hg mines. *Daily fluxes (storm events) are in g d^{-1}, although otherwise specified; numbers in parenthesis indicate the duration of the event.*

3.5 Conclusions

Mercury geochemistry is studied in different hydrologic conditions in the Paglia River watershed, which is heavily polluted by anthropogenic activity, mainly due to the past mining activity of Mt. Amiata. After more than 30 years from the end of the mining activity, this study shows that a Hg persistent contamination affects both waters and particulate matter of the Paglia River. Calculated EF_{Li}^{Hg} and I_{geo} suggest that river suspended matter is enriched in Hg up to 100 times with respect to the natural background levels. Minor, but still significant, contamination of suspended matter in As and Sb is reported. Using tracer injection and water sampling, loads of Hg, As and Sb along the Paglia River are quantified. Particulate loads and partition coefficients show that Hg transport mainly occurs as Hg bound to particulate; Hg fluxes are 1 to 2 orders of magnitude higher than dissolved ones. Mercury partitioning in the Paglia River is mainly the result hydrological conditions and mine runoff. High loads of Hg (As) are the result of runoff from ASSM, the most important Hg producing mine in the Mt. Amiata district, as Hg (As) loads substantially decrease downstream from the mine area. Sharp change of the hydrological gradient along the river course causes the deposition of particulate Hg, which forms a sink, from which it is later mobilized during periods of low flows, representing a constant source of Hg to the basin. This mechanism of Hg transport in

the PRB is unaffected by the hydrological conditions of the river, while rainfall and the associated river discharge determine the quantities of Hg (i.e. load) released from the basin.
The yearly Hg flux of 11 kg yr^{-1} represents the first reliable estimate of Hg transported by the Paglia River from the Mt. Amiata district during base flow conditions. However, such a value may highly underestimate the real amount of Hg transported in this area, as huge amount of SPM could be mobilized in the Paglia River as a consequence of multiple rainy days and/or storm events. Future studies are therefore needed in order to have additional information about temporal SPM fluctuations in the Paglia River, and to quantitatively determine the importance of flood events to mobilize particulate Hg. Particularly, due to the human-altered river morphodynamic, which favours downstream transport of Hg accumulated on the bottom of the river bed, data of this study highlight that elevated quantities of Hg could directly be delivered to the Tiber River, thus representing an hazard for its ecosystem. Additional investigations should be carried out in the Tiber River Basin to determine the impact of Hg discharged by the Paglia River, and to quantify the loads of Hg that are consequently discharged to the Mediterranean Sea.

Acknowledgements

This study was financially supported by the University of Florence, and the Municipality of Abbadia San Salvatore (Italy). I do acknowledge Regione Toscana (geologists Andrea Salvadori and Marco Nannucci) and Servizio Idrografico Regionale Umbria for providing field support during the discharge measurements, and Dr.ssa Francesca Podda (University of Cagliari) for providing heavy metals analysis in waters and SPM. Daniele Rappuoli, Marcello Niccolini (Municipality of Abbadia San Salvatore) Mario Paolieri, and Francesca Dughetti (University of Florence) are gratefully thanked for their assistance during fieldwork.

References

APPELO C.A.J. AND POSTMA D. (1993). Geochemistry, Groundwater and Pollution. Rotterdam, Brookfield, pp. 536.

ARISI ROTA F., BRONDI A., DESSAU G., FRANZINI M., MONTE AMIATA S.P.A. (1971), STABILIMENTO MINERARIO DEL SIELE, STEA B., VIGHI L. (1971). I Giacimenti minerari. In: La Toscana meridionale. *Rend. Soc. Ital. Mineral. Petrol.*, **27**, Spec. Is.: 357–544.

BACCI E. (1989). Mercury in the Mediterranean. *Mar. Pollut. Bull.*, **20**: 59−63.

BALOGH S.J., MEYER M.L., JOHNSON D.K. (1997). Mercury and Suspended Sediment Loadings in the Lower Minnesota River. *Environ. Sci. Technol.*, **31**: 198−202.

BENCALA K. E., MCKNIGHT D. M., ZELLWEGER G. W. (1990). Characterization of transport in an acidic and metal−rich mountain stream based on a lithium tracer injection and simulations of transient storage. *Water Resour. Res.*, **26**: 989–1000.

BENVEGNÙ E., BRONDI A., COLICA A., CONTI P., GUASPARRI G., POLIZZANO C., SABATINI G., TASSONI E. (1993). Studies of migration factors in clay in real situation; study of fractures in clays the neogenic basin of Siena. Nuclear Sc. Tech., Commission of European Communities Report. pp.1–53.

BLOOM N. (1989). Determination of Picogram Levels of Methylmercury by Aqueous Phase Ethylation, Followed by Cryogenic Gas Cromatography with Cold Vapour Atomic Fluorescence Detector. *Can. J. Fish. Aquat. Sci.*, **46**: 1131−1140.

CASTALDI F. AND CHIOCCHINI U. (2012). Effects of land use changes on badland erosion in clayey drainage basins, Radicofani, Central Italy. *Geomorphology*, **169-170**: 98−108.

CENCETTI C., FREDDUZZI A., MARCHESINI A. (2004). Processi di erosione in alvei ghiaiosi dell'Italia Centrale. Il fiume Paglia (Bacino del Tiber). Atti della 8° conferenza italiana ASITA "Geomatica Standardizzazione, interoperabilità e nuove tecnologie. Roma, 14-17 dicembre, vol. 1: 731-736.

CICCACCI S., D'ALESSANDRO L., FREDI P., LUPIA PALMIERI E. (1988). Contributo dell'analisi geomorfica quantitativa allo studio dei processi di denudazione nel bacino idrografico del Torrente Paglia (Toscana meridionale−Lazio settentrionale). *Suppl. Geogr. Dinam. Quat.*, **1**: 171−188.

CICCACCI S. GALIANO M., ROMA M.A., SALVATORE M.C. (2009). Morphodynamics and morphological changes of the last 50 years in a badland sample area of Southern Tuscany (Italy). *Z. Geomorph. N. F.*, **53**, 273−297.

CHOE K.−Y., GILL G.A., LEHMAN R. (2003). Distribution of particulate, colloidal, and dissolved mercury in San Francisco Bay estuary. 1. Total mercury. *Limn. Ocean.,* **48**: 1535–1546.

CIDU R. AND FRAU F. (2009). Distribution of trace elements in filtered and non filtered aqueous fractions: Insights from rivers and streams of Sardinia (Italy). *Appl. Geochem.*, **24**: 611−623.

COQUERY M., COSSA D., SANJUAN J. (1997). Speciation and sorption of mercury in two macro-tidal estuaries. *Mar. Chem.*, **58**: 213−227.

COSSA D., MARTIN J.-M., TAKAYANAGI K., SANJUAN J. (1997). The distribution and cycling of mercury species in the western Mediterranean. *Deep-Sea Res. Pt. II*, **44**: 721-740.

COSSA D. AND COQUERY M. (2005). The Mediterranean Mercury Anomaly, a Geochemical or a Biologocal Issue. *Hdb. Env. Chem.*, **5**, Part K: 177–208.

COVELLI S., PIANI R., ACQUAVITA A., PREDONZANI S., FAGANELI J. (2007). Transport and dispersion of particulate Hg associated with a river plume in coastal Northern Adriatic environments. *Mar. Pollut. Bull.*, **55**: 436−450.

COYNEL A., SCHÄFER J., BLANC G., BOSSY C. (2007). Scenario of particulate trace metal and metalloid transport during a major flood event inferred from transient geochemical signals. *Appl. Geochem.*, **22**: 821–836.

DASKALAKIS K.D. AND O' CONNOR T.P. (1995). Normalization and Elemental Sediment Concentrations in the Coastal United States. *Environ. Sci. Technol.*, **29**: 470−477.

DAVID N., MCKEE L.J., BLACK F.J., FLEGAL A.R., CONAWAY C.H., SCHOELLHAMER D.H., GANJU N.K. (2009). Mercury concentrations and loads in a large river system tributary to San Francisco Bay, California, USA. *Environ. Toxicol. Chem.*, **28**: 2091–2100.

DELLA SETA M., DEL MONTE M., FREDI P., LUPIA PALMIERI E. (2007). Direct and indirect evaluation of denudation rates in Central Italy. *Catena*, **71**: 21-30.

DI TRIA L., GRIMALDI S., NAPOLITANO F., UBERTINI L. (1999). Rainfall forecasting using limited area models and stochastic models. Proc. of EGS Plinius Conference, Maratea, 193–204.

D'ORAZIO M., INNOCENTI F., SERRI G., PETRINI R. (1994). Il vulcano di Radicofani nel quadro del magmatismo neogenico − quaternario dell'Appennino settentrionale. *Studi Geologici Camerti*, **1**: 79–92.

DOMAGALSKI J.L., ALPERS C.N., SLOTTON D.G., SUCHANEK T.H., AYERS S.M. (2004). Mercury and methylmercury concentrations and loads in the Cache Creek watershed, California. *Sci. Total Environ.*, **327**: 215–237.

DREVER J.I. (1997). The Geochemistry of Natural Waters. Prentice Hall, Upper Saddle River, NJ (USA), pp. 436.

EATON A.D., CLESCERI L.S., GREENBER A.E. (1999). Standard methods for the Examination of Water and Wastewater, 2540D, 19th Ed. American Public Health Association 1995. Washington, DC.

EISLER R. (1987). Mercury hazards to fish, wildlife, and invertebrates: A synoptic review. US Fish and Wildlife Service, Biological Report 85 (1.10), pp. 63.

FAGANELI J., HORVAT M., COVELLI S., FAJON V., LOGAR M., LIPEJ L., CERMELJ B. (2003). Mercury and methylmercury in the Gulf of Trieste (northern Adriatic Sea). *Sci. Total Environ.*, **304**: 315−326.

FENG H., HAN X., ZHANG W., YU L. (2004). A preliminary study of heavy metal contamination in Yangtze River intertidal zone due to urbanization. *Mar. Pollut. Bull.*, **49**: 910–915.

FERRARA R., MASERTI B.E., BREDER R. (1991). Mercury in abiotic and biotic compartments of an area affected by a geochemical anomaly (Mt. Amiata, Italy). *Water Air Soil Poll.,* **56**: 219-233.

FERRARA R., MASERTI B.E., ANDERSSON M., EDNER H., RAGNARSON P., SVANBERG S. (1997). Mercury degassing rate from mineralized areas in the Mediterranean basin. *Water Air Soil Poll.*, **93**: 59−66.

FLANDERS J.R., TURNER R.R., MORRISON T., JENSEN R., PIZZUTO J., SKALAK K., STAHL R. (2010). Distribution, behavior, and transport of inorganic and methylmercury in a high gradient stream. *Appl. Geochem.*, **25**: 1756–1769.

FRONDINI F., CALIRO S., CARDELLINI C., CHIODINI G., MORGANTINI N. (2009). Carbon dioxide degassing and thermal energy release in the Monte Amiata volcanic-geothermal area (Italy). *Appl. Geochem.*, **24**: 860−875.

GANGULI P.M., MASON R.P., ABU−SABA K.E., ANDERSON R.S., FLEGAL A.R. (2000). Mercury Speciation in Drainage from the New Idria Mercury Mine, California. *Environ. Sci. Technol.*, **34**: 4773−4779.

GRAY J.E., THEODORAKOS P.M., BAILEY E.A., TURNER R.R. (2000). Distribution, speciation, and transport of mercury in stream−sediment, stream−water, and fish collected near abandoned mercury mines in southwestern Alaska, USA. *Sci. Total Environ.,* **260**: 21−33.

GURI (GAZZETTA UFFICIALE DELLA REPUBBLICA ITALIANA) (2006a). Decreto legislativo 3 aprile 2006, n. 152: Norme in materia ambientale. Gazzetta Ufficiale della Repubblica Italiana n. 88 del 14-4-2006, suppl. ord. n. 96, Tab.1/A. Istituto Poligrafico dello Stato, Roma.

GURI (GAZZETTA UFFICIALE DELLA REPUBBLICA ITALIANA) (2006b). Decreto legislativo 3 aprile 2006, n. 152: Norme in materia ambientale. Gazzetta Ufficiale della Repubblica Italiana n. 88 del 14-4-2006, suppl. ord. n. 96, Titolo V, All.5. Tab. 1. Istituto Poligrafico dello Stato, Roma.

HISSLER C. AND PROBST J.-L. (2006). Chlor-alkali industrial contamination and riverine transport of mercury: Distribution and partitioning of mercury between water, suspended matter, and bottom sediment of the Thur River, France. *Appl. Geochem.*, **21**: 1837−1854.

HOLMES P., JAMES K.A.F., LEVY L.S. (2009). Is low-level environmental mercury exposure of concern to human health? *Sci. Total Environ.*, **408**: 171−182.

HOROWITZ A.J., ELRICK K.A., SMITH J.J. (2001). Estimating suspended sediment and trace element fluxes in large river basins: methodological considerations as applied to the NASQAN programme. *Hydrol. Process.,* **15**: 1107–1132.

HORVAT M., KOTNIKA J., LOGARA M., FAJONA V., ZVONARI T., PIRRONE N. (2003). Speciation of mercury in surface and deep−sea waters in the Mediterranean Sea. *Atm. Environ.*, **37**, Suppl. No. 1: S93–S108.

HUDSON R. AND FRASER J. (2002). Alternative methods of flow rating in small Coastal streams. Forest Research, Extension Note EN-014, pp. 11. Vancouver Forest Region, BCMOF.

HUDSON R. AND FRASER J. (2005). Introduction to Salt Dilution Gauging for Streamflow Measurement Part IV: The Mass Balance (or Dry Injection) Method. *Streamline Watershed Management Bull.*, **9**: 6−12.

HURLEY J., BENOIT J., BABIARZ C., SHAFER M., ANDREN A., SULLIVAN J., HAMMOND R., WEBB D. (1995). Influences of Watershed Characteristics on Mercury Levels in Wisconsin Rivers. *Environ. Sci. Technol.,* **29**: 1867–1875.

KILPATRICK F.A. (1993). Simulation of soluble waste transport and buildup of in surface waters using tracers. *US Geological Survey Techniques of Water-Resources Investigations*, Vol. 3, chap. A20., pp. 37. Open-File Report: 92-457.

KILPATRICK F.A., AND COBB E.D. (1985). Measurement of discharge using tracers: *US Geological Survey Techniques of Water−Resources Investigations*, Vol. 3, chap. A16, pp. 52.

KILPATRICK F.A., RATHBUN R.E., YOTSUKURA N., PARKER G.W., DELONG L.L. (1989). Determination of stream reaeration coefficients by use of tracers. *US Geological Survey Techniques of Water−Resources Investigations*, Vol. 3, chap. A18, pp. 87.

KIMBALL B.A. (1997). Tracer Injection & Synoptic Sampling. US Geological Survey Fact Sheet FS−245−96, pp. 7.

KIMBALL B.A., BIANCHI F., WALTON−DAY K., RUNKEL R.L., NANNUCCI M., SALVADORI A. (2007). Quantification of Changes in Metal Loading from Storm Runoff, Merse River (Tuscany, Italy). *Mine Water Environ.*, **26**: 209–216.

KIMBALL B.A. AND RUNKEL R.L. (2009). Spatially Detailed Quantification of Metal Loading for Decision Making: Metal Mass Loading to American Fork and Mary Ellen Gulch, Utah. *Mine Water Environ.*, **28**: 274−290.

KIMBALL B.A., RUNKEL R.L., GERNER L.J. (2001). Quantification of mine−drainage inflows to Little Cottonwood Creek, Utah, using a tracer-injection and synoptic-sampling study. *Environ. Geol.*, **40**: 1390−1404.

KIMBALL B.A., RUNKEL R.L., WANTY R.B., VERPLANCK P.L. (2010). Reactive solute−transport simulation of pre−mining metal concentrations in mine-impacted catchments: Redwell Basin, Colorado, USA. *Chem. Geol.*, **269**: 124−136.

KITE G. (1993). Computerized streamflow measurement using slug injection. *Hydrol. Process.*, **7**: 227−233.

KOCMAN D., KANDUČ T., OGRINC N., HORVAT M. (2010). Distribution and partitioning of mercury in a river catchment impacted by former mercury mining activity. *Biogeochemistry*, doi:10.1007/s10533-010-9495-5, pp. 19.

LANGELIER W. AND LUDWING H. (1942). Graphical methods for indicating the mineral character ofnatural waters. *J. Am. Water Assoc.*, **34**: 335 - 352.

LEERMAKERS M., MEULEMAN C., BAEYENS W. (1995). Mercury speciation in the Scheldt estuary. *Water Air Soil Poll.*, **80**: 641-652.

LEITCH D.R., CARRIE J., LEAN D., MACDONALD R.W., STERN G.A., WANG F. (2007). The delivery of mercury to the Beaufort Sea of the Arctic Ocean by the Mackenzie River. *Sci. Total Environ.*, **373**: 178–195.

LIN C., HE M., LI Y., LIU S. (2012). Content, enrichment, and regional geochemical baseline of antimony in the estuarine sediment of the Daliao river system in China. *Chem. Erde−Geochem.*, **72**: S4: 23–28.

LORING D.H. (1990). Lithium – a new approach for the granulometric normalization of trace metal data. *Mar. Chem.*, **29**: 155−168.

LORING D.H. AND RANTALA R.T.T. (1992). Manual for the geochemical analyses of marine sediments and suspended particulate matter. *Earth-Sci. Rev.*, **32**: 235−283.

LOSKA K., WIECHUŁA D., KORUS I. (2004). Metal contamination of farming soils affected by industry. *Environ. Int.*, **30**: 159– 165.

MARTIN J.-M. AND MEYBECK M. (1979). Elemental mass-balance of material carried by major world rivers. *Mar. Chem.,* **7**: 173−206.

MOATAR F., PERSON G., MEYBECK M., COYNEL A., ETCHEBER H., CROUZET P. (2006). The influence of contrasting suspended particulate matter transport regimes on the bias and precision of flux estimates. *Sci. Total Environ.*, **370**: 515−531.

MORETTI G.P., CIANFICCONI F., PERONI E., RONCA M. (1988). Considerazioni sulle comunità macrobentoniche del sistema fluviale Paglia-Chiani. *Boll. Mus. St. Nat. Lunigiana*, **6-7**: 157–161.

MORTEANI G., RUGGIERI G., MÖLLER P., PREINFALK C. (2011). Geothermal mineralized scales in the pipe system of the geothermal Piancastagnaio power plant (Mt. Amiata geothermal area): a key to understand the stibnite, cinnabarite and gold mineralization of Tuscany (central Italy). *Miner. Deposita*, **46**: 197–210.

MÜLLER G. (1981). Die Schwermetallbelastung der Sedimenten des Neckars und Seiner Nebenflüsse. *Chem. Ztg.,* **6**: 157– 64.

PARAQUETTI H.H.M., AYRES G.A., DE ALMEIDA M.D., MOLISANI M.M., DE LACERDA L.D. (2004). Mercury distribution, speciation and flux in the Sepetiba Bay tributaries, SE Brazil. *Water Res.*, **38**: 1439−1448.

PASCUCCI, V., COSTANTINI, A., MARTINI, P.I., DRINGOLI, R. (2006). Tectono sedimentary analysis of a complex, extensional, Neogene basin formed on thrust faulted, Northern Apennines hinterland: Radicofani Basin, Italy. *Sediment. Geol.*, **183**: 71–97.

PECCERILLO A. (2002). Plio-Quaternary magmatism in Central-Southern Italy: a new classification scheme for volcanic provinces and its geodynamic implications. *Boll. Soc. Geol. It.,* Spec. Vol. **1**: 113−127.

PROTANO, G., RICCOBONO, F., SABATINI, G. (1998). La cartografia geochimica della Toscana meridionale. Criteri di realizzazione e rilevanza ambientale attraverso esempi di Hg, As, Sb, Pb e Cd. – *Mem. Descr. Carta Geol. It.*, **55**: 109–140.

RAJAR R., ČETINA M., HORVAT M., ŽAGAR D. (2007). Mass balance of mercury in the Mediterranean Sea. *Mar. Chem.*, **107**: 89−102.

REIMANN C. AND DE CARITAT P. (2005). Distinguishing between natural and anthropogenic sources for elements in the environment: regional geochemical surveys versus enrichment factors. *Sci. Total Environ.*, **337**: 91– 107.

RENZONI A., ZINOAND F., FRANCHI E. (1998). Mercury Levels along the Food Chain and Risk for Exposed Populations. *Environ. Res. A*, **77**: 68−72.

RIMONDI V., GRAY J.E., COSTAGLIOLA P., VASELLI O., LATTANZI P. (2012). Concentration, distribution, and translocation of mercury and methylmercury in mine-waste, sediment, soil, water, and fish collected near the Abbadia San Salvatore mercury mine, Mt. Amiata district, Italy. *Sci. Total Environ.*, **414**: 318−327.

RUDNICK S. AND GAO S. (2003). Composition of the continental crust. In: Holland H.D., Turekian K.K. (Eds.), The Crust., Treatise on Geochemistry, vol. 3. Elsevier, Oxford, pp. 1–64.

SCHÄFER J., BLANC B., AUDRY S., COSSA D., BOSSY C. (2006). Mercury in the Lot–Garonne River system (France): Sources, fluxes and anthropogenic component. *Appl. Geochem.*, **21**: 515−527.

ŠIRCA A., HORVAT M., RAJAR R., COVELLI S., ŽAGAR D., FAGANELI J. (1999). Estimation of mercury mass balance in the Gulf of Trieste. *Acta Adriatica*, **40**: 75−85.

SONG L., LIU C.-Q., WANG Z.-L., ZHU X., TENG Y., LIANG L., TANG S., LI J. (2011). Iron isotope fractionation during biogeochemical cycle: Information from suspended particulate matter (SPM) in Aha Lake and its tributaries, Guizhou, China. *Chem. Geol.*, **280**: 170–179.

STORDAL M.C., GILL G.A., WEN L.−S., SANTSCHI P.H. (1996). Mercury phase speciation in the surface waters of three Texas estuaries: Importance of colloidal forms. *Limnol. Oceanogr.*, **41**: 52-61.

SUTHERLAND RA. (2000). Bed sediment-associated trace metals in an urban stream, Oahu, Hawaii. *Environ. Geol.*, **39**: 611– 27.

SZEFER (1990). Mass−balance of metals and identification of their sources in both river and fallout fluxes near Gdańsk Bay, Baltic Sea. *Sci. Total Environ.*, **95**: 131−139.

TANELLI G. (1983). Mineralizzazioni metallifere e minerogenesi della Toscana. *Mem. Soc. Geol. It.*, **25**: 91–109.

TAYLOR S.R. AND MCLENNAN S.M. (1995). The geochemical evolution of the continental crust. *Rev. Geophys.*, **33**: 241–265.

THOMAS M.A., CONAWAY C.H., STEDING D.J., MARVIN-DI PASQUALE M., ABU-SABA K.E., FLEGAL A.R. (2002). Mercury contamination from historic mining in water and sediment, Guadalupe River and San Francisco Bay, California. *Geochem.: Explor. Environ. Anal.*, **2**: 211−217.

ULLRICH S.M., TANTON T.W., ABDRASHITOVA S.A. (2001). Mercury in the Aquatic Environment: A Review of Factors Affecting Methylation. Crit. Rev. *Environ. Sci. Technol.*, **31**: 241–293.

UNEP/ECE/UNIDO/FAO/UNESCO/WHO/IAEA (1984). Pollutants from land-based sources in the Mediterranean. *UNEP Regional Seas Reports and Studies No. 32*. Geneva, pp. 99.

UNEP/WHO (1996). Guidelines for treatment of effluents prior to discharge into the Mediterranean Sea. *MAP Technical Reports Series No. 111*. Athens, pp. 247.

US EPA (1996). Method 1669, Sampling Ambient Water for Trace Metals at EPA Water Quality Criteria Levels. U.S. Environmental Protection Agency, Washington DC

US EPA (1997). Mercury study report to Congress. U.S. Environmental Protection Agency. I−VIII, EPA−452/R−97−003.

US EPA (2002). Method 1631, Revision E: Mercury in water by oxidation, purge and trap, and cold vapor atomic fluorescence spectrometry. U.S. Environmental Protection Agency. 821−R−02−01.

US EPA (2009). National Recommended Water Quality Criteria. United States Environmental Protection Agency. http:/www.epa.gov/ost/criteria/wqctable/.

YIĞITERHAN O. AND MURRAY J.M. (2008). Trace metal composition of particulate matter of the Danube River and Turkish rivers draining into the Black Sea. *Mar. Chem.*, **111**: 63−76.

WALL G.R., INGLESTON H.H., LITTEN S. (2005). Calculating mercury loading to the tidal Hudson River, New York, using rating curve and surrogate methodologies. *Water Air Soil Pollut.*, **165**: 233–248.

WAYNE D.M., WARWICK J.J., LECHLER P.J., GILL G.A., BERRY LYONS W. (1996). Mercury contamination in the Carson River, Nevada: a preliminary study of the impact of mining wastes. *Water Air Soil Pollut.*, **92**: 391−408.

WEDEPOHL H. (1995). The composition of the continental crust. *Geochim. Cosmochim. Acta*, **59**: 1217–1239.

WHO (1976). Environmental Health Criteria no. 1: Mercury. World Health Organization, Geneva, Switzerland.

WHYTE D.C. AND KIRCHNER J.W. (2000). Assessing water quality impacts and cleanup effectiveness in streams dominated by episodic mercury discharges. *Sci. Total Environ.*, **260**: 1−9.

WOOD P.J. AND DYKES A.P. (2002). The use of salt dilution gauging techniques: ecological considerations and insights. *Water Res.*, **36**: 3054–3062.

CHAPTER 4

PART III - MERCURY SPECIATION IN THE MINING DISTRICT OF MT. AMIATA (SOUTHERN TUSCANY, ITALY)

Abstract

A fundamental step in order to evaluate the biogeochemical and, in particular, the eco–toxicological significance of Hg diffusion in the environment is to determine, rather than its absolute content, its speciation and reactivity in solid matrices. Various independent techniques, such as SEM–EDS, sequential extractions (SCE), and X–Ray Absorption Spectroscopy (XAS), are applied in this study in order to unravel the Hg speciation in samples coming from the Hg mining district of Mt. Amiata, located in Southern Tuscany (Italy). Different geological materials, like waste calcines, soils, sediments, and water particulate matter were analyzed. Due to the complex mineralogy of the samples, the results obtained by the different techniques are sometimes ambiguous, or conflicting. Results show that the samples are mainly composed by insoluble sulphide minerals (cinnabar and metacinnabar), together with a significant proportion of soluble Hg compounds. Their formation is presumably the result of ore-roasting process, post-depositional weathering reactions, and waste calcine runoff. In addition, the wide distribution of elemental Hg (Hg^0) in sediments draining the mining area at present or in the recent past, highlights the strong impact of anthropogenic activity in this area. Nowadays, the principal environmental concern in the Mt. Amiata district is represented by the diffusion downstream of the mine of soluble ionic Hg compounds, which could provide Hg(II) species for methylation reactions. In spite of some unresolved ambiguities, a multi-technique approach to study Hg speciation appears of fundamental importance to fully characterize complex matrices, particularly in order to overpass the inherent limitations that characterize each methodology.

Keywords: mercury, speciation, X-Ray Absorption Spectroscopy, Sequential chemical extractions

4.1 Introduction

Mercury is a heavy metal of environmental concern, indicated by the U.S. Environmental Protection Agency (US EPA) as the most impacting to human health of all the pollutants

included in the Clean Air Act (US EPA, 1997). The greatest potential threat of Hg is its natural conversion to methyl–Hg, an organic compound that is at least one order of magnitude more mobile than inorganic Hg, 50-100 times more toxic, and more readily bioaccumulated especially in the aquatic food web (Compeau and Bartha, 1984; Bloom and Porcella, 1994; US EPA, 2001; Gabriel et Williamson, 2004).

As for other metals, Hg speciation is fundamental because it controls its solubility, reactivity, bioavailability, and therefore its toxicity. The solubility of Hg compounds extends across both ends of the solubility range, from Hg sulfides, which are chemically unreactive and stable over geological times, to Hg-chloride/sulphates/oxides, which show a much higher solubility. Consequently, Hg sulfides, although representing the most abundant Hg compounds in mining sites, are by far the least toxic compounds.

A significant risk associated to dismissed and active Hg mines worldwide is the natural erosion by local streams and rivers of roasted mine wastes (calcines), which are often improperly disposed. Due to the inefficiency of retorting processes, calcines still contain appreciable amount of Hg in the form of unconverted cinnabar and metacinnabar, but more importantly in the form of Hg^0 and ionic Hg compounds formed during ore processing (Kim et al., 2000, 2003, 2004; Gray et al., 2006; Esbrí et al., 2010). These water soluble Hg compounds may adversely impact the environment because they release Hg(II) species, which are the main precursors to the formation of methyl-Hg (Compeau and Bartha, 1984; Ullrich et al., 2001). Therefore, environmental studies addressed to determine the speciation of Hg in areas impacted by mining are essential to establish effective cleanup strategies, and to protect humans and biota from exposure to highly toxic methyl-Hg.

The speciation of dilute Hg levels in complex mixed inorganic and organic matrices, such as soils and sediments, can be determined by means of different techniques: sequential chemical extractions (SCE) (Neculita et al., 2005; Sanchéz et al., 2005), sequential thermal desorption (Biester et al., 1999, 2000; Teršič et al., 2011), microbeam analysis (SEM-EDS and TEM), and X–Ray Absorption Spectroscopy (XAS). Differently from the others, SCE do not yield indications about mineralogical phases in the samples, but define an *operational* speciation (fractionation), that is assumed to indicate the biogeochemical behaviour of the fractions present in the sample. SCE offer therefore a direct tool to evaluate the behaviour of Hg in natural conditions, and have been widely applied for speciation studies in mining districts (Martín-Doimeadios et al., 2000; Kocman et al., 2004; Lin et al., 2010). On the other hand, XAS has been shown to provide direct in situ information on Hg major phases in different matrices, and has been intensively applied to study Hg speciation in minerals (Behra et al.,

2001), plants (Patty et al., 2009), fish (Kuwabara et al., 2007), and particularly to characterize high grade Hg geological materials such as waste calcine (Kim et al., 2000; 2003; 2004; Bernaus et al., 2006a; Esbrì et al., 2010) and contaminated soils (Bernaus et al., 2006b; Terzano et al., 2010). All these techniques suffer for some inherent limitations, which include a non fully specific removal of Hg phases over multiple extraction steps for SCE, and a high Hg concentration threshold (usually ~ 1-100 μg/g) for XAS, preventing the application of this spectroscopy to highly dilute (ppb) Hg compounds, which is the usual concentration of methyl-Hg found in contaminated areas. A further limitation of XAS is that the phases contained in low relative proportions (< ~10%) are usually difficult to detect because their signal is hindered by the species occurring in higher relative proportions; on the other hand, even small percentages can be quantified by SCE. Nevertheless, information deriving from these two techniques is complementary, therefore their combined application should provide a reliable picture of metal speciation in many environmentally relevant materials (Kim et al., 2003; Terzano et al., 2010).

Starting from this consideration, the present study combines routine microbeam analysis (SEM–EDS) with SCE and XAS in order to characterize Hg speciation in samples coming from the Mt. Amiata Hg district and particularly the Abbadia San Salvatore Hg mine (Southern Tuscany, Italy; Fig. 4.1). At a continental scale, this district belongs to the large circum–Mediterranean Hg belt, which hosts about 65% of world cinnabar deposits (Bargagli et al., 1986). Although mining activity in this area ceased in 1980s, abandoned and untreated mine wastes continue to release Hg in the environment, where it is actively methylated (Rimondi et al., 2012). Furthermore, the presence of elemental Hg is well visible in soils of the mining area. To our knowledge, only a previous speciation study was conducted in this area by application of SEC (Malferrari et al., 2011); however investigations coupling XAS and SCE were never conducted in this important Hg district. A comprehensive set of samples, ranging from 27–1,500 μg/g Hg, are analyzed in this work. They include: 1) waste calcines and soils of the mining area; 2) particulate dispersed in stream waters, and stream sediments collected from the watercourse receiving drainage from the Hg mines; 3) pre-industrial stream sediments. This dataset was chosen in order to delineate a complete picture of Hg speciation in different geological and mine samples, starting from the source of Hg to the environment (calcines and soils of the mining area) down to the targets of contamination (lake and stream sediments), while the present-day transport conditions are monitored by means of particulate matter in waters. The study of Hg speciation in sediments presumably deposited in pre-

industrial times, and therefore not affected by anthropogenic activities, should provide an indication of the local natural background.

4.2 Experimental Section

4.2.1 Investigated site

Southern Tuscany, located in central Italy, has been one of the most important mining districts in Italy, since the Pre-Roman Age. Mining activities for exploitation of cinnabar at the Mt. Amiata volcano–geothermal area started during the Etruscan period, although discontinuously and not extensively; after a prolonged period of inactivity, Hg mining went on without interruptions from 1870 to 1982, when the exploitation of Hg mines was definitely abandoned. The Mt. Amiata Hg mines produced a total of more than 102,000 t of Hg (3 million flasks of Hg of 34.5 kg each) (Ferrara et al., 1998) in about one century of activity, making it the 4th largest Hg producing district worldwide. The Abbadia San Salvatore Hg mine, located few km east of Mt. Amiata (Fig. 4.1), was the most important mine of the entire district, and where the samples of this study were collected.

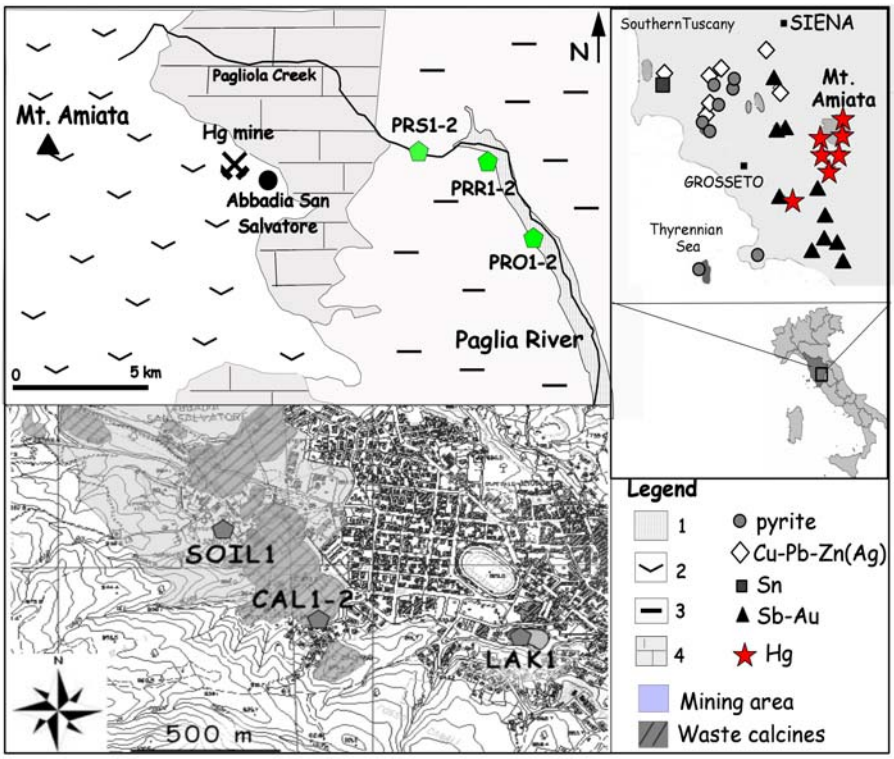

Fig. 4.1. *Localization of the study area and sampling sites, and schematic representation of main outcropping formations: 1) Alluvial deposits (Holocene); 2) Volcanic rocks (Pleistocene); 3) Neogene deposits (Pliocene); 4) Ligurian Domain (Oligocene−Late Cretaceous).*

As it is common to the majority of Hg mines, Hg ore at the studied site is essentially cinnabar, while the presence of stibnite, piryte, realgar, and orpiment was also reported (Morteani et al., 2011). The mineralization is located in flysch complexes belonging to the Ligurian Domain (Cretaceous-Oligocene), and partially in the volcanic rocks of Quaternary age related to the magmatism of Mt. Amiata volcano (Tanelli et al., 1983). Mercury, and associate Sb metallogeny in Tuscany is considered to be the result of shallow convective hydrothermal circulation triggered by the emplacement of granitoids in the mid-crust (Tanelli et al., 1983; Klemm and Neumann, 1984).

4.2.2 Sample collection and preparation

Samples were recovered from the dismissed plant of Abbadia San Salvatore, and its main drainage network, represented by the Pagliola Creek and thereafter Paglia River (Fig. 4.1). A list of the samples analyzed in this study, and a brief description is presented in Table 4.1.

ID	Sampling area	Material
PRR1-2	Paglia River, ~ 5 km downstream the mine	Sediment from the Paglia River internal terrace; recent sediment
PRO1-2	Paglia River, ~ 5 km downstream the mine	Sediment from the Paglia River external terrace, fossil sediment
PRS1-2	Pagliola Creek, ~ 5 km downstream the mine	Stream sediment of the Pagliola Creek, present-day stream sediment
PM1	Pagliola Creek, ~ 5 km downstream the mine	Suspended particulate matter of Pagliola Creek
SOIL1	Mine and metallurgical plant	Forest soil from the mining area
CAL1-2	Mine and metallurgical plant	Calcination waste
LAK1	La Gora lake, town centre	Lake sediment receiving the runoff from the mine

Table 4.1. *Samples location in the mining district of Mt. Amiata.*

Particularly, based on field surveys, sedimentologic characterization and paleohydrographic reconstructions, different orders of terraced fluvial deposits located in the modern valley of Paglia River were recognized in this area. Thanks to this reconstruction, both sediments considered to pre-date industrial activity and sediments dated to the recent-past, i.e. the time of mining, were sampled. In the following we refer to these samples as fossil (PRO) and recent sediments (PRR), respectively. Lastly, active stream sediments of Pagliola Creek (PRS) were collected because they are considered to geochemically represent the catchment

area they are draining. Calcines, sediments and soils were sampled in polyethylene bags, air-dried, sieved at 180 mm, and ground before analysis. Particulate matter was collected by filtering a known amount of water at 0.45 μm with sterilized cellulose filter, oven-dried at 60 °C until a constant weight, and then scrap off from the filter.

4.2.3 Mineralogical and chemical characterization

Samples of calcine, soil, sediment and suspended matter were analyzed for total Hg concentrations at the Dipartimento di Scienze della Terra, Università di Firenze, by digestion with aqua regia (3:1 HCl:HNO_3), and analysis by cold vapor atomic absorption spectroscopy (CVAAS). The data were reported as an average of a duplicate analysis with a mean internal reproducibility of 19%. The analytical quality was checked by using international standards; differences with respect to the certified Hg values was <10%.
For a mineralogical characterization of samples, XRD diffraction spectra were collected using a Philips PW 1050/37 diffractometer equipped with a Cu X–ray tube, using a step-scanning the range from 0 to 70° 2θ at angular increments of 0.05°. SEM observations coupled with EDX spectrometry were also performed on all samples, with a specific attention to the presence of Hg-bearing compounds. The SEM study was conducted on a ZEISS EVO MA15 instrument, equipped with an OXFORD INCA 250 EDX detector.

4.2.4 X-Ray Absorption Spectroscopy

XAS measurements were conducted at the European Synchrotron Facility (ESRF) in Grenoble (France) at the beamline BM25 (SPLINE) at the Hg L_{III}-edge (12,284 eV). The main optical elements included a pseudo channel-cut type monochromator with two fixed Si(111) crystals and Rh coated mirrors, placed upstream and downstream the monochromator, for collimation, vertical focusing, and rejection of higher harmonics. XANES spectra were collected at room temperature in fluorescence–yield mode using a 13-element solid state (Si(Li)) detector (e2v Scientific Instruments) optimized for the detection of dilute elements. Al–filters of suitable thickness were used in order to attenuate the strong fluorescence signal from the matrix (especially Fe). Depending on the concentration of Hg, two or three consecutive scans were acquired to improve statistic. Portions of the same samples used for chemical characterization were newly ground for synchrotron analysis in an agate mortar, then mixed and homogenized with cellulose, and finally pressed to a pellet. This procedure should ensure a homogenous distribution of Hg in the analyzed samples.

Several Hg reference compounds were chosen on the basis of the knowledge of the mineralogy of the studied area, and of the possible weathering and anthropogenic processes that could have occurred. Spectra for these compounds were acquired in transmission mode using ionization chambers. The set of reference compounds included natural and synthetic phases: Hg^0, Hg_2Cl_2 (calomel), $HgCl_2$, Hg_2SO_4, HgO, HgS_{red} (cinnabar), HgS_{black} (metacinnabar), $Hg_2NCl_{0.5}(SO_4)_{0.3}(MoO_4)_{0.1}(CO_3)_{0.1} \cdot H_2O$ (Hg_{mos}; mosesite) and $Hg_3(SO_4)O_2$ (Hg_{sch}; schuetteite).

In addition, an Hg^0 reference spectrum, prepared embedding a fine emulsion of elemental Hg in epoxy resin, was simultaneously acquired at each energy scan for accurate energy calibration using a third ionization chamber. Principal Component Analysis (PCA) and Least Combination Fitting (LCF) were applied to the XANES spectra to obtain quantitative information on the sample speciation. PCA allows determining the minimum number of components necessary to reconstruct an experimental spectrum, and to identify the best candidates among a set of reference compounds through a procedure called "target transformation". LCF consists in a weighted linear combination of the reference standards suggested by PCA able to reconstruct a given experimental spectrum. Therefore, provided that the set of reference compounds is sufficiently representative, LCF can reveal the relative amounts of the main phases present in the samples. PCA and LCF were performed using the SIXPACK and IFEFFIT packages, respectively (Ravel and Newville, 2005; Webb, 2005).

4.2.5 Sequential Chemical Extractions

In sequential extractions the sample is treated with a series of different reagents which are expected to selectively dissolve specific mineral phases. Besides the most common protocol (Tessier et al., 1979), more specific procedures have been formulated in these years for Hg analysis (see Issaro et al., 2009 for a complete review), because most procedures applied to other metals are not suitable for Hg. It has been demonstrated, for example, that Hg is rarely associated with the *exchangeable* fractions (Martín-Doimeadios et al., 2000), while on the contrary it is often bound to humic/fulvic phase, which deserves a specific extraction step (Di Giulio and Ryan, 1987). Finally, as Hg silicates are rare, a final residual step with hydrofluoric acid can be avoided, while an *aqua regia* step is fundamental in order to solubilize sulphide minerals, the most important carriers of Hg in the environment. Taking all the above into account, in this study the protocol of Bloom et al. (2003) was applied to samples analyzed by XAS spectroscopy. Furthermore, Bloom's procedure included a specific extraction step for the determination of metallic Hg (Hg^0), which is a highly probable phase in

our samples. The SCE consisted of five steps, including: (a) water soluble (F1); (b) "human acid stomach" soluble (F2); (c) organo-chelated (F3); (d) elemental Hg (F4); and (e) mercuric sulphide. It should be noted that as natural Hg carbonated are not known, a "carbonatic" step in order to recover Hg from this fraction is usually not present (Issaro et al., 2009). The sequential extraction steps, the reagents employed, and Hg phases that are typically removed at each step are reported in Table 4.2. Extractions were conducted by continuous agitation of 0.4 g of solid for 18 ± 4h at room temperature at a solid/liquid ratio of 1:100. After each step, the supernatant was separated from the remained solid by centrifugation for 10 min at 10,000 rpm. Dissolved Hg concentrations in the supernatants were determined by CV–AAS with a lower detection limit of 1 μg/l, corresponding to an Hg concentration in each step of 0.2 μg/g. Blanks were analyzed for each extraction steps. The accuracy of the analysis was assessed by comparing the sum of Hg extracted in the five extraction steps with Hg concentrations coming from a single extraction with aqua regia. Percentages of recovery ranged between 70 and 104% (mean 91%), well within the error commonly accepted for SCE (Cuong and Obbard, 2006).

Step	Extractant	Description	Compounds removed
F1	milliQ water	hydro-soluble Hg	$HgCl_2$
F2	0.01M HCl/0.1M HOAc	"human stomach acid"	HgO, $HgSO_4$
F3	1M KOH	Hg in reducible forms	Organo-complexed (i.e. Hg-humic/fulvic),Hg_2Cl_2, CH_3Hg
F4	12M HNO_3	strong complexed Hg and/or in oxidizable form	Hg in mineral lattice, Hg_2Cl_2, Hg^0
F5	Aqua regia	mercuric sulphides	HgS, m-HgS, HgSe

Table 4.2. *Sequential extraction method developed by Bloom et al. (2003).*

Generally, one of the main drawbacks of SCE is the lack of a standard that certifies the percentage of recovery for each extraction step. However, the sequential extraction method developed by Bloom et al. (2003) makes use of the international standard, NIST–2710 (Soil, Montana), furnishing a term of comparison. Bloom's SCE was therefore applied in our laboratories to NIST-2710, obtaining a Hg recovery for each step well comparable to that of Bloom et al. (2003) (Table 4.3), thus confirming the good accuracy of the analysis. An

additional quality control consisted in replicates on samples CAL1 and PRO1 to check for reproducibility.

Sample name		Hg (µg/g)						
		F1	**F2**	**F3**	**F4**	**F5**	**sum**	**% recovered**
NIST–2710	this study	< d.l.	< d.l.	1	15	16	32	**97**
	Bloom et al. (2003)	0.2	0.02	1.5	12.0	19.0	32.7	**102**

Table 4.3. *Comparison between the recoveries for the international standard NIST-2710 obtained in this study and by Bloom et al. (2003).*

4.3 Results and discussion

4.3.1 Chemical and mineralogical characterization

Total Hg contents in the analyzed samples vary between 27 and 1,480 µg/g (Table 4.4). Higher concentrations are found in calcines of the mining area, as due to the inefficiency of ore roasting process considerable amounts of Hg are still present in roasted materials (Rimondi et al., 2012).

Sample	**material**	**Hg (µg/g)**
PRR1	river sediment	671
PRR2	river sediment	368
PRO1	river sediment	108
PRO2	river sediment	516
PRS1	stream sediment	665
PRS2	stream sediment	154
PM1	suspended matter	27
SOIL1	soil	396
CAL1	calcine	688
CAL2	calcine	1480
LAK1	lake sediment	348

Table 4.4. *Mercury contents in samples from the Mt. Amiata mining district.*

The high Hg concentrations reported for soils, stream and lake sediments located downstream the mine (Table 4.4) suggest that the runoff from contaminated waste and/or of Hg-bearing rocks determines high availability of Hg in this ecosystem. Particularly, concentrations in stream sediments are much higher than those previously observed (Rimondi et al., 2012), suggesting an intensive local accumulation of Hg in the Paglia River sediments. Although particulate matter shows the lowest concentration of Hg (27 μg/g; Table 4.4), this Hg content indicates a still active transport of Hg from the mine even 30 years after the ending of mining operations.

The results of XRD and SEM/EDS studies conducted on the same portion of samples analyzed by XAS are summarized in Table 4.5. XRD shows that the matrix of all samples but calcines is predominantly composed by plagioclase, micas (biotite or muscovite), pyroxene, k-feldspar, quartz, and clay minerals (clinochlore, illite). This mineralogy is consistent with the geology of Mt. Amiata, where the major outcropping formations are made of volcanics, shales, and carbonate rocks; clay minerals result from weathering of mafic minerals. Electron microscope studies reveal the presence of other minor mineral phases, associated to the silicatic matrix, particularly Fe, Ti and Fe-Ti (ilmenite) oxides, zircon, apatite, and REE (-Ce) silicates. Specifically, perrierite-(Ce) $[(Ce,La,Ca)_4(Fe^{2+},Mg)_2(Ti,Fe^{3+})_3Si_4O_{22}]$ and allanite-(Ce) $[(Ce,Ca,Y)_2(Al,Fe^{3+})_3(SiO_4)_3(OH)]$, have been extensively reported as accessory phases, together with ilmenite, magnetite, apatite, and zircon in the volcanites of Mt. Amiata (Van Bergen, 1984; Tonarini et al., 2003; MacDonald et al., 2009). Barite is also observed in this study, probably as a product of hydrothermal alteration from the active circulation of hydrothermal fluids (Brogi et al., 2011). XRD and SEM/EDX of calcines show that they are mainly composed by calcite, gypsum, quartz, and minor phyllosilicates (muscovite). Accessory phases are represented by hematite, allanite-(Ce), and zircon. Quartz is an abundant mineral in the primary assemblage of the ore deposits, thus it should be considered as a residual phase of the roasting process, together with minor allanite and zircon. Calcite and gypsum are instead secondary minerals, formed as a result of the roasting process, which generally involved the addition of lime (calcination). Hematite and oxyhydroxides are common phases in calcines (Gray et al., 2006) and are responsible for the red-violet color that characterizes these materials.

As expected, no Hg phases were detected by XRD because they represent a very minor proportion of the mineralogy of the samples (below 5%). On the contrary, numerous Hg-bearing phases were identified by electron microscopy in all samples, with the exception of PRO1, PRS1, and PM1. SEM images reveal that Hg is present as discrete particles of

diameters ranging from few up to tens or hundreds of μm (Fig. 4.2); the corresponding EDX analysis identifies these phases as HgS, Hg_2Cl_2 (calomel), and HgO (montroydite) as shown in Fig. 4.2. Additional particles containing Hg-S-Cl-O, probably corresponding to Hg hydroxyhalides such as kleinite [$Hg_2N(Cl,SO_4) \cdot n(H_2O)$], were identified by EDX, although the limitations of this technique prevents their certain identification.

	XRD	SEM-EDS	Hg compounds
SOIL1	quartz, orthopyroxene, K-feldspar, biotite	ilmenite, ox Fe	HgS (8), Hg-S-Cl (1), Hg_2Cl_2 (1), HgO (1)
PRO1	quartz, calcite, clay minerals (clinochlore, illite)	ilmenite, barite	/
PRO2	quartz, calcite, plagioclase, clay minerals (clinochlore)	barite, sphalerite, aluminocerite-(Ce), allanite, apatite	HgS (4)
PRS1	quartz, calcite, albite, phyllosilicates	Barite, biotite, pyrite, ox Fe	/
PRS2	quartz, calcite, muscovite, clay minerals (clinochlore)	barite, ilmenite, ox Fe, clorite, biotite, aluminocerite-(Ce)	HgS (3), HgO (1)
LAK1	quartz, K-feldspar, plagioclase, biotite	ilmenite, Au, ox Fe, perrierite, zircone, ox Ti	HgS (6), Hg-S-Cl (1)
PRR1	quartz, calcite, muscovite, clay minerals (clinochlore)	apatite, ox Fe, aluminocerite-(Ce)	HgS (1)
PRR2	quartz, calcite, muscovite, clay minerals (clinochlore)	Barite	HgS (7)
CAL-1	calcite, gypsum, quartz	ox Fe, qz, barite, zircone	HgS (4)
CAL-2	calcite, gypsum, quartz	biotite, gypsum, allanite, ox Fe, ox Fe (pseud py)	HgS (7), HgO (1)
PV1	quartz, muscovite, clay minerals (clinochlore), plagioclase	ox Fe	/

() number of grains identified for each phase

Table 4.5. *Mineralogical characterization of the samples analyzed in this study by XRD and microbeam analysis (SEM/EDS).*

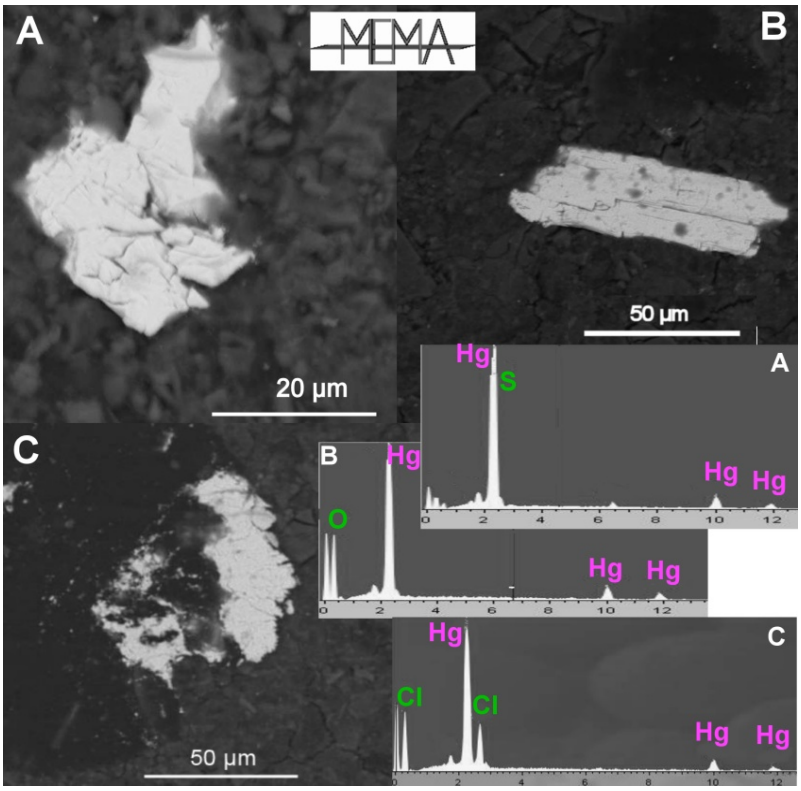

Fig. 4.2. *SEM backscattered electron images of Hg-bearing grains identified as HgS (A), HgO (B) and Hg_2Cl_2 (C) phases. The insets show the corresponding EDX spectra.*

4.3.2 XAS

The normalized near edge absorption spectra (XANES) of the samples and reference compounds are reported respectively in the left and right panels of Fig. 4.3, together with the best linear combination fitting curve (in left panel) and the Target Transform (TT) curves (right panel). The XANES of the standards compounds show the distinctive spectral features, supporting the validity of the PCA and LCF analysis presented in the following. PCA was applied to the XANES spectra, suggesting that one single component is mainly responsible for the variation of the spectra, while TT applied on the set of reference compounds showed that the statistical indicators (χ_ν^2 and R) underwent to a steep increase after the six standard compounds: HgS_{red}, Hg^0, HgS_{black}, Hg_2Cl_2, $HgCl_2$, and Hg_{mos}. The results of TT using six components are reported in Table 4.6 and the TT curves are plotted in the right panel of Fig. 4.3 superimposed with the corresponding target spectrums. LCF, performed using these six standards, led to excellent matches with the samples' spectra. The results of the LCF are reported in Table 4.6 and the fitted curves are plotted in the left panel of Fig. 4.3, superimposed to the corresponding samples spectra. All possible two to six components fits were optimized by minimizing the reduced χ_ν^2. Starting from the best two components fit, the

best fit with n + 1 components was considered to be significantly better than the best n-component one, if its χ_ν^2 was at least 15% lower than that of the best n-component fit. The precision of the fractions obtained from LCF was previously estimated to be between 10 and 20% of the total Hg (Isaure et al., 2002; Panfili et al, 2005; Bardelli et al., 2011), but it strongly depends on the signal to noise ratio and on the errors in the normalization procedure. Fractions occurring in amounts <10% were found to improve the fits negligibly and were therefore ignored. The sum of the fractions is 100% for all samples (Table 4.6), supporting the correctness of the fitting procedure. Results from LCF analysis generally quantify Hg sulphides for much more than 50% of the total Hg compounds and confirm the extremely heterogeneous nature of the samples, as already pointed out by SEM-EDS analysis. Metallic Hg (Hg^0) is found as one of the main phases in both recent stream sediments (PRS), and industrialized sediments (PRR), where it accounts for remarkable fractions, ranging from 22 up to 40% (Table 4.6). The other relevant mineral species is mosesite ($Hg_2NCl_{0.5}(SO_4)_{0.3}(MoO_4)_{0.1}(CO_3)_{0.1}\cdot H_2O$, theoretical formula), which occurs in almost half of the samples.

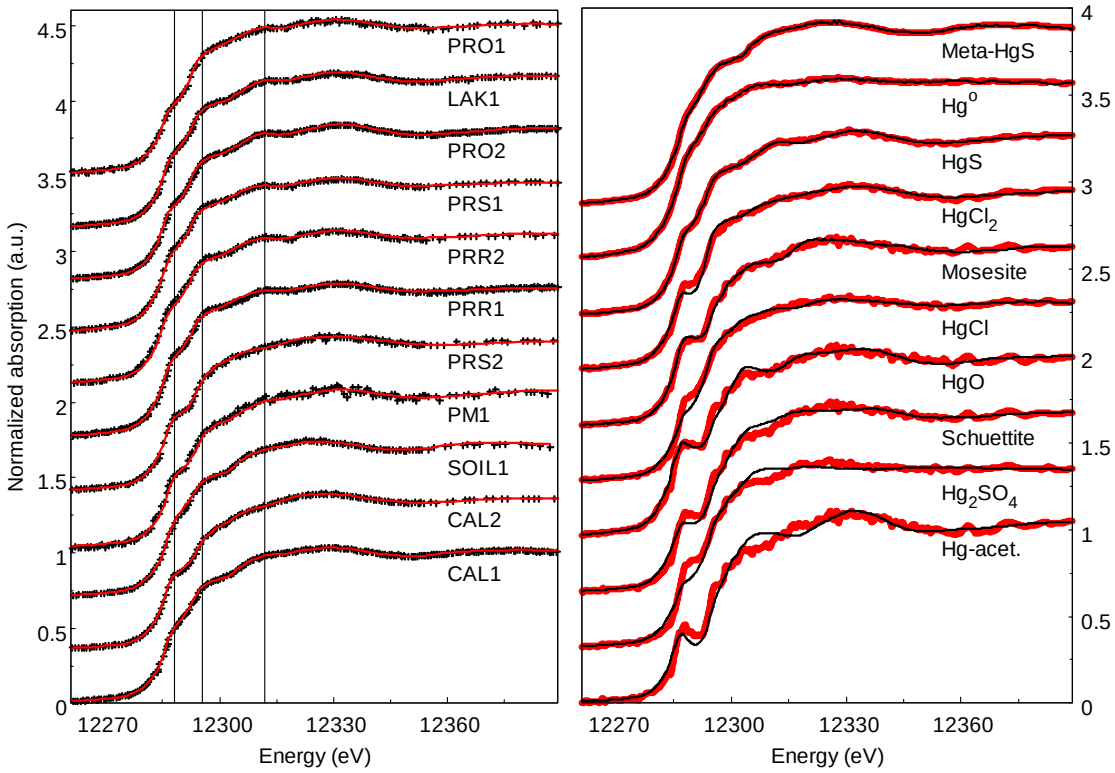

Fig. 4.3. *Left panel: XANES spectra of the samples (points) with linear combination fit curves superimposed (solid lines). The vertical dashed lines serve to highlight some of the main spectral features. Right panel: XANES spectra of the Hg reference compounds (thinner lines) with Target Transforms curves superimposed (thicker lines).*

	$HgS_{(red)}$	$HgS_{(black)}$	Hg_2Cl_2	$HgCl_2$	Hg_{mos}	Hg^0	Σ	χ_v^2
CAL1	40	60	--	--	--	--	100	0.00017
CAL2	21	37	--	--	42	--	100	0.00014
SOIL1	--	100	--	--	--	--	100	-
PRR1	60	--	--	--	--	40	100	0.00076
PRR2	67	--	--	--	--	32	100	0.00095
PRS1	63	--	--	--	--	37	100	0.00079
PRS2	20	--	--	22	36	22	100	0.00075
PRO2	100	--	--	--	--	--	100	-
PRO1	61	--	39	--	--	--	100	0.00090
LAK1	76	24	--	--	--	--	100	0.00051
PM1	60	20	--	--	20	--	100	0.0030*

Table 4.6. *Hg fractions derived from LCF. The sum of the fractions (Σ), which is 100% for all samples, and the value of the reduced χsquare (χ_v^2), both indicate good matches with the experimental spectra. *The higher value of the χ_v^2 for PM1 is due to the low signal to noise ratio of this spectrum.*

The phases identified by XAS are generally comprised in those reported by the EDS analysis, with the exception of montroydite (HgO), that was not detected by XAS. However, it should note that bulk XAS analysis, as such performed in this work, gives information on the average composition of the samples, while EDS, being a microprobe technique, gives punctual analysis. Therefore, the differences between EDS and XAS techniques are due to the high heterogeneity of the samples. Moreover, minor Hg phases, occurring in fractions <10%, can be present but were ignored considering the large error associated with XAS procedure (10 - 20%).

4.3.3 SCE

The results of SCE expressed as cumulative percentage and absolute contents of extracted Hg are reported in Fig. 4.4 and Table 4.7, respectively. Mercury is extensively recovered in all samples during F5 and F4 steps, which account for Hg bound to sulphide fraction, strong complexed plus Hg^0, respectively. Particularly, the sulphide fraction generally extracts more than 80% of Hg (Fig. 4.4), corresponding to Hg range of 72-1,016 µg/g (Table 4.7). The only exception is for samples CAL1 and PM1, where F4 extraction accounts for more than 50% of the total Hg budget. Lesser extent of Hg is mobilized by F1-F3, which cumulative percentages are <15% (Fig. 4.4). Particularly, steps F1-F2 indicate the presence of low proportions of

soluble Hg compounds, which are generally ascribed as the "*bioaccessible" Hg* (Bloom et al., 2003). Although representing only the 12% of total Hg budget, the absolute content of this fraction is particularly elevated in sample CAL2, when up to 144 µg/g Hg are extracted during F1-F2.

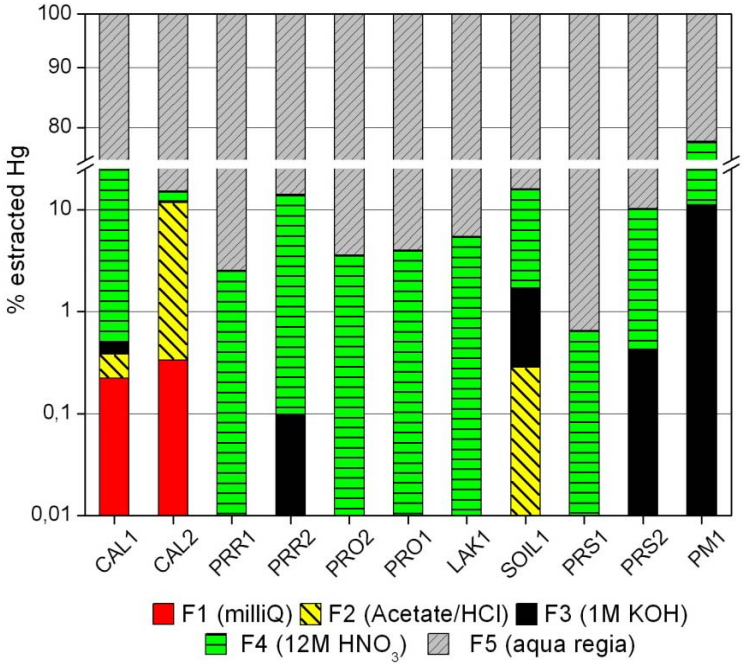

Fig. 4.4. *Percent of Hg extracted in each fraction of SCE for the samples analyzed in this study.*

Sample	F1	F2	F3	F4	F5
CAL1	2	1	1	368	360
CAL2	4	136	6	36	1,016
PRR1	u.d.l.	u.d.l.	u.d.l.	14	540
PRR2	u.d.l.	u.d.l.	u.d.l.	48	297
PRO2	u.d.l.	u.d.l.	u.d.l.	17	459
PRO1	u.d.l.	u.d.l.	u.d.l.	3	72
LAK1	u.d.l.	u.d.l.	u.d.l.	16	278
SOIL1	u.d.l.	1	5	50	296
PRS1	u.d.l.	u.d.l.	u.d.l.	4	610
PRS2	u.d.l.	u.d.l.	1	16	144
PM1	u.d.l.	u.d.l.	3	18	6

Table 4.7. *Hg concentrations (µg/g) resulting from the five steps extraction procedure applied in this study. (u.d.l. stays for under detection limit).*

Comparison of the replicated SEC steps to samples CAL1 and PRO1 shows good agreement for high concentrations of Hg, i.e. for steps F4 and F5 when much of Hg is extracted (Table 4.8). In this case, the differences are less than 15%. However, lower reproducibility is reported for the F1-F3 steps when the amount of recovered Hg is generally low (< 10 μg/g), and differences between replicated steps may reach 80% (CAL1). As outlined by SEM analysis, despite grinding, Hg compounds are widespread as isolated grains of considerable dimensions in the matrix, reflecting their inhomogeneous distribution in the samples. This observation is common for Hg, that thanks to physical resistance of its compounds, is common to nugget effect, resulting in scarce reproducibility also for total digestion procedures (Kocman et al., 2006). As a consequence, a scarce reproducibility of SCE was achieved in this study for those compounds which are present in lower concentrations, and may or may not be present in the portions of samples being digested.

Sample name	**Hg (μg/g)**						
	F1	**F2**	**F3**	**F4**	**F5**	**Σ step**	**% recovered**
CAL1-I	0.3	< d.l.	0.6	326	347	674	**98**
CAL1–II	0.6	0.2	0.5	348	313	663	**96**
CAL1–III	1.6	1.2	0.9	368	360	732	**106**
PRO1–I	< d.l.	< d.l.	< d.l.	3	72	75	**70**
PRO1–II	< d.l.	< d.l.	< d.l.	3	72	75	**70**

Table 4.8. *Replicated SCE procedures for samples CAL1 and PRO1.*

4.3.4 Mercury speciation

The qualitative results deriving from the two independent speciation methods, SCE and XAS, are generally similar, although some discrepancies are evident for specific samples. Both techniques indicate Hg sulphides as the principal Hg-bearing phase in most of the samples analyzed, in agreement with the fact that cinnabar (HgS_{red}) is the primary ore mineral in Hg deposits. The inefficiency of roasting process, designed to extract metallic Hg from ores, results in significant amount of unconverted cinnabar in waste calcine deposits worldwide (Kim et al., 2000, 2004; Esbrí et al., 2010). Although cinnabar represents the thermodynamically stable form of HgS at low temperatures and reducing conditions (Dickson and Tunell, 1959), metacinnabar (HgS_{black}), the metastable polymorph of HgS, is widely diffused both in waste calcines and soils of the Mt. Amiata area. The occurrence of matacinnabar is common in slag materials and derived soils whenever the high temperatures

(~ 600 °C) of mineral processing trigger the structural conversion of cinnabar to metacinnabar (Kim et al., 2003; 2004; Bernaus et al., 2005). The transition between the two polymorphs occurs at 345 °C (Kullerud, 1965) and, once formed, metacinnabar is stabilized by the presence of impurities such as Zn, Se, and Fe. These elements then prevent the reversion of metacinnabar to the original red form by lowering the phase transition temperature and retarding the conversion kinetic (Dickson and Tunell, 1959). Both polymorphs of HgS are extremely insoluble mineralogical phases (K_{ps} are in the range of 10^{-36}; Schwarzenbach and Widmer, 1963), and are kinetically resistant to oxidation; therefore, once formed in anoxic conditions, they are stable even in oxidizing environments (Barnett et al., 2001). Physical weathering and erosion of cinnabar-bearing rocks and waste calcines of mining area result then in cinnabar/metacinnabar mobilization by water and consequent transport in the form of particulate to the lake and streams of Mt. Amiata, where it accumulates in sediments.

The prevalence of chloride-bearing phases (calomel, mosesite and $HgCl_2$) in calcines, stream and fossil sediments shown by XAS, is typical of Hg deposits located in hot spring areas (Kim et al., 2000, 2004; Bernaus et al., 2005), as it is the case of the Mt. Amiata Hg district (Rytuba, 2003), where the local salinity levels in geothermal fluids may favor the formation of Hg chloride minerals (Kim et al., 2003, 2004). Higher proportions of mosesite in calcines particularly implies that this phase is primarily formed during secondary processes, either during ore roasting, or, at a later time, during chemical weathering reactions. The high proportion of residual Hg in roasted materials has probably reacted with free Cl^-, which became available for vaporization of residual water, or decomposition of hydrothermal minerals, such as clays (Kim et al., 2004). Mosesite is moreover found in present-day stream sediments draining the Mt. Amiata (PRS2), where it may be present as: a) secondary mineral accumulated as a result of its chemical/physical transport from calcines, or b) secondary in situ product of supergene alteration of cinnabar. Although active transport of mosesite from calcines is documented by the recovering of this phase in water particulate matter, free Hg available for formation of Hg-chlorides may have produced even in the fluvial system of Paglia River by dissolution of primary cinnabar. In spite of its resistance to chemical alteration, cinnabar solubility can be enhanced by particular environmental conditions, such as in presence of elemental sulfur, chloride-rich waters, organic matter, and Fe^{3+} during mine drainage (Burkstaller et al., 1975; Paquette et al., 1997, Ravichandran et al., 1999a,b). Furthermore, oxidative dissolution of cinnabar has been documented in fluvial environments (Holley et al., 2007). Moreover, since the interaction of calomel with ammonia-rich waters is reported as the dominant mechanism for the formation of mosesite (Switzer et al., 1953), the

high contents of NH^{4+} reported for the thermal waters (Duchi and Prati, 1985) and geothermal fluids of Mt. Amiata (Bertini et al., 1995) can validate the hypothesis that mosesite additionally formed as a secondary product of calomel alteration. In addition, the discharge of NH^{4+}-rich waters from the sewage system of Abbadia (Rimondi et al., 2012) may further promote the formation of mosesite along the river course. Besides mosesite, Hg(II)-chloride ($HgCl_2$) is observed in present-day stream sediments, suggesting a current leaching of this phase from calcines, where it is commonly formed as a consequence of roasting and/or later processes (Kim et al., 2000; Esbrí et al., 2010), although XAS does not indicate its presence in roasted materials. However, the presumably small percentages of $HgCl_2$ in calcines possibly prevent its identification by XAS, where mineral phases less than 20% were generally omitted in this study. Moreover, the heterogeneous distribution of soluble Hg-species in the samples matrices, as outlined by SEC, may result in lacking of this phase in the sample analyzed by XAS. However, small amounts of compounds like $HgCl_2$ and HgO in calcines and soil of the mining area are confirmed by SCE and SEM/EDX. Although representing just 0.3-12% of the total Hg budget (SCE analysis), these phases may release to the environment enormous quantities of Hg, being much more soluble than the Hg sulfides. Particularly, the amounts of such phases now observed in calcines possible underestimate their initial quantities, as much of them underwent chemical leaching and transport in downstream environment.

XAS indicates that fossil sediments of Paglia River may locally host, beside major amounts of cinnabar, considerable proportions of Hg-chlorides phases, in the form of the Hg(I)-chloride (calomel). Hg-chlorides are notably absent of in the primary mineral assemblage of the Mt. Amiata ores (Arisi Rota et al., 1971; Dini et al., 2003; Morteani et al., 2011), however calomel could represent a secondary mineral, formed as a consequence of post-depositional alteration of primary cinnabar as documented elsewhere (Roberts et al., 2003).

Results from SCE and XAS generally mismatch to identify Hg-halides species in the analyzed samples. Lacking of a specific selective extraction step for this phase, SCE was not able to quantify mosesite in PRS2, PM, and CAL2. Particularly, due to its insolubility in water, acetic acid, and HNO_3, mosesite is decomposed by concentrated HCl (Switzer et al., 1953), probably solubilizing during the F5 step. The presence of mosesite was then masked by the simultaneous dissolution of sulphides; as a consequence, the % of sulphides determined by SCE is generally higher than those obtained by XAS. Similarly, SCE did not succeed to identify calomel and $HgCl_2$ in those samples where they were indicated in remarkable amounts (> 20%) by XAS, i.e. PRO1 and PRS2, respectively. It should however be

considered that one of the main drawbacks of SCE methods is the overlapping of extraction steps, resulting in lacking of minerals complete solubilization in one defined step and/or re-adsorption reaction phenomena (Issaro et al., 2009). Particularly, it is observed that for Bloom's protocol the results from F1-F3 are unambiguous only when the total concentration of Hg in the samples is high (1000 – 10,000 μg/g) (Issaro et al., 2009), while discrepancies appear evident for lower contents. Specifically, al lower concentrations soluble species leached between F1-F3, as HgCl or $HgCl_2$, are re-adsorbed on clay surfaces (Bloom et al., 2003; Malferrari et al., 2011), therefore overlapping to mineral species solubilized in later steps.

Results from XAS report metallic Hg in the present and recent sediments of Paglia River, suggesting that extensive runoff of Hg^0 from the mining area of Abbadia San Salvatore goes on even after 30 years from the end of industrial activity. Notably, Hg^0 was not detected in pre-industrialized (fossil) deposits, supporting the fact that abiotic and biotic reduction of Hg(II) to the metallic form (Ullrich et al., 2001) could not be invoked for the high percentages of free Hg^0 found in present-day stream sediments. High proportions of Hg^0 are however surprising in sediments, because Hg^0 due to its high volatility readily partitions to the gas phase, suggesting sorption reactions with sediments could have concurred to delay the migration of Hg^0 (Schlüter, 2000). The accurate determination of Hg^0 by SCE is particularly complicated because other compounds as Hg(I), Hg-Au amalgams, crystalline Fe/Mn oxides, and amorphous organo-sulfur can be extracted by cold 12 M HNO_3 (75% v/v) beside Hg^0 (Bloom et al., 2003). The F4 step of Bloom's protocol is therefore not completely selective for Hg^0, resulting in an uncertain quantification of this phase (Bloom et al., 2003; Covelli et al., 2009). Moreover, possible problems could arise when 75% HNO_3 extraction is applied to finely ground samples, which leads to an increased solubility of sulphides, resulting in their extraction during the penultimate step (F4), with successive underestimate of the following (Kim et al., 2003; Hall et al., 2005). Such finding can possibly explain the observations coming from SCE for samples CAL1 and PM1, where their fine grained nature, coupled with the abundant presence of Fe oxides, could have given rise to a particle size effect with increased solubility of HgS, and solubilization of Hg-bearing Fe oxides, overestimating Hg extracted in F4. Particularly, in the case of CAL1, Hg removed by 12 M HNO_3 (50%; Fig. 4.4) almost corresponds to the amount of metacinnabar determined by XAS (60%; Table 4.6), confirming, as already observed by Kim et al. (2003), the possible higher solubility of this phase in natural samples than the one modeled by Bloom's extraction procedure. Then, because Hg^0 reaches saturation in water at 50 μg/l, only values near this level in F1 confirm

that the sample contains free metallic Hg, that can be consequently estimated by F4 (Bloom et al., 2003).

Contrary to XAS, data from SCE suggest that metallic Hg is present only in calcines samples, although in small percentages, ~ 10% for CAL1, and 3% for CAL2. As previously explained, because the great part of Hg recovered in F4 for CAL1 is believed to be the result of metacinnabar and Hg-bearing Fe oxides solubilization, Hg^0 can be grossly estimated by the difference between Hg recovered in F4 and the percentage of metacinnabar obtained by XAS. The occurrence of metallic Hg is well explainable in these type of deposits, where Hg^0 is a residue, due to the recovery inefficiency during roasting (Biester et al., 1999; Gray et al., 2004, 2006).

Results for elemental Hg by XAS and SCE are generally in disagreement pointing out the inherent limitations of these techniques. Small percentages of Hg^0 (<15%) were indeed commonly overlooked by XAS, due to the common elevated errors associated with this analysis. Similarly, the non-identification of Hg^0 in sediments by SCE was mainly due to its heterogeneous distribution in the materials. Despite this mismatching, the data of this study demonstrate that Hg^0 is still eroded and transported from the Abbadia San Salvatore mine contaminated site, where it accumulates in sediment, and it could remain for many years thanks to its chemical stability under mildly oxidizing or reducing conditions (Ullrich et al., 2001). The presence of Hg^0 in the environment should be carefully monitored as this species may undergo oxidation to Hg(II) (Yamamoto et al., 1996), supplying ionic Hg for methylation.

4.4 Conclusions

Speciation results obtained by the application of XAS and SCE generally show Hg sulphides as the dominant mineral phases in most of the analyzed samples, although secondary chemical reaction and mine downstream leaching complicate the mineral assemblage of the analyzed samples. Anthropogenic processes such as ore roasting have considerable effects on the speciation of the waste calcines, mainly resulting in: a) residual minor amount of Hg^0; b) conversion of cinnabar to metacinnabar; c) secondary formation of moderately soluble Hg(I)-chlorides and Hg-N-Cl-compounds; d) formation of extremely soluble Hg species such as $HgCl_2$, HgO and $HgSO_4$. In particular, mercuric chloride, oxide and sulphates, although do not represent more than ~ 10% of global Hg species, may result in mobilization of environmentally significant amounts of Hg (up to 136 μg/g; Table 4.7).

Due to their improper disposal, waste calcines are highly impacting for the environment, as they undergo physical and chemical weathering, resulting in cinnabar transport as particulate by water, and chemical leaching of Hg ionic compounds. Such ionic compounds found in the sediments of the Paglia River represent the main environmental concern of this area because, differently from cinnabar, can solubilize and release free Hg^{2+}, which may be readily available for methylation reactions. Thus, the overall dominant effect of mining activity, and particularly of roasting process, is the increase of Hg toxicity, by enhancing its mobility in the environment. The speciation results coming from this study, and particularly the presence of remarkable percentages of soluble Hg-bearing minerals in sediments, can possibly correlate with the significant bioavailability of methyl-Hg previously documented for the Mt. Amiata district (Rimondi et al., 2012).

The presence of elemental Hg in the present-day and recent stream sediments of Paglia River further highlights the huge impact of mining activity in this area. Even if mining ceased more than three decades ago, Hg^0 is transported downstream the Abbadia San Salvatore mine, and possible contribute to methyl-Hg formation by oxidation to Hg(II).

The use of multiple analytical methods allows to define a complete picture of Hg speciation in the Hg district of Mt. Amiata, and helps to improve the predictions of Hg mobility and bioavailability in the environment. The phases detected by SEM/EDS are generally comprised in the compounds resulting from XAS spectroscopy, although the additional presence of soluble compounds as HgO is reported. Nevertheless it should be pointed out that microscope techniques, differently from XAS, give punctual information about mineralogical phases, thus extensive searching and fortuitous cases may lead to identification of mineral phases which are present in very minor amounts in the matrix, and are not statistically significant for the description of Hg mineralogy. Differences in speciation between SCE and XAS mainly arose when trying to quantify the non-sulfide fractions of the samples, and particularly Hg^0. In this case, the inherent limitation of each technique appear evident. Particularly, lacking of modeled extractions for specific phases, lack of selectivity, and matrix effects are the main problems encountered in application of SCE techniques. On the other hand, the high detection limits associated with XAS may prevent identification of the Hg compounds present in low amounts, nonetheless significant to predict Hg bioavailability in the environment. Results from this study therefore confirm the importance of a multidisciplinary approach in order to study Hg speciation in natural systems.

Acknowledgements

This study was financially supported by the University of Florence. I was in debt with Fabrizio Bardelli (Istitute de Geosciences, Grenoble), who interpreted the XAS spectra and J.E. Gray (USGS) for providing some Hg compounds employed as standards in this study.

References

ARISI ROTA F., BRONDI A., DESSAU G., FRANZINI M., MONTE AMIATA S.P.A. (1971), STABILIMENTO MINERARIO DEL SIELE, STEA B., VIGHI L. (1971). I Giacimenti minerari. In: La Toscana meridionale. *Rend. Soc. Ital. Mineral. Petrol.*, **27**, Spec. Is.: 357–544.

BARDELLI, F., CATTARUZZA, E., GONELLA, F., RAMPAZZO G., VALOTTO, G. (2011). Characterization of road dust collected in Traforo del San Bernardo highway tunnel: Fe and Mn speciation. *Atmos. Environ.,* **45**: 6459−6468.

BARGAGLI R., BARGHIGIANI C., MASERTI B.E. (1986). Mercury in vegetation of the Mount Amiata area (Italy). *Chemosphere*, **15**: 1035−1042.

BARNETT M.O., TURNER R.R., SINGER P.C. (2001). Oxidative dissolution of metacinnabar (β-HgS) by dissolved oxygen. *Appl. Geochem.*, **16**: 1499−1512.

BEHRA P., BONNISSEL–GISSINGER P., ALNOT M., REVEL R., EHRHARDT J.J. (2001). XPS and XAS Study of the Sorption of Hg(II) onto Pyrite. *Langmuir*, **17**: 3970–3979.

BERNAUS A., GAONA X., VALIENTE M. (2005). Characterisation of Almadén mercury mine environment by XAS technique. *J. Environ. Monit.*, **7**: 771−777.

BERNAUS A., GAONA X., ESBRÍ J.M., HIGUERAS P., FALKENBERG G., VALIENTE M. (2006A). Microprobe Techniques for Speciation Analysis and Geochemical Characterization of Mine Environments: The Mercury District of Almadén in Spain. *Environ. Sci. Technol.*, **40**: 4090−4095.

BERNAUS A., GAONA X., VAN REEB D., VALIENTE M. (2006B). Determination of mercury in polluted soils surrounding a chlor–alkali plant. Direct speciation by X–ray absorption spectroscopy techniques and preliminary geochemical characterisation of the area. *Anal. Chim. Acta*, **565**: 73–80.

BERTINI G., CAPPETTI G., DINI I., LOVARI F. (1995). Deep drilling results and updating of geothermal knowledge of the Monte Amiata area. Proc. World Geotherm. Congr., Firenze, Italy 18–31May 1995, pp 1283–1286.

BIESTER H., GOSAR M., MÜLLER G. (1999). Mercury speciation in tailings of the Idrija mercury mine. J. Geochem. Explor., **65**: 195−204.

BIESTER H., GOSAR M., COVELLI S. (2000). Mercury Speciation in Sediments Affected by Dumped Mining Residues in the Drainage Area of the Idrija Mercury Mine, Slovenia. *Environ. Sci. Technol.*, **34**: 3330−3336.

BLOOM N.S. AND PORCELLA D.B. (1994). Less Mercury? *Nature*, **367**: 694−694.

BLOOM N.S., PREUS E., KATON J., HILTNER M. (2003). Selective extractions to assess the biogeochemically relevant fractionation of inorganic mercury in sediments and soils. *Anal. Chim. Acta*, **479**: 233–248.

BROGI A., FABBRINI L., LIOTTA D. (2011). Sb–Hg ore deposit distribution controlled by brittle structures: The case of the Selvena mining district (Monte Amiata, Tuscany, Italy). *Ore Geol. Rev.*, **41**: 35–48.

BURKSTALLER J.E., MCCARTY P.L., PARKS G.A. (1975). Oxidation of Cinnabar by Fe(lll) in Acid Mine Waters. *Environ. Sci. Technol.,* **9**: 676−678.

COMPEAU G.C. AND BARTHA R. (1984). Methylation and demethylation of mercury under controlled redox, pH and salinity conditions. *Appl. Environ. Microbiol.,* **48**: 1203−1207.

COMPEAU G.C. AND BARTHA R. (1985). Sulfate–Reducing Bacteria: Principal Methylators of Mercury in Anoxic Estuarine Sediment. *Appl. Environ. Microbiol.*, **50**: 498–502.

COVELLI S., ACQUAVITA A., PIANI R., PREDONZANI S., DE VITTOR C. (2009). Recent contamination of mercury in an estuarine environment (Marano lagoon, Northern Adriatic, Italy). *Estuar. Coast. Shelf Sci.,* **82**: 273–284.

COUNG D. AND OBBARD J.P. (2006). Metal speciation in coastal marine sediments from Singapore using a modified BCR–sequential extraction procedure. *Appl. Geochem.*, **21**: 1335–1346.

DICKSON F.W AND TUNELL G. (1959). The stability relations of cinnabar and metacinnabar. *Am. Mineral.*, **44**: 471−487.

DI GIULIO R.T. AND RYAN E.A. (1987). Mercury in soil, sediments, and clams from a North Carolina peatland. *Water Air Soil Poll.*, **33**: 205−219.

DINI A. (2003). Ore deposits, industrial minerals and geothermal resources. In: Poli G., Perugini D., Rocchi S., Dini A. (Eds.). Miocene to Recent Plutonism and Volcanism in the Tuscan Magmatic Province. *Per. Mineral.*, special issue, **72**: 41−52.

DUCHI V. AND PRATI F. (1985). Indagine geochimica su acque e gas dei sistemi termali a bassa temperatura dell'area amiatina. *Boll. Soc. Geol. It.*, **104**: 527−538.

ESBRÍ J.M., BERNAUS A., ÁVILA M., KOCMAN D., GARCÍA-NOGUERO E.M., GUERRERO B., GAONA X., ÁLVAREZ R., PEREZ-GONZALEZ G., VALIENTE M., HIGUERAS P., HORVAT M., LOREDO J. (2010). XANES speciation of mercury in three mining districts – Almadén, Asturias (Spain), Idria (Slovenia). *J. Synchrotron Rad.*, **17**: 179–186.

FERRARA R., MAZZOLAI U.B., EDNER H., SVANBERG S., WALLINDER E. (1998). Atmospheric mercury sources in the Mt. Amiata area, Italy. *Sci. Total Env.*, **213**: 12–23.

GABRIEL M.C. AND WILLIAMSON D.G. (2004). Principal biogeochemical factors affecting the speciation and transport of mercury through the terrestrial environment. *Environ. Geochem. Health*, **26**: 421–434.

GRAY J.E., HINES M.E., BIESTER H. (2006). Mercury methylation influenced by areas of past mercury mining in the Terlingua district, Southwest Texas, USA. *Appl. Geochem.*, **21**: 1940–1954.

GRAY J.E., HINES M.E., HIGUERAS P.L., ADATTO I., LASORSA B.K. (2004). Mercury speciation and microbial transformations in mine wastes, stream sediments, and surface waters at the Almadén mining district, Spain. *Environ. Sci. Technol.*, **38**: 4285–4292.

HALL G.E.M., PELCHAT P., PERCIVAL J.B. (2005). The design and application of sequential extractions for mercury, Part 1. Optimization of HNO3 extraction for all non-sulphide forms of mercury. *Geochem.: Explor. Environ. Anal.*, **5**: 107−113.

HOLLEY E.A., MCQUILLAN A.J., CRAW D., KIM J.P., SANDER S.G. (2007). Mercury mobilization by oxidative dissolution of cinnabar (α-HgS) and metacinnabar (β-HgS). *Chem. Geol.*, **240**: 313−325.

ISAURE M-P, LABOUDIGUE A., MANCEAU A, SARRET G., TIFFREAU C, TROCELLIER P, LAMBLE G, HAZEMANN J-L, CHATEIGNER D. (2002). Quantitative Zn speciation in a contaminated dredged sediment by -PIXE, -SXRF, EXAFS spectroscopy and principal component analysis. *Geochim. Cosmochim. Acta*, **9**: 1549–1567.

ISSARO A., ABI-GHANEM C., BERMOND A. (2009). Fractionation studies of mercury in soils and sediments: A review of the chemical reagents used for mercury extraction. *Anal. Chim. Acta*, **631**: 1–12.

KIM C.S., BLOOM N.S., RYTUBA J.J., BROWN JR. G.E. (2003). Mercury Speciation By X–Ray Atomic Absorption Fine Structure Spectroscopy and Sequential Chemical Extractions: A Comparison of Speciation Methods. *Environ. Sci. Technol.*, **37**: 5102–5108.

KIM C.S., BROWN JR. G.E., RYTUBA J.J. (2000). Characterization and speciation of mercury–bearing mine wastes using X–ray absorption spectroscopy. *Sci. Total Environ.*, **261**: 157–168.

KIM C.S., RYTUBA J.J., BROWN JR. G.E. (2004). Geological and anthropogenic factors influencing mercury speciation in mine wastes: an EXAFS spectroscopy study. *Appl. Geochem.*, **19**: 379–393.

KLEMM D.D. AND NEUMANN N. (1984). Ore-controlling factors in the Hg–Sb province of southern Tuscany, Italy. In: Wauschkuhn A. et al. (Eds.). Syngenesis and Epigenesis in the Formation of Mineral Deposits, Springer-Verlag, Heidelberg, pp. 482−503.

KOCMAN D., BLOOM N.S., AKAGI H., TELMER K., HYLANDER L., FAJON V., JEREB V., JAĆIMOVIĆ R., SMODIŠ B., IKINGURA J.R., HORVAT M. (2006). Preparation and characterization of a soil reference material from a mercury contaminated site for comparability studies. J. *Environ. Manage.*, **81**: 146–154

KOCMAN D., HORVAT M., KOTNIK J. (2004). Mercury fractionation in contaminated soils from the Idrija mercury mine region. *J. Environ. Monitor.*, **6**: 696-703.

KULLERUD G. (1965). The Mercury–sulfur System. Carnegie Institute of Washington Year Book, Vol. 64, pp. 193–195.

KUWABARA J.S., TOPPING B.R., PICKERING G., GEORGE G. (2007). Mercury Speciation in Piscivorous Fish from Mining–Impacted Reservoirs. *Environ. Sci. Technol.*, **41**: 2745–2749.

LIN Y., LARSSEN T., VOGT R.D., FENG X. (2010). Identification of fractions of mercury in water, soil and sediment from a typical Hg mining area in Wanshan, Guizhou province, China. *Appl. Geochem*., **25**: 60–68.

MACDONALD R., BELKIN H.E., WALL F., BAGIŃSKI B. (2009). Compositional variation in the chevkinite group: new data from igneous and metamorphic rocks. *Mineral. Mag.*, **73**: 777−796.

MALFERRARI D., BRIGATTI M.F., ELMI C., LAURORA A. (2011). Determination of Hg binding forms in contaminated soils and sediments: state of the art and a case study approaching abandoned mercury mines from Mt. Amiata (Siena, Italy). *N. Jb. Miner. Abh.*, **188**: 65–74.

MARTÍN-DOIMEADIOS R.C.R., WASSERMAN J. C., GARCÍA BERMEJO L.F., AMOUROUX D., BERZAS NEVADO J. J., DONARD O.F.X. (2000). Chemical availability of mercury in stream sediments from the Almadén area, Spain. *J. Environ. Monitor.*, **2**: 260−266.

MORTEANI G., RUGGIERI G., MÖLLER P., PREINFALK C. (2011). Geothermal mineralized scales in the pipe systemof the geothermal Piancastagnaio power plant (Mt. Amiata geothermal area): a key to understand the stibnite, cinnabarite and gold mineralization of Tuscany (central Italy). *Miner. Deposita*, **46**: 197–210.

NECULITA C.-M., ZAGURY G.J., DESCHÊNES L. (2005). Mercury Speciation in Highly Contaminated Soils from Chlor-Alkali Plants Using Chemical Extractions. *J. Environ. Qual.*, **34**: 255-262.

PANFILI F., MANCEAU A., SARRET G., SPADINI L., KIRPICHTCHIKOVA T., BERT V., LABOUDIGUE A., MARCUS M.A., AHAMDACH N., LIBERT M-F. (2005). The effect of phytostabilization on Zn speciation in a dredged contaminated sediment using scanning electron microscopy, X-ray fluorescence, EXAFS spectroscopy, and principal components analysis. *Geochim.. Cosmochim. Acta*, **69**: 2265−2284.

PAQUETTE K.E. AND HELZ G. R. (1997). Inorganic Speciation of Mercury in Sulfidic Waters: The Importance of-Valent Sulfur. *Environ. Sci. Technol.,* **31**, 2148-2153.

PATTY C., BARNETT B., MOONEY B., KAHN A., LEVY S., LIU Y., PIANETTA P. ANDREWS J.C. (2009). Using X–ray Microscopy and Hg L3 XANES To Study Hg Binding in the Rhizosphere of *Spartina* Cordgrass. *Environ. Sci. Technol.*, **43**: 7397–7402.

RAVEL B. AND NEWVILLE M. (2005). Athena, Artemis, Hephaestus: Data analysis for X-ray absorption spectroscopy using Ifeffit. *J. Synchrotron Radiat.*, **12**: 537−541.

RAVICHANDRAN M., AIKEN G.R., REDDY M.M., RYAN J.N. (1999A). Enhanced Dissolution of Cinnabar (Mercuric Sulfide) by Dissolved Organic Matter Isolated from the Florida Everglades. *Environ. Sci. Technol.*, **32**: 3305−3311.

RAVICHANDRAN M., AIKEN G.R., RYAN J.N., REDDY M.M. (1999B). Inhibition of precipitation and aggregation of metacinnabar (mercuric sulfide) by dissolved organic matter isolated from the Florida Everglades. *Environ Sci. Technol.*, **33**: 1418–1423.

RIMONDI V., GRAY J.E., COSTAGLIOLA P., VASELLI O., LATTANZI P. (2012). Concentration, distribution, and translocation of mercury and methylmercury in mine–waste, sediment, soil, water, and fish collected near the Abbadia San Salvatore mercury mine, Mt. Amiata district, Italy. *Sci. Tot. Environ.*, **414**: 318–327.

ROBERTS A.C., COOPER M.A., HAWTHORNE F.C., GAULT R.A., GRICE J.D., NIKISCHER A.J. (2003). Artsmithite, a new Hg^{1+}–Al phosphate–hydroxide from the Funderburk prospect, Pike County, Arkansas, U.S.A. *Can. Mineral.,* **41**: 721−725.

RYTUBA J.J. (2003). Mercury from mineral deposits and potential environmental impact. *Environ. Geol.*, **43**: 326–338.

SANCHÉZ D.M., QUEJIDO A.J., FERNÁNDEZ M., FERNÁNDEZ C., SCHMID T., MILLÁN R., GONZÁLEZ M., ALDEA M., MARTÍN R., MORANTE R. (2005). Mercury and trace element fractionation in Almaden soils by application of different sequential extraction procedures. *Anal. Bioanal. Chem.*, **381**: 1507−1513.

SCHWARZENBACH G. AND WIDMER M. (1963). Die Loslichkeit von Metallsulfiden I. Schwarzes Quecksilbersulfid. *Helv. Chim. Acta*, **46**: 2613−2628.

SCHLÜTER K. (2000). Review: evaporation of mercury from soils. An integration and synthesis of current knowledge. *Environ. Geol.*, **39**: 249−271.

SWITZER G., FOSHAG W.F., MURATA K.J., FAHEY J.J. (1953). Re-Examination of Mosesite. *Amer. Mineral.*, **38**: 1225–1234.

TANELLI G. (1983). Mineralizzazioni metallifere e minerogenesi della Toscana. *Mem. Soc. Geol. It.*, **25**: 91−106.

TERŠIČ T., GOSAR M., BIESTER H. (2011). Environmental impact of ancient small-scale mercury ore processing at Pšenk on soil (Idrija area, Slovenia). *Appl. Geochem.*, **26**: 1867−1876.

TERZANO R., SANTORO A., SPAGNUOLO M., VEKEMANS B., MEDICI L., JANSSENS K., GÖTTLICHER J., DENECKE M.A., MANGOLD S., RUGGIERO P. (2010). Solving mercury (Hg) speciation in soil samples by synchrotron X–ray microspectroscopic techniques. *Environ. Poll.*, **158**: 2702–2709.

TESSIER A., CAMPBELL P.G.C., BISON M. (1979). Sequential Extraction Procedure for the Speciation of Particulate Trace Metals. *Anal. Chem.*, **51**: 844−851.

TONARINI S., FORTE C., PETRINI R., FERRARA G. (2003). Melt/biotite 11B/10B isotopic fractionation and the boron local environment in the structure of volcanic glasses. *Geochem. Cosmochim. Acta*, **67**: 1863−1873.

ULLRICH S.M., TANTON T.W., ABDRASHITOVA S.A. (2001). Mercury in the Aquatic Environment: A Review of Factors Affecting Methylation. Crit. Rev. *Environ. Sci. Technol.*, **31**: 241–293.

US EPA (2001). US EPA (2001). Water quality criterion for the protection of human health: Methylmercury. U.S. Environmental Protection Agency, EPA-823-R-01-001. Washington, DC.

US EPA (1997). Mercury study report to Congress. U.S. Environmental Protection Agency, I-VIII, EPA-452/R-97-003.

VAN BERGEN (1984). Perrierite in siliceous lavas from Mt. Amiata, central Italy. *Miner. Mag.*, **48**: 553−556.

YAMAMOTO M. (1996). Stimulation of elemental mercury oxidation in the presence of chloride ion in aquatic environments. *Chemosphere,* **32**: 1217−1224.

WEBB S.M. (2005). SIXpack: a graphical user interface for XAS analysis using IFEFFIT. *Phys. Scr.*, **T115**: 1011−1014.

CHAPTER 5

PART IV – A GEOCHEMICAL SURVEY FOR HG AND AS CONCENTRATIONS IN SEDIMENTS OF THE MT. AMIATA REGION (SOUTHERN TUSCANY, ITALY)

Abstract

The Mt. Amiata area (Southern Tuscany, Italy) hosts one of the most important Hg district in the world, determining a widespread Hg (and associated As) geochemical anomaly. The Hg ores have been exploited for Hg production up to the last century, resulting in an extensive Hg contamination of the Pagliola Creek ecosystem, draining the important mine of Abbadia San Salvatore (ASSM). Presently, a remediation project is carrying on at this mine site. The principal aim of this study is to characterize Hg(As) diffusion in different sediments of this area in relation to the past mining activity. Sediments of different age were then sampled along the Pagliola Creek in order to reconstruct the history of Hg(As) diffusion in this region, from pre-industrial to present-day times. Pre-mining sediments were in particular sampled in order to try to establish a reliable regional background for Hg and As, which can help to define the remediation strategy for the ASSM. Furthermore, a paleo-hydrographic reconstruction of the Pagliola Creek was attempted. A preliminary Hg regional background of 2-6 μg/g is defined for the Mt. Amiata area, which largely exceeds the Hg established contamination level of Italy. As a result of this study, a new reliable regulation for Hg should be defined for this area, taking into account the high natural occurring Hg levels in the environment.

Keywords: mercury, Mt. Amiata, geochemical background, multivariate analysis

5.1. Introduction

The term geochemical background originates from geochemical exploration and refers to the "normal abundance of an element in a determined barren earth material" (Hawkes and Webb, 1962). The concept was introduced to localize geochemical anomalies, i.e. ore deposits, defined as the deviations of one of more elements with respect to normal values (Reimann and Garrett, 2005). In the last few decades, the concept of geochemical background has become increasingly important in environmental sciences, and many international projects were

dedicated to geochemical mapping (http://www.globalgeochemicalbaselines.eu/) for a complete review of the papers and reports produced within this framework). In environmental sciences, the concept of geochemical background differs from the traditional sense used in exploratory geochemistry (Gałuska et al., 2007; Gałuska and Migaszewski, 2011). In this context, the background is then referred to the concentration of an element without the influence of human activity (Vidal et al., 2004; Gałuska, 2007; Gałuska and Migaszewski, 2011). The term baseline is sometimes employed as a synonym (Nieto et al., 2005), although it refers to the present concentration of a substance in a contemporary environmental sample, which it might be subjected to variations in the future. However, some authors do not support the use of this term (Reimann and Garrett, 2005).

Much of the geochemical research for background is focused on heavy metals because their concentrations in the environment negatively affect wildlife and humans (Salomons, 1995). Many works were then devoted to the distinction between natural (geogenic) and anthropogenic source of contamination at regional or sub-regional scale in the whole Europe (Macklin et al., 1994; Salminen and Tarvainen 1997; Albanese et al., 2007; Breward, 2007; Galàn et al., 2008; Reimann et al., 2009; Bini et al., 2011; Gosar and Žibret, 2011; Guillèn et al., 2011). This distinction represents a challenging task of modern research as the strong human civilization exacerbates the diffusion of contaminants in the environment, resulting in an overlapping of anthropogenic and natural imprints. The establishment of background trace metals in superficial environments is however important because it allows: 1) to distinct between contaminated and uncontaminated areas, and 2) to model the influence of metal distribution as a consequence of human influence. In mining areas, the levels of heavy metals in the environment can be raised naturally up by the weathering of mineralized rocks (Loredo et al., 1999), although the release of heavy metals by human activities occurs generally at higher rates than natural weathering processes. In these areas, however, the definition of a pre-mining background is extremely important to design realistic remediation strategies (Kelley and Taylor, 1997), as the remediation of mine sites should be conducted up to the pristine background concentrations disregarding the regulation limits that may be lower than the local geogenic element concentrations.

Since the first regional geochemical background surveys conducted in the 1960s and 1970s, active stream sediments have been the most widely used medium (Garret et al., 2008) because they usually provide a solid, easy-to-sample and relatively cost-effective way to assess trace metals concentrations in upstream catchment basins. Nonetheless, their validity has been questioned in a number of works **(**Ottesen et al. 1989; De Vos et al. 1996; Swennen et al.

1998; Swennen and Van der Sluys 1998**)**, which showed that the main drawbacks using the stream sediments as a proxy for the geochemical background estimation are: i) their heterogeneous sources and their temporal fluctuations; ii) the difficulty to distinct between the geogenic versus the anthropogenic sources in areas with long-time mining or industrial activity (Reimann and Garret, 2005); in these conditions, remobilization of contaminated bottom stream sediments and contaminated river banks may lead to wrong estimations of the geochemical background (Kocman et al., 2010). Quaternary sediments may then represent a good alternative to present-day and overbank sediments in mining areas with strong historical disturbance. A detailed geochemical characterization of sediments is moreover necessary in order to elucidate the geochemical processes determining the natural fluctuations of the analyzed element in a specific region. The background is indeed more realistic represented by a range of values, which takes into consideration the natural variability of the element, rather than by a single value Reimann and Garrett, 2005).

The Mt. Amiata region (Southern Tuscany, Italy) hosts a broad Hg geologic anomaly, due to the wide occurrence of cinnabar ore deposits (Arisi Rota et al., 1971; Tanelli, 1983). Ore bodies were extensively mined in the last century and determined the production of elevated amounts of mining wastes improperly disposed to the surface environment. This study focuses on the Pagliola Creek, which represents the first mountain tract of the Paglia River Basin (PRB). Here, the Abbadia San Salvatore Mine (ASSM), the largest in the Mt. Amiata district, is located (Fig. 5.1); a remediation strategy for this mine started in 2012. Previous studies on the Hg diffusion in the area are scarce, and a reliable Hg background has not yet been clearly established. Environmental studies on the stream sediments of Paglia River (Ferrara et al., 1991), suggested a Hg baseline of 9.4 μg/g. However, scarce information about field sampling methodology, number of samples for each medium, considered grain size and statistical elaboration of data, suggests that this value could hardly be taken as a reference. In addition, active transport of mine waste as sediment load is observed in the Paglia River (Rimondi et al., 2012), suggesting a possible overestimation of this value.

The present paper attempts to finally assess the geogenic Hg background of the Mt. Amiata area, proposing Quaternary sediments as sample media. In particular, thanks to morphological and paleo-hydrological reconstruction of the Pagliola drainage course, fossil stream sediments referred to the ancient Pagliola were considered as pristine, and sampled. The dataset was then completed with present-day stream sediments and sediments from a recently formed fluvial terrace (i.e. coeval to the mining and smelting activities), which are expected to represent the modern and the historical ambient background, respectively.

5.2 Geological outline

The study area is located in Southern Tuscany, centered on the Mt. Amiata region (Southern Tuscany, Italy) (Fig. 5.1). The Mt. Amiata is the central relief of the homonymous volcano-geothermal area, which develops in the inner part of Northern Apennines. The building of the Apennines during the Tertiary as a thrust and fold chain and the related post-collisional events determined the modern setting of Southern Tuscany.

From geophysical data, it is supposed that a magmatic body is presently emplaced beneath the Mt. Amiata at 6-7 km depth (Gianelli et al., 1988). The emplacement of this intrusion during the Early Pliocene (Jacobacci et al., 1967; Pasquarè et al., 1983) determined the surface uplift of this area (Acocella, 2000; Brogi, 2008), the volcanic eruptions of Mt. Amiata (300-180 ka; Bigazzi et al., 1981; Barberi et al., 1994; Cadoux and Pinti, 2009), and a still active hydrothermal circulation. To this convective flow is attributed the ore genesis of the epithermal cinnabar deposits of Mt. Amiata (Tanelli et al., 1983), to which minor quantities of As minerals are associated (Arisi Rota et al., 1971). Although Hg was produced already by the Etruscans, the industrialization of this area began in the 1860s and Hg production ended in 1982 with the closure of the Abbadia San Salvatore Hg mine.

In this study, we focus on the Paglia River, which drains the east side of the Mt. Amiata area (Fig. 5.1). This river flows in the Radicofani Basin (RB) (Fig. 5.1), a Neogene tectonic depression elongated NW-SE, bordered by the Mt. Centona ridge on the east and the Mt. Amiata−Castell'Azzara on the west (Bonini and Sani, 2002; Castaldi and Chiocchini, 2012). Traditionally, the RB has been interpreted as a *graben* and/or *semi-graben* (Brogi, 2004; 2008) (Cetona and Radicofani Faults; Collettini et al., 2006) (Martini and Sagri, 1993; Liotta and Salvatorini, 1994; Liotta, 1996; Collettini et al., 2006; Pascucci 2006; Brogi, 2008), although different theories indicated the RB as a syn-tectonic *thrust-top* basin (Bonini and Sani, 2002). The RB is filled up with 2500 m thick marine Pliocene deposits (Barberi et al., 1994), which extensively outcrop along the Paglia River (Fig. 5.1). Pliocene sediments, overlaying the Miocene deposits, are documented only by the deep wells of Paglia 1 and Radicofani 1 (Fig. 5.1) (Bonini and Sani, 2002), and unconformably rest on the pre-Neogene Units (Bonini and Sani, 2002; Brogi and Liotta, 2008). In the Neogene deposits, four principal angular unconformities-bounded stratigraphic units (UBSU) (Salvador, 1987) were recently recognized (Bonini and Sani, 2002). The Sedimentary Unit 3, composed by upper early middle Pliocene (*G. margaritae* to *G. puncticulata* zone) marine clays, sandy-clays and conglomerates (Liotta, 1996), is the main formation cropping out in the RB. Along the Paglia

River, this unit is represented by gray-blue clays interbedded with sandy layers or conglomerates (Bonini and Sani, 2002; Ghinassi and Lazzarotto, 2005; Pascucci et al., 2006), the so-called "Argille di Fabro" (Girotti and Mancini, 2003). Due to the evolution of RB during the Neogene (Pasquaré et al., 1983; Barberi et al., 1994 Pascucci et al., 2006), no younger sedimentary record are present in this area.

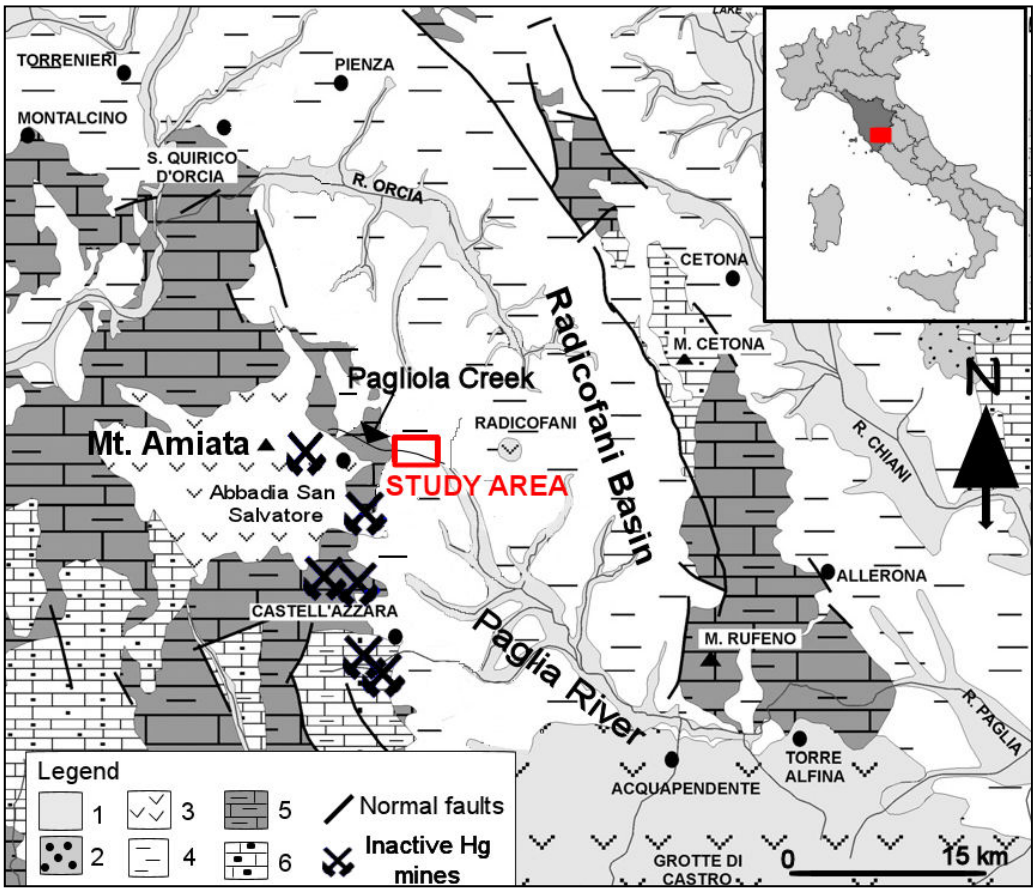

Fig. 5.1. *Location of the study area, inactive Hg mines, and schematic geological map of the Mt. Amiata region. Numbers refer to the main geological formations outcropping in the area: 1) alluvial deposits (Holocene); fluvial-lacustrine sediments (Holocene-Pleistocene); 3) volcanic rocks (middle-late Pleistocene); 4) marine deposits (early-late Pliocene); 5) Ligurian Units (late Cretaceous- Oligocene); 6) Tuscan Nappe (Triassic-Oligocene) (modified after Castaldi et al., 2012). The study area is enlarged in Fig. 5.2.*

5.3 Methods

5.3.1 Sampling sites and procedures

The Pagliola Creek is the first mountain tract of Paglia River, which is formed by the union of the Pagliola, Vascio and Cacarello Creeks (Fig. 5.2). The present-day Pagliola Creek flows in

a narrow valley, with a torrential character, and a river bed morphology made by steps and pools (Photo 5.1). Along the Pagliola Creek, it is possible to identify scarps of about 1-2m high (Photo 5.2a), mainly composed by clasts ranging from pebble to cobble in a silty-clay matrix, alternated to sandy-silt beds, that in the 1:10,000 geological map of Italy (section 321090) have been interpreted as Holocene deposits, terraced and not terraced (Fig. 5.2). In this study these deposits are interpreted as fluvial terraces of an old Pagliola Creek, thereafter called as paleo-Pagliola, and they are indicative of a complex drainage reorganization during the Quaternary, with alternating episodes of deposition and incision. Like the modern Pagliola, the paleo-Pagliola flowed SE from Mt. Amiata, and the sedimentologic characteristics of the fluvial terraces indicate a river bed made by step and pool bed even for that paleo-creek. Moreover, morphological reconstructions of this area suggests that the paleo-Pagliola has deposited a fluvial conoid in the last part of its river course (the shadow area in Fig. 5.2). This observation is more convincing if we consider the strong variation in hydrological gradients that marks the transition between the Pagliola Creek and the Paglia River (Fig. 5.2), which results even today in a marked deposition of particulate matter in this river tract (§ part II).

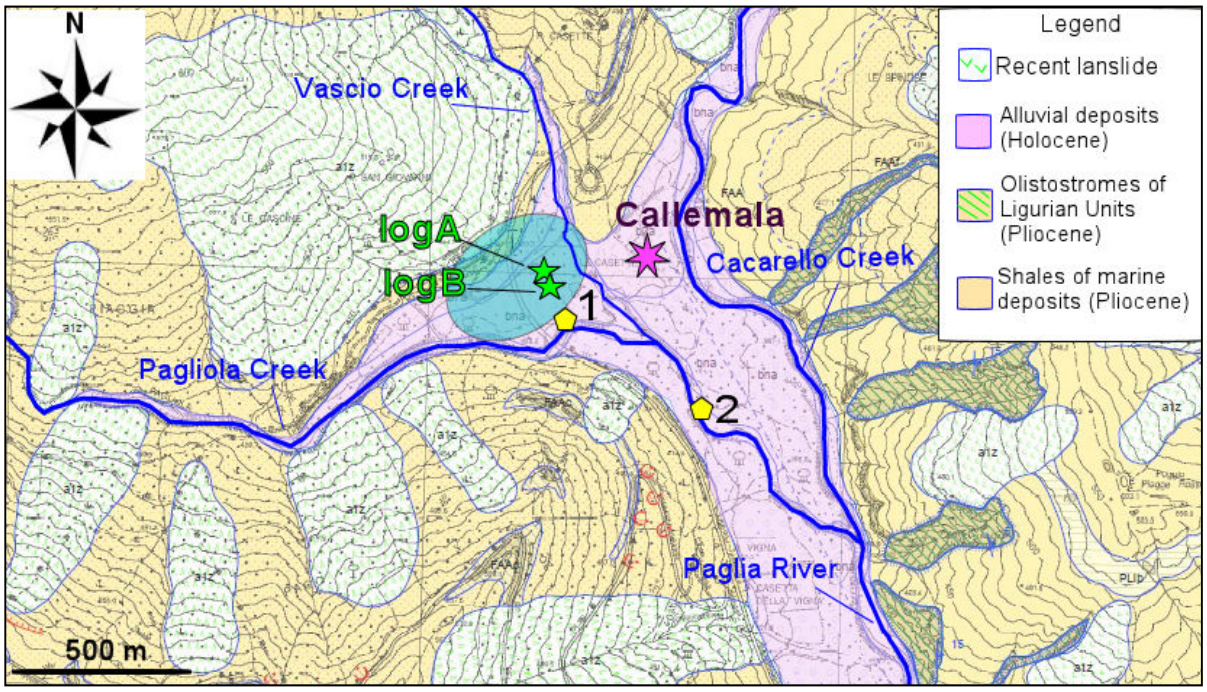

Fig. 5.2. *Enlarged geological map of the study area reported in Fig. 5.1 (section 321090). The position of two excavations, indicated as logA and logB, is indicated by the green stars, whereas the yellow symbols 1 and 2 refer to the sampling sites for the fluvial terraces and stream sediments. The position of the paleo-Pagliola conoid is indicated by the blue oval.*

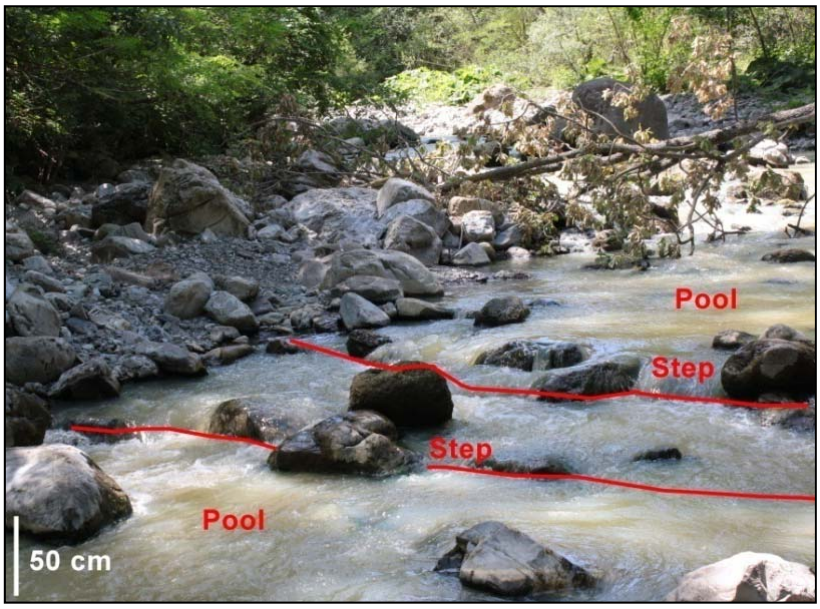

Photo 5.1. *Steps and pools riverbed morphology for the present-day Pagliola Creek.*

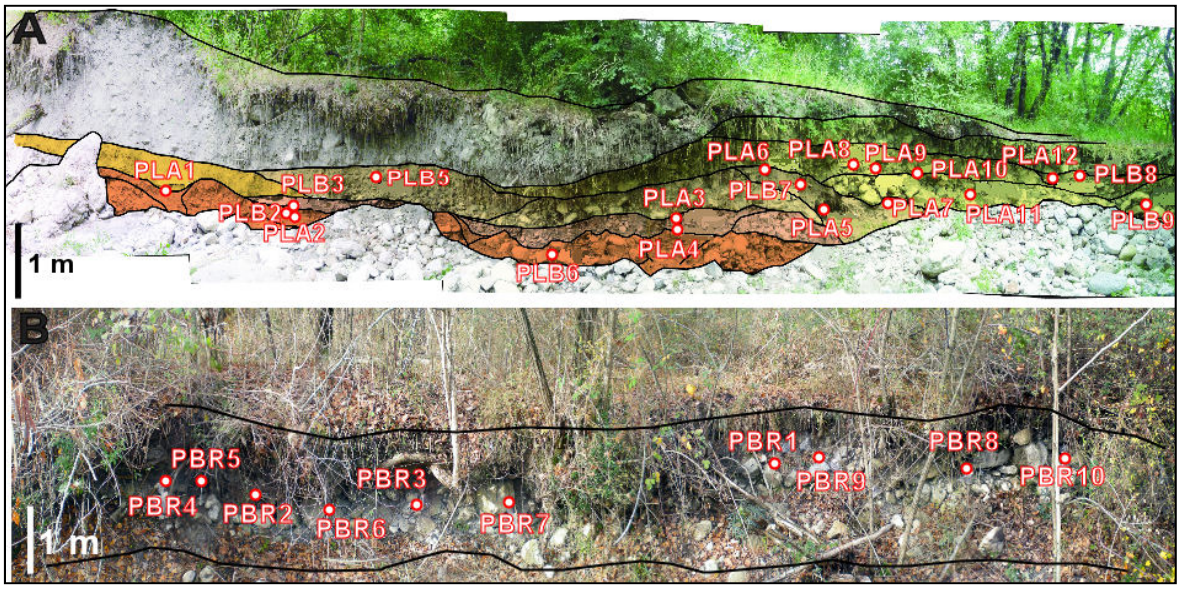

Photo. 5.2a,b. *Scarps of 1-2 m encountered along the Pagliola Creek and interpreted as fluvial terraces. A) External fluvial terrace formed before the mining activity; the black lines delimited the steps and pools of the ancient morphology; the samples collected in this terrace, whose position is reported in the photo, belong to the PS group; B) Internal fluvial terrace formed by the current Pagliola Creek and considered coeval to mining activity; the samples collected in this terrace, whose position is reported in the photo, belong to the BR group.*

Despite the lack of an exact chronological constraints on this conoid and associated fluvial terraces, the presence in this area of the buried roman village of Callemala found in 876 A.D (*Callis Malus*; Francovich, 1999) represents an indirect way to date these deposits. This village was an important stop of the so-called *Via Francigena*, an old itinerary that connected Canterbury to Rome starting from the X century A.D., testifying with its position that the

present-day morphology of Pagliola Valley was already defined when the village was funded. The formation of the paleo-Pagliola conoid and the related paleo-hydrography reconstruction then largely precedes the large-scale mining activity for Hg in this region, which started at the end 1800. Therefore, sediments belonging to the paleo-Pagliola hydrography are considered pristine and have been employed in this study to reconstruct the background for Hg. Two excavations of 2-4 m depth were then made in this area (logA and logB; Fig. 5.2) in order to: i) investigate about the paleo-hydrographic evolution of the Pagliola Creek; and ii) sample the stream sediments related to the ancient paleo-Pagliola. Sediment samples were in addition recovered from: a) an external fluvial terrace recognized on the left side of the present-day Pagliola Creek (locations 1 and 2 in Fig. 5.2) referred to the paleo-Pagliola course, which could be additionally employed to reconstruct the background (Photo 5.2a); ii) an internal fluvial terrace (location 1 in Fig. 5.2; Photo 5.2b), which is an example of the very recent morphodynamic development of the present-day Pagliola Creek, and is then possible considered coeval with the industrial exploitation of Hg mines; these deposits were then sampled to delineate the historical Hg contamination related to the peak of Hg production; and iii) the present-day Pagliola Creek stream sediments in order to evaluate the recent impact of the past mining activity in this area. A total of 74 sediment samples (2-5 kg) were recovered in the main sampling area and summarized in Table 5.1.

All samples were air dried, dry sieved to < 160 μm and finally powdered. The 160 μm grain size as representative of the fine fraction was used in order to compare the results with those of a recent survey in the region (Rimondi et al. 2012). Thereafter, we refer to the groups with the acronyms reported in Table 5.1.

Group	Number of samples	Sampling location	Description
PS	24	1&2	Pre-mining stream sediment; external fluvial terrace of paleo-Pagliola
BR	13	1&2	Recent stream sediment, coeval with mining; internal fluvial terrace
SS	15	1	Present-day stream sediments of Pagliola Creek
TR	22	logA&logB	Pre-mining stream sediment from the boreholes

Table 5.1. *Description of the different group of sediments collected in this study, and acronyms of groups that are used in the text. Sampling location is referred to Fig. 5.2.*

5.3.2 Chemical characterization

Quantitative chemical analyses of major elements (Na, Mg, Al, Si, P, K, Ca, Ti, Mn, and Fe) were performed by X-ray fluorescence (XRF) using a Philips PW1480/10 X-ray spectrometer The analytical quality was controlled by using international standards, and the relative differences between our result and certified values are less than 5%. Loss of ignition (L.O.I.) was carried out at 950 °C. Analytical solutions for Hg and As were obtained through aqua regia digestion of powdered samples. The concentrations of As was determined by a Perkin Elmer FIAS 100 Hydride Generator Perkin Elmer AAnalist100 spectrophotometer (AAS). Mercury was analyzed by the same spectrophotometer coupled with cold vapor (CV) technique. For random samples replicates were performed to provide a measure of the analytical precision. Accuracy was checked against international standards (2710, 2711, DS-1). The relative percent error was <10% for Hg and <5% for As.

5.4 Results and discussion

5.4.1 Paleohydrographic reconstruction of the Pagliola Valley

The stratigraphy succession of the two boreholes is reported in Fig. 5.3. From the bottom three main units are recognized (see Table 5.2 for detailed description of each lithotypes), based on the lithological and sedimentological characteristics of the deposits:

- *S1 (150 cm)*, encountered only in the logB, it mainly consists of massive plastic grayish clays, or sandy clays of 10-30 cm thick, with subordinate10-20 cm thick fine to coarse sandy beds. In the upper portion of the unit, two levels of silty or silty/sandy matrix-supported pebbles and cobbles (15-20 cm thick) are observed. Between these lithologies, 20-30 cm of gray clay and silt with sporadic pebbles are interposed (Fig. 5.3). An erosional surface separates this Unit from the upper one.
- *S2 (80-90 cm)*, mainly constituted by pebble, cobble, and occasional boulder-sized conglomerates, with a minor percentage of sandstone. The deposit is massif, poorly sorted, and without an internal stratification. Clasts are mainly carbonatic, probably resulting from the dismantling of Ligurian Units. This unit approximates 90 cm in logA, while it is observable its pitch-out in logB.
- *S3 (140-150 cm)*, mainly represented by clast-supported clay-sandy silt, with outsized reddish-violet clasts derived from the Mt. Amiata vulcanites. A normal gradation is observed, with angular carbonatic clasts of the Ligurian Units located in the lower part of the unit, and a silt-clay lithotype which prevails in the last 50 cm.

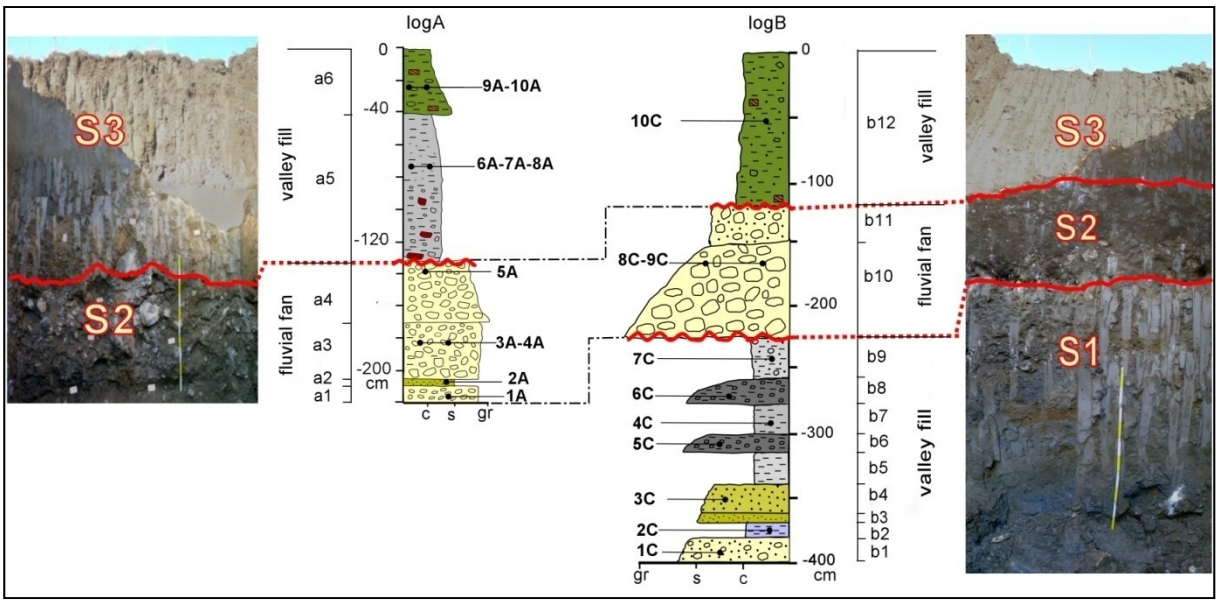

Fig. 5.3. *Correlations between logs A and B (refer to Fig. 5.2 for their locations), showing the different lithologies and units recognized. Grain size codes in logs - c: clay; s: sand; gr: gravel. The acronyms on the left and right of the stratigraphic profiles (a1-a6; b1-b12) refer to the lithotypes described in detail in Table 5.2. The names and the positions of the collected samples along the profiles are reported (1A-10A and 1C-10C).*

On the base of the different Units recognized in the boreholes, the paleo-hydrograpic evolution of the Pagliola Creek articulates in four main stages, explained graphically by Fig. 5.4. During the first stage, documented by S1 at the bottom of the log B, a paleo-Pagliola filled a NW-SE large paleo-valley, and similarly to present condition, flowed NE from the Mt. Amiata, discharging in the paleo-Paglia River. The coarser deposits observed in the profiles (b6 and b8 lithotypes of Table 5.2) are related to the deposition that occurred in the fluvial channels of the paleo-course, while finer lithologies identify the deposition in more peripheral areas, such as in the floodplain. During the second stage (S2), this valley was sharply deactivated, as suggested by the erosional surface delimiting the S1 at its top, and an alluvial fan started to form. This depositional stage suggests that a major change affected the paleo-Pagliola river system during that time, and the sediments that in the previous stage had been transported up to the paleo-Paglia River, were in this phase deposited in the alluvial fan. Uplift and subsidence of the paleo-Pagliola bed, possible triggered by main tectonic events such as Mt. Amiata eruptions, controlled the beginning of fan deposition. In the third stage (S3), the paleo-Pagliola started to incise its fluvial conoid, and a new deposition of sediments started in a more recent paleo-valley. The nowadays first order of fluvial terrace deposits, belonging to the PS group in this study, represents the remnants of sediments that filled the valley at that time along the main river channel, while the sediments of S3 testify the

occasional overflow of those deposits in the floodplain (Fig. 5.4). The extensive finding of the Mt. Amiata trachytes starting from the S3 unit collocates the formation of the new Pagliola Valley and its deposits (sediment PS) after the emplacement of the Mt. Amiata vulcanites (200-300 ka). On the contrary, the minor finding of vulcanites in the paleo-Pagliola conoid may suggest: i) the absence of vulcanites in the paleo-Pagliola drainage basin, and/or ii) the low availability of these rocks at the time this basin was formed, suggesting a possible formation of these deposits before the emplacement of the vulcanite rocks. During the last stage of the Pagliola evolution (S4), the alternation of sedimentation and erosion processes resulted in the formation of different order of fluvial terraces, and to the narrowing of the Pagliola Valley to its present-day position. To the recent morphodynamic evolution of Pagliola Creek is particularly attributed the formation of the internal terrace, considered potentially coeval with the mining activity (Fig. 5.4).

In this reconstruction, the sediments belonging to S3 and to the first fluvial terrace (PS) are coeval, representing only the deposition in different areas of the Pagliola Valley (Fig. 5.4.). In the perspective of this study, these sediments may be considered as pristine and may be therefore employed to establish the Mt. Amiata Hg regional background.

log A	log B
a1: gravel with maximum Φ = 50 cm	**b1**: massive, sandy matrix-supported pebbles and cobbles
a2: massive, medium- to coarse-grained sand	**b2**: massive plastic grayish clay
a3: massive pebble and cobble in mud matrix	**b3**: massive low-grained sand
a4: matrix-supported clasts ranging from pebbles to boulders	**b4**: massive medium-grained sand
a5: normally graded clay-sandy mud with root traces, with cm-mm clasts and outsized volcanic cobbles	**b5**: silty clay, with lenses of sand
a6: massive clay with mm/cm angular clasts	**b6**: matrix-supported sandy-gravel
	b7: silty clay, often with scattered granules and pebbles
	b8: silty supported-matrix pebbles and cobbles
	b9: silty sands with scattered clasts
	b10: massive, matrix-supported cobbles and pebbles
	b11: sandy clay silt with clasts

Table 5.2. *Main characteristics of the lithologies encountered in logA and logB.*

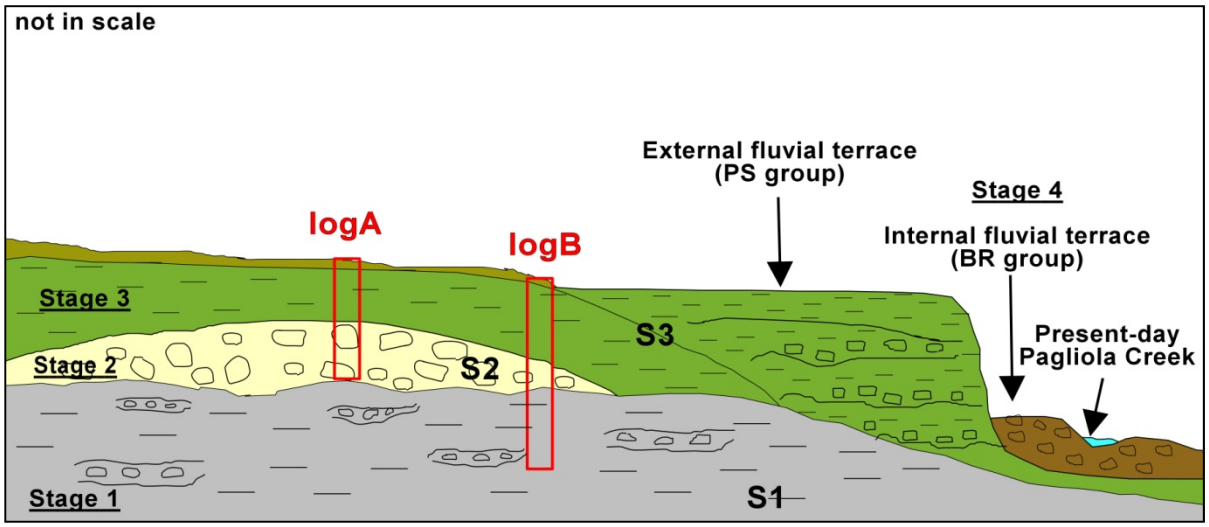

Fig. 5.4. *Schematic representation of the paleo-hydrographic evolution of the Pagliola Valley, following the four stage described in detail in the text. S1, S2 and S3 refer to the stratigraphic units reported in Fig. 5.3. Stage 1-4 refers to the four stages in which is articulated the paleohydrographic reconstruction of the Pagliola Creek (refer to the text for any detail). The position of the two boreholes made in this study (logA and logB) is shown.*

5.4.2 Major chemistry

The chemical composition of the analyzed samples, expressed as oxides (%), is reported in Table 5.3. Sediment composition is described by the four compounds, SiO_2, Al_2O_3, Fe_2O_3 and CaO, which represent the 65% of oxides, reflecting the silico-clastic nature of these deposits. In order to investigate the relationships between the groups identified by the stratigraphy, multivariate statistical analysis was applied to the database of this study. The main objective of this analysis was to observe if the operational subdivisions of sediments was supported by remarkable differences in main geochemistry.

As the relationship among major oxides obeys a numerical constrain that it is not free to vary from $-\infty$ and $+\infty$ but it is closed to 100%, this kind of data are known as compositional data (Aitchision, 1986). The constant sum constraint implies the application of a special geometry, the Aitchison geometry to the simplex (Filzmoser et al., 2009). In this space, the Euclidian descriptive statistics is not informative (Pawlowsky-Glahn et al., 2007) and the data should be properly transformed. The most common way to transform the data is considering the log-ratios between variables rather than their absolute values (Aitchison, 1986; Pawlowsky-Glahn and Egozcue, 2006). The application of these techniques to different field of geological sciences is well documented (Buccianti and Esposito, 2004; Buccianti and Pawlowsky-Glahn, 2005; Borgheresi et al., 2012).

Group	Sample	H_2O	Na_2O	MgO	Al_2O_3	SiO_2	P_2O_5	K_2O	CaO	TiO_2	MnO	Fe_2O_3
PS	PLA1	9.48	0.60	2.77	17.08	54.02	0.09	2.64	4.49	0.77	0.08	7.48
	PLA2	9.86	0.59	2.96	18.94	48.53	0.08	3.13	5.69	0.73	0.69	8.38
	PLB2	9.97	0.64	2.97	18.45	52.58	0.09	2.89	4.08	0.76	0.08	7.16
	PLB6	8.26	0.66	2.66	18.27	52.61	0.09	3.13	4.70	0.79	0.11	8.33
	PLA3	8.67	0.54	2.63	17.14	45.99	0.08	2.66	4.03	0.69	0.35	16.72
	PLA4	8.30	0.57	2.80	18.27	51.09	0.08	3.02	4.73	0.79	0.16	9.80
	PLB3	9.80	0.59	2.89	18.95	51.28	0.09	3.19	4.54	0.79	0.11	7.45
	PLA5	9.59	0.53	2.72	17.61	47.81	0.09	2.77	4.47	0.72	0.19	13.04
	PLA6	11.09	0.57	2.81	16.58	48.39	0.08	2.75	7.95	0.68	0.15	8.66
	PLB5	9.79	0.57	2.80	18.70	49.89	0.09	3.05	5.00	0.79	0.27	8.68
	PLB7	10.31	0.59	2.79	17.23	48.97	0.08	2.93	5.40	0.90	0.11	10.29
	PLA7	8.49	0.61	2.82	18.15	50.76	0.08	2.90	3.84	0.76	0.17	10.99
	PLA8	10.64	0.56	2.79	16.86	47.62	0.09	2.81	6.18	0.80	0.12	11.14
	PLA9	10.17	0.52	2.79	16.81	46.44	0.08	2.76	6.22	0.70	0.23	12.76
	PLA10	9.61	0.57	2.76	17.14	49.56	0.09	2.83	5.47	0.76	0.15	10.74
	PLA11	9.67	0.52	2.88	18.79	49.39	0.09	3.12	4.60	0.76	0.16	9.63
	PLA12	9.58	0.47	2.90	17.99	47.49	0.10	2.97	4.52	0.75	0.13	12.65
	PLB8	9.42	0.54	2.84	18.27	49.99	0.09	3.11	4.67	0.78	0.11	9.83
	PLB9	8.86	0.50	2.78	17.60	47.33	0.09	2.81	3.59	0.73	0.15	14.92
	PLB1	9.93	0.41	1.38	18.83	50.32	1.07	2.82	5.72	0.77	0.12	8.21
	PLB4	9.70	0.61	2.85	18.43	52.35	0.09	3.04	4.50	0.80	0.09	7.24
	PLB11	9.11	0.65	2.68	18.15	52.22	0.09	3.14	4.90	0.80	0.11	7.82
	PLB12	8.75	0.70	2.47	17.89	52.07	0.09	3.16	4.91	0.81	0.12	8.73
	PLB13	8.03	0.70	2.47	17.66	52.03	0.09	3.11	3.82	0.88	0.13	10.61
BR	PLB10	10.94	0.55	2.92	18.03	49.43	0.09	3.05	6.32	0.73	0.11	7.48
	PLA13	12.56	0.50	2.50	15.11	42.71	0.11	2.39	9.55	0.70	0.13	12.18
	PLA14	12.96	0.39	2.32	13.69	38.85	0.12	2.00	9.88	0.63	0.15	18.02
	PBR1	11.80	0.53	2.78	15.77	44.57	0.09	2.64	9.11	0.77	0.12	11.36
	PBR2	12.57	0.50	2.75	16.05	44.94	0.09	2.67	9.08	0.71	0.12	9.99
	PBR3	12.48	0.46	2.59	14.42	41.63	0.10	2.26	9.11	0.69	0.13	15.46
	PBR4	12.06	0.49	2.71	16.96	45.93	0.09	2.65	8.33	0.70	0.12	9.48
	PBR5	10.78	0.57	2.76	18.09	49.43	0.09	2.89	6.07	0.72	0.12	8.10
	PBR6	10.50	0.59	2.81	18.39	49.80	0.09	2.96	5.95	0.71	0.12	7.76
	PBR7	13.97	0.46	2.51	15.89	43.39	0.10	2.32	10.25	0.66	0.12	9.92
	PBR8	10.68	0.56	2.69	18.13	50.08	0.09	2.75	5.89	0.71	0.12	8.07
	PBR9	11.60	0.52	2.51	17.51	46.54	0.09	2.63	7.80	0.74	0.12	9.38
	PBR10	12.36	0.47	2.44	16.20	46.11	0.09	2.47	10.03	0.72	0.12	8.47
SS	PGA1	6.40	0.57	3.00	18.69	50.48	0.15	2.88	8.26	0.78	0.14	7.76
	PGA3	6.60	0.42	2.52	21.17	48.43	0.27	2.63	7.05	0.73	0.20	9.00
	PGA5	5.72	0.59	2.89	17.68	51.50	0.13	2.79	8.89	0.80	0.12	8.05
	PSS1	12.02	0.57	3.35	15.58	47.25	0.11	3.09	9.00	0.75	0.10	7.75
	PSS2	12.57	0.55	3.14	15.54	46.77	0.11	2.98	9.47	0.73	0.10	7.51
	PSS3	11.90	0.56	3.20	16.00	47.63	0.11	3.00	8.61	0.74	0.10	7.75
	PSS4	12.03	0.53	3.21	16.41	47.53	0.12	2.98	8.12	0.73	0.10	7.83
	PSS5	11.50	0.53	3.08	17.29	48.07	0.10	2.97	7.71	0.73	0.09	7.51
	PSS6	12.11	0.53	2.91	17.43	47.35	0.13	2.80	7.93	0.70	0.11	7.52
	PSS7	12.40	0.52	2.92	17.76	47.33	0.11	2.80	7.85	0.67	0.09	7.25
	PSS8	12.64	0.46	2.84	18.05	47.04	0.11	2.81	8.11	0.65	0.09	6.89
	PSS9	12.15	0.50	2.78	18.47	47.39	0.09	2.80	8.10	0.64	0.08	6.61
	PSS10	12.16	0.48	2.72	18.75	47.36	0.11	2.75	7.68	0.65	0.09	6.89
	PSS11	11.75	0.48	2.75	19.55	48.25	0.09	2.79	7.07	0.61	0.07	6.22
	PSS12	12.26	0.48	2.67	19.55	46.92	0.09	2.69	7.68	0.62	0.08	6.48
TR	1A	7.98	0.62	2.68	18.82	54.14	0.09	3.09	3.82	0.79	0.13	7.84
	2A	7.97	0.60	2.78	19.49	53.56	0.09	3.26	3.47	0.81	0.13	7.85
	3A	7.92	0.61	2.70	18.98	54.11	0.10	3.14	3.3	0.80	0.15	8.20
	4A	8.47	0.57	2.83	19.34	53.08	0.10	3.29	3.34	0.81	0.15	8.02

Table 5.3−Continued on next page

Table 5.3−Continued

5A	8.33	0.58	2.79	19.25	53.49	0.10	3.2	3.35	0.79	0.16	7.95
6A	8.69	0.59	2.75	18.18	54.39	0.10	2.90	3.79	0.79	0.11	7.71
7A	8.97	0.58	2.76	18.15	54.19	0.11	2.78	4.08	0.76	0.12	7.51
8A	9.06	0.58	2.71	18.36	53.94	0.10	2.88	3.80	0.79	0.11	7.66
9A	8.27	0.61	2.66	19.00	55.51	0.12	2.90	2.47	0.80	0.12	7.54
10A	8.41	0.57	2.60	18.14	55.46	0.12	3.06	2.29	0.88	0.13	8.35
1B	10.17	0.49	2.98	18.43	50.22	0.09	3.20	5.59	0.72	0.18	7.94
2B	8.13	0.53	2.77	19.43	53.57	0.10	3.25	3.42	0.79	0.15	7.86
1C	8.26	0.62	2.88	19.15	53.47	0.10	3.19	3.73	0.77	0.13	7.69
2C	9.21	0.65	2.76	18.08	54.23	0.09	2.84	4.35	0.77	0.07	6.96
3C	7.95	0.63	2.81	19.64	53.99	0.09	3.28	3.59	0.78	0.05	7.19
4C	7.61	0.58	2.78	18.95	56.45	0.10	3.11	2.16	0.85	0.04	7.38
5C	8.37	0.57	2.76	18.74	53.46	0.09	3.10	3.90	0.76	0.18	8.06
6C	8.23	0.58	2.78	19.04	53.38	0.09	3.17	3.87	0.77	0.18	7.92
7C	7.95	0.61	2.79	19.29	54.30	0.10	3.16	3.63	0.78	0.06	7.32
8C	10.25	0.54	2.85	17.93	52.74	0.10	2.85	4.20	0.76	0.10	7.68
9C	9.47	0.50	2.9	18.88	51.76	0.09	3.16	4.53	0.76	0.13	7.82
10C	9.24	0.56	2.75	18.54	53.65	0.11	2.99	3.33	0.81	0.13	7.89

Table 5.3. *Chemical characterization of the four groups of sediments in which data have been divided. Main oxides are expressed as weight %.*

The analysis was then articulated in three steps in order to determine: i) the centre, which is a measure of central tendency for the dataset and it is defined as the closed geometric mean (Daunis-i-Estadella et al. 2006); ii) the variation matrix (Daunis-i-Estadella et al. 2006), expressed as the variance of log-ratios, which describes the dispersion of the variables; iii) the biplot graph (Gabriel, 1971; Aitchinson and Greenacre, 2002); as a biplot represents in two dimensions all the variables under consideration, it is an useful graph in order to visualize the data variability and to identify important subcompositions, which may differentiate the geochemical processes.

The centre for each oxide in each group is reported Table 5.4. The main differences between groups relate to the CaO and SiO_2 or Al_2O_3 contents. CaO is in particular higher for the BR and SS groups (> 9%), and lower for TR and PS (3-5%), while the opposite behavior is observed for SiO_2 or Al_2O_3 (Table 5.4). These oxides may then represent suitable variables in order to discriminate between the recent/present-day sediments and the fossil pre-mining ones.

Group	Na_2O	MgO	Al_2O_3	SiO_2	P_2O_5	K_2O	CaO	TiO_2	MnO	Fe_2O_3
PS	0.64	3.00	19.96	55.67	0.11	3.28	5.40	0.86	0.16	10.92
BR	0.58	3.04	18.92	52.49	0.11	2.97	9.33	0.81	0.14	11.61
SS	0.58	3.31	20.13	54.24	0.13	3.22	9.14	0.79	0.11	8.34
TR	0.63	3.04	20.60	58.89	0.11	3.37	3.90	0.86	0.13	8.47

Table 5.4. *Centres of the composition of major oxides (in %) of each sediment group.*

The relative variability of each oxide within each group is reported in Table 5.5 by means of the centred log-ratio (clr)-variance and the total variance which is the sum of these values within each group. The clr-tranformations for the data were obtained by dividing each variable of the composition by the geometric mean of the closed array, and then by taking natural logarithms (Aitchison, 1986). As the variance is low both for each oxide taken into consideration and for the total variance, each group can be considered as homogeneous.

Group	Na_2O	MgO	Al_2O_3	SiO_2	P_2O_5	K_2O	CaO	TiO_2	MnO	Fe_2O_3	Total variance
PS	0.040	0.044	0.030	0.032	0.146	0.032	0.042	0.033	0.120	0.052	0.576
BR	0.014	0.010	0.013	0.011	0.011	0.015	0.027	0.009	0.010	0.038	0.163
SS	0.011	0.010	0.012	0.008	0.028	0.009	0.010	0.007	0.023	0.007	0.128
TR	0.014	0.011	0.011	0.012	0.015	0.012	0.029	0.012	0.073	0.010	0.203

Table 5.5. *Centred log-ratio variances and total variances for major oxides of each sediment group.*

In order to examine the covariance structure of the data, the variation matrix was determined by using the log-ratio variances, where each *ij*- component of the Table 5.6. is expression of the var[ln*(xi/xj)*]. The extremely low log-ratios for Al_2O_3/SiO_2, SiO_2/K_2O, Al_2O_3/Na_2O indicate low variabilities of these variables and a probable similar geochemical behavior in the system investigated. On the contrary, the ratios involving P_2O_5 present the highest variability, particularly the P_2O_5/MnO and P_2O_5/MgO, showing the presence of a possible geochemical process able to differentiate these oxides. Additional relationships among variables were then better analyzed by the biplot.

	Na_2O	MgO	Al_2O_3	SiO_2	P_2O_5	K_2O	CaO	TiO_2	MnO	Fe_2O_3	Group
Na_2O		0.0209	0.0161	0.0100	0.3387	0.0119	0.0531	0.0116	0.2586	0.0874	PS
		0.0046	0.0027	0.0026	0.0344	0.0017	0.0903	0.0063	0.0277	0.1224	BR
		0.0030	0.0270	0.0072	0.0896	0.0045	0.0034	0.0053	0.0709	0.0131	SS
		0.0075	0.0048	0.0032	0.0119	0.0083	0.0582	0.0048	0.1873	0.0091	TR
MgO	0.0209		0.0249	0.0245	0.4159	0.0225	0.0596	0.0274	0.2297	0.0674	PS
	0.0046		0.0045	0.0028	0.0205	0.0043	0.0643	0.0026	0.0155	0.0908	BR
	0.0030		0.0253	0.0068	0.0862	0.0012	0.0034	0.0057	0.0713	0.0110	SS
	0.0075		0.0013	0.0024	0.0113	0.0024	0.0374	0.0041	0.1600	0.0030	TR
Al_2O_3	0.0161	0.0249		0.0021	0.2443	0.0016	0.0373	0.0046	0.2232	0.0621	PS
	0.0027	0.0045		0.0006	0.0297	0.0022	0.0817	0.0056	0.0231	0.1187	BR
	0.0270	0.0253		0.0069	0.0609	0.0159	0.0249	0.0201	0.0588	0.0185	SS
	0.0048	0.0013		0.0012	0.0096	0.0011	0.0476	0.0021	0.1617	0.0024	TR
SiO_2	0.0100	0.0245	0.0021		0.2532	0.0030	0.0368	0.0030	0.2498	0.0693	PS
	0.0026	0.0028	0.0006		0.0250	0.0026	0.0738	0.0034	0.0188	0.1083	BR
	0.0072	0.0068	0.0069		0.0646	0.0029	0.0068	0.0048	0.0550	0.0073	SS
	0.0032	0.0024	0.0012		0.0062	0.0038	0.0530	0.0008	0.1699	0.0028	TR
P_2O_5	0.3387	0.4159	0.2443	0.2532		0.2649	0.2573	0.2567	0.5495	0.3469	PS
	0.0344	0.0205	0.0297	0.0250		0.0385	0.0310	0.0174	0.0020	0.0364	BR
	0.0896	0.0862	0.0609	0.0646		0.0784	0.0837	0.0540	0.0044	0.0378	SS
	0.0119	0.0113	0.0096	0.0062		0.0139	0.0756	0.0055	0.1671	0.0083	TR
K_2O	0.0119	0.0225	0.0016	0.0030	0.2649		0.0374	0.0035	0.2296	0.0667	PS
	0.0017	0.0043	0.0022	0.0026	0.0385		0.0928	0.0074	0.0313	0.1310	BR
	0.0045	0.0012	0.0159	0.0029	0.0784		0.0036	0.0052	0.0664	0.0090	SS
	0.0083	0.0024	0.0011	0.0038	0.0139		0.0480	0.0039	0.1568	0.0030	TR
CaO	0.0531	0.0596	0.0373	0.0368	0.2573	0.0374		0.0399	0.2291	0.0994	PS
	0.0903	0.0643	0.0817	0.0738	0.0310	0.0928		0.0520	0.0337	0.0384	BR
	0.0034	0.0034	0.0249	0.0068	0.0837	0.0036		0.0057	0.0668	0.0114	SS
	0.0582	0.0374	0.0476	0.0530	0.0756	0.0480		0.0614	0.1534	0.0480	TR
TiO_2	0.0116	0.0274	0.0046	0.0030	0.2567	0.0035	0.0399		0.2566	0.0662	PS
	0.0063	0.0026	0.0056	0.0034	0.0174	0.0074	0.0520		0.0119	0.0826	BR
	0.0053	0.0057	0.0201	0.0048	0.0540	0.0052	0.0057		0.0401	0.0023	SS
	0.0048	0.0041	0.0021	0.0008	0.0055	0.0039	0.0614		0.1698	0.0027	TR
MnO	0.2586	0.2297	0.2232	0.2498	0.5495	0.2296	0.2291	0.2566		0.1892	PS
	0.0277	0.0155	0.0231	0.0188	0.0020	0.0313	0.0337	0.0119		0.0398	BR
	0.0709	0.0713	0.0588	0.0550	0.0044	0.0664	0.0668	0.0401		0.0287	SS
	0.1873	0.1600	0.1617	0.1699	0.1671	0.1568	0.1534	0.1698		0.1351	TR
Fe_2O_3	0.0874	0.0674	0.0621	0.0693	0.3469	0.0667	0.0994	0.0662	0.1892		PS
	0.1224	0.0908	0.1187	0.1083	0.0364	0.1310	0.0384	0.0826	0.0398		BR
	0.0131	0.0110	0.0185	0.0073	0.0378	0.0090	0.0114	0.0023	0.0287		SS
	0.0091	0.0030	0.0024	0.0028	0.0083	0.0030	0.0480	0.0027	0.1351		TR

Table 5.6. *Variation matrix, expressed as* $Var(\ln Xi/Xj)$.

In this study, the biplot is able to characterize the 67% of the total variability of the dataset (Fig. 5.5), suggesting that an appreciable association between variables is present. The 9 observable vectors (some of them have been eliminated as unnecessary to describe data variability), intersecting in a common origin, represents the clr-variables, while each markers represents a clr-transformed sample in the biplot space. The centre of the biplot is the barycentre of the dataset, $\xi = [g1, \ldots, gD] = [g\mathrm{H_2O}, g\mathrm{Na_2O}, g\mathrm{MgO}, g\mathrm{Al_2O_3}, g\mathrm{SiO_2} g, g\mathrm{P_2O_5}, g\mathrm{K_2O}, g\mathrm{CaO}, g\mathrm{Ti_2O}, g\mathrm{MnO}, g\mathrm{Fe_2O_3}] = [9.9, 0.6, 2.8, 18.1, 50.5, 0.1, 2.9, 5.4, 0.8, 0.1, 8.8]$, where gi is the geometric mean for each variable in the closed dataset.

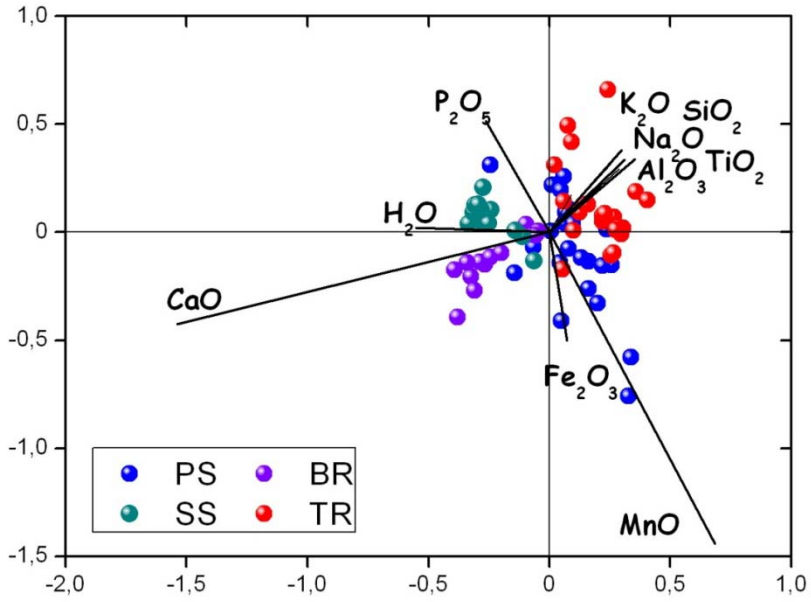

Fig. 5.5. *Biplot showing the relationships between each group of sediment with respect to the variables affecting composition. Intersecting vectors represent the clr-components; markers are related to the sediment samples belonging to each group.*

The graphical configuration of vectors in the biplot may supply additional information about the analyzed dataset. In the biplot formalism, the length of each vector is then approximately equal to the variance of each log-centred variance, whereas the links (the joints among the vertices of the vectors) provides information on the covariance structure (Aitchison and Greenacre, 2002; Daunis-i-Estadella et al., 2006). In particular, the following characteristics of the biplot are observed to describe this dataset: i) the cosines of the angles between links, which give indications about the correlations between log-ratios; then if angles are at 90°, zero association is expected between the considered log-ratio; ii) the coincidence of the vertices of two or more vectors, which indicate that the variance of the correspondent log-ratio is zero and the ratio among variables is constant; iii) the collinearity of some vertices in

opposite quadrants of the biplot, whose vectors identify subcompositions that can be analyzed separately. The length of the vectors of the biplot and the clr-variance of Table 5.5 indicates that for this dataset the variability can be described by the following sequence of oxides: CaO>MnO>P_2O_5>SiO_2. As the vertices of SiO_2, Al_2O_3, K_2O and TiO_2 practically coincide, the variance of the log-ratio of these variables is zero, or nearly so (Table 5.6), meaning that their absolute ratios are constant. Then the only vector SiO_2 (or Al_2O_3) is taken as representative of the total variability expressed by this quadrant of the biplot as the other variables only carry on redundant information. The biplot shows that the variability of fossil sediments, TR and PS groups, is mainly expressed by the SiO_2 and MnO vectors, whereas the recent and modern sediments are described by the variables CaO and P_2O_5, suggesting that minor chemical differences are able to operate a discrimination among the four groups of sediments. However, the clustering of all groups around the barycentre of the biplot indicates that all sediments, notwithstanding some differences, are linked by a common geochemical composition.

Combining the information of Table 5.4 and Fig. 5.5, it was possible to select three variables that were sufficient to operate a discrimination among groups in a ternary diagram. The variables whose centres are very different and whose rays form angles higher than 90° in the biplot were chosen (Table 5.4; Fig. 5.5). In addition, the approximately collinearity of vertices CaO, SiO_2 and Al_2O_3 and P_2O_5, MnO and Fe_2O_3 reveals the possible presence of patterns in the ternary diagram and the two subsets were analyzed separately. In order to better visualize compositional lines, the data were reported in the ternary diagram by means of a mathematical operation called perturbation, i.e. the barycentre of the dataset is moved to the centre of the ternary diagram (Buccianti et al., 1999; Von Eynatten et al. 2002). In our case, only the subcomposition SiO_2-MnO-CaO is able to distinct, at least partially, the four sediment groups (Fig. 5.6). In particular, the TR group presents higher SiO_2 content, while the SS and BR groups point toward the CaO vertex; the PS group almost overlaps in the ternary diagram to the TR one, suggesting similar geochemical characteristics of these sediments.

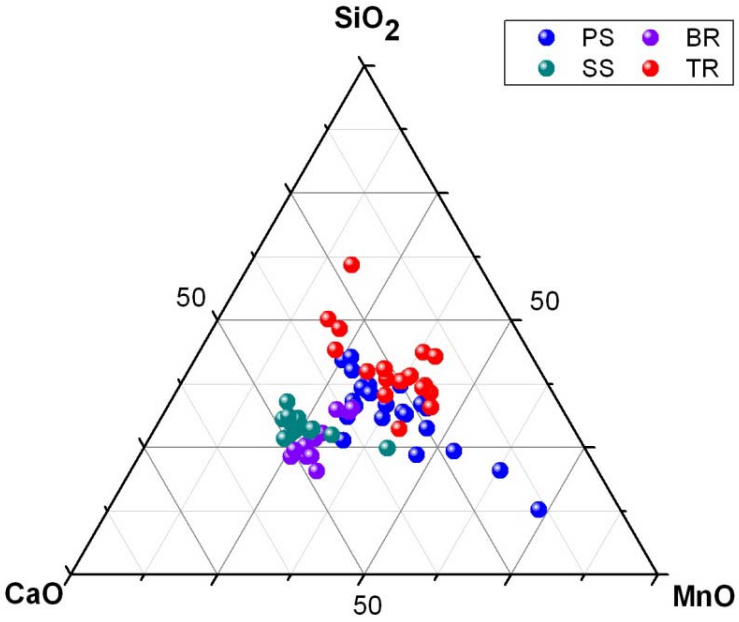

Fig. 5.6. *Ternary diagram of SiO_2-MnO-CaO(centred dataset).*

Examination of the ternary diagram CaO-SiO_2-Al_2O_3 shows that this subcomposition has a one-dimensional variability, i.e. the data plot along a compositional line characterized by $(SiO_2)/(Al_2O_3) \cong 1$ (Fig. 5.7). Along this trend, groups are distinguished on the base of their CaO%, with contents lower and higher than about 45% for TR-PS and BR-SS, respectively.

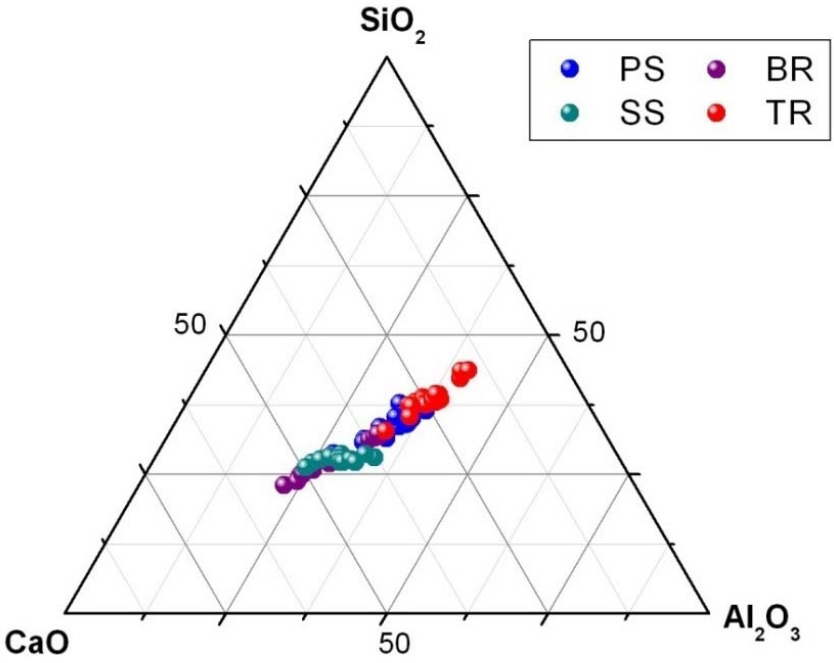

Fig. 5.7. *Ternary diagram of CaO-SiO_2-Al_2O_3 (centred dataset).*

This data pattern, moving from the SiO_2−Al_2O_3 side of the ternary diagram towards the vertex, depicts a geochemical evolution trend for sediments, showing a progressive enrichment in CaO as they become younger in age. The existence of a significant correlation in the system CaO-SiO_2-Al_2O_3 was moreover verified after the application of an isometric log-ratio transformation of data (Daunis-i-Estadella et al., 2006; Filzmoser and Hron, 2009), by considering the balances $1/\sqrt{2} \times \ln(CaO/SiO_2)$ and $1/\sqrt{6} \times \ln[(CaO \times SiO_2)/(Al)^2]$ (not shown). This graph then explains the relative variation of two groups of parts (variables or components of the composition) in an orthogonal system (Borgheresi et al., 2012). The correlation was found equal to $R^2 = 0.95$, suggesting that these variables strictly correlate, allowing in theory a modelization to be made, which is however beyond the scope of this work.

On the base of the main geochemistry, the four different groups can be clustered in two main subdivisions, PS-TR and BR-SS, discriminated by the ratio Al_2O_3/CaO, and corresponding to pre-mining and post-mining sediments, respectively. The clustering of all groups around the barycentre of the biplot and the similar Al_2O_3/SiO_2 ratio for all groups suggest a common parent rock for both recent and pre-mining sediments, generally represented by the silicatic rocks abundant in this area. Nevertheless, the particular geochemical fingerprint of recent sediments, enriched in CaO with respect to pre-mining conditions, indicates the presence of an additional Ca-rich source of sediments in the drainage basin of Pagliola Creek. As this geochemical marker is found only in recent and present-day stream sediments, being coeval and/or subsequent to mining activity, the Ca-rich source could be supposed to relate to the industrial exploitation of Hg mines, representing the natural weathering of an anthopogenic material connected to Hg production.

5.4.3 Minor chemistry

Mercury and arsenic contents for each samples divided in the four groups are reported in Table 5.7 together with the main descriptive statistics. Arsenic contents are in the range of the established 7 μg/g background for Southern Tuscany (Benvegnù et al., 1993; Protano et al., 1998). However, with few exceptions, all the concentrations are beneath 20 μg/g, which is the Italian maximum permissible limit in soils designated to public green, private and residential use (GURI, 2006). Although slight higher levels of As are reported for the BR and PS groups, As concentrations in different groups are of the same order of magnitude, suggesting that the present-day environmental availability of As is comparable to that characterizing the industrial period.

Group	Trace elements (mg/kg)	
	Hg	**As**
PS	7	5
	2	8
	15	6
	6	10
	16	22
	41	10
	2	7
	3	14
	10	9
	17	10
	108	16
	3	12
	34	14
	15	17
	3	11
	1	12
	2	16
	1	14
	58	22
	19	11
	3	7
	66	8
	16	12
	44	16
median	**12**	**12**
mean	**10***	**12**
std dev	**4***	**5**
max	**108**	**22**
min	**0.8**	**5**
BR	54	7
	732	20
	420	29
	620	17
	458	16
	368	25
	450	13
	145	10
	51	8
	280	17
	70	8
	441	12
	2103	10
median	**420**	**13**
mean	**290***	**15**
std dev	**3***	**7**
max	**2103**	**29**
min	**51**	**7**

Group	Trace elements (mg/kg)	
	Hg	**As**
TR	7	5
	9	5
	4	6
	3	6
	2	6
	0.7	7
	0.8	8
	0.6	7
	2	12
	2	11
	0.3	6
	5	6
	3	5
	1	5
	0.4	2
	0.7	3
	0.6	6
	0.9	6
	3	4
	0.5	6
	1	6
	2	8
median	**2**	**6**
mean	**2***	**6**
std dev	**2***	**2**
max	**9**	**12**
min	**0.3**	**2**
SS	13	7
	47	12
	29	6
	36	6
	64	7
	38	7
	31	8
	32	7
	36	9
	29	8
	29	7
	26	7
	35	8
	28	6
	50	6
median	**32**	**7**
mean	**32***	**7**
std dev	**1***	**1**
max	**64**	**12**
min	**26**	**6**

***Table* 5.7.** *Data for Hg and As for the dataset analyzed in this study.* refers to the calculated mean and the standard deviation for Hg distributions, which have been calculated by taking the natural logarithmic of data in order to obtain a normal distribution.*

Concentrations of Hg on the analyzed samples vary between 0.3 to 2,103 µg/g (Table 5.7), suggesting a wide range of variability. More than 85% of samples is above the Hg Italian law limit of 1 µg/g, reflecting the large diffusion of this contaminant in the Mt. Amiata region. Distribution of Hg among the four groups ranges between 1-108 (PS), 51-2103 (BR), 13-50 (SS), and 0.3-9 (TR) µg/g, for PS, BR, SS and TR groups, respectively (Table 5.7). Positive skewed distributions characterize Hg in all groups but PS (Fig. 5.8), then indicating the geometric mean as the most suitable parameter to describe the barycentres of the groups (Table 5.7). Outliers are abundant, particularly for the PS group, indicating the presence of anomalously high Hg concentrations in some samples, which can be related to a nugget effect which is a common problem for Hg analysis. Unlike As, significant different Hg levels are reported between groups; in particular, the 290 µg/g Hg barycentre for the BR group is two orders of magnitude higher than that of fossil sediments TR (2 µg/g), and one fold higher than the present-day stream sediments SS (32 µg/g) (Table 5.7). This observation suggests that high environmental Hg characterized the formation and deposition of these sediments, indirectly confirming that the age of the internal terrace of Pagliola can be coeval to the exploitation of Hg mines.

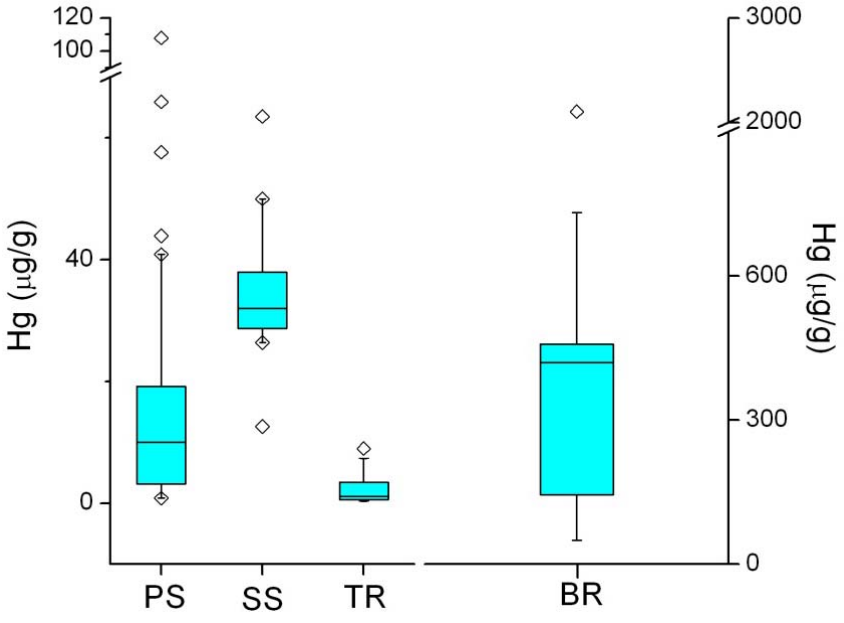

Fig. 5.8. *Mercury box plots for the groups SS, TR, PS and BR. Note the BR group (right) has a different scale with respect to the others (left).*

In order to highlight the geochemical processes which can explain the Hg contents in the analyzed groups, the subcomposition Hg-Al_2O_3-CaO (Fig. 5.9) was investigated, as the ratio Al_2O_3/CaO was found to mainly discriminate within the recent and pre-mining sediment

groups. In the ternary space, the four groups plot along a linear trend which connects the Hg vertex to the CaO-Al_2O_3 axis. The highest Hg levels are associated to lowest Al_2O_3/Ca ratios (Al_2O_3/Ca ≈ 1), i.e. to the SS and BR groups, whereas higher Al_2O_3/Ca (Al_2O_3/Ca >1) are reported for the SS and BR groups. Furthermore, the diagram discloses a quasi-linear data pattern in the subcomposition CaO-Hg-Al_2O_3, which was better clarified by the isometric log-ratio data transformation (Fig. 5.10).

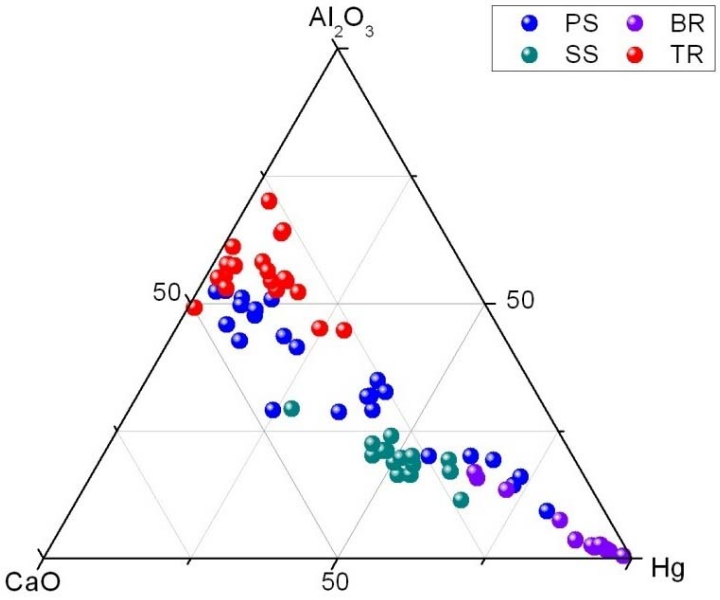

Fig. 5.9. *Ternary diagram of CaO-SiO_2-Al_2O_3 (centred dataset).*

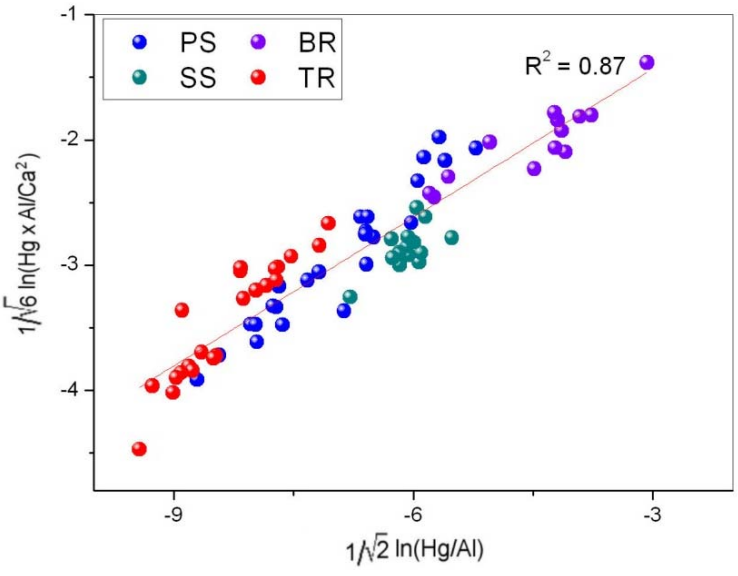

Fig. 5.10. *Isometric transformation of the trend observed in the ternary diagram CaO-SiO_2-Al_2O_3.*

The presence of a good correlation in the system CaO-Hg-Al_2O_3 (R^2 = 0.87) suggests that Hg in the Mt. Amiata samples is not random distributed but can be modeled and predicted on the base of CaO, suggesting that this oxide may act as a proxy for Hg in this area. Common to most Hg mines, a calcination process was carried out at the Mt. Amiata mines and particularly at the Abbadia San Salvatore's analyzed in this work, consisting in the addition of lime to a first roasted material in order to recover the residues of metallic Hg. The lime-addicted material was then new-roasted, and the final discarded wastes, enriched in CaO and Hg, were termed calcines. The natural weathering of these materials may then be considered the cause of the CaO-enrichment of recent and present-day stream sediments of Pagliola, which are directly impacted by the runoff from the Abbadia San Salvatore mine site, where elevated quantities of calcines are piled up. Consequently to the chemical/physical weathering of calcines, Hg is highly diffused in the recent and present-day environment of the Pagliola Creek. On the contrary, the absence of calcine deposits at the time when the pre-mining sediments were formed, determines lower CaO levels in the PS and TR groups and corresponding lower Hg. The linear trend observed in the ternary diagram or by the isometric transformation of Hg-Al-Ca variables, may then represent an indirect estimate of the mass of calcines being altered: higher the quantity of weathered calcines in sediments, higher the corresponding Hg contents.

5.4.4 Mercury and arsenic in the Pagliola Creek evolution

In order to highlight main differences in Hg and As contents as a consequence of the paleo-geographical evolution of the paleo-Pagliola, the profiles of Hg and As concentrations at increasing depth for the TR group are reported (Fig. 5.11). The highest values of Hg are generally observed for the conoid-sediments, ranging 0.5− 9 μg/g, while sediments referred to the infill of the paleo- and modern valleys by the Pagliola Creek, collected beneath and above the conoid, report lower Hg with respect of the conoid lithotypes. Arsenic does not correlate with Hg ones, and its concentrations are variable without apparent connection with the different lithotypes along the profiles. Common to both As and Hg small increases in metal contents are generally reported in sediments collected near the surface.

It is useful to remember that sediments collected above the conoid (S3) are coeval to those forming the first order fluvial terrace of Pagliola Creek (PS groups), although Hg concentration in the PS group is generally higher than those of S3. This observation highly reflects the non-homogeneous distribution of Hg in sediments filling the paleo-Pagliola

Valley, which is characterized by higher contents along the main river channel and lower contents in the floodplain.

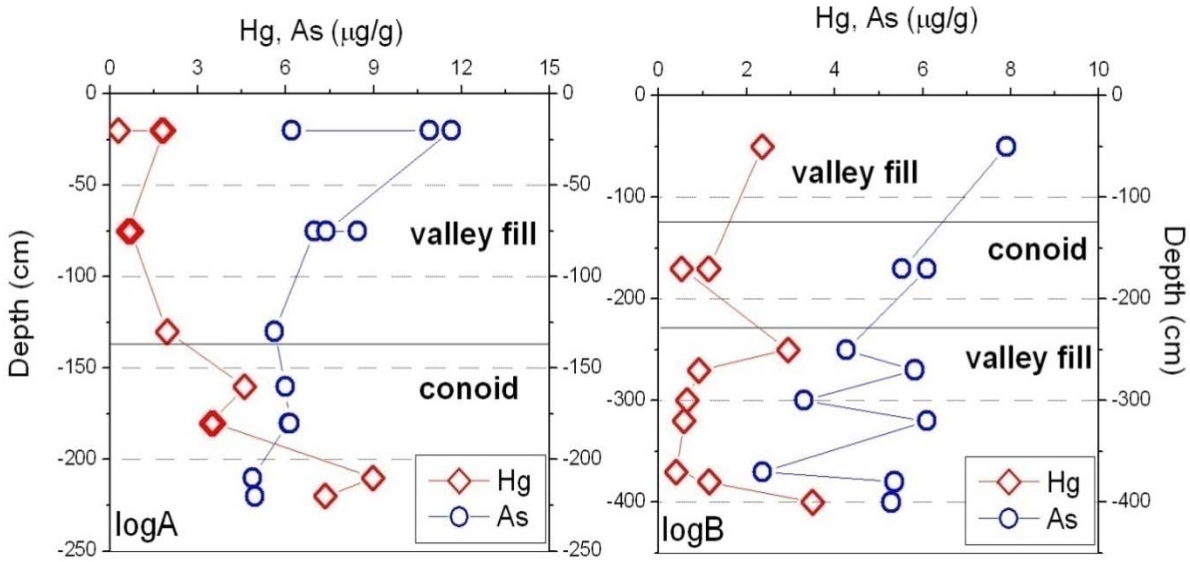

Fig. 5.11. *Profiles of Hg and As versus depth in the two excavations logA and logB.*

The results of this study testify that in the environment of Mt. Amiata a geochemical mobilization of Hg was already taking place at the time of the paleo-Pagliola Creek, whose concentrations are much higher than the clarke values of 0.056 μg/g (Rudnik and Gao, 2003). The distribution of Hg along the profile furthermore suggests that the geochemistry of the paleo-Pagliola basin changed during the evolution of the creek, registering an increase during the conoid deposition. After the reestablishment of the river course, a marked increase in Hg contents is again reported along the main channel of the paleo-Pagliola, indicating that an important change in the geochemistry of the Pagliola drainage basin has occurred as a consequence of: i) natural physical modifications of the Pagliola River catchment basin and/or ii) chemical changes in the parent rocks being altered. The zoning of Hg in the paleo-Pagliola Valley suggests moreover the presence of different Hg-enriched sources of sediments in the basin: a Hg-rich one, which fed the paleo-Pagliola main river channel, and a Hg-poor one, characterizing the floodplain of the paleo-Pagliola. Arsenic on the contrary does not register perceptible variations, highlighting that the As geochemistry of the Pagliola drainage basin was constant during the evolution of the system.

5.4.5 Mercury and arsenic geochemical background

On the base of the paleo-hydrographic reconstruction of the Pagliola Creek, the sediments belonging to the TR and PS groups were considered pristine, i.e. the levels of the

contaminants are unaffected by the mining activity of this area. If the two groups derive from the same population, the background can then be calculated by clustering together these two distributions. The non-parametric median and Mann-Whitney tests were then run, in order to test the null hypothesis H_0 that the median values of the two samples were not significantly different. The tests indicate however that the two datasets cannot be considered as extracted by a single population at the significant level of 0.5 (H_0 is rejected). Presently, there is no way to establish if these differences between medians are the result of geochemical processes operating in this area, or they happen by chance due to the low number of samples collected in this study.

In this context, a geochemical background for Hg and As can then be considered to be comprised between the barycentre of the TR and PS distributions, which define a minimum and maximum estimates. The regional backgrounds for the Mt. Amiata area then range 2-6 μg/g and 6−11 μg/g for Hg and As, respectively. However, these ranges must be considered as preliminary estimates, as further research is needed in this area in order to increment the number and the spatial distribution of samples in the Pagliola Basin. The concept of geochemical background is interconnected with that of regional variability (Matschullat et al., 2000), then in order to establish a reliable background, samples must extend spatially in order to account for the natural fluctuations of the element being characterized (Reimann and Garrett, 2005). Moreover a detailed characterization of the sampling media represents a fundamental precursor step to determine the geochemical processes occurring in a determined area, and influencing the background. This study put then the necessary premises to further study the geochemical background of the Mt. Amiata, determining: i) the spatial fluctuations of Hg(As) along the paleo-Pagliola Valley, and ii) the geochemical processes affecting the chemistry of Mt. Amiata sediments.

Notwithstanding some inherent limitations, this study first documents the presence of a wide geogenic anomaly centered in the Mt. Amiata area, resulting in Hg levels that are two orders of magnitude higher than the crustal clarke (0.056 μg/g; Rudnick and Gao, 2003). The defined background range is moreover much higher than that previously reported for this area, 0.3 μg/g (Protano et al., 1998). The range for As background is on the contrary well comprised in that generally defined for this element in Southern Tuscany (7 μg/g; Protano et al., 1998), although higher than that common encountered in the UCC (4.8 μg/g; Rudnick and Gao, 2003).

5.5 Conclusions

The extensive mining activity in the Mt. Amiata highly affects the geochemistry of the Pagliola Creek, which drains the Abbadia San Salvatore Hg mine. As a result of the weathering and downstream transport of the calcine deposits by the river, elevated CaO% contents are reported in the recent and current stream sediments of the Pagliola Creek, which well correlate with Hg concentrations. Mercury mobilization in the environment is then strictly related to that of calcines, suggesting that the CaO oxide may be regarded as a geoindicator of environmental quality in the Mt. Amiata area. During mining activity for Hg, in particular, the diffusion of Hg in the environment of Mt. Amiata was extremely elevated, determining up to hundreds of μg/g Hg in the sediments draining the mining areas during that time. Although Hg levels reported in the current stream sediment testify a decrease of Hg availability in the environment with respect to the industrial period, mean concentrations are still 35-folds higher than those accepted by the Italian legislation.

Mercury concentrations in pre-mining sediments of the ancient Pagliola river course are two orders of magnitude higher than the normal concentrations encountered in the crust, indicating the presence of a wide geogenic anomaly as a result of the natural denudation of Hg-rich rocks and the dismantling of cinnabar deposits. The Hg background for the Mt. Amiata region is then estimated between 2 and 6 μg/g. This concentration range, although representing only a preliminary estimate, is much higher than the 1 μg/g limit established by the Italian legislation for Hg. A most reliable contamination level should be then defined for this area in order to properly discriminate between the natural baseline and the anthropic contamination, helping to define reliable and cost-effectiveness thresholds for the remediation project carrying on at the Abbadia San Salvatore Hg mine.

Acknowledgements

This study was financially supported by the University of Florence, and the Municipality of Abbadia San Salvatore (Italy). I'm really grateful to M. Benvenuti (University of Florence), who helped me to reconstruct the paleogeography of the Pagliola Creek, and Antonella Buccianti (University of Florence) for her introduction to the world of compositional, for her suggestions and for her helpful reviews to the test.

References

ACOCELLA V. (2000). Space accommodation by roof lifting during pluton emplacement at Amiata Mt (Italy). *Terra Nova*, **12**: 149–155.

AITCHISON J. (1986). The statistical analysis of compositional data. London, UK: Chapman and Hall, 416 pp.

AITCHISON J. AND GREENACRE M.(2002).Biplots for compositional data. *Journal of the Royal Statistical Society, Series C*, **51**: 375–392.

ALBANESE S., DE VIVO B., LIMA A., CICCHELLA D. (2007). Geochemical background and baseline values of toxic elements in stream sediments of Campania region (Italy). *J. Geochem. Exploror.*, **93**: 21−34.

ARISI ROTA F., BRONDI A., DESSAU G., FRANZINI M., MONTE AMIATA S.P.A. (1971), STABILIMENTO MINERARIO DEL SIELE, STEA B., VIGHI L. (1971). I Giacimenti minerari. In: La Toscana meridionale. *Rend. Soc. Ital. Mineral. Petrol.*, **27**, Spec. Is.: 357–544.

BARBERI F., BUONASORTE G., CIONI R., FIORDELISI A., FORESI L., LACCARINO S., LAURENZI M.A., SBRANA A., VERNIA L., VILLA I.M. (1994).Plio-Pleistocene geological evolution of the geothermal area of Tuscany and Latium. *Mem. Descr. Carta Geol. It.*, **49**: 77−134.

BENVEGNÙ E., BRONDI A., COLICA A., CONTI P., GUASPARRI G., POLIZZANO C., SABATINI G., TASSONI E. (1993). Studies of migration factors in clay in real situation; study of fractures in clays the neogenic basin of Siena. Nuclear Sc. Tech., Commission of European Communities Report. pp.1–53.

BIGAZZI G., BONADONNA F.P., GHEZZO C., GIULIANI O., DI BROZOLO RADICATI F., RITA F. (1981). Geochronological Study of the Monte Amiata Lavas (Central Italy). *Bull. Vulcanol.*, **44**: 455−465.

BINI C., SARTORI G., WAHSHA M., FONTATA S. (2011).Background levels of trace elements and soil geochemistry at regional level in NE Italy. *J. Geochem. Expl.*, **109**: 125–133.

BONINI M. AND SANI F. (2002). Extension and compression in the northern Apennines (Italy) hinterland: Evidence from the late Miocene-Pliocene Siena-Radicofani Basin and relations with basement structures. *Tectonics*, **22**: 1–35.

BORGHERESI M., BUCCIANTI A., DI BENEDETTO F., VAUGHAN D.J. (2012).Application of Compositional Techniques in the Field of Crystal Chemistry: A Case Study of Luzonite, a Sn-Bearing Mineral. *Math. Geosci.*, DOI 10.1007/s11004-012-9422-5.

BREWARD N. (2007). Arsenic and presumed resistate trace element geochemistry of the Lincolnshire (UK) sedimentary ironstones, as revealed by a regional geochemical survey using soil, water and stream sediment sampling. *Appl. Geochem.*, **22**: 1970−1993.

BROGI A. (2004). Miocene extension in the inner northern Apennines: the Tuscan Nappemegaboudins in the Mt. Amiata geothermal area and their influence on Neogene sedimentation. *Boll. Soc.Geol. It.*, **123**: 513–529.

BROGI A. (2008). The structure of the Monte Amiata volcano-geothermal area (Northern Apennines, Italy): Neogene-Quaternary compression versus extension. *Int. J. Earth Sci.*, **97**: 677–703.

BROGI A. AND LIOTTA D. (2008). Highly extended terrains, lateral segmentation of the substratum and basin development: the Middle–Late Miocene Radicondoli Basin (Inner Northern Apennines, Italy). *Tectonics*, **27**: 1–20.

BUCCIANTI A. AND ESPOSITO P. (2004). Insights into Late Quaternary calcareous nannoplankton assemblages under the theory of statistical analysis for compositional data. *Palaeogeogr. Palaeocl.*, **202**: 209−227.

BUCCIANTI A. AND PAWLOWSKY-GLAHN (2005).New Perspectives on Water Chemistry and Compositional Data Analysis. *Math. Geol.,* **37**: 703−727.

BUCCIANTI A., PAWLOWSKY-GLAHN V., BARCELÓ-VIDAL C., JARAUTA-BRAGULAT E. (1999). Visualization and modeling of natural trends in ternary diagrams: A geochemical case study. InLippard S. J., Naess A., Sinding-Larsen R. (Eds.), Proceedings of IAMG'99−The fifth annual conference of the International Association for Mathematical Geology: Trondheim, pp. 139−144.

CADOUX A. AND PINTI D.L. (2009). Hybrid character and pre-eruptive events of Mt Amiata volcano (Italy) inferred from geochronological, petro-geochemical and isotopic data. *J. Volcanol. Geoth. Res.*, **179**: 169–190.

CASTALDI F. AND CHIOCCHINI U. (2012). Effects of land use changes on badland erosion in clayey drainage basins, Radicofani, Central Italy. *Geomorphology*, **169-170**: 98−108.

COLLETTINI C., DE PAOLA N., HOLDSWORTH R.E., BARCHI M.R. (2006). The development and behaviour of low-angle normal faults during Cenozoic asymmetric extension in the Northern Apennines, Italy. *J. Struct. Geol.*, **28**: 333–352.

DAUNIS-I-ESTADELLA J., BARCELÓ-VIDAL C., BUCCIANTI A. (2006).Exploratory compositional data analysis. In: Buccianti A., Mateu-Figueiras G., Pawlowsky-Glahn V. (Eds.), Compositional Data Analysis in the Geosciences. Geological Society, London, Spec. Pub., **264**: 161–174.

DE VOS W., EBBING J., HINDEL R., SCHALICH J., SWENNEN R., VAN KEER I. (1996). Geochemical mapping based on overbank sediments in the heavily industrialised border area of Belgium, Germany and The Netherlands. *J. Geochem. Explor.*, **56**: 91–104.

FERRARA R., MASERTI B.E., BREDER R. (1991). Mercury in abiotic and biotic compartments of an area affected by a geochemical anomaly (Mt. Amiata, Italy). *Water Air Soil Pollut.,* **56**: 219-233.

FILZMOSER P., HRON K., REIMANN C. (2009).Univariate statistical analysis of environmental (compositional) data: Problems and possibilities. *Sci. Total Environ.*, **407**: 6100-6108.

FRANCOVICHR. (1999).L'archeologia in Toscana fra alto e basso medioevo: una rassegna bibliografica. *Archivio Storico Italiano*, CLVII/579, pp. 131−176.

GABRIEL K. R. (1971). The biplot-graphic display of matrices with application to principal component analysis. *Biometrika*, **58**: 453−467.

GALÁN E., FERNÁNDEZ-CALIANI J.C., GONZÁLEZ I., APARICIO P., ROMERO A. (2008).Influence of geological setting on geochemical baselines of trace elements in soils. Application to soils of South–West Spain. *J. Geochem. Expl.*, **98**: 89−106.

GAŁUSKA A. (2007). A review of geochemical background concepts and an example using data from Poland. *Environ. Geol.*, **52**: 861–870.

GAŁUSZKA A. AND MIGASZEWSKI Z.M. (2011). Geochemical background – an environmental perspective. *Mineralogia*, **12**: 7−17.

GARRETT R.C., REIMANN C., SMITH D.B., XIE X. (2008). From geochemical prospecting to international geochemical mapping: a historical overview. *Geochem.: Expl. Environ. An.*, **8**: 205−217.

GHINASSI M. AND LAZZAROTTO A. (2005). Different source areas feeding the Early Pliocene marine Radicofani Basin (Siena): geological and paleogeographical implications. *Boll. Soc. Geol. It.*, Spec. Vol., **3**: 15−28.

GIANELLI G., PUXEDDU M., BATINI F., BERTINI G., DINI I., PANDELI E.,NICOLICH R. (1988). Geological model of a young volcanoplutonic system: the geothermal region of Monte Amiata (Tuscany Italy). *Geothermics*, **17**:719–734.

GIROTTI O. AND MANCINI M. (2003).Plio – Pleistocene stratigraphy and relations between marine and non – marine successions in the middle valley of Tiber river (Latium, Umbria). *Il Quaternario*, **16**: 89–106.

GOSAR M. AND ŽIBRET G. (2011). Mercury contents in the vertical profiles through alluvial sediments as a reflection of mining in Idrija (Slovenia). *J. Geochem. Explor.*,110: 81−91.

GUILLÉN M.T.,DELGADOJ., ALBANESE S., NIETO J.M., LIMA A., DE VIVO B. (2011). Environmental geochemical mapping of Huelva municipality soils (SW Spain) as a tool to determine background and baseline values. *J. Geochem. Explor.*, **109**: 59−69.

GURI (GAZZETTA UFFICIALE DELLA REPUBBLICA ITALIANA) (2006). Decreto legislativo 3 aprile 2006, n. 152: Norme in materia ambientale. Gazzetta Ufficiale della Repubblica Italiana n. 88 del 14-4-2006, suppl. ord. n. 96, Titolo V, All.5. Tab. 1. Istituto Poligrafico dello Stato, Roma.

HAWKES H.E. AND WEBB J.S. (1962). Geochemistry in Mineral Exploration. New York Harper, 415 pp.

JACOBACCI A., MARTELLI N., NAPPI G. (1967) - Note illustrative della Carta Geologica d'Italia alla scala 1:100.000, Foglio 129 Santa Fiora. *Serv. Geol. d'It.*, 61 pp.

KELLEY K. D. AND TAYLOR C. D. (1997). Environmental geochemistry of shale-hosted Ag-Pb-Zn massive sulfide deposits in northwest Alaska: natural background concentrations of metals in water from mineralized areas. *Appl. Geochem.*, **12**: 397-409.

KOCMAN D., KANDUČ T., OGRINC N., HORVAT M. (2010).Distribution and partitioning of mercury in a river catchment impacted by former mercury mining activity. *Biogeochemistry*, doi:10.1007/s10533-010-9495-5, pp. 19.

LIOTTA D. (1996). Analisi del settore centro-meridionale del bacino pliocenico di Radicofani (Toscana meridionale). *Boll. Soc. Geol. It.*, **115**: 115−143.

LIOTTA D. AND SALVATORINI G. (1994). Evoluzione sedimentaria e tettonica della parte centro.meridionale del bacino pliocenico di Radicofani. *Studi Geologici Camerti*, Sp. Vol., **1**: 65−77.

LOREDO J., ORDÓÑEZ A., GALLEGO J.R., BALDO C., GARCÍA-IGLESIAS J. (1999). Geochemical characterisation of mercury mining spoil heaps in the area of Mieres (Asturias, northern Spain). *J. Geochem. Explor.*, **67**: 377−390.

MACKLIN M.G., RIDGWAY J., PASSMORE D.G., RUMSBY B.T. (1994). The use of overbank sediment for geochemical mapping and contamination assessment: results from selected English and Welsh floodplains. *Appl. Geochem.*, **9**: 689−700.

MARTINI I.P. AND SAGRI M. (1993). Tectono sedimentary characteristics of late Miocene - Quaternary extensional basins of the Northern Apennines, Italy. *Earth-Sc. Rev.*, **34**: 197−233.

NIETO P., CUSTODIO E., MANZANO M. (2005). Baseline groundwater quality: a European approach. *Environ. Sci. Policy*, **8**: 399–409.

OTTESEN R.T., BOGEN J., BØLVIKEN B., VOLDEN T. (1989). Overbank sediment: a representative sample medium for regional geochemical mapping. *J. Geochem. Explor.*, **32**: 257–277.

PASCUCCI V., COSTANTINI A., MARTINI I.P., DRINGOLI R. (2006). Tectono-sedimentary analysis of a complex, extensional, Neogene basin formed on thrust-faulted, Northern Apennines hinterland: Radicofani Basin, Italy. *Sediment.Geol.*, **183**: 71–97.

PASQUARÈ G., CHIESA S., VEZZOLI L. ZANCHI A. (1983). Evoluzione paleogeografica e strutturale di parte della Toscana meridionale a partire dal Miocene superiore. *Mem. Soc. Geol. Ital.*, **25**: 145–157.

PAWLOWSKY-GLAHN V. AND EGOZCUE J.J. (2006). Compositional data and their analysis: an introduction. In: Buccianti A., Mateu-Figueiras G., Pawlowsky-Glahn V. (Eds.), Compositional Data Analysis in the Geosciences, Geological Society, London, Sp. Pub., **264**: 1–10.

PAWLOWSKY-GLAHN V., EGOZCUE J.J., TOLOSANA-DELGADO R. (2007). Lecture Notes on Compositional Data Analysis. http://hdl.handle.net/10256/297.

PROTANO, G., RICCOBONO, F., SABATINI, G. (1998). La cartografia geochimica della Toscana meridionale. Criteri di realizzazione e rilevanza ambientale attraverso esempi di Hg, As, Sb, Pb e Cd. – *Mem. Descr. Carta Geol. It.*, **55**: 109–140.

REIMANN C. AND GARRETT R.G. (2005). Geochemical background − concept and reality. *Sci. Total Environ.*, **350**: 12−27.

REIMANN C., MATSCHULLAT J., BIRKE M., SALMINEN R. (2009). Arsenic distribution in the environment: The effects of scale. *Appl. Geochem.*, **24**: 1147−1167.

RIMONDI V., GRAY J.E., COSTAGLIOLA P., VASELLI O., LATTANZI P. (2012). Concentration, distribution, and translocation of mercury and methylmercury in mine-waste, sediment, soil, water, and fish collected near the Abbadia San Salvatore mercury mine, Mt. Amiata district, Italy. *Sci. Total Environ.*, **414**: 318−327.

RUDNICK S. AND GAO S. (2003). Composition of the continental crust. In: Holland H.D., Turekian K.K. (Eds.), The Crust, Treatise on Geochemistry, Vol. 3. Elsevier, Oxford, pp. 1–64.

SALMINEN R. AND TARVAINEN T. (1997). The problem of defining geochemical baselines. A case study of selected elements and geological materials in Finland. *J. Geochem. Explor.*, **60**: 91–98.

SALOMONS W. (1995). Environmental impact of metals derived from mining activities: Processes, predictions, prevention. *J. Geochem. Explor.*, **52**: 5−23.

SWENNEN R. AND VAN DER SLUYS J. (1998). Zn, Pb, Cu and As distribution patterns in overbank and medium-order stream sediment samples: their use in exploration and environmental geochemistry. *J. Geochem. Explor.*, **65**: 27−45.

SWENNEN R., VAN DER SLUYS J., HINDEL R., BRUSSELMANS A. (1998). Geochemistry of overbank and large order stream sediments in Belgium and Luxembourg: a way to assess environmental pollution. *J. Geochem. Explor.*, **62**: 67–79.

TANELLI G. (1983). Mineralizzazioni metallifere e minerogenesi della Toscana. *Mem. Soc. Geol. It.*, **25**: 91–109.

SALVADOR A. (1987). Unconformity-bounded stratigraphic units. *Geol. Soc. Am. Bull.*, **98**: 232-237.

VIDAL J., PÉREZ-SIRVENT C., MARTÍNEZ-SÁNCHEZ M.J., NAVARRO M.C. (2004). Origin and behaviour of heavy metals in agricultural Calcaric Fluvisols in semiarid conditions. *Geoderma*, **121**: 257–270.

VON EYNATTEN H., PAWLOWSKY-GLAHN V., EGOZCUE J.J. (2002). Understanding Perturbation on the Simplex: A Simple Method to Better Visualize and Interpret Compositional Data in Ternary Diagrams. *Math. Geol.,* **34***:* 249−257.

CHAPTER 6

– CONCLUSIONS –

As part of the broad Mediterranean Hg belt, the Mt. Amiata region (Central Italy) hosts a wide geochemical anomaly in Hg, mainly in the form of cinnabar ores. More than 103,000 tons of liquid Hg were produced by these mines and introduced to the global market, ranking this district as one of the most important at a global level. The produced Hg was extensively used almost in all sectors of human life as far as the risk associated to Hg use was elucidated by different cases of human mass poisonings in the 1950s and 1970s. The following contraction of worldwide demand for Hg resulted in the closure of all the Hg mines in the Mt. Amiata region at the beginning of the 1980s. The Abbadia San Salvatore mine was the last one to close in 1982, and the main centre of this work. Due to its pervasive character, Hg contamination is long-lasting in time, maintaining high levels in all environmental compartments belonging to the mine districts. Moreover, the impact of Hg is often not limited to the local scale, but it becomes of regional importance, extending hundreds of kms away from the local source of contamination. Cleanup strategies of abandoned Hg mines are therefore essential to limit Hg diffusion in the environment. Presently, almost no remediation strategies have been carried out at the Abbadia Hg mine and estimated 120,000 m^2 of roasted cinnabar banks are located next to the mining area without proper disposal. Calcine deposits are a well known long-term source for Hg due to the presence of unconverted cinnabar, not recovered liquid Hg and secondary formed Hg minerals.

A widespread Hg diffusion in the environment of Mt. Amiata was already documented during the mining activity and confirmed in field surveys made in the years following the end of mining. In this thesis, the extent of Hg diffusion in the Mt. Amiata environment is evaluated after 30 years mining is ceased, focusing on Hg dispersion by action of a natural river course, the Paglia River. The waters of this river represent indeed the main carriers for the Hg drained by the Abbadia San Salvatore mine. Different aspects of Hg environmental impact of mining activity in the Mt. Amiata Hg mines are taken into consideration in order to: i) delineate an updated picture of the extent of Hg and MMHg diffusion in the environment of Paglia River (part I); ii) have a first reliable assess of the quantities of Hg transported by Paglia River waters (part II); iii) define the real availability of Hg from the contaminated

sediments and matrices (part III); iv) proper discriminate Hg background values from Hg anthropogenic contamination (part IV).

After three decades from the end of mining, the results of this study indicate that a still pervasive Hg diffusion is present in all environmental compartments belonging to the Paglia River. In sediments, Hg contents exceed both the Probable Effect Concentrations and the Italian regulation limits for soils, although they are generally lower than those encountered in other mining districts worldwide. The main risk associated to these Hg mines is represented by the presence of methyl-Hg, the most toxic Hg compound, which is actively produced in all compartments of the Paglia River. These levels are in particular in the range or higher than those encountered in other mining districts which are however significantly more contaminated by total Hg, suggesting the peculiar high bioavailability of MMHg in the Mt. Amiata. High methyl-Hg concentrations in small fish living in this river, largely exceeding the recommended value of 0.3 µg/g w/w US EPA, further suggest favourable conditions for methylation reactions in this ecosystem.

The main environmental problem associated with the mining activity of Abbadia San Salvatore is the widespread occurrence of waste calcines, highly contaminated in Hg (up to 1500 µg/g), piled up without proper disposal. Weathering/leaching of these deposits is then highly impacting for the downstream environment of the Paglia River, affecting: i) the major and minor chemical composition of sediments; and ii) the Hg speciation in geological matrices. Results of this thesis show that the recent and present-day sediments draining the Hg mine are partly composed by the dismantled calcine deposits; the CaO% content in sediments, which is the chemical fingerprint of calcines, can be used to predict Hg levels in the deposits. The increase of Hg mobility in the environment is another main problem associated to the past roasting process for Hg production, forming secondary Hg compounds in waste rocks which are more soluble than the original ones. As documented in this work, leaching of these Hg mineral phases severely alters the Hg speciation in the draining sediments. While in pre-mining sediments, Hg is dominantly in the form of cinnabar, which is an extremely insoluble Hg phase that naturally limit the availability of Hg, in post mining sediments Hg is present in more soluble forms, such as elemental Hg and $HgCl_2$. These phases, which are directly drained from the mining area, may strongly affects the bioavailability of Hg in the Paglia River ecosystem. As they may easily dissolve, they can release Hg(II), entering the aquatic Hg cycle, and possible methylating. The presence of these Hg soluble phases may represent a possible explanation for the elevated levels of MMHg registered in the Paglia River ecosystem.

The first reliable estimate of Hg load of Paglia River made in this work reflects the importance of waters as vectors for Hg diffusion. In baseline conditions, the transport of Hg by the river is quantified to 11 kg yr^{-1}, occurring mainly in the form of particulate Hg. Due to the strong association of Hg to particulate matter, hydrological and morphological modifications of the Paglia River results in strong variation of Hg loads along the river reach. In this study, in particular, the marked deposition of Hg along the river, forming a natural sink, is identified few kms downstream the mine. Rather than representing a way to decontamination of the river, this in-river deposit is a nearly continuous source of Hg to the environment, supplying the river with: i) particulate Hg independently from the river hydrological conditions (i.e. river discharge); ii) dissolved Hg as a result of chemical reactions promoting Hg desorbing from particulate and increasing the availability of dissolved species along the Paglia River. This sink is then only a transient storage for Hg, which is later remobilized and transported further away from the local source up to the Tiber River. The impact of Hg mining in the Mt. Amiata therefore is not limited to the local environment of Paglia River but it extends further away from the local mines.

The main effect of human activity in mining districts is the alteration of the local Hg cycle, introducing to the environment the Hg stored in the geological traps. This represents an exacerbation of the natural dismantling of cinnabar mineralization and Hg-rich rocks, which determines high Hg backgrounds in the areas where the Hg global belts are located. Evaluate and quantify this process is a fundamental step in order to proper discriminate between anthropogenic and background levels in these regions. This study represents the first attempt to establish a reliable Hg background for the Mt. Amiata by employing Quaternary pre-mining sediments of the paleo-Paglia river course. This preliminary estimate indicates that a wide Hg geochemical anomaly characterizes the Mt. Amiata area, ranging 2-6 µg/g, which is two orders of magnitude higher than those commonly reported for the upper continental crust. These concentrations suggest the importance of defining reliable contamination levels for Hg in this area, taking into consideration such elevated natural background. The CaO% content in sediments may in particular represents a suitable geoindicator for Hg contamination, representing an easy way to discriminate between anthropogenic and background levels in the sediments of Mt. Amiata.

This thesis may represent an useful base to further investigate specific aspects of Hg geochemistry in the Mt. Amiata region and may help with the ongoing remediation strategy that is carrying on at the Abbadia San Salvatore Hg mine. One of the main problem elucidated in this work is connected with MMHg, whose high concentrations in the Paglia River basin is

largely unexplained although some hypothesis have been made. Additional research on the peculiar factors influencing and enhancing methyl-Hg reactions in the Mt. Amiata area is then required, due to the potential high impact of this compound to biota living in this ecosystem and to humans. Moreover, as the importance of the Mt. Amiata district is not limited to the local scale but may extend far away from this region, a study focusing on the Tiber River abiotic and biotic compartments is projected in order to quantify the impact of Paglia River on this basin and then to the Mediterranean Sea.

PHD RESEARCH ACTIVITY

Italian and abroad studying experiences

- USGS, US Geological Survey (Denver Federal Center, Colorado). 4/5/2011-30/6/2011. Research and laboratori activity for the analysis of the Mt. Amiata fish.
- Sardinia, 30/5/2012-5/6/2012. Field and laboratory activity for the application of tracer dilution methods to determine flow discharges in the mining sites of Inglesiente-Sulcis (supervisor Briant A. Kimball, USGS-Utah Water Science Center).

National and International collaborations

- Regione Toscana
- USGS, US Geological Survey (J.E. Gray)
- ESRF, European Synchrotron Radiation Facility

School attendances

- ISFG - International School of Fluid Geochemistry, 36 – 37. 21-24th September 2010, Abbadia San Salvatore Italy.
- ISTT - International School on Travertine and Tufa, 5-9th September 2011, Abbadia San Salvatore, Italy.
- International School "Minerals and Biosphere", 23-27th September 2011, Campiglia Marittima, Livorno, Italy.

Congress attendances

- ICOBTE-11th International Conference on the Biogeochemistry of Trace Elements, 3-7th July 2011 Firenze, Italy.
- FIST 2011– Federazione Italiana Scienze Terra, 19-23rd September 2011, Torino, Italy.
- EMC 2012 - European Mineralogical Conference, 2-6 September Frankfurt, Germany.
- ICHMET 2012 - 16th International Conference of Heavy Metals in the Environment, 23-27 September 2012 Rome.

Awards

- GABeC (group of Georisorse, Ambiente, Beni Culturali) grant for the participation to the International School "Minerals and Biosphere"
- GABeC grant for the participation to the EMC 2012.

Pubblications

Congress abstracts

V. Rimondi, P. Costagliola, O. Vaselli, P. Lattanzi, F. Tassi (2010). Mercury distribution in the environment: the case of Abbadia San Salvatore (Mt. Amiata). International School of Fluid Geochemistry, 36 – 37. 21-24 September 2010, Abbadia San Salvatore, Italy.

V. Rimondi, P. Costagliola, J.E. Gray, O. Vaselli, M.M. Benvenuti, F. Di Benedetto, P.Lattanzi. Mercury diffusion in fish of the Hg mining district of Monte Amiata (Southern Tuscany, Italy). EGU General Assembly 2011, Geophysical Research Abstracts, vol. 13, EGU2011-11820. 3-8 April 2011, Vienna, Austria.

V. Rimondi, P. Costagliola, J.E. Gray, P. Lattanzi, O. Vaselli, M. Benvenuti (2011). Mercury distribution and transport in the ecosystem of Paglia River (Monte Amiata, Italy). Geoitalia 2011, Epitome, vol. 4, 87. 19-23 September 2011, Torino, Italy.

A. Ciardi, M. Benvenuti, P. Costagliola, P. Lattanzi, M. Paolieri, V. Rimondi (2011). Anomalous arsenic concentrations in soils from the Viterbo area. Geoitalia 2011, Epitome, vol. 4, 87. 19-23 September 2011, Torino, Italy.

V. Rimondi, P. Costagliola, J.E. Gray, P. Lattanzi, M. Nannucci, A. Salvadori, and O. Vaselli (2012). Mass loading of mercury in the Monte Amiata mining district, Southern Tuscany (Italy). EMC 2012, European Mineralogical Conference vol. 1, EMC2012-614. 2-6 September 2012, Frankfurt, Germany.

Extended Abstracts

V. Rimondi, P. Costagliola, J.E. Gray, M.M. Benvenuti, F. Di Benedetto, P.F Lattanzi, O. Vaselli (2011). Mercury diffusion and distribution in the Hg mining district of Monte Amiata (Southern Tuscany, Italy). ICOBTE 2011, 11th International Conference on the Biogeochemistry of Trace Elements, S13_118. 3-7 July 2011, Firenze, Italy.

F. Bardelli, M. Benvenuti, P. Costagliola, F. Di Benedetto, L. Valenzano, P.F. Lattanzi, C. Meneghini, V. Rimondi, M. Romanelli (2011). Arsenic incorporation in natural calcite: a structural and spectroscopic study. ICOBTE 2011, 11th International Conference on the Biogeochemistry of Trace Elements, pp. 2. 3-7 July 2011, Firenze, Italy.

V. Rimondi, P. Costagliola, J.E. Gray, P. Lattanzi, M. Nannucci, A. Salvadori, O. Vaselli (2012). Mass loading of Hg in the mine district of Monte Amiata, Southern Tuscany (Italy). ICHMET 2012, 16th International Conference of Heavy Metals in the Environment, pp. 4. 23-27 September 2012, Roma, Italy.

Journal papers

V. Rimondi, J.E. Gray, P. Costagliola, O. Vaselli, P. Lattanzi (2012). Concentration, distribution, and translocation of mercury and methylmercury in mine-waste, sediment, soil, water, and fish collected near the Abbadia San Salvatore mercury mine, Monte Amiata district, Italy. Science of the Total Environment, 414: 318-322.

P. Costagliola, F. Bardelli, M. Benvenuti, F. Di Bendetto, M. Romanelli, M. Paolieri, V. Rimondi, G. Vaggelli (2012). "Arsenian calcite" in natural travertines: evidence from sequential extraction, μ-XAS AND μ-XRF. Submitted to Environment Science and Technology.

ACKNOWLEDGMENTS

I would like to thank all the people that believed in this project, actively contributed to its realization, and helped me during my PhD activity:

Pilario Costagliola, my supervisor, for the infinite energy, enthusiasm and funds he invested in this work;

Orlando Vaselli, my co-supervisor, for the suggestions, the indications and the bureaucracy he took care at my place;

Piefranco Lattanzi, for the useful suggestions to the manuscript, for the support and help he always gave me in these years;

John E. Gray, for the introduction to the world of mercury, for its hospitality during the months I spent in the USGS, and its great help in the realization of this project;

Daniele Rappuoli, *Marcello Niccolini* and *Andrea Esposito* (Municipality of Abbadia San Salvatore), for the unlimited availability in the realization of this work. I'm especially in debt with Marcello for its ubiquitous presence in the field works, the enthusiasm demonstrated for the project, for the fish he caught…and for the delicious wild boar we ate along the Paglia River!

Andrea Salvadori and *Marco Nannucci* (Regione Toscana), for their essential and appreciable help in the realization of mass loads along the Paglia River;

Mario Paolieri, for its great experience in the laboratory, to have repaired the FIAS every time it did not work, for its help in the field;

Francesca Podda, to have provided part of the analysis reported in this work and for her help to clarify all my doubts.

Elena Pecchioni, for the help she gave me every I needed and for the delicious cakes and biscuits she cheers up the PhD student office;

Fabrizio Bardelli, *Marco G. Benvenuti*, *Marco M. Benvenuti*, *Antonella Buccianti*, for the time you dedicated to my work, and for the collaborations we started and I hope we will carry on in the future;

Lastly but not least, all my colleagues of the "Ex Biblioteca" are acknowledge to have shared with me the nice and bad moments of the working life. I especially remember the PhD students MAG group, *Francesca*, *Matteo* and *Giovanni*, historical friends of the first years of university, for the infinite number of coffees we took together at the coffee machine of the department, for the kebab and Chinese food we ate at lunch, for the scientific and semi-scientific questions we shared and the support they gave me in these years.

RINGRAZIAMENTI

Desidero ringraziare tutte le persone che hanno creduto in questo progetto, che hanno contribuito attivamente alla sua realizzazione e mi hanno aiutato nello svolgimento del dottorato:

Pilario Costagliola, il mio supervisore, per l'infinita energia, l'entusiasmo e gli investimenti profusi in questo lavoro;

Orlando Vaselli, il mio co-supervisore, per i suggerimenti, le indicazioni, gli investimenti e per tutte le noiose pratiche burocratiche di cui si è occupato al mio posto;

Pierfranco Lattanzi, per gli utili commenti al manoscritto, per il grande supporto e disponibilità dimostrati in questi anni;

John E. Gray, per l'introduzione al mondo del mercurio, per l'ospitalità nei mesi passati all'USGS, per la disponibilità e l'aiuto nella realizzazione di questo progetto;

Daniele Rappuoli, *Marcello Niccolini*, *Andrea Esposito* (Comune di Abbadia S. Salvatore), per l'infinita disponibilità dimostrata nella realizzazione di questo lavoro. A Marcello, in particolare, vanno i più sentiti ringraziamenti per la sua onnipresenza in campagna e per l'entusiasmo travolgente verso questo progetto, per la pesca …e per lo squisito cinghiale mangiato lungo il Paglia!

Andrea Salvadori e *Marco Nannucci* (Regione Toscana), per aver fornito il valido e indispensabile aiuto fornito nella realizzazione dei bilanci di massa sul Paglia;

Mario Paolieri, per le grande esperienza di laboratorio, per aver "riparato" il FIAS tutte le volte che si bloccava, per l'aiuto in campagna e per le gran risate che ci siamo fatti;

Francesca Podda, per aver svolto parte delle analisi inserite in questo lavoro e aver risolto i dubbi amletici;

Elena Pecchioni, per l'aiuto dimostrato qualsiasi volta ce ne sia stato bisogno …e per le meravigliose torte e biscotti con cui allieta la nostra stanza dottorandi;

Marco M. Benvenuti, *Marco G. Benvenuti*, *Antonella Buccianti*, *Fabrizio Bardelli*, per il tempo che mi avete dedicato e per collaborazioni che abbiamo iniziato e che spero porteremo aventi.

Infine, ringrazio tutti il gruppo dei colleghi della "Ex biblioteca", con i quali abbiamo condiviso gioie e dolori della vita lavorativa comune. Desidero in particolare ringraziare il gruppo MAG dei dottorandi, *Francesca*, *Matteo* e *Giovanni*, amici storici dei primi anni di università, per tutti i caffè bevuti alla macchinetta del dipartimento, i kebab mangiati all'ora di pranzo, i cinesi da asporto procacciati, le domande scientifiche e semi-scientifiche condivise e in generale per il supporto manifestato nel corso di questi anni.